Analysis of the applicability of iPS cell-based approaches to bypass senescence and to re-establish rejuvenation features in human MSCs from aged individuals

Dissertation
zur Erlangung des akademischen Grades
Doctor rerum naturalium (Dr. rer. nat.)

am Fachbereich für Biologie, Chemie und Pharmazie
der Freien Universität Berlin

vorgelegt von

Matthias Megges

Berlin 2015

1. Gutachter: Professor Dr. James Adjaye

2. Gutachter: Professor Dr. Petra Knaus

Disputation am: 18. 04. 2016

Unser Wissen ist ein Tropfen, unser Unwissen ein Ozean.

Sir Isaac Newton

Acknowledgments

First of all I would like to thank Professor Dr. James Adjaye for assigning this very interesting PhD project to me and for his supervision and career support over the years despite moving to a different Institute and starting a very demanding new position as a Professor and director of the Institut für Stammzellforschung und Regenerative Medizin, Düsseldorf. I would like to thank him for the great scientific advices that helped to develop and finish this work as well as for reviewing it and for having always the right idea or solution for scientific problems. In addition, I would like to thank him for always finding the time to discuss the project.

Furthermore, I would like to thank Professor Dr. Petra Knaus for the effort to be the second supervisor of this external PhD project despite already supervising many other internal PhD students. I would like to thank her for the scientific advice for this project and for her support and scientific discussions.

I would like to thank all members of the Institut für Stammzellforschung und Regenerative Medizin, Düsseldorf, who supported this project and helped with organisation and advice. I would like to thank Wasco Wruck for his help with bioinformatics and Silke Wehrmeyer for taking care of ordering.

Moreover, I would like to thank all former group members of the Molecular Embryology and Ageing Group at the Max Planck Institute for Molecular Genetics, Berlin, who helped with scientific advice, discussions, methodological advice and who made the time at work enjoyable.

In addition, I would like to thank all members of the Max Planck Institute for Molecular Genetics, who contributed to this work with good advice or by making sure that everything in the institute runs smoothly and who made the time enjoyable at the institute.

Apart from that, I would like to thank all external collaborators of this project for the fruitful teamwork.

Furthermore, I would like to thank Klaus, Susann and my father for their help with proof reading this work. Thank you very much.

Especially I would like to thank my parents and my parents-in-law for all their support during the last years.

Most importantly I would like to thank my wonderful wife Anett for her patience, understanding, support, faith in me, her humour and for taking care of our son so I could have more time to finalise this work. Without you it would not have been possible to find the strength to go through these not always easy times. Thank you very, very, very much. Finally, I would like to thank my son for making me smile even on bad days.

Contents

List of Figures

List of Tables

List of abbreviations

8-OHdG	8-Oxo-2'-deoxyguanosine
ACVR I/II	activin A receptor, type 1/II
AFP	α Fetoprotein
AKT	AKT kinase
ALDH1A3	aldehyde dehydrogenase 1 family, member A3
ALDH5A1	aldehyde dehydrogenase 5 family, member A1
ALDOC	aldolase C, fructose-bisphosphate
ALDOC	fructose-1,6-(bis)phosphate aldolase
ALK4	activin receptor like kinase receptor 4
ALK5	activin receptor like kinase receptor 5
ALK7	activin receptor like kinase receptor 7
ALPL	alkaline phosphatase
APC	adenomatosis polyposis coli protein
APOD	apolipoprotein D
ATM	ataxia telangiectasia mutated
ATP	adenosine triphosphate
Atp5a1	ATP synthase, H+ transporting, mitochondrial F1 complex, alpha subunit 1
Atp5f1	ATP synthase, H+ transporting, mitochondrial F0 complex, subunit B1
B27	serum free supplement for cell culture
BCL2	B-cell CLL/lymphoma 2
BGLAP	bone gamma-carboxyglutamate (gla) protein (osteocalcin)
BMP 4	bone morphogenetic protein 4
BMP6	bone morphogenetic protein 6
BMPRI/II:	BMP receptor I/II
BOP1	block of proliferation 1
BSA	bovine serum albumin
C2orf40	chromosome 2 open reading frame 40
CAMs	cell adhesion molecules
CAPRIN2	caprin family member 2
CCNB1	cyclin B1
CCND1	cyclin D1
CCNDBP1	cyclin D-type binding-protein 1
CCNE2	cyclin E2
CD9	cluster of differentiation 9

CD11b	integrin, alpha M (complement component 3 receptor 3 subunit), cluster of differentiation 11b
CD14	cluster of differentiation 14
CD34	hematopoietic progenitor cell antigen, cluster of differentiation 34
CD45	protein tyrosine phosphatase, cluster of differentiation 45
CD73	ecto-5'-nucleotidase, cluster of differentiation 73
CD79α	immunoglobulin-associated alpha, cluster of differentiation 79α
CD90	Thy-1 cell surface antigen / cluster of differentiation 90
CD105	endoglin, cluster of differentiation 105
CD271	nerve growth factor receptor, cluster of differentiation 271
CDC7	cell division cycle 7 homolog
CDK4	cyclin-dependent kinase 4
CDK6	cyclin-dependent kinase 6
CDKN1C	cyclin-dependent kinase inhibitor 1C
CDKN2A	cyclin-dependent kinase inhibitor 2A, P16INK4A
CFU-f	colony forming unit-fibroblastoid cell
CITED2	Cbp/p300-interacting transactivator, with Glu/Asp-rich carboxy-terminal domain, 2
c-MYC	v-Myc myelocytomatosis avian viral oncogene homolog
CNDP2	CNDP dipeptidase 2 (metallopeptidase M20 family)
COL1A1	collagen, type I, alpha 1
COX7A1	cytochrome c oxidase subunit VIIa polypeptide 1 (muscle)
Cox7a2	cytochrome c oxidase subunit VIIa polypeptide 2 (liver)
Cox7b	cytochrome c oxidase subunit VIIb
CREG	cellular repressor of E1A-stimulated genes 1
C_t	threshold cycle
DAPI	4',6-diamidino-2-phenylindole
DCF	fluorescent 2',7'-dichlorofluorescein
DCFDA	2’,7’–dichlorofluorescin diacetate
DEPC	diethylpyrocarbonate
DMEM	Dulbecco's Modified Eagle's Medium
DMSO	dimethyl sulfoxide
DNAse	deoxyribonuclease
dNTP	deoxynucleotide triphosphate
DPPA4	developmental pluripotency associated 4
DSB	DNA double-strand breaks
DUSP1	dual specificity phosphatase 1

DVL	segment polarity protein dishevelled
DZNep	3-deazaneplanocin A
E2F2	E2F transcription factor 2
EBNA1	Epstein–Barr nuclear antigen 1
ECM	extracellular matrix
EDTA	ethylenediaminetetraacetic acid
EGR1	early growth response 1
EHHADH	enoyl-Coenzyme A, hydratase/3-hydroxyacyl Coenzyme A dehydrogenase
ERK1/2	extracellular signal regulated kinase1 / 2
ETS1	v-ets erythroblastosis virus E26 oncogene homolog 1 (avian)
ETS2	v-ets erythroblastosis virus E26 oncogene homolog 2 (avian)
EXO1	exonuclease 1
FACS	fluorescence activated cell sorting
FADS1	fatty acid desaturase 1
FBS	fetal bovine serum
FCS	forward scatter
FGF2	basic fibroblast growth factor
FGF4	fibroblast growth factor 4 (heparin secretory transforming protein 1, Kaposi sarcoma oncogene)
FGFR	basic fibroblast growth factor receptor
FITC	fluorescein isothiocyanate
Foxo1	forkhead box O1
Frizzled	WNT receptor
gag	group-specific antigen
GAPDH	glyceraldehyde-3-phosphate dehydrogenase
GCAT	glycine C-acetyltransferase (2-amino-3-ketobutyrate coenzyme A ligase)
GCLM	glutamate-cysteine ligase, modifier subunit
GFP	green fluorescent protein
GGCT	gamma-glutamyl cyclotransferase
GnRH	gonadotropin-releasing hormone 1
GO	gene ontology
GPI	glucose-6-phosphate isomerase
Gpx1	glutathione peroxidase 1
GPX2	glutathione peroxidase 2
GPX3	glutathione peroxidase 3
GPX8	glutathione peroxidase 8
GSH	guthatione

GSK3β	glycogene synthase kinase 3 β
Gsta2	glutathione S-transferase A2
Gstm2	glutathione S-transferase M2 (muscle)
GTG banding	Giemsa stain based banding
HEK293T	transformed human embryonic kidney cell line
HeLa	epithelial cell line derived from cervical cancer cells 1951 from Henrietta Lacks
HEPES	4-(2-hydroxyethyl)-1-piperazineetanesulfonic acid
hESC	human embryonic stem cells
hFF	human fetal foreskin fibroblasts
HGPS	lamin A/C
HLA-DR	major histocompatibility complex, class II, DR beta 1
hMSCs	human bone marrow -derived mesenchymal stem cells
ID1	inhibitor of DNA binding 1, dominant negative helix-loop-helix protein
ID2	inhibitor of DNA binding 2, dominant negative helix-loop-helix protein
IDE	insulin-degrading enzyme
IGF-1	insulin-like growth factor 1
IGFBP5	insulin-like growth factor binding protein 5
IGFR	insulin-like growth factor receptor
IgG1	immunoglobulin heavy constant gamma 1
IgG2a	gamma-2a immunoglobulin heavy chain
IMDM	Iscove's Modified Dulbecco's Medium
iMSCs	mesenchymal stem cell-like cells derived from pluripotent stem cells
INK4A/ARF locus	locus encoding INK4A, INK4B, and ARF
iPSC	induced pluripotent stem cells will be named
IRES2	internal ribosome entry site 2
IRS1	insulin receptor substrate 1
JUN	jun oncogene
KEGG	Kyoto Encyclopedia of Genes and Genomes
KLF4	Kruppel-like factor 4
KRT25	keratin 25
LEFTY1	left-right determination factor 1
LIN28	lin-28 homolog
LPL	lipoprotein lipase
MAP2K1	mitogen-activated protein kinase kinase 1
MCM7	minichromosome maintenance complex component 7
MEF2D	myocyte enhancer factor 2D

MEK	mitogen-activated protein kinase kinase 1
MET	mesenchymal-to-epithelial transition
MGST2	microsomal glutathione S-transferase 2
MIF	macrophage migration inhibitory factor (glycosylation-inhibiting factor)
MMLV	Moloney Murine Leukemia Virus
MORC3	MORC family CW-type zinc finger 3
MRPL28	mitochondrial ribosomal protein L28
MSRA	methionine sulfoxide reductase A
MSRB2	methionine sulfoxide reductase B2
MSRB3	methionine sulfoxide reductase B3
mTOR	mammalian target of Rapamycin
N2	chemically defined, serum-free supplement based on Bottenstein's N-1 formulation
NANOG	Nanog homeobox
NEK6	NIMA (never in mitosis gene a)-related kinase 6
NES	Nestin
NF-κB	nuclear factor of kappa light polypeptide gene enhancer in B-cells 1
NOD scid gamma mouse	immunodeficient NOD.Cg-Prkdcscid Il2rgtm1Wjl/SzJ mouse
NOX4	NADPH oxidase 4
NUAK1	NUAK family, SNF1-like kinase, 1
OCT4 / POU5F1	octamer-binding protein 4 / POU class 5 homeobox 1
OGDHL	oxoglutarate dehydrogenase-like
OriP	origin of replication of episomal plasmid
ORX1	olfactory receptor, family 13, subfamily H, member 1
OXR1	oxidation resistance 1
P16INK4A	cyclin-dependent kinase inhibitor 2A
P19ARF	ARF tumor suppressor, alternate reading frame protein product of the INK4A/ARF locus
P21	Cip1, cyclin-dependent kinase inhibitor 1A
P53	tumor protein P53
PARP3	poly (ADP-ribose) polymerase family, member 3
PAX6	paired box 6
PBS	phosphate-buffered saline
pCMV	cytomegalovirus immediate-early promoter
PCR	polymerase chain reaction
PDCD4	programmed cell death 4 (neoplastic transformation inhibitor)
PDK1	pyruvate dehydrogenase lipoamide kinase isozyme 1

PDLIM1	PDZ and LIM domain 1
Pdpk1	3-phosphoinositide dependent protein kinase-1
PE	phycoerythrin
pEF	eukaryotic elongation 1α promoter
PerCP	peridinin
PFKFB3	6-phosphofructo-2-kinase/fructose-2,6-bisphosphatase 3
Pfkl	phosphofructokinase, liver
PFKP	phosphofructokinase, platelet
Pfu	Pfu DNA polymerase from Pyrococcus furiosus
PGAM1	phosphoglycerate mutase 1 (brain)
PI3K	phosphatidylinositol-4,5-bisphosphate 3-kinase
PI3K	Phosphatidylinositol-4,5-bisphosphate 3-kinase
PML	promyelocytic leukemia
PNPT1	polyribonucleotide nucleotidyltransferase 1
PODXL	podocalyxin-like
pol	retroviral DNA polymerase
POLR2H	polymerase (RNA) II (DNA directed) polypeptide H
POLR3G	polymerase (RNA) III (DNA directed) polypeptide G (32kD)
poly(I:C)	polyinosinic:polycytidylic acid
PPARγ	peroxisome proliferator-activated receptor gamma
PRKAG1	protein kinase, AMP-activated, gamma 1 non-catalytic subunit
PRKDC	protein kinase, DNA-activated, catalytic polypeptide
PRR11	proline rich 11
PTGS1	prostaglandin-endoperoxide synthase 1 (prostaglandin G/H synthase and cyclooxygenase)
qRT-PCR	quantitative real-time PCR
Raf	rat fibrosarcoma protein
Rapgef1	rap guanine nucleotide exchange factor (GEF) 1
Ras	rat sacoma protein
RCAN1	regulator of calcineurin 1
RFC3	replication factor C (activator 1) 3
RFC5	replication factor C (activator 1) 5
RNase	ribonuclease
ROCK	rho-associated protein kinase 1
ROI	regions of interest
ROMO1	reactive oxygen species modulator 1
ROS	intracellular reactive oxygen species

RSL1D1	ribosomal L1 domain containing 1
RT	room temperature
RUNX2	runt-related transcription factor 2
SB	sodium borate
SCARA3	scavenger receptor class A, member 3
SERPINB2	serpin peptidase inhibitor, clade B (ovalbumin), member 2
SERPINE1	serpin peptidase inhibitor, clade E (plasminogen activator inhibitor type 1)
SHMT2	serine hydroxymethyltransferase 2 (mitochondrial)
SMA	smooth muscle actin
SMAD2	SMAD family member 2
SMOC1	SPARC related modular calcium binding 1
SON	SON DNA binding protein
SOX17	SRY (sex determining region Y)-box 17
SOX2	SRY (sex determining region Y)-box 2
SRXN1	sulfiredoxin 1 homolog
SSC	side scatter
SSEA-1	stage-specific antigene 1
SSEA-4	stage-specific antigene 4
SV40LT	SV40 large T antigen (Simian Vacuolating Virus 40 TAg)
Taq	taq polymerase, thermostable DNA polymerase
TBE	Tris/Borate/EDTA
TBX2	T-box 2
TBX3	T-box 3
TCA cycle	tricarboxylic acid cycle
TDG	thymine DNA glycosylase
TEMED	tetramethylethylenediamine
TERT	telomerase reverse transcriptase
TGF-β	transforming growth factor, beta 1
THBS1	thrombospondin 1
THY1	Thy-1 cell surface antigen
TLR3	toll-like receptor 3
TOR	target of Rapamycin
TRA-1-60	tumour related antigen -1-60
TRA-1-81	tumour related antigen -1-81
tRNA	transfer RNA
TSPO	translocator protein
TUJ1	βIII-tubulin

TWIST1	twist homolog 1 (Drosophila)
UV light	ultraviolet light
VASH1	vasohibin 1
VIM	vimentin
VNTR	variable numbers of tandem repeats
VPA	valproic acid
WNT:	wingless-type MMTV integration site family member protein
ZNF277	zinc finger protein 277
γH2AX	histone H2AX phosphorylated at Serin 139

Semantics

%	per cent
°C	degree Celcius
x g	times gravity
µg	microgram
µl	microlitre
µM	micromolar
cm	centimetre
cm^2	square centimetre
g	gram
h	hour
M	molar concentration, 1 mol per litre
mg	milligram
min	minute
ml	millilitre
mm	millimetre
mM	millimolar
N	equivalent concentration
ng	nanogram
nM	nanomolar
rpm	revolutions per minute
s	second
U	enzyme unit

Abstract

Ageing-related limits in the propagation and the application possibilities of primary human bone marrow-derived mesenchymal stem cells (hMSCs) can be circumvented by generating induced pluripotent stem cells (iPS cells) from them. iPS cells are able to self-renew without senescence and have potential as clinically relevant source of hMSC-like cells (iMSCs). Recent evidence suggests that donor cell type specific gene expression is retained in iPS cells, whereas ageing-related processes are most likely reverted to a younger state during pluripotency induction. Moreover, ambiguous results have been reported addressing the retention of ageing processes in iMSCs and other iPS derivatives. Therefore, the extent of the retention of ageing hallmarks in iPS cells and iMSCs from aged hMSCs needs more detailed clarification. To shed light on these aspects, ageing-related features and gene expression patterns were comparatively characterised in hMSCs of fetal femur isolated 53 days post-conception and in hMSCs of donors of 60-74 years before and after pluripotency induction and redifferentiation to iMSCs. Comparative viral and non-viral reprogramming of hMSCs with different age background suggested an age-related decline in reprogramming efficiency. iPS cells could be derived from fetal hMSCs with viral and non-viral methods and from an aged donor with non-viral methods with addition of vitamin c. iMSCs were derived from iPS cells of fetal and aged background. Cell type identity and according functionality could be confirmed in primary hMSCs, corresponding iPS cells and iMSCs irrespective of age. Further, comparison of ageing features and related gene expression patterns indicated age-related differences in senescence and oxidative stress-related processes in primary hMSCs. Upon pluripotency induction, these ageing-related differences were not detectable and most likely reverted to a more immature state. Moreover, the presence of oxidative DNA damage, response to oxidative stress was decreased in both age groups. Moreover, processes related to energy metabolism and glutathione metabolism were changed irrespective of age. Despite this, ageing-related processes seemed to be re-introduced in iMSCs. In particular, gene expression signatures annotated to senescence, oxidative stress response, ageing, insulin signalling, oxidative phosphorylation, glycolysis and cytoskeleton suggested reflection of donor age in iMSCs. However, glutathione metabolism and DNA damage repair-associated gene expression indicated a reversion to a more immature state. The results described herein suggest a reflection of donor age in iPS cells and iMSCs derived from hMSCs next to reversion of particular ageing aspects to a more fetal-like state in both cell types. Further exploration of these previously undescribed processes in hMSC-derived iPS cells and iMSCs will help to translate regenerative approaches of these cells tailored for elderly patients into clinical applications.

Zusammenfassung

Die Zellexpansion und Anwendbarkeit von primären humanen mesenchymalen Stammzellen (hMSCs) unterliegen Einschränkungen aufgrund ihrer Alterung. Durch Umwandlung in induziert pluripotente Stammzellen (iPS-Zellen) kann dies umgangen werden. iPS-Zellen besitzen die Fähigkeit der Selbsterneuerung ohne Seneszenz und haben Potential als Quelle von hMSC-ähnlichen Zellen (iMSCs). Aktuelle Studien zeigen den Erhalt von Zelltyp-spezifischen Genexpressionsmustern in iPS-Zellen, während molekularer Alterungsprozesse in einen verjüngten Zustand versetzt werden. Ob Alterungsmerkmale in iMSCs und iPS-Zellen aus hMSCs erhalten bleiben, ist nicht ausreichend bekannt. Eine Aufklärung dieser Aspekte in iPS-Zellen und iMSCs aus hMSCs älterer Spender ist daher für eine sichere Anwendung notwendig. Diesbezüglich vergleicht diese Arbeit Alterungsmerkmale in hMSCs aus dem fetalen Oberschenkelknochen (Isolation 53 Tage nach Empfängnis) und in hMSCs älterer Spender (Isolation im Alter von 60-74 Jahren) vor und nach der Induktion von Pluripotenz und der Differenzierung zu iMSCs. Reprogrammierung von hMSCs unterschiedlichen Alters zu iPS-Zellen zeigte eine Verminderung der Reprogrammierungseffizienz. iPS-Zellen konnten aus fetalen hMSCs mittels viraler und nicht-viraler Methoden und aus hMSCs eines älteren Spenders nicht-viral hergestellt werden. Ebenfalls konnten iMSCs aus iPS-Zellen der verglichenen Altersgruppen hergestellt werden. Die Identität und Funktionalität primärer hMSCs und entsprechender iPS-Zellen und iMSCs konnte unabhängig vom Alter belegt werden. Eine vergleichende Analyse von Alterungsprozessen und Genexpressionsmustern deutete auf altersbedingte Unterschiede in der Seneszenz und oxidativen Stress in primären hMSCs hin. Nach der Induktion von Pluripotenz konnten diese Alterungsmerkmale nicht nachgewiesen werden. Zum Beispiel wurden der Energie- und Glutathion-Stoffwechsel unabhängig vom Spenderalter verändert. Im Gegensatz dazu wurden Alterungsmerkmale in iMSCs sehr wahrscheinlich wieder aktiviert. Insbesondere wurde das Spenderalter in den Expressionsmustern von solchen Genen widergespiegelt, die eine Rolle in der Seneszenz, der zellulären Antwort auf oxidativen Stress, der Alterung, im Insulin-Signalweg, der Oxidative Phosphorylierung, der Glykolyse, der Adhäsion und dem Zytoskelett spielen. Darüber hinaus deuteten Expressionsmuster von Genen des Glutathion-Stoffwechsels und der DNA-Reparatur einen potentiell verjüngten Zustand in iMSCs aus älteren Spendern an. Diese Studie zeigt, dass das Spenderalter sehr wahrscheinlich einen Einfluss auf Alterungsprozesse in aus hMSCs hergeleiteten iPS-Zellen und iMSCs hat. Daneben deuten die Ergebnisse eine Veränderung bestimmter Alterungsprozesse hin zu einem Zustand jüngeren Alters in beiden Zellarten an. Die weitere Erforschung dieser bisher nicht charakterisierten Prozesse wird helfen, eine auf das Spenderalter zugeschnittene medizinische Anwendung dieser Zellen zu ermöglichen.

1 Introduction

1.1 Implications of ageing in human bone marrow-derived mesenchymal stem cells for regenerative applications based on induced pluripotent stem cells

The following text will give a short overview of the inter-relation of the research fields converging in this study. This will be followed by a more detailed explanation of the state of the art in the fields themselves.

Ageing is defined as functional decline of cells, tissues and organs over the course of time leading to age-related diseases and death in all organisms. Ageing itself is a complex process, the molecular basis of which has been increasingly investigated in the last decades (de Magalhães 2014, López-Otín et al. 2013). One emerging research field, which constantly develops new cures for organ dysfunctions related to diseases of ageing, is the field of regenerative medicine (Mason and Dunnill 2008). Regenerative medicine is defined as research and therapies with the aim of regenerating or repairing organs, tissues and cells with reduced function due to diseases, ageing or injuries. The approaches of regenerative medicine comprise for example stem cell transplantation, tissue engineering and the use of cellular reprogramming (Mason and Dunnill 2008). One of the goals of research in regenerative medicine is to provide patient-tailored cell therapeutics for the cure of ageing-related diseases, such as cardiovascular or diseases of the nerve system (Bellin et al. 2012). One cell type with tremendous potential for curing age-related neurodegenerative diseases, diabetes and skeletal diseases, such as osteoarthritis or osteoporosis, are mesenchymal stem cells (González et al. 2009, Ito 2014, Jurewicz et al. 2010, Koç et al. 2000, Koga et al. 2008, Lee et al. 2006, Zappia et al. 2005, Jing Zhang et al. 2005). Mesenchymal stem cells were first isolated from the bone marrow (Friedenstein et al. 1974) and later from other sources such as adipose tissue, umbilical cord and dental pulp (Erices et al. 2000, Gronthos et al. 2000, Zuk et al. 2001). Moreover, MSCs were isolated from human fetal bone marrow and the multipotency and proliferative properties of these cells were demonstrated (Campagnoli et al. 2001, Mirmalek-Sani et al. 2006). In addition, MSCs are already analysed in various clinical trials and used as cell therapeutics in autologous and allogenic cell transplantation (Escacena et al. 2015). As MSCs will be applied in adult and aged patients rather than in young patients, it is important to understand the effect of donor age on hMSCs. Higher donor age leads to shorter *in vitro* life spans, enhances senescence in hMSCs (Stenderup et al. 2003) as well as a decrease in abundance of MSCs (M. Fan et al. 2010, Kasper et al. 2009, Katsara et al. 2011, Siegel et al. 2013). Moreover, ageing impairs the function and seems to cause changes in the differentiation potential of these cells (Kretlow et al. 2008, Siegel et al. 2013, Stolzing and Scutt 2006, Wagner et al. 2009, Ji Min Yu et al. 2011, Zhou et al. 2008). In addition, the *in vitro* expansion potential of MSCs is limited as MSCs undergo changes upon

long-term culture which eventually lead to functional decline and replicative senescence (Baker et al. 2015, Geißler et al. 2012, Wagner et al. 2009, Wagner et al. 2010). In addition to that, donor age has an effect on therapeutic efficacy of MSCs of aged background (Bajek et al. 2012, Golpanian et al. 2015, Khan et al. 2011). One very promising approach to overcome these limitations associated with applications of MSCs and MSCs of elderly donors in particular, is to reprogram them to induced pluripotent stem cells (iPSCs). iPSCs are pluripotent cells that can be differentiated in all cell types of the body, are able to self-renew and to be propagated in the undifferentiated state without the limitation of *in vitro* senescence, which makes them very similar to human embryonic stem cells (hESCs) (Takahashi et al. 2007, Takahashi and Yamanaka 2006, Yu et al. 2007). Since the discovery of induced pluripotent stem cells, the number of protocols to directly differentiate these cells into lineages of all three germ layers has grown exponentially. Thus, in the future it is very likely that cells of all lineages can be generated with a low variability and at large scale without limitations associated with the use of primary somatic cells. In addition, iPS cells have been generated from mesenchymal stem cells (Frobel et al. 2014, Megges et al. 2015, Nasu et al. 2013, Ohnishi et al. 2012, Park et al. 2008a, Shao et al. 2013, Yulin et al. 2012).

However, many aspects associated with the potential use of iPS technology to counteract shortfalls of primary hMSCs and hMSCs of aged background in particular need to be analysed in more detail. For example, the higher reprogramming efficiency of cells from fetal tissues has been demonstrated (Galende et al. 2010, Wolfrum et al. 2010). However, nothing is known about the susceptibility of fetal hMSCs from the bone marrow to pluripotency induction. Moreover, the process of reprogramming reverses aspects of ageing such as senescence and leads to a rejuvenated state (Boulting et al. 2011, Lapasset et al. 2011, Miller et al. 2013, Ohmine et al. 2012, Prigione et al. 2011a, Yagi et al. 2012) and high age most likely impairs reprogramming efficiency (Cheng et al. 2011, Kim et al. 2010, Li et al. 2009, Soria-Valles et al. 2015). However, iPSCs most likely retain a functional memory of their somatic origin, which has potential implications for cures of skeletal diseases and injuries in hMSC-iPSCs (Kim et al. 2010, Kim et al. 2011, Ohi et al. 2011, Polo et al. 2010, Rizzi et al. 2012, Thomas et al. 2015). This makes iPS cells a potential tool to model complex gene regulatory networks of diseases and to conduct patient-tailored drug testing (Bellin et al. 2012). Yet, the extent to which hMSCs as somatic origin and their age is reflected in the features of the respective iPS cells and how it affects pluripotency induction is not clear as both aspects are still a matter of debate (Ishiy et al. 2015, Nasu et al. 2013, Nejadnik et al. 2015, Rohani et al. 2014, Shao et al. 2013). As iPSCs can give rise to tumours (Masuda et al. 2015), it might be safer to generate progenitor cells from iPS cells and apply these in regenerative approaches. A cell type of great interest for applications of regenerative medicine of the skeletal system are mesenchymal stem cell-like cells derived from iPS cells and hESCs (iMSCs). The derivation and characterisation of iMSCs has been demonstrated by various groups (Frobel et al. 2014, Hong et al. 2015, Ishiy et al. 2015, Kimbrel et al. 2014, Raynaud et al. 2013, Wang et al. 2014). In addition, the regenerative functionality of iMSCs has

been demonstrated in animal disease models including ageing-related diseases (Hong et al. 2014, Kimbrel et al. 2014, Nejadnik et al. 2015, Wang et al. 2014). These studies demonstrate the potential of iMSCs for circumventing shortcomings associated with primary MSCs of aged individuals such as fast *in vitro* senescence and functional decline. However, it is not well understood whether organismal age has an effect on the features of cells re-differentiated from iPSCs as demonstrated by studies in fibroblasts (Lapasset et al. 2011, Miller et al. 2013, Prigione and Adjaye 2010, Suhr et al. 2010, Wen et al. 2013). Likewise, the reflection of ageing in iMSCs is still debated (Frobel et al. 2014, Zhang et al. 2011). In particular, whether organismal age is reflected in the functionality and transcriptome of iMSCs derived from fetal hMSCs or from hMSCs with aged background is not clear and has to be determined further before the tremendous potential of these cells can be translated into therapeutic applications.

1.2 Aspects of ageing and their presence in hMSCs

Ageing has been defined as an inevitable complex process, taking place throughout life, which leads to decline of organ, tissue and cellular functionality, eventually resulting in disease and death determining the lifespan of an organism (Studer et al. 2015). The molecular events taking place in ageing have been concluded to involve senescence, stability of the genome, the shortening of telomeres, epigenetic changes, decline of mitochondrial function and oxidative stress, impaired stem cell function, deregulated nutrient sensing and changes in cellular communication and dysfunctional proteostasis. There is no consensus on the exact processes taking place during ageing, yet (López-Otín et al. 2013). Furthermore, there are several theories of ageing. In the DNA damage theory of ageing accumulation of DNA damage by telomere shortening or mutation as well as oxidative damage causes age-related functional decline (Aubert and Lansdorp 2008, Moskalev et al. 2013). Moreover, recent evidence suggests that ageing is caused by changes of the interaction of stem cells with their microenvironment or niche (Reitinger et al. 2015). In contrast to that, the mitochondria free radical theory of ageing states that ageing is caused by reactive oxygen species (ROS) produced by mitochondrial dysfunction which react with DNA, proteins and lipids in the cells and damage them impairing cellular function and leading to oxidative stress and ageing of tissues (Liu et al. 2014). However, this theory is rejected by the metabolic stability theory of ageing, which states that the ability to maintain ROS levels determines the pace of ageing (Brink et al. 2009).

1.2.1 Cellular senescence

Cellular senescence was first described as in human fibroblasts as a state of non-reversible growth arrest after continuous passaging *in vitro* (Hayflick and Moorhead 1961). This effect was later attributed to be caused by telomere shortening (Bodnar et al. 1998). The number of senescent cells increases with ageing (Dimri et al. 1995). Furthermore, higher numbers of senescent cells have been found in aged mice (Wang et al. 2009) using DNA damage and senescence-associated β-galactosidase

(SABG) as markers (Dimri et al. 1995). Moreover, senescence can be triggered prematurely by transcription of the INK4/ARF locus or by DNA damage (Collado et al. 2007). Interestingly, the locus on the genome encoding P16INK4A and P19ARF, the INK4/ARF locus, was linked to the most ageing-associated diseases in a genome wide association study (Jeck et al. 2012). Furthermore, the number of senescent cells was described to be dependent on donor age in human (Zhou et al. 2008).
In MSCs, senescence was not altered by higher age in studies of the rat (Geißler et al. 2012). In contrast to that, MSCs have been reported to go into a senescent state during *in vitro* long-term culture (Baxter et al. 2004, Bork et al. 2010, Geissler et al. 2012, Wagner et al. 2009, Wagner et al. 2010).

1.2.2 DNA damage, DNA damage repair and stability of the genome

DNA damage in the form of somatic mutations accumulates throughout life and has been associated with ageing (Moskalev et al. 2013). Moreover, ageing is associated with elevated accumulation of chromosomal aberrations (Faggioli et al. 2012, Forsberg et al. 2012). The damage of the DNA can be caused by extrinsic factors, such as radiation or chemicals or by endogenous factors, such as replication errors or reactive oxygen species. The constantly occurring DNA lesions are repaired by processes that are able to repair most types of DNA damage (Lord and Ashworth 2012). Accordingly, defective DNA repair negatively influences lifespan (Gregg et al. 2012). Furthermore, apart from the damage of nuclear DNA, increased damage of mitochondrial DNA has been associated with ageing (Kazak et al. 2012). Moreover, DNA double-strand breaks (DSB) are some of the most consequential DNA lesions in genomic instability and can be caused by ROS generated by oxidative phosphorylation, by stalled replication forks or by radiation. The immediate response of the cell to the presence of DNA double-strand breaks is the phosphorylation of histone H2AX within minutes after the double-strand break. This leads to the generation of γH2AX foci at the adjacent sites to the DSB. Therefore, immunofluorescence labelling of γH2AX is used as indicator for the presence of DSB (Pilch et al. 2003, Rogakou et al. 1998). In addition to that, telomeres are gradually lost during cell division and in the course of ageing, as somatic cells do not express telomerase (Blasco 2007). Yet, whether ageing is caused by short telomeres or short telomeres are caused by the ageing process is still debated (Aubert and Lansdorp 2008).
Accumulation of DNA damage with ageing has been described in MSCs (Beauséjour 2007, Wagner et al. 2009). Moreover, genes involved in DNA damage repair were found to be down-regulated in MSCs of aged background (Hacia et al. 2008, Wagner et al. 2009, Wagner et al. 2008). Yet`, independent from age, MSCs were found to have a frequency of ~4% of chromosomal aberrations in a high throughput study analysing 144 MSC samples with 139 human MSC samples among them (Ben-David et al.). Moreover, whether MSCs develop chromosomal instabilities *in vitro* is not clear as there are studies reporting ambiguous results of chromosomal analyses after long-term culture (Bernardo et al. 2007, Røsland et al. 2009, Takeuchi et al. 2009, Zhang et al. 2007).

1.2.3 Mitochondrial dysfunction, reactive oxygen species and oxidative stress

The role of reactive oxygen species (ROS) was first described in the mitochondrial free radical theory of ageing which states that ageing-related decline in mitochondrial function causes increased levels of reactive oxygen species that in turn further enhance mitochondrial dysfunction (Harman 1965). The functionality of the respiratory chain declines with age, leading to electron leakage, which in turn leads to the development of ROS (Green et al. 2011). This results in the development of free radicals or reactive oxygen species, which are molecules with an unpaired electron. This molecule category consists of hydrogen peroxide, superoxide anions and hydroxyl radicals (Poyton et al. 2009). Elevated levels of ROS lead to oxidative stress, which is defined as an imbalance of ROS production and antioxidants (Reuter et al. 2010). Reactive oxygen species can react with lipids, proteins and DNA and damage them (Reuter et al. 2010). The reaction of reactive oxygen species with DNA can cause a variety of damages. 8-hydroxy-2' -deoxyguanosine (8-OHdG) or 8-oxo-7,8-dihydro-2'-deoxyguanosine (8-oxodG) is one of the most predominant forms of oxidative DNA damage (Jacob et al. 2013). Therefore, 8-OHdG is one of the most widely used biomarkers of oxidative stress-induced DNA damage (Valavanidis et al. 2009).

In MSCs elevated ROS levels were detected upon long-term culture independent of age (Geissler et al. 2012). There are studies supporting the notion that elevated levels of ROS in MSCs might, in addition to cell intrinsic mitochondrial dysfunction, be effected by age-related changes of paracrine factors or extracellular matrix compositions (Geissler et al. 2013, Sun et al. 2011). Moreover, it has been shown that high oxygen levels, and therefore higher intracellular ROS, causes genomic instability in MSCs, which can be prevented by culturing them under hypoxic conditions (Estrada et al. 2012, Holzwarth et al. 2010, Li and Marbán 2010, Tsai et al. 2011). Likewise, culture of MSCs in the presence of antioxidants was shown to reduce DNA damage in them (Alves et al. 2013).

1.2.4 The metabolic instability theory of ageing

The free radical theory of ageing has been rejected by a study corroborating the metabolic stability-longevity principle. This principle describes the lifespan of organisms to be determined by the homeostasis of ROS (Brink et al. 2009). The principle is based on a mathematical model of metabolic stability, which described ROS and other metabolites to be maintained by dissipative and stabilizing regulatory networks (Demetrius 2004). Brink et al. confirmed the principle through detection of changes in pathways associated with ageing that were predicted by this model (Brink et al. 2009).

More specifically, Brink et al. described the age-related deregulation of glutathione metabolism, insulin signalling and oxidative phosphorylation in mice. (i) Glutathione metabolism is involved in the maintenance of ROS levels in the cell. The age-related up-regulation of the glutathione metabolism associated genes *Gclm*, *Gpx1*, *Gpx3*, *Gsta2* and *Gstm2* was detected in aged mouse hearts in the study

by Brink et al. (Brink et al. 2009). (ii) *Foxo1* is a gene, which regulates the expression of genes involved in glycolysis and insulin signalling. Moreover, *Foxo1* is involved in ageing (Curran and Ruvkun 2007). The age-related down regulation of *Foxo1* was found by Brink et al.. Other insulin signalling-associated genes which were found to be differentially expressed in the tissue of aged mice were *Map2k1*, *Pdpk1*, *Pfkl* and *Rapgef1* (Brink et al. 2009). (iii) The process of oxidative phosphorylation produces ATP by nutrient oxidation. Genes involved in oxidative phosphorylation such as *Atp5a1*, *Atp5f1*, *Cox7a2*, *Cox7b* were deregulated in the heart of aged mice in the study of Brink et al. (Brink et al. 2009).

Moreover, Brink et al. proposed a model of a gene regulatory network in the aged mouse heart in which insulin signalling and glutathione metabolism are positively regulated and the tricarboxylic acid (TCA) cycle and oxidative phosphorylation are negatively regulated. In the regulatory network insulin signalling leads to enhanced TOR (target of Rapamycin) signalling reducing the expression levels of genes involved in TCA cycle, mitochondrial ribosomes and oxidative phosphorylation, thus reducing cell respiration (Shamji et al. 2000). Furthermore, glucose concentration is regulated by insulin, which is linked to TCA cycle by glycolysis and pyruvate, whereas the TCA cycle is linked to the respiratory chain via fumarate and succinate (Figure 1). In agreement with this model, recent studies suggest that catabolic signalling increases ageing, whereas decreased nutrient signalling extends lifespan (Fontana et al. 2010).

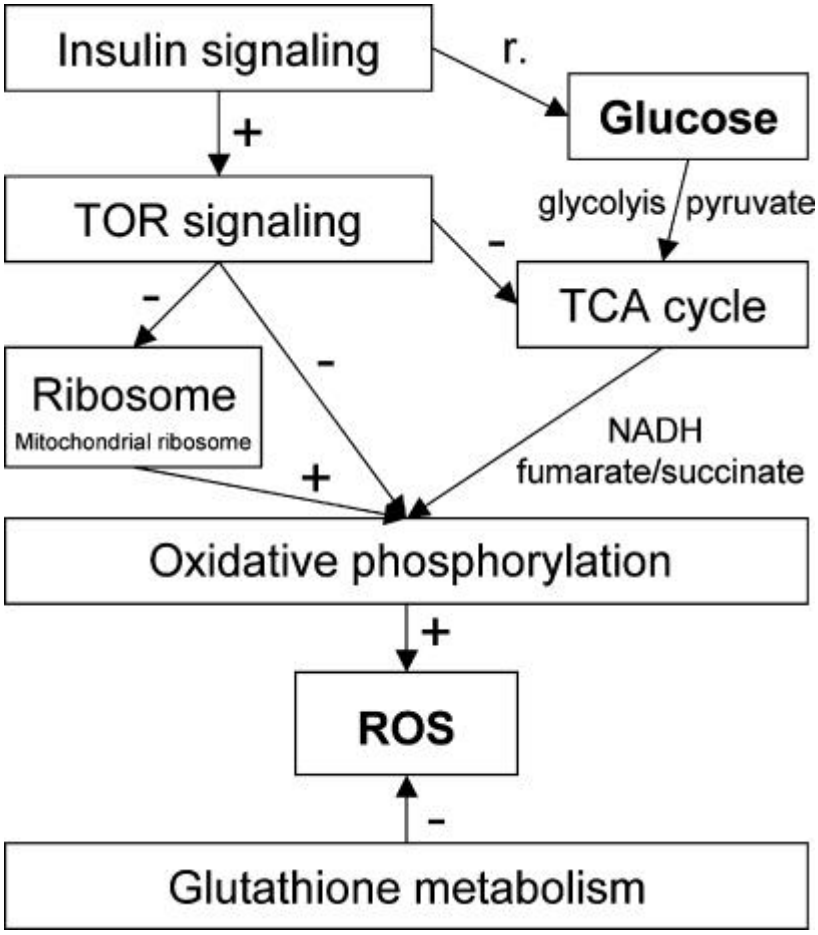

Figure 1 Model of the regulatory network based on the metabolic stability theory of ageing.
r.: regulation, -: down-regulation of genes, +: up-regulation of genes. TOR: target of Rapamycin, TCA cycle: tricarboxylic acid cycle, ROS: reactive oxygen species. Taken from (Brink et al. 2009)

Whether the network based on the metabolic stability theory of ageing is applicable to ageing of bone marrow-derived mesenchymal stem cells remains to be determined. However, there are studies describing age-related alterations in hMSCs in components of the network. For example, antioxidant capacity was altered in aged MSCs. Yet, antioxidative processes were down-regulated in MSCs upon long-term cultivation independent from age (Geißler et al. 2012). Furthermore, even exposure to serum of aged MSCs induced elevated ROS levels and underlined the systemic nature of ageing in MSCs and the importance of ROS homeostasis (Geissler et al. 2013, Shipounova et al. 2010). In addition, the role of TOR signalling in ageing of MSCs has been shown (Gharibi et al. 2014, Dayong Zhang et al. 2015). Likewise, genes associated with TOR signalling were found to be up-regulated in transcriptomes of MSCs of aged donors (Zhou et al. 2015).

1.2.5 Age-related changes of interaction with the stem cell niche

Stem cells reside in a tissue in a particular microenvironment called niche (Rando 2006). However, the niche has been found to be changed upon ageing and these changes in turn were shown to have an impact on stem cell function (Kurtz and Oh 2012, Pan et al. 2007). Yet, to which extent intrinsic changes of the interaction with the niche or changes of the niche itself cause the ageing-related changes is still debated (Rando 2006). One of the main components of the niche is the extracellular matrix (ECM), which plays an important role in tissue maintenance and regeneration (Bonnans et al. 2014). The effect of extracellular matrix composition on age-related changes has been demonstrated in fibroblasts as modulation of ECM could revert senescence in these cells (Choi et al. 2011). Moreover, systems biology-based approaches analysing ageing and metabolism-related genes provided evidence that genes involved in cell-cell and cell-matrix adhesion are associated with ageing and longevity (Wolfson et al. 2009).

Comparative analyses of the transcriptome revealed the up-regulation of genes involved in ECM-receptor interaction and focal adhesion in MSCs derived from osteoporosis patients (Zhou et al. 2015). Furthermore, ECM from fetal MSCs was shown to enhance proliferative properties of adult MSCs (Ng et al. 2014). Likewise, declining proliferation in aged MSCs could be restored by culture on ECM derived from fetal MSCs (Sun et al. 2011).

1.2.6 Age-related changes in the cytoskeleton

Changes in the cytoskeleton were shown to be associated with ageing (Baird et al. 2014, Liu et al. 2015). Moreover, ageing has been shown to lead to altered tissue biomechanics by senescence-associated changes of the cytoskeleton (Morgan et al. 2015). Furthermore, comparative meta analyses of *in vivo* aged tissue and *in vitro* cellular senescence revealed the de-regulation of genes involved in actin cytoskeleton-related functions in both processes (Voutetakis et al. 2015).

Ageing of hMSCs seems to be associated with changes in their cytoskeleton, as indicated by a study that compared young and aged MSCs of the rat (Kasper et al. 2009). A further study described the down-regulation of cytoskeleton-associated genes upon long-term cultivation in MSCs with a young and aged background (Geissler et al. 2012). Moreover, changes levels of cytoskeleton-associated proteins were found in hMSCs cultivated for higher passage numbers (Madeira et al. 2012).

1.2.7 Further aspects of ageing

Apart from the above-described aspects of ageing, there are more processes, which are important and are subject of research. One such aspect is the involvement of proteostasis in ageing which is the process of protein folding and protein degradation. The impairment of proteostasis is associated with age-related diseases and lifespan could be enhanced by alterations of gene expression associated with proteostasis (Zhang and Cuervo 2008). A further aspect of ageing, which is discussed as one of the

main contributors of ageing are age-related epigenetic changes. Changes in global DNA methylation patterns, changes in modifications of histones as well as changes in the chromatin status, have been associated with ageing and diseases of accelerated ageing such as progeroid syndromes (Horvath 2013, Kanfi et al. 2012, Mostoslavsky et al. 2006). A recent study described changes in heterochromatin as one of the main drivers of ageing and of an accelerated ageing syndrome called Werner syndrome (Weiqi Zhang et al. 2015). However, these age-related features are not analysed in the comparative analysis of ageing aspects in pluripotency induction and redifferentiation of hMSCs in this work.

1.3 Mesenchymal stem cells

Mesenchymal stem cells, which are also termed mesenchymal stromal cells, were first described by Friedenstein as non-hematopoietic progenitor cells in the bone marrow that have a spindle-shaped morphology in monolayer culture (Friedenstein et al. 1974, Friedenstein et al. 1968). In addition, MSCs were isolated from different tissues such as umbilical cord, dental pulp and adipose tissue (Collart-Dutilleul et al. 2015, Crisan et al. 2009, da Silva Meirelles et al. 2006, Suzuki et al. 2015, Vangsness et al. 2015). The clonogenic cells today known as MSCs were named colony forming unit fibroblasts (Friedenstein et al. 1974). *In vivo* MSCs represent 0.0001% of the nucleoted cells of the bone marrow and their number declines with age (Caplan 2009). The International Society for Cellular Therapy defined the minimal criteria of MSCs to be (i) plastic adherence, (ii) expression of the cell surface markers CD105 (endoglin), CD73 (ecto-5'-nucleotidase) and CD90 (THY1) and no expression of CD34, CD14, CD79α CD11b, CD45, HLA-DR as well as (iii) multipotency as progenitors of osteoblasts, adipocytes and chondrocytes (Dominici et al. 2006). MSCs are defined as stem cells as they are able to self-renew. Moreover, the multipotency of MSCs has first been described for MSCs derived from the bone marrow (Caplan 1991). However, their ability to trans-differentiate into ectodermal and endodermal lineages is still debated (Kopen et al. 1999, Pittenger et al. 1999) (Figure 2). Moreover, MSCs have immuno-modulatory properties and are involved in tissue regeneration (Baker et al. 2015). Yet, there is a debate about characteristics and lineage markers of MSCs (Calloni et al. 2013, Frenette et al. 2013, Lv et al. 2014). The reason for this is that MSC populations were described as heterogeneous population with different subpopulations of distinct immunophenotypes (Caplan 2005), whereas a different study described CD271 (low-affinity nerve growth factor receptor) positivity as marker for MSCs (Eghbali-Fatourechi et al. 2005). Furthermore, the extend of the changes of the features of MSCs upon *in vitro* cultivation compared to the *in vivo* features of these cells is not entirely clear yet (Bara et al. 2014). MSCs are at this point already applied as cellular therapeutic agents, they are part of numerous clinical trials, and there are many preclinical models of the use of MSCs in tissue repair. In addition, MSCs were shown to play a role in wound healing and were proven to enhance healing of injuries of the digestive system as well as of liver, of diabetic limb

ischemia, of burned skin, of injuries of the musculoskeletal system as well as lung and brain injuries (Wei et al. 2013).

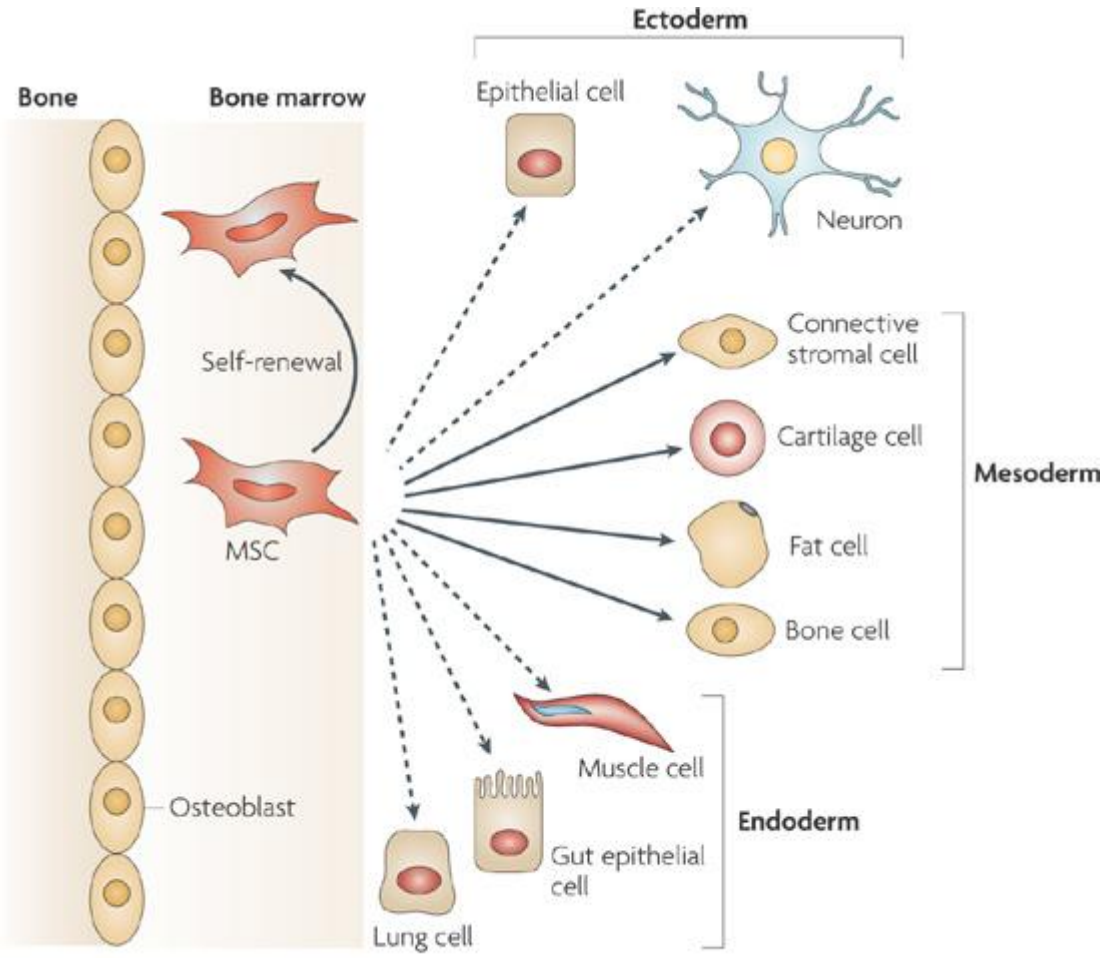

Figure 2 Characteristics and differentiation potential of bone marrow derived mesenchymal stem cells.

MSC: mesenchymal stem cell, dotted line: differentiation propensity of MSCs still debated. Taken from (Uccelli et al. 2008)

1.3.1 Fetal MSCs

The isolation of fetal MSCs from the bone marrow of first trimester foetuses was first described by Campagnoli et al. (Campagnoli et al. 2001). Frist trimester fetal MSCs have the same immunophenotype as adult bone marrow derived MSCs, proliferate faster than their adult counterparts and they have a fibroblast-like morphology, which does not change *in vitro* for at least 20 passages (Campagnoli et al. 2001, Campagnoli et al. 2002). Moreover, fetal MSCs go later into senescence, compared to their adult counterparts (Guillot et al. 2006). Apart from MSCs of aged donors, mesenchymal stem cells derived from fetal femur were used in this study. The isolation of these cells was described by Mirmalek-Sani and colleagues, who isolated these cells from the cartilage anlage of

femurs of foetuses with 8 weeks of age (Mirmalek-Sani et al. 2006). The cells used in this study were isolated with the same procedure. Fetal femur-derived MSCs were confirmed to be multipotent and were tested towards their osteogenic potential on different scaffold surfaces for tissue engineering (Kanczler et al. 2009, Mirmalek-Sani et al. 2009). Moreover, fetal hMSCs were used to model bone development *in vitro* as well as to study epigenetic changes during bone development (de Andrés et al. 2013, El-Serafi et al. 2011).

1.3.2 Ageing-associated shortfalls of MSCs

Despite their regenerative potential, there are shortfalls associated with ageing of MSCs that might represent roadblocks for their application (Diederichs and Tuan 2014). One aspect of ageing in this context is the age related decline of colony forming unit fibroblastoid cells (CFU-f) in MSC populations of the bone marrow. However, this feature is still a matter of debate (Ming Fan et al. 2010, Kasper et al. 2009, Katsara et al. 2011, Sethe et al. 2006). There are studies describing increased senescence *in vivo* in MSCs as primary cause of this (Geißler et al. 2012, Kasper et al. 2009). Moreover, ageing has been reported to lead to decreased proliferation rates (Sethe et al. 2006). Yet, the effect of organismal ageing on the proliferation rate of MSCs is still unclear (Ming Fan et al. 2010, Geißler et al. 2012, Katsara et al. 2011, Kretlow et al. 2008, Sun et al. 2011, Ji Min Yu et al. 2011). In addition, age-related changes of the differentiation capacity of MSCs were reported (Sethe et al. 2006). Moreover, aged MSCs demonstrated an ageing-related decline in regenerative potential (Bustos et al. 2014, Ming Fan et al. 2010, Kang et al. 2012, Yao et al. 2012, Hao Zhang et al. 2005). Moreover, MSCs have to be propagated *ex vivo* before application. However, the potential effects of *in vitro* culture are not understood in detail, yet (Baker et al. 2015). Upon long-term culture, MSCs lost their differentiation potential and showed changes in their immunophenotype as well as increased cell size (Wagner et al. 2010). The causes of these changes were described to be related to decline in self-renewal and increased differentiation and accumulation of mutations and DNA damage due to telomere loss eventually leading to decreased proliferation and increased senescence (Bork et al. 2010, Wagner et al. 2009, Wagner et al. 2010).

The limits of the application potential of MSCs by age-related decline in functionality and *in vitro* senescence could be solved by reprogramming MSCs to induced pluripotent stem cells.

1.4 Pluripotent stem cells

1.4.1 Human embryonic stem cells

Isolation of pluripotent self-renewing stem cells from inner cell mass of mammals was first described by Evans and Kaufman (Evans and Kaufman 1981). Similarly, human embryonic stem cells are cells derived from the inner cell mass of the blastocyst stage of *in vitro* fertilised embryos, which was described for the first time in humans by Thomson and colleagues (Thomson et al. 1998). These cells

are pluripotent as they have the potential to give rise to lineages of all three germ layers, which are formed during gastrulation, namely ectoderm, endoderm and mesoderm. In addition, hESCs express pluripotency markers such as OCT4, NANOG, SOX2, SSEA-4 or TRA-1-60 (Chan et al. 2011, Thomson et al. 1998). The morphology of human embryonic stem cells is characterised by their small size. In addition, hESCs grow in colonies, which are flat and have sharp edges and the cells have a high nucleus to cytoplasm ratio. Furthermore, embryonic stem cells can be cultured for long periods without differentiation and without showing signs of senescence. Moreover, hESCs form teratomas when injected into mice, which are immune-compromised. In addition, hESCs express telomerase, enabling self-renewal without senescence. Furthermore, hESCs are epithelial cells expressing cell-cell adhesion molecules such as desmosomes, tight junctions and adherence junctions, which leads to low survival rates of single cells (Thomson et al. 1998).

1.4.1.1 Applications of human embryonic stem cells

Due to theoretically limitless propagation potential without senescence and pluripotent differentiation propensity, hESCs are a potential unlimited source of cells types that are difficult to isolate or to study. These features raised the hopes for applications of these cells in toxicity testing and drug discovery (Daley 2014, Jensen et al. 2009). However, applications involving human embryonic stem cells are associated with ethical concerns. It is still debated whether research on human embryonic stem cells is still needed as they can be replaced by induced pluripotent stem cells, which have very similar properties (Hug and Hermerén 2011).

1.4.1.2 Regulation of the pluripotent state

The pluripotent state of hESCs is controlled by a regulatory network consisting of transcription factors, micro RNAs and chromatin modifying enzymes as well as regulatory signalling pathways (Jaenisch and Young 2008). Within this regulatory network, the transcription factors OCT4, SOX2 and NANOG were shown to play key roles in maintaining pluripotency in mammalian stem cells (Avilion et al. 2003, Babaie et al. 2007, Chambers et al. 2003, Hart et al. 2004, Hay et al. 2004, Jaenisch and Young 2008, Jung et al. 2010, Matin et al. 2004, Nichols et al. 1998). These three transcription factors repress or activate genes, which are part of processes taking place during differentiation, eventually leading to maintenance of the pluripotent state. The role of OCT4, SOX2 and NANOG in the complex regulatory network of pluripotency was first described by Boyer et al. (Boyer et al. 2005). Moreover, pluripotency is maintained in hESCs and iPSCs through extracellular signalling molecules resulting in repression of genes associated with differentiation and development and activating transcriptional programs associated with pluripotency. Among these extracellular factors, basic fibroblast growth factor (bFGF or FGF2) plays one of the most important roles. FGF2 is an essential additive to hESC and iPS cell media for *in vitro* culture of these cells in order to maintain

pluripotency (Amit et al. 2000, Greber et al. 2007, Thomson et al. 1998). Furthermore, the transforming growth factor β (TGF-β)/Nodal/Activin A signalling pathway was shown to play a key role in pluripotency maintenance (Greber et al. 2007, James et al. 2005, Vallier et al. 2005, Vallier et al. 2009). Likewise, the WNT signalling pathway was described to play an important role in pluripotency regulation (Davidson et al. 2012, Sato et al. 2004). Figure 3 shows the context between different signalling pathways in the maintenance of pluripotency and how the extracellular signals are transduced to activate the pluripotency core transcription factors in hESCs and iPSCs. Due to the role of FGF2 in pluripotency maintenance in hESCs and iPS cells, mouse embryonic fibroblasts (MEFs) are used as feeder cells for co-culture. The reason for this is that MEFs provide the right surface and secrete signalling molecules for the maintenance of the pluripotency upon stimulation with FGF2 (Greber et al. 2007)

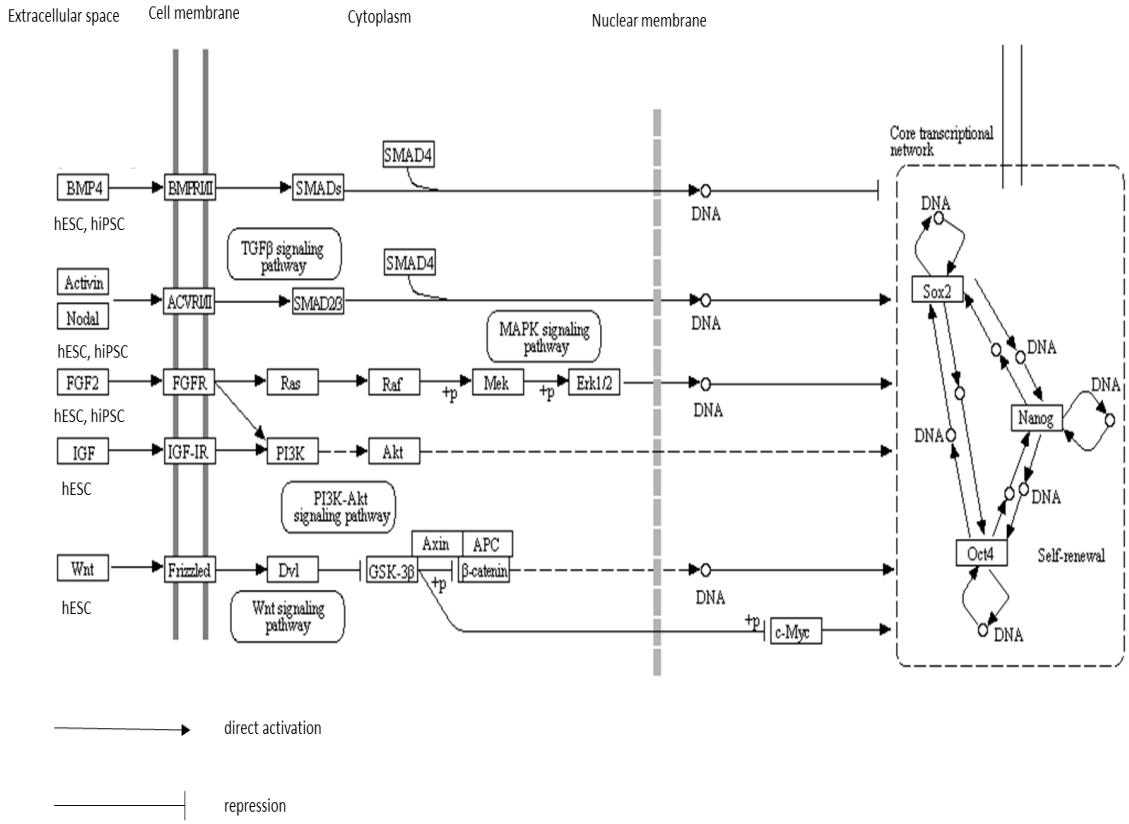

Figure 3 Interplay of signal transduction pathways in maintenance of self-renewal and the pluripotent state in human pluripotent stem cells.

Differentiation inducing signalling molecules such as BMP4 interact with the BMP receptor (BMPR//II) and activate SMAD1/5/8 which, via SMAD4, activates differentiation-associated gene expression. During pluripotency maintenance, the interaction between BMPs and the receptor is hindered by the receptor antagonists CER1 (Cerberus protein) and GREM1 (Gremlin 1 protein) which are secreted upon FGF stimulation. (not shown) Activin A and Nodal interaction with the TGFβ receptor (ACVR I/II) activate SMAD 2/3 and lead to gene expression

involved in pluripotency maintenance. FGF2 interacts with the FGF2 receptor (FGFR) and activates the MAP kinase signalling cascade as well as downstream signalling involving PI3K and AKT, which in turn is activated by insulin-like growth factor 1 (IGF-1) signalling. These processes result in the maintenance of gene expression networks controlling pluripotency. WNT signalling is leading to differentiation. However, the inhibition of GSK3β, which is part of the WNT signalling pathway enhances pluripotency induction. Finally, all these pathways converge leading to a self-regulatory network involving OCT4, SOX2 and NANOG as key components.
BMP 4: Bone Morphogentic Protein 4; BMPRI/II: BMP receptorI/II; SMADs: SMAD 1/5/8; ACVR I/II: TGF-β receptor; FGF2: basic fibroblast growth factor; FGFR: basic fibroblast growth factor receptor; Ras: Rat sacoma protein; Raf: Rat fibrosarcoma protein; ERK1/2: Extracellular signal regulated kinase1/2; IGF-1: Insulin-like growth factor 1; IGFR: Insulin-like growth factor receptor; PI3K: Phosphatidylinositol-4,5-bisphosphate 3-kinase; AKT: AKT kinase; WNT: wingless-type MMTV integration site family, member protein; Frizzled: WNT receptor; DVL: segment polarity protein dishevelled; GSK-3 β: Glycogene synthase kinase 3 β; APC: adenomatosis polyposis coli protein. Taken from Kyoto Encyclopedia of Genes and Genomes (Kanehisa and Goto 2000, Kanehisa et al. 2014), http://www.genome.jp/kegg-bin/show_pathway?map04550 (03.09.2015), KEGG-map signalling pathways regulating pluripotency of stem cells.

1.4.2 Induced pluripotent stem cells

The background of discoveries in the field of embryonic stem cells led to the establishment of a protocol for the induction of pluripotency in fibroblasts of the mouse in 2006 by Takahashi and Yamanaka (Takahashi and Yamanaka 2006). In the following year the induction of pluripotency in human fibroblasts was reported by Takahashi et al. by using retroviral overexpression of the transcription factors OCT4 (octamer-binding transcription factor 4), SOX2 (sex determining region Y box 2), KLF4 (Krueppel-like factor 4) and c-MYC (v-Myc myelocytomatosis avian viral oncogene homolog) (Takahashi et al. 2007). Yu et al., using ectopic expression of OCT4, SOX2, NANOG and LIN28, reported the same (Yu et al. 2007). Both studies described the reprogramming of human fibroblasts by means of ectopic expression of transcription factors to iPS cells which are able to self-renew without senescence and which are pluripotent as they can give rise to lineages of all three germ layers (Takahashi et al. 2007, Yu et al. 2007). In addition, iPSCs are very similar to hESCs in terms of expression of pluripotency-related genes and the ability to give rise to teratoma in mice. Moreover, it could be shown that mouse iPS cells could give rise to chimeras and germ line transmission in mice (Okita et al. 2007, Takahashi and Yamanaka 2006). One additional feature of hESCs and iPSCs is that they form spheres when cultured in low-attachment culture dishes. These spherical structures are

called embryoid bodies. One way to test the pluripotency of generated induced pluripotent stem cells *in vitro* is to seed embryoid bodies on a gelatine-coated surface in medium without FGF2 for random differentiation of the cells. This promotes the outgrowth of cells from the seeded embryoid bodies. This outgrowth is tested towards the presence of cells of mesodermal, endodermal and ectodermal lineages by analysis of the respective markers. Markers for mesodermal differentiation are brachiury and α smooth muscle actin. In addition, ectodermal markers are PAX6, Nestin and TUJ1 (β-III-Tubulin). Finally, endodermal marker proteins used in this pluripotency test are α fetoprotein (AFP) and SOX17 (Takahashi et al. 2007).

1.4.2.1 Applications of iPS cells

The development of iPS technology led to new directions of research. The tremendous potential of iPS cells in regenerative medicine became increasingly clear through several preclinical studies. The first study describing such an approach was the treatment of sickle cell anaemia with autologous iPS-derived cells in mice (Hanna et al. 2007). Further applications of iPS cells have been described for Parkinson's disease (Rakovic et al. 2015), spinal cord injury (Nori et al. 2011), macular degeneration (Singh et al. 2013)), muscular dystrophy (Filareto et al. 2013), ischemic stroke (Oki et al. 2012, Polentes et al. 2012) and limb ischemia (Suzuki et al. 2010). Moreover, the potential application of iPS technology for the regeneration of cartilage and bone has been demonstrated (Jin et al. 2013, Medvedev et al. 2010). A further field based on iPS technology is disease modelling and drug screening. The first studies describing such applications of iPS cells were published in 2008 (Dimos et al. 2008, Park et al. 2008a). When applied for disease modelling, iPS cells are generated from patients and in most studies used to recapitulate disease-related phenotypical changes in patient-derived iPS cells and their derivatives. Today there are numerous studies describing the modelling of diseases with this approach. For example, iPS-technology has been used to model Alzheimer´s disease (Hossini et al. 2015, Yagi et al. 2011), Parkinson´s disease (Imaizumi and Okano 2014) or cardiac diseases (Moretti et al. 2010).

1.4.2.2 The process of pluripotency induction

The process of induction of pluripotency in somatic cells is not known in detail. The comparative analysis of the transcriptome during reprogramming revealed that reprogramming most likely consists of several steps (Mah et al. 2011). In the first phase it has been shown that processes such as cell adhesion and cell contact are down-regulated, whereas genes involved in proliferation and DNA replication are up-regulated. The reprogramming factors used initiate the development of somatic cells to pre-iPS cells. Yet, only a small fraction of these become fully reprogrammed iPS cells (Polo et al. 2012). Moreover, it has been shown that the process of cellular reprogramming consists of a stochastic and a hierarchical phase (Buganim et al. 2012, Hanna et al. 2009, Smith et al. 2010). In addition,

epigenetic changes take place during reprogramming. These changes include expression of proteins regulating the chromatin status and chromatin dynamics (Apostolou and Hochedlinger 2013, Gładych et al. 2015, Watanabe et al. 2013).

1.4.2.3 Methods for iPS derivation

The first reports of iPS generation were using retroviruses or lentiviruses, which randomly integrate into the genome and could cause insertional mutagenesis with negative effects (Aasen et al. 2008, Aoi et al. 2008, Judson et al. 2009, Jeong Beom Kim et al. 2009, Kim et al. 2008, Takahashi et al. 2007, Yu et al. 2007). To circumvent these problems, various approaches resulting in integration free pluripotency induction were developed since 2006. Among these methods for delivery of reprogramming factors are episomal plasmid-based methods (Yu et al. 2009), viral plasmid-based methods (Okita et al. 2011, Okita et al. 2008), methods based on synthesised RNA (Warren et al. 2010), on proteins (Dohoon Kim et al. 2009), on Sendai virus (Ban et al. 2011, Fusaki et al. 2009, Ono et al. 2012) and on adenovirus (Stadtfeld et al. 2008). Notably, a recent report described reprogramming of mouse embryonic fibroblasts using six small molecule compounds, namely VPA, CHIR99021, 616452, Tranylcypromine, Forskolin and DZNep. The same study confirmed the similarity between the chemically generated iPS cells and ESCs (Hou et al. 2013).

One of the most widely used non-integrating vector systems for reprogramming is the Epstein–Barr virus-derived oriP/EBNA1 episomal vector system. This method enables transgene expression during reprogramming. Subsequently, the vectors are lost after about 15 passages post isolation in the iPS cell lines (Hu and Slukvin 2013, Yu et al. 2009). The episomal plasmid system developed by Yu et al. was furthermore optimised using particular vector combinations and the addition of small molecule inhibitors (J. Yu et al. 2011). In addition, the reprogramming efficiency was reported to be lower than in retroviral reprogramming. Yet, compared to other reprogramming methods employing plasmids, one nucleofection of episomal plasmids is enough to induce pluripotency in somatic cells, even when more reprogramming factors are needed, such as SV40LT and LIN28 (Guokai Chen et al. 2011, Chou et al. 2011, Hu et al. 2011, Okita et al. 2011, Yu et al. 2011, Yu et al. 2009). There are no studies at this point that describe iPS generation by non-viral reprogramming methods for hMSCs of fetal or aged origin.

1.4.2.4 Chemical enhancement of reprogramming efficiency

Yu et al. have described a combination of chemical inhibitors that enhance reprogramming efficiency during iPS generation from fibroblasts based on episomal plasmids. This combination consisted of the TGF-β receptor I kinase inhibitor or ALK5 inhibitor A-83-01, the MEK inhibitor PD0325901, the GSK3β inhibitor CHIR99021, and the ROCK inhibitor HA-100 (J. Yu et al. 2011). In addition, the

combination of TGF-β receptor I kinase inhibition and MEK inhibition was previously described to increase the reprogramming efficiency of fibroblasts over 100-fold (Lin et al. 2009).

Modulation of ageing-associated pathways and features

Hypoxia and antioxidants

Pluripotent cells meet their higher need for energy through enhanced glycolysis, whereas energy in somatic cells is generated mainly through oxidative phosphorylation (Kondoh et al. 2007, Zhang et al. 2012). Consistently, it has been described that pluripotency induction can be enhanced by hypoxia in murine and human cells (Yoshida et al. 2009). In a following study, it has been shown that pluripotency induction could be enhanced by blocking oxidative phosphorylation (Zhu et al. 2010). The addition of antioxidants was reported to enhance iPS quality in terms of the stability of the genome. One antioxidant that was used in this context is N-acetyl-cysteine, which reduced the induction of reactive oxygen species and the associated instability of the genome during reprogramming (Luo et al. 2014).

Vitamin c

Addition of vitamin c increased the efficiency of pluripotency induction in human skin fibroblasts and stromal cells derived from the adipose tissue during retroviral reprogramming with OCT4, SOX2, KLF4 and c-MYC (Esteban et al. 2010). In addition, vitamin c was described to enhance the quality of iPS cells during reprogramming. This is most probably due to the restoration of epigenetic features by vitamin c (Stadtfeld et al. 2012). Next to its function as antioxidant, vitamin c was found to most likely enhance reprogramming efficiency through its function as cofactor of enzymes involved in epigenetic gene regulation (Loenarz and Schofield 2008, Tao Wang et al. 2011). Moreover, pre-iPS cells could be converted into fully reprogrammed iPS cells using vitamin c most likely mediated through the histone demethylases KDM3/4 (Chen et al. 2013).

Inhibitors of epigenetic enzymes

The important role of chromatin remodelling during reprogramming enabling pluripotency induction through granting access to loci for the transcriptional activation of pluripotency-associated genes is still a matter of debate (Apostolou and Hochedlinger 2013). Yet, the inhibition of histone deacetylases which take part in chromatin remodeling by valproic acid (VPA), or sodium butyrate, enhanced reprogramming efficiency (Huangfu et al. 2008b, Luo et al. 2013, Mali et al. 2010). In addition, VPA was reported as a substitute of Klf4 and c-Myc (Huangfu et al. 2008a, Onder et al. 2012).

Inhibition of the IGF-1 (Insulin-like growth factor 1) pathway

The insulin and IGF-1 pathway which is associated with metabolism and ageing is a determinant of lifespan in worms and vertebrates and is involved in longevity in humans (Kenyon 2010, Suh et al. 2008). So far, it has been shown that inhibition of the IGF-1 receptor with the chemical compounds PQ401 or with LY294002 which inhibits PI3K, a downstream effector of the IGF-1 receptor, increased reprogramming efficiency in mouse fibroblasts (Taotao Chen et al. 2011).

Modulation of senescence-associated factors and P53

Cellular senescence has been described to occur during reprogramming and to interfere with the establishment of pluripotency by lowering the pace and efficiency of pluripotency induction (Zhao and Daley 2008). In addition, the absence of senescence-associated P16INK4A and P19ARF (Banito et al. 2009) and P53 or P21 enabled a more efficient generation of iPS cells (Hanna et al. 2009, Hong et al. 2009). Therefore, inhibition of P53 might be a possibility to enhance ageing-associated decline of reprogramming efficiency in hMSCs. A P53 inhibitor used in this study is pifithrin α (Komarov et al. 1999).

Modulation of the activity of the toll-like receptor

A recent study described that, apart from their function in delivering the reprogramming factors, retroviruses most likely contribute to pluripotency induction by activation of innate immunity in part through activation of the toll-like receptor 3 (TLR3). In the study, reprogramming efficiency was much lower when OCT4, SOX2, KLF4 and c-MYC were delivered as non-viral peptides. Moreover, the efficiency could be restored by additionally utilising polyinosinic:polycytidylic acid (Poly I:C) which is an antagonist of TLR3 and activates the innate immune response. Accordingly, knockdown of TLR3 reduced reprogramming efficiency when retroviral vehicles were used for delivery (Lee et al. 2012). Moreover, ageing has been described to lead to impairment of the function of toll-like receptors (Shaw et al. 2011). However, it is not known whether it is possible to enhance reprogramming efficiency of hMSCs derived from aged donors by means of activation of innate immunity through TLR3 activation.

1.4.3 Pluripotency induction in hMSCs

iPS cell generation from human bone marrow-derived MSCs was first described by Park et al. Conflicting with the notion that less mature cells such as mesenchymal stem cells may be reprogrammed faster than terminally differentiated cells, the study described that OCT4, SOX2, KLF4 and c-MYC did not suffice to induce pluripotency in hMSCs. The factors TERT (telomerase reverse transcriptase) and the viral gene SV40LT had to be used in addition to the classical combination of ectopic transcription factors OCT4, SOX2, KLF4 and c-MYC. However, compared to fibroblasts, the reprogramming efficiency was low (Park et al. 2008a). In a further report published few months later,

hMSCs from a patient were reprogrammed using retroviral transduction with only OCT4, SOX2, KLF4 and c-MYC without additional factors (Park et al. 2008b). In addition, human bone marrow-derived MSCs, which were stored as frozen stock could be reprogrammed to iPS cells. The reprogramming efficiency ranged from 0 to 0.0008% in three primary hMSC preparations that were reprogrammed (Ohnishi et al. 2012). Moreover, a recent study comparatively reprogrammed hMSCs and fibroblasts using retroviral overexpression of OCT4, SOX2, KLF4, c-MYC. The reprogramming efficiency was between 1.6 up to 10-fold lower in hMSCs compared to dermal fibroblasts (Nasu et al. 2013). In addition, a recent study described the iPS generation from bone marrow-derived hMSCs from a 48-year-old male donor using lentiviral reprogramming by means of OCT4, SOX2, KLF4 and c-MYC overexpression. The hMSC-iPS cells were successfully differentiated towards MSC-like cells (Diederichs and Tuan 2014). In addition to that, iPS cells could be generated from bone marrow-derived hMSCs by means of retroviral delivery of OCT4, SOX2, KLF4 and c-MYC in combination with P53 knock down by siRNA, supplementation with valproic acid and vitamin c (Yulin et al. 2012). So far, there are no reports describing iPS cell generation from hMSCs without viruses. Furthermore, there are no reports describing either viral or non-viral pluripotency induction in fetal hMSCs derived from the femur. Finally, it is not clear whether the pluripotency induction follows similar processes in fetal hMSCs and hMSCs of aged donors. Moreover, it is not clear how similar iPS cells derived from fetal hMSCs and hMSCs from aged donors are to hESCs and whether there are differences between iPS cells derived from fetal hMSCs and aged hMSCs according to their origin. Therefore, more research is needed to evaluate fetal hMSCs and aged hMSCs as potential cell sources for iPS generation. The possible age-related effects in hMSCs and the changes of age-related features through the reprogramming process need to be characterised in more detail before hMSCs can be used for iPS-based regenerative applications that exploit the likely higher potential of hMSC-iPSCs to give rise to mesenchymal cell lineages.

1.4.4 Somatic donor cell memory in iPS cells

iPS cells which were generated from murine fibroblasts, precursor cells of skeletal muscle, or granulocytes or B cells from the spleen displayed gene expression patterns related to their parental cell type (Polo et al. 2010). A further study found that residual DNA methylation patterns in iPS cells were similar to the patterns detected in their somatic origin and leading to preference of the differentiation into the lineage of the parental cell type. This memory of the somatic donor cell could be attributed to retention of donor-specific DNA methylation patterns (Kim et al. 2011). Moreover, it has been shown, that this somatic donor cell memory can be modulated by treatment with chromatin modifying molecules (Kim et al. 2010). Therefore, it is very likely that iPS cells generated from hMSCs will retain a memory of the donor cell and therefore tend to differentiate more efficiently into tissue developmentally related to hMSCs such as osteoblasts. However, a recent study comparing iPS cells

derived from fibroblasts and bone marrow-derived MSCs from the same donor reported a retention of epigenetic characteristic related to the somatic origin. However, no clear effect on the differentiation propensity could be shown when osteogenic and chondrogenic potential of the iPS cells of different background were tested (Nasu et al. 2013). Yet, it remains to be determined whether the effect of epigenetic memory on the differentiation propensity of iPS cells from bone marrow MSCs depends on the age of the donor.

1.5 The role of age related processes in reprogramming and occurrence pluripotent stem cells

1.5.1 Pluripotency induction in cells with aged background

There are few studies that addressed the effect of the age of the donor on the process of reprogramming. Initial studies in mice showed that increased donor age leads to a decline in the efficiency of reprogramming (Cheng et al. 2011, Kim et al. 2010, Li et al. 2009, Bo Wang et al. 2011). In addition, few studies compared the effect of age in the process of pluripotency induction in human cells. In contrast to the studies in mice, the first report addressing the effect of donor age on reprogramming efficiency in human cells could not find a correlation between age and efficiency of pluripotency induction. In this study, over 100 iPS cell lines were generated from fibroblasts of donors between 8-64 years of age. Independent from donor age, iPS cells were successfully generated from all cell preparations and the generated iPS cells could be differentiated into the endodermal lineage (Somers et al. 2010). Consistently, a further study could not detect a negative effect of high age on reprogramming efficiency and differentiation propensity of the generated iPS cell lines with different age background. In this study 16 iPS cell lines were generated from donor cells between 29 and 82 years of age. The iPS cells could be re-differentiated into functional motor neurons (Boulting et al. 2011). However, a decline in reprogramming efficiency of fibroblasts from a 78-year-old patient compared to fibroblasts of 47-year-old donor derived control was reported. In this study high age resulted in fewer fully reprogrammed colonies (Wen et al. 2013). In addition, Miller et al. reported the iPS generation from fibroblast populations from donors of three different age groups. Reprogrammed were young donors 11 years of age, from aged donors 82 years of age as well as fibroblasts from patients suffering from the premature ageing syndrome called Hutchinson-Gilford progeria syndrome (HGPS) with 14 years of age using OCT4, SOX2, KLF4 and c-MYC and Sendai virus-based reprogramming. The study showed that fibroblasts of all ages and the HGPS-fibroblasts could be reprogrammed to pluripotency. In addition, donor age and HGPS background had no impact on the karyotype of the iPS cells. Moreover, after reprogramming age-associated markers were absent in the generated iPS cells, irrespective of age background (Miller et al. 2013). In addition, a recent study on ageing and reprogramming efficiency utilised retroviral reprogramming or Sendai virus-based

reprogramming with the factors OCT4, SOX2, KLF4 and c-MYC to induce pluripotency in human newborn fibroblasts compared to fibroblasts derived from donors between 1 and 83 years of age. That study reported a decline of reprogramming efficiency with increasing donor age. In addition, the age related decline in reprogramming could be mimicked in younger cells when they were reprogrammed in high passages indicating similar effects between organismal ageing and *in vitro* senescence or ageing (Trokovic et al. 2015).

The generation of fully reprogrammed iPS cells from cells derived from aged human donors has been described in a number of studies (Lapasset et al. 2011, Ohmine et al. 2012, Prigione et al. 2011a, Suhr et al. 2009, Yagi et al. 2012). One of these studies described the pluripotency induction in human keratinocytes from donors of the ages 56-76 years using OCT4, SOX2, KLF4 and c-MYC. With a value of 0.0001%, the reprogramming efficiency was lower than initially described for adult fibroblasts (Takahashi et al. 2007). However, the pluripotency status of generated iPS cells did not vary with age (Ohmine et al. 2012). Notably, successful generation of iPS cells from fibroblasts, which were derived from centenarians, were described by two studies (Lapasset et al. 2011, Yagi et al. 2012).

These studies confirmed that ageing does not necessarily block reprogramming. However, in which way ageing interferes with the process of reprogramming, in particular in hMSCs, is not known. Likewise, until now, no study comparatively described the effect of ageing on reprogramming efficiency and the process of pluripotency induction in bone marrow-derived hMSCs from aged donors and hMSCs from fetal femur-derived MSCs. Such a study would help to elucidate details of ageing-related effects for the application of cellular reprogramming in hMSCs.

1.5.2 Senescence

Numerous studies in mice described that senescence could be one of the main reasons for an age-related decline of reprogramming efficiency (Banito et al. 2009, Hong et al. 2009, Kawamura et al. 2009, Li et al. 2009, Marión et al. 2009, Utikal et al. 2009, Zhao et al. 2008). As described above upon senescence, cells undergo a decline in proliferation resulting in a stop of the progression of the cell cycle (Campisi 2011, Kuilman et al. 2010). Therefore, senescence could interfere with reprogramming of aged cells as a change in proliferation is a crucial process involved in reprogramming (Hanna et al. 2009, Hanna et al. 2010). Moreover, reprogramming-induced senescence is likely to contribute to senescence-associated blocks of reprogramming in aged cell populations (Banito et al. 2009). More specifically, increased expression levels of the senescence-associated genes P16INK4 and P19ARF, encoded in the INK4A/ARF locus, which downregulates proliferation, was described to be associated with the negative effect of ageing on reprogramming efficiency. Consistently, silencing of the genes rescued reprogramming efficiency (Li et al. 2009). In addition, absence of senescence-associated genes P53 and P21CIP1 resulted in higher efficiencies of pluripotency induction (Kawamura et al.

2009, Li et al. 2009). Moreover, it has been described that cells from a 74-year-old donor could be reprogrammed after senescence had been induced *in vitro* through long-term culture. As re-differentiated fibroblasts of these iPS cells showed proliferation rates of younger fibroblasts and lower rates of senescence after long-term culture, a reversion of senescence into a rejuvenated state through reprogramming is likely. This indicates that cellular senescence can be circumvented and reverted by pluripotency induction (Lapasset et al. 2011). In a further study senescence was confirmed to contribute to decline of reprogramming efficiency in fibroblasts from aged donors as well as from senescent young and aged fibroblasts compared to fibroblasts derived from young donors (Trokovic et al. 2015).

1.5.3 Oxidative stress

As described above, two features likely causative of ageing are oxidative stress and the functional decline of mitochondria (Moiseeva et al. 2009, Passos et al. 2007). As pluripotent stem cells proliferate faster than somatic cells, they mainly rely on glycolysis-associated metabolism and less on oxidative phosphorylation. This difference in energy metabolism leads to lower production rates of reactive oxygen species, which are a by-product of oxidative phosphorylation and therefore a reduction of oxidative stress (Kondoh et al. 2007, Prigione et al. 2010). Likewise, in hESCs, mitochondria were reported to have a more effective DNA damage repair, less mass and a more anaerobic metabolism relying on glycolysis (Cho et al. 2006, Prigione et al. 2010, Saretzki et al. 2008, Suhr et al. 2010). Moreover, the expression of genes involved in oxidative stress and metabolism of mitochondria was changed through reprogramming in fibroblasts of centenarians. In addition, the features of mitochondria in iPSCs were found to be very similar to mitochondria in hESCs indicating a rejuvenation (Lapasset et al. 2011). Moreover, it has been shown that higher levels of anti-oxidative glutathione are present in pluripotent stem cells and promote enhanced protection from oxidative DNA damage further reducing oxidative stress (Dannenmann et al. 2015).

1.5.4 Genomic instability in pluripotent stem cells

It has been shown that damage of nuclear and mitochondrial DNA is enhanced with age (Garinis et al. 2008). In addition, the derivation of iPS cells from somatic cells of aged individuals led to iPSCs with chromosomal aberrations (Boulting et al. 2011, Prigione et al. 2011a). In addition to that, the development of genomic instabilities and chromosomal aberrations has been detected during reprogramming and in cultured iPS cells and ESCs (Gore et al. 2011, Hussein et al. 2011, Laurent et al. 2011, Mayshar et al. 2010). Moreover, mutations of mitochondrial DNA were detected in iPS cells (Prigione et al. 2011b). On the other hand, recent studies described iPS cells to be less sensitive to DNA damage than their somatic counterparts and derivatives (Dannenmann et al. 2015). The role of DNA damage response and DNA repair in reprogramming and in pluripotent cells has been confirmed by studies looking at enzymes such as ATM (Kinoshita et al. 2011, Lee et al. 2013, Nayler et al. 2012)

as well as the DNA repair processes homologous recombination (González et al. 2013, Soyombo et al. 2013) and non-homologous end joining (Molina-Estevez et al. 2013, Tilgner et al. 2013). Moreover, pluripotent stem cells showed a higher efficiency of repairing DNA damage than HeLa cells and fibroblasts (Maynard et al. 2008). Furthermore, a study described the up-regulation of genes involved in DNA repair and confirmed the presence of respective proteins in pluripotent cells compared to differentiated cells (Fan et al. 2011). However, whether DNA damage response and repair processes and genomic stability differ in iPS cells from hMSCs of aged donors and fetal hMSCs due to donor age-related difference remains to be clarified.

1.5.5 Remodelling of pathways associated with metabolic stability theory of ageing during pluripotency induction and in pluripotent cells

Mitochondrial energy metabolism

As described above in more detail, several studies reported the changes of the properties of mitochondria in the process of pluripotency induction, rendering their metabolism and morphology less mature and more similar to the mitochondria of hESCs (Lapasset et al. 2011, Ohmine et al. 2012, Prigione et al. 2010, Suhr et al. 2009). In addition, recent studies described that a metabolic switch is occurring during reprogramming as the energy metabolism is changed from aerobic respiration relying on oxidative phosphorylation to a more anaerobic energy metabolism relying on glycolysis (Prigione et al. 2010, Suhr et al. 2010). When the metabolic switch cannot take place, reprogramming to pluripotency is impaired (Kida et al. 2015). The occurrence of the changes in metabolism during reprogramming seems to be independent of the age of the parental cell as the same changes of mitochondrial properties were taking place when fetal fibroblasts as well as when fibroblasts of an 84 year old donor (Prigione et al. 2010) and fibroblasts of a centenarian were reprogrammed to pluripotency (Lapasset et al. 2011).

Insulin signalling

Moreover, insulin signalling has been reported to be necessary to maintain pluripotency in iPS cells and ESCs (Guokai Chen et al. 2011). In addition, Brink et al. found that age results in the differential regulation of insulin signalling associated genes in mice such as *Foxo1*, *Pdpk1* and *Pfkl* (Brink et al. 2009). From these genes 3-phosphoinositide-dependent protein kinase-1 (Pdpk1) is a key part of the signalling response triggered by ligand binding to the insulin receptor and activates numerous downstream signalling molecules (King and Newton 2004) Pdpk1 or PDK1 has been described to be necessary for pluripotency maintenance in embryonic stem cells (Ling et al. 2013). In addition, PDK1 is activated by PI3K, which has been shown to increase the efficiency of reprogramming (Taotao Chen

et al. 2011). Downstream of PDK1 is mTOR, which has been shown to regulate lifespan (Kapahi et al. 2010, Kapahi and Zid 2004). mTOR signalling very likely is involved in reprogramming as inhibition of mTOR was described to enhance reprogramming efficiency (Hanna et al. 2009, Hanna et al. 2010).

Glutathione metabolism

Ageing is dependent on the ability of the organism to maintain the levels of reactive oxygen species (Reinisalo et al. 2015). Guthatione (GSH) plays a key role in the maintenance of ROS levels by decreasing them. In addition, GSH is involved in decreasing ROS that were generated by UV light and ROS, which were generated in mitochondria through oxidative phosphorylation (Murakami 2006). The glutathione metabolism comprises biosynthesis of GSH, the detoxification of ROS by oxidation of GSH to the oxidised form and the catalysis of conjugation of toxic residues, e.g. from lipids which were peroxidised to GSH to detoxify them (Brink et al. 2009). Brink et al. have found an age-dependent regulation of genes involved in glutathione metabolism such as *Gclm, Gpx1, Gpx3, Gsta2* and *Gstm2* in the cardiac tissue of aged mice (Brink et al. 2009). Moreover, glutathione metabolism changes during pluripotency induction as described in a recent study. The same study reported higher levels of glutathione and of GPX2 (glutathione peroxidase 2) in iPS cells compared to fibroblasts. This enhanced protection from DNA damage as well as decreased oxidative stress in iPS cells (Dannenmann et al. 2015)

Although the remodelling of processes involve in ROS maintenance and metabolic stability during pluripotency induction were described, it is still unclear which impact the age has on these processes when human mesenchymal stem cells are reprogrammed to induced pluripotency.

1.5.6 Changes in the cytoskeleton and adhesion during reprogramming

The tension and the state of the cytoskeleton are associated with regulation of self-renewal and differentiation in pluripotent stem cells. This was reported to be mediated by rho-associated kinase, myosin II and E-cadherin, which control the self-renewal, differentiation and survival of pluripotent stem cells (James et al. 2005, Xu et al. 2005). During pluripotency induction, mesenchymal-to-epithelial transition (MET) was described to be an important step. In particular, mesenchymal transcription factors are down-regulated and epithelial markers such as E-cadherin are induced (Lamouille et al. 2014). The regulation of the remodelling of the cytoskeleton by novel kinases during MET in reprogramming has been described recently (Hu et al. 2014, Sakurai et al. 2014). Moreover, cytoskeleton-associated molecules are involved in the maintenance of pluripotency (Jiang et al. 2013). However, the impact of age-specific changes of the cytoskeleton in MSCs during pluripotency induction is not clear. Likewise, nothing is known about a potential effect of donor age of human MSCs on adhesion-associated processes during reprogramming. In addition, whether ageing leads to

particular patterns of gene expression of adhesion-associated genes in MSC-iPSCs remains to be elucidated.

1.6 Redifferentiation of pluripotent cells to mesenchymal stem cell-like cells (iMSCs)

1.6.1 Differentiation methods

Various publications described the derivation of mesenchymal stem cell-like cells from embryonic stem cells and from iPS cells (Barberi et al. 2005, Fukuta et al. 2014, Hwang et al. 2008, Lian et al. 2007, Liu et al. 2012, Luzzani et al. 2015, Olivier et al. 2006, Trivedi and Hematti 2007, Trivedi and Hematti 2008, Villa-Diaz et al. 2012). Moreover, Chen et al. reported a simple method to derive iMSCs from pluripotent cells, which is also used in this work. The study described that the application of the TGF-β receptor inhibitor SB-431542 to pluripotent stem cells and subsequent passaging of the cells by trypsinisation in different seeding densities resulted in the generation of iMSCs. The generated iMSCs met all criteria of mesenchymal stromal cells (Yen Shun Chen et al. 2012). The treatment of pluripotent stem cells with the inhibitor SB-431542 that blocks the phosphorylation of TGF-β receptors ALK4, ALK5, and ALK7 and therefore phosphorylation of SMAD2 resulted in a lower expression of pluripotency-associated genes and induced differentiation (Galvin et al. 2010).

1.6.2 Properties of iMSCs and similarity to primary MSCs

Most studies reported that the generated iMSCs showed the typical immunophenotype, which is defined by positivity for CD105, CD73 and CD90 and negativity for hematopoietic markers. Therefore, iMSCs met the minimal criteria for MSCs described by The International Society for Cellular Therapy (Dominici et al. 2006). However, different surface-marker expression patterns of iMSC were reported. ESC-derived iMSCs by Olivier et al. were CD73 and CD105 positive. Yet the cells also expressed SSEA4 (Olivier et al. 2006), which is a marker of pluripotency. In addition, iMSCs derived in the study of Hwang et al. did not express CD73 (Hwang et al. 2006). Furthermore, most studies demonstrated the potential iMSCs to differentiate into osteoblasts, adipocytes and chondrocytes as described by the International Society for Cellular Therapy (Dominici et al. 2006). Yet; lower efficiency of adipogenesis from iMSCs has been described by several studies using various protocols (Boyd et al. 2009, Yen Shun Chen et al. 2012, Diederichs and Tuan 2014, Frobel et al. 2014, Kang et al. 2015). In a further study, hMSCs were reprogrammed to iPS cells using lentiviral expression of OCT4, SOX2, KLF4 and c-MYC from one vector. In that study iMSCs were generated with four distinct derivation protocols and compared to their parental origin. The MSC-like surface marker profile was confirmed in the iMSCs. However, the generated iMSCs were reported to

differentiate less efficiently into osteoblast than into adipocytes and chondrocytes and to show distinct gene expression patterns compared to their parental primary hMSCs (Diederichs and Tuan 2014).

1.6.3 Application potential

It has been suggested that iMSCs represent a more standardised cell type which could be used for regenerative approaches and circumvent variability in primary MSCs (Diederichs and Tuan 2014). IN this respect, bone formation of iMSCs *in vivo* was described by several studies (Arpornmaeklong et al. 2010, Bilousova et al. 2011, Diederichs and Tuan 2014, Hu et al. 2010, Koyama et al. 2013, Kuhn et al. 2014, Mahmood et al. 2010). Furthermore, the potential in regeneration of cartilage defects could be confirmed (Nejadnik et al. 2015, Wang et al. 2014, Zhang et al. 2013). Additional applications of iMSCs were described in various studies (Xiao Chen et al. 2012, de Peppo et al. 2010, Deyle et al. 2012, Gruenloh et al. 2011, Hajizadeh-Saffar et al. 2015, Himeno et al. 2013, Hu et al. 2015, Kimbrel et al. 2014, Yang et al. 2014, Jieyuan Zhang et al. 2015).

1.6.4 Ageing-related properties in derivatives of iPS cells

As described above, ageing features are in part remodelled during reprogramming, and even higher age does not represent an unsurmountable roadblock in reprogramming. Despite this, it is not yet well understood whether the aspects of ageing are reintroduced upon differentiation of iPS cells from aged backgrounds compared to iPS cells with a younger background (Mahmoudi and Brunet 2012, Rohani et al. 2014). Concerning this, it was reported that mitochondria are reverted into a developmentally younger state, which is similar to ESCs during reprogramming. Yet, it is not clear to which extent the mitochondria return to their initial age and development-related phenotype (Armstrong et al. 2010). Yet, fibroblasts differentiated from iPS cells derived from an aged donor displayed rejuvenated mitochondrial properties indicating the maintenance of the rejuvenated state (Prigione and Adjaye 2010, Suhr et al. 2009). A further study reported a rejuvenation of the stress response in mitochondria in iPS-derived fibroblasts (Lapasset et al. 2011). In addition, metabolism and signalling processes associated with mitochondria were reset to a state similar to the parental cells upon redifferentiation of fibroblast iPS cells in a further study (Prigione et al. 2010). Furthermore, the premature senescence of fibroblasts derived from centenarians and the iPS generation from these cells were described. Notably, fibroblasts derived from the respective iPS cells did not show signs of premature senescence indicating a rejuvenation through pluripotency induction (Lapasset et al. 2011). However, several cell types differentiated from iPS cells were described to undergo early senescence compared to cells derived from ESCs (Feng et al. 2010). Yet, Gokoh et al. described differentiated cells from iPS cells, which did not show the same early senescence (Gokoh et al. 2011). The most extensive study on the changes of ageing-associated features during reprogramming and redifferentiation is the study by Miller et al.. In this study the change of ageing aspects such as DNA-damage response, γH2AX DNA damage foci, age-related increased ROS, epigenetic features, changes associated with the lamina of the nucleus,

number of senescent cells and length of telomeres were investigated in iPS cell derived from old donor fibroblasts and re-differentiated fibroblasts. All ageing aspects were reset to a younger state upon reprogramming and ageing-like features were not re-introduced when the iPS cells were re-differentiated into fibroblast-like cells indicting a permanent reset of the ageing processes (Miller et al. 2013). However, mesenchymal stem cells and vascular smooth muscle cells re-differentiated from iPS cells derived from patients suffering from an accelerated ageing syndrome called Hutchinson-Gilford progeria (HGPS) displayed again ageing features similar to the parental cells, which could not be detected in the pluripotent state (Liu et al. 2011, Zhang et al. 2011). On the other hand, reprogramming-induced rejuvenation interferes with modelling of the molecular pathology of late onset diseases of the nervous system (Srikanth and Young-Pearse 2014). These studies indicate that although in some cases ageing features are re-introduced upon redifferentiation, redifferentiation mostly results in a rejuvenated cell type. Whether this rejuvenation depends on the age of the donor in particular in hMSCs and respective iPS cells and iMSCs remains to be determined.

1.6.5 Transcriptional and epigenetic aspects of ageing in iMSCs

Although it has been reported that iMSCs fulfilled the minimal criteria of MSCs defined by the International Society for Cellular Therapy (Dominici et al. 2006), differences between hMSCs and iMSCs were reported in particular when the transcriptomes were compared to primary hMSCs (Barbet et al. 2011, Karlsson et al. 2009, Kopher et al. 2010, Lee et al. 2010). Concerning the similarity between the transcriptomes, a recent study compared the transcriptomes of primary MSCs and iMSCs derived from hESCs. The same study reported that the iMSCs showed gene expression related to an immature developmental state in between primary MSCs and the pluripotent stem cells they were derived from (Barbet et al. 2011). In addition, iMSCs generated from hMSC-derived iPS cells showed distinct gene expression patterns compared to their parental primary hMSCs (Diederichs and Tuan 2014). Moreover, the methylation of DNA has been described to have a role in ageing (Horvath 2013). A recent study described the successful generation of iMSCs from primary hMSCs of 56- to 73-year-old donors, which showed the required properties characterising MSCs in terms of immunophenotype and capacity to differentiate into osteoblasts and chondrocytes. Yet, the loss of age-related epigenetic features was described for iMSCs. However, the same study reported a high similarity between the transcriptomes of iMSCs and their corresponding primary MSCs although they were derived from aged patients (Frobel et al. 2014). In contrast to that, the presence of ageing-related features in MSCs derived from patients with Hutchinson Gilford Progeria has been reported (Zhang et al. 2011).

These studies show that knowledge about the effect of the somatic donor cell and donor age on features of iMSCs has to be broadened further. This will provide more detailed insights into applicability and regenerative potential of iMSCs. In particular, there are no studies comparing iMSCs of a young and aged background which were derived from primary hMSCs. Likewise, nothing is

known about the effect of donor age on the gene expression associated with ageing processes such as senescence, response to oxidative stress and DNA damage repair in iMSCs derived from fetal and aged hMSCs. In addition, it is not known whether ageing-related gene expression patterns are reverted to a more fetal-like state when iMSCs are generated from hMSCs of aged donors. In this respect, the direct comparison of iPS cell and iMSC generation from a fetal and aged donor hMSCs would help to get more insight into these aspects. In addition, the effect of reprogramming technology in this context is not known and comparison of viral and episomal plasmid-based reprogramming and subsequent iMSC generation from fetal and aged MSCs would elucidate these aspects. Finally, the analysis of the gene expression patterns would help to understand the extent of reflection of age in hMSC-derived iPS cells and its maintenance in the corresponding iMSCs.

1.7 Aim of this work

This study seeks to provide more detailed knowledge about the effect of donor age and age-related features in human bone marrow-derived mesenchymal stem cells on the process of the generation, the features of the derived iPS cells and on corresponding iMSCs. These efforts aim to provide insights into the applicability of iPS and iMSC-based approaches to change ageing features in hMSCs from elderly donors in comparison to fetal hMSCs as a very young cell type. In order to reach the aim, the following questions will be addressed using the described approaches:

- What are age-related differences between fetal hMSCs and hMSCs of aged donors that potentially could interfere with reprogramming of hMSCs into iPS cells?

  -Comparative characterisation of primary hMSCs of fetal and aged background in terms of surface marker expression and trilineage differentiation potential.

  -Comparative characterisation of ageing-related features, such as intracellular ROS levels, senescence, cell cycle regulation and comparative transcriptome analysis based on microarray data of primary hMSCs of fetal and aged background.

- Can hMSCs derived from aged individuals be reprogrammed to pluripotency with the same efficiency as hMSCs with fetal background and can the manipulation of known pathways implicated in aging improve the efficiency of iPS generation from aged hMSCs?

  -Comparative reprogramming of fetal hMSCs and hMSCs from elderly donors using retroviral and non-viral reprogramming.

  -Comparative reprogramming under conditions known to modulate reprogramming efficiency and to modulate ageing-associated features and signalling.

  -Characterisation of the generated iPS cells in terms of pluripotency and somatic origin.

- Are MSC-specific features and aspects of aging reflected in iPS cells reprogrammed from hMSCs of fetal and high age origin?

  -Detection of ageing-related fetaures, such as DNA damage and ROS in hMSC-iPS cells of different age backgrounds.

  -Comparison of retained donor cell-specific gene expression patterns in iPSCs of fetal and aged background.

  -Analysis of gene expression patterns comparing hMSC-iPSCs with fetal and aged background based on gene sets specific for ageing-related processes.

-Analysis of retained gene expression related to osteogenesis in hMSC-derived iPS cells compared to fibroblast-derived iPS cells and of a potential effect of donor cell background on osteoblast differentiation.

- Can hMSC-iPSCs be re-differentiated to iMSCs and are features of ageing or rejuvenation reflected in iMSCs of fetal and high age origin?

  -Derivation of iMSCs from hMSC-iPSCs of fetal and aged background and from hESCs.

  -Characterisation of surface marker expression and trilineage potential.

  -Analysis of age-related gene expression patterns in iMSCs of fetal and aged background based on gene sets specific for ageing-related processes.

  -Comparison of the transcriptional profiles of iMSCs with primary hMSCs of different age background.

2 Materials and Methods

2.1 Ethics statement

Fetal hMSCs and aged hMSCs were kindly provided by Professor Richard Oreffo of the Bone and Joint Research Group, Institute of Developmental Sciences, Southampton General Hospital, Southampton, United Kingdom. Primary hMSCs fetal hMSC 1, fetal hMSC 2 and fetal hMSC 3 were isolated from human fetal femur that was obtained after termination of pregnancy according to guidelines issued by the Polkinghorne Report and with approval of from the Southampton & South West Hampshire Local Research Ethics Committee. Primary aged hMSC (60y), aged hMSC (62y) and aged hMSC (70y) were isolated from the bone marrow and used after written informed consent of the patient. Ethical approval was obtained from the Southampton & South West Hampshire Local Research Ethics Committee. Aged hMSC (74y) were kindly provided by Professor Georg Duda and Dr. Sven Geissler of the Julius Wolff Institute, Charité - Universitätsmedizin Berlin, Berlin, Germany. Aged hMSC (74y) were isolated and used with written informed consent of the patient and the use of the cells was approved by the research ethics board of the Charite - Universitätsmedizin, Berlin.

2.2 Cell culture

Mesenchymal stem cells were maintained under normoxic conditions in an incubator (INNOVA CO-170 Incubator, New Brunswick Scientific) under humidified atmosphere at 37°C and 5% CO_2. Pluripotent cells were maintained under hypoxic conditions in a hypoxia incubator (C-200, LABOTECT) at 37°C, 5% CO_2 and 5% O_2. Reprogramming experiments were conducted under hypoxic or normoxic conditions. Cell culture procedures were carried out under aseptic conditions under clean benches with laminar flow (HeraSafe, Thermo Scientific).

2.2.1 Primary cells and cell lines

The primary hMSCs fetal hMSC 1, fetal hMSC 2, fetal hMSC 3, aged hMSC (60y), aged hMSC (62y), aged hMSC (70y) used in the course of this thesis were isolated in the Bone and Joint Research Group, Institute of Developmental Sciences, Southampton General Hospital, Southampton, United Kingdom and were transported to the Max Planck Institute as cryopreserved samples. The primary aged hMSC (74y) were isolated at the Julius Wolff Institute, Charité, Berlin, Germany. The reprogramming of aged hMSC (74y) was described as part of my master thesis (Megges 2010). The further characterisation of aged hMSC (74y) and the respective iPS cell line as well as corresponding iMSCs were carried out as part of this PhD thesis. All cells used in the experiments of this work are listed in Table 1.

Table 1 Primary hMSCs, pluripotent cell lines and iMSCs.

primary hMSCs				
Name	**Sex**	**Age of donor**	**Isolated from**	**Received from**
fetal hMSC 1	m	55 days post conception	bone marrow of femur	Bone & Joint Research Group, Southampton General Hospital
fetal hMSC 2	m	55 days post conception	bone marrow of femur	Bone & Joint Research Group, Southampton General Hospital
aged hMSC (60y)	f	60 years	bone marrow of hip bone	Bone & Joint Research Group, Southampton General Hospital
aged hMSC (62y)	f	62 years	bone marrow of hip bone	Bone & Joint Research Group, Southampton General Hospital
aged hMSC (70y)	f	70 years	bone marrow of hip bone	Bone & Joint Research Group, Southampton General Hospital
aged hMSC (74y)	f	74 years	bone marrow of hip bone	Julius Wolff Institute, Charité, Berlin
induced pluripotent cell lines				
Name	**Derived from**	**Reprogramming method**		
iPSC (hMSC, fetal line 1, viral)	fetal hMSC 1	retroviral transduction		
iPSC (hMSC, fetal, line 1, episomal 1)	fetal hMSC 1	episomal plasmids		
iPSC (hMSC, fetal, line 1, episomal 2)	fetal hMSC 1	episomal plasmids		
iPSC (hMSC, 62y, episomal)	aged hMSC (62y)	episomal plasmids		
iPSC (hMSC, 74y, viral)	aged hMSC (74y)	retroviral transduction		
human embryonic stemm cell lines				
Name	**Purchased from**	**Cell line**	**Sex**	
hESC H1	WiCell Research Institute	WA 01	male	
hESC H9	WiCell Research Institute	WA-09	female	
iMSC preparations				
Name	**Derived from**			
iMSC (fetal, line 1, viral)	iPSC (hMSC, fetal line 1, viral)			
iMSC (74y, viral)	iPSC (hMSC, 74y, viral)			
iMSC (hESC H1)	hESC H1			

HEK293T: transformed Human Embryonic Kidney cell line (Max Planck Institute for Molecular Genetics, Berlin)

Mouse Embryonic Fibroblasts (MEFs): MEFs were isolated from pregnant female mice (CF-1, Harlan, USA) after they were sacrificed by a technician of the Max Planck Institute for Molecular Genetics Berlin.

The iPS cell line iPSC (hFF, viral) was generated by Dr. Ying Wang, a post-doc in the Molecular Embryology and Ageing Group at the Max Planck Institute for Molecular Genetics, Berlin. The respective iPS cell line was generated using the same retroviral approach for reprogramming as for iPSC (hMSC, 74y, viral), however without addition of inhibitors. In this work, the transcriptome data of iPSC (hFF, viral) were used that were detected by microarray.

2.2.2 Isolation of primary bone marrow-derived mesenchymal stem cells

Fetal hMSC 1, fetal hMSC 2 and fetal hMSC 3 were isolated from bone marrow of fetal femur as previously described (Cheung et al. 2014). Primary aged hMSC (60y), aged hMSC (62y) and aged hMSC (70y) were isolated from the bone marrow of the hip bone. Primary hMSCs aged hMSC (74y) were isolated at the Julius Wolff Institute, Charité, Berlin, Germany, from bone marrow aspirates from the hip bone in an operation. After separation by density gradient centrifugation the part of the bone marrow containing mononuclear cells was seeded in cell culture dishes in order to isolate hMSCs via plastic adherence. All primary hMSCs were transported to Max Planck Institute for Molecular Genetics as cryopreserved samples.

2.2.3 Maintenance and expansion of hMSCs, mouse embryonic fibroblasts (MEFs) and iMSCs

After being defrosted, MEFs were initially seeded at a density of 3000 cells per cm^2 and split in a ratio of 1:6 when subconfluent. hMSCs were seeded at a density of $1000cm^2$. MEFs were cultured in MEF maintenance medium (7.1.1.1). hMSCs and iMSC were cultured in hMSC maintenance medium (7.1.1.2). The seeding density of iMSCs was $1000cm^2$ after passage four. This seeding density was maintained when hMSCs were split when subconfluency was reached. To split the cells, the medium was removed with a pump and sterile glass pipette. As a next step, the cells were washed with PBS without Magnesium and Calcium ions for three times. Subsequently, 0.01% Trypsin/EDTA (Life Technologies) was used to detach the cells from the surface by applying a volume enough to cover the surface of the dish and keeping the dish at 37°C and 5% CO_2 until full detachment was reached. At this point, the trypsin was inactivated by adding 2.5-10ml culture medium containing FBS depending on the size of the dish. The cell suspension was collected in tubes with conic ends (Falcon) and spun down for 5min at 500 x g. The supernatant was removed and the cell pellet was resuspended for cell counting using a Neubauer haemocytometer. After the calculation of the cell number, the volume of the cell suspension was adapted to reach a concentration that seeding the cells in the respective seeding density could be carried out. For seeding the new cell culture, the dish was filled with the appropriate volume of culture medium and the cell suspension was applied containing the calculated amount of cells. The cells were evenly distributed before the dish was placed into an incubator. Growth of the cells was controlled using a bright-field microscope. Medium change was carried out every three days.

2.2.4 Freezing and thawing of primary hMSCs, MEFs and iMSCs

hMSCs or MEFs were washed, detached and spun down as described in the previous section. To freeze hMSCs, the cell pellet was resuspended in hMSC freezing medium containing 10% DMSO HYBRY Max, sterile filtered (Sigma-Aldrich, D26509) and 90% FBS (Biochrom AG). To freeze MEFs and mitotically inactivated MEFs, the cell pellet was resuspended in MEF freezing medium containing 10% of DMSO HYBRY Max, sterile filtered (Sigma-Aldrich, D26509), 40% of DMEM (High Glucose, Life Technologies) and 50% of FBS (Biochrom AG). The mix was shared to cryovials and put into a freezing container (Nalgene). After an overnight incubation at -80°C the cryovials were transferred into liquid nitrogen tanks with appropriate racks at -196°C. To thaw hMSCs, MEFs and iMSCs, the cryovials were transferred from liquid nitrogen to a 37°C water bath to quickly defrost. The cryovial was then sterilised using 70% Ethanol before it was opened under a laminar flow hood. Medium warmed to 37°C was prepared and the thawed cell suspension was resuspended in 10ml of it using a 1ml pipette for this procedure. Subsequently, the defrosted cells were spun down for 5min at 500 x g, the supernatant was removed and the cell pellet was resuspended in 10ml culture medium for

assessment of the number of living cells using Trypan Blue (Sigma-Aldrich, 72-57-1) and a Neubauer counting chamber. The concentration of living cells in the suspension was calculated on the base of trypan blue negative cells and the respective number needed to reach the wished seeding density was transferred to the cell culture dish, which contained fresh culture medium.

2.2.5 Maintenance and expansion of pluripotent cells

iPS cells and human embryonic stem cells were cultured in six well cell culture plates coated with Matrigel and inactivated feeder cells using unconditioned medium (7.1.1.3) supplemented with 4ng/ml FGF2. The cells were split when colonies covered 80% of the well surface. When the cells had not grown enough to be split after one week the maintenance medium was switched to conditioned medium supplemented with 4ng/ml FGF2. The medium was changed every day using 2.5ml -4ml per well depending on the confluence. One day before passaging the cells, inactivated MEFs (feeder cells) were seeded onto Matrigel-coated six well plates at a density of $2x10^5$ cells per well of a six well plate and cultured in MEF maintenance medium until the next day. Directly before splitting, the feeder cell coated cell culture dishes were washed with PBS for three times and unconditioned medium was warmed to 37°C and supplemented with 4ng/ml of FGF2 and subsequently added to the culture dish using 2ml of medium per well.

To passage the cells they were cut manually using a BD Microlance™ 3 injection needle (Becton Dickinson) and a Stereo Microscope of the model Leica MZ 95 under a HERAguard Clean Bench (Heraeus, Thermo Fischer Scientific). By using the needle, the undifferentiated cells detached from the surface. The old medium was removed and the cut colonies were washed with PBS twice. Next 1ml of unconditioned medium was added to each well and the pluripotent stem cell colonies were detached from the surface by scraping using a cell scraper. The suspension was mixed and distributed to three prepared wells resulting in a 1:3 split ratio, which was used for the maintenance of all pluripotent cell lines in this study. The seeded pluripotent cells were distributed evenly in the well by agitation and carefully placed in the middle of a shelf in the incubator under hypoxic conditions for attachment.

2.2.6 Mitotic inactivation of mouse embryonic fibroblasts

MEFs were cultured in $150cm^2$ tissue culture dishes until 80% confluence was reached. In addition, MEFs were only cultured until passage 2 before they were inactivated. To inactivate them, MEFs were cultured in MEF maintenance medium containing 10µg/ml of mitomycin c (Roche) for 2h at 37°C. Subsequently, the inactivation medium was removed and the cells were washed three times with PBS, detached using trypsin and either seeded immediately as feeder cells for maintenance of pluripotent stem cells or cryopreserved and stored at 196°C.

2.2.7 Preparation of Matrigel-coated plates

In order to avoid the polymerisation, Matrigel (Becton Dickinson) was slowly defrosted overnight at 4°C. Subsequently, a stock solution was prepared by adding the appropriate amount of Knockout™ DMEM to the thawed Matrigel solution for a final concentration of 5mg/ml. The stock solution was then aliquotted on ice in pre-cooled 15ml plastic tubes and stored at -20°C. To coat cell culture dishes using Matrigel, a frozen vial of the 5mg/ml stock solution was resuspended using 14ml 4°C cold Knockout™ DMEM for 1ml of the stock solution. 1ml per well of a six well plate of the 4°C Matrigel suspension was then transferred to the surface of the cell culture dish and distributed to cover the whole bottom of the well. The cell culture plates were subsequently wrapped with Para film and left overnight at 4°C for polymerisation of the Matrigel. Before use, the leftover Matrigel solution was removed and washed with PBS twice before using it for feeder-free maintenance of pluripotent stem cells.

2.2.8 Preparation of conditioned medium

Conditioned medium was used to culture pluripotent stem cells under feeder-free conditions and after one week of culture on feeder cells to ensure maintenance in the pluripotent state. First, mitotically inactivated MEFs were seeded in 150cm^2 cell culture flasks at a density of 5.6x10^4 cells/cm^2. After attachment of the MEFs, the medium was removed and the cells were washed four times using PBS. Next, the medium was replaced with unconditioned medium supplemented with 4ng/ml FGF2 using a volume of 0.5ml/cm^2. The cell culture dish was placed in an incubator under normoxic conditions for 24 h and the conditioned medium was collected. The medium was changed another six times. Finally, the collected conditioned medium was pooled, frozen and stored at -80°C. For use in feeder-free maintenance of pluripotent stem cells, the conditioned medium was defrosted and supplemented with 4ng/ml of FGF2.

2.2.9 Feeder-free maintenance of pluripotent stem cells

Pluripotent stem cells were cultured without feeders before isolation of RNA and DNA, before being injected when tested in the Teratoma assay and before being differentiated into Osteoblasts or iMSCs. The pluripotent stem cells were seeded onto Matrigel-coated plates. For maintenance, conditioned medium supplemented with 4ng/ml FGF2 was used. In addition, mTeSR 1 (Stem Cell Technologies) was used for feeder-free culture of hMSC-iPSCs.

2.2.10 Freezing and thawing of pluripotent cells

For cryopreservation of pluripotent stem cells, they were cut into pieces and detached from the surface using a cell scraper as described for passaging. The cell suspension was spun down for 5min at 500 x g and 4ºC. The supernatant was removed and the cell pellet was resuspended in pluripotent stem cell

freezing medium containing 10% DMSO (Sigma-Aldrich), 40% Knockout™ DMEM (Life Technologies) and 50% Knockout ™ Serum Replacement (Life Technologies). Subsequently, the freezing medium mixed with cell clumps was transferred to cryovials and put into a freezing container (Nalgene) which was placed in a -80°C freezer overnight. On the next day, the cryovials were transferred into liquid nitrogen tanks with appropriate racks at -196°C.

To defrost pluripotent stem cells, the cryovial was removed from the liquid nitrogen tank and defrosted in a 37°C water bath. The defrosted cell suspension was quickly transferred into 10ml of conditioned medium, which was pre-warmed, to 37°C under aseptic conditions. The solution was spun down at 500 x g and 4ºC for 5min and the supernatant was removed. The cell pellet was resuspended in unconditioned medium suppelemented with 8ng/ml FGF2 and seeded onto feeder coated cell culture dishes with a culture volume of 2.5ml per well of a six well plate. 10µM Rho-associated kinase (ROCK) inhibitor Y-27632 (Tocris, 1254) were added to the culture medium to support the attachment of the pluripotent stem cells as previously described (Watanabe et al. 2007)

2.3 Analysis of nucleic acids

2.3.1 Isolation of genomic DNA

Genomic DNA was isolated in order to be used in PCR applications to analyse the somatic origin of iPS cells generated and to detect sequences of episomal plasmids. To isolate genomic DNA, the pluripotent cells were cultured under feeder free conditions. The FlexiGene DNA Kit (Qiagen) was used to isolate genomic DNA following the instructions of the manufacturer. hMSCs were trypsinised, whereas pluripotent cells were detached by scraping. The cells were spun down at 300 x g, for 5min. The supernatant was removed and the cell pellet was resuspended in 300µl FG1 buffer and transferred to a 1.5ml micro tube followed by addition of 300µl FG2 buffer containing 3µl Quiagen protease provided with FlexiGene DNA Kit and a 10min incubation at 65ºC. After the incubation the 600µl 2-propanol were added and the suspension was mixed thoroughly until the DNA precipitated. This was followed by a centrifugation step for 3min at 10,000 x g and subsequent removal of the supernatant. The tube was left to dry for a short time and 600µl 70% ethanol were added and the mix was vortexed for 5s. Next, the solution was centrifuged at 10,000 x g for 3min. After discarding the supernatant the DNA pellet at the bottom of the tube was left to dry for 5min. Finally, the pellet was dissolved in 200µl of buffer FG3 by vortexing for 5s at low speed and an incubation for 30min at 65°C. The isolated DNA was stored at -80°C after the concentration was measured and the quality was checked with a spectrophotometer type NanoDrop® ND-1.000.

2.3.2 Polymerase chain reaction

PCR was used to detect specific sequences of episomal plasmids in iPS cell lines generated with the episomal plasmid-based non-viral method and for DNA fingerprinting.

Reaction mix for one DNA sample:

2.5µl	10 x B1 buffer (7.1.2.1)
0.2µl	dNTP-Mix (dATP, dCTP, dGTP, dTTP each 25mM)
0.5µl	50µM forward primer
0.5µl	50µM reverse primer
0.4µl	*Taq* DNA Polymerase (10U/µl)
0.1µl	*Pfu* DNA Polymerase (10U/µl)

Equivalent volume for 50ng template DNA

ad 25µl $_{dd}H_2O$

The PCR reaction was conducted in a Dyad thermal cycler (BioRad, Hercules, CA) using the following programs:

DNA fingerprinting:

Initial denaturation 94°C for 2min 30s, denaturation 94°C for 1min, primer annealing 56°C for 1min, primer extension 72°C for 1min, final extension 72°C for 10min for 40 cycles followed by a final hold at 4°C.

Episomal plasmid-specific sequence detection:

Initial denaturation 94°C for 5min, denaturation 94°C for 15s, primer annealing 55°C for 30s, primer extension 68°C for 1min, final extension 68°C for 7min for 35 cycles followed by a final hold at 4°C.

The primers sequences used in the respective PCR reaction are listed in Table 2.

2.3.3 Agarose and acrylamide gel electrophoresis

Products of PCR reactions used to detect sequences within episomal plasmids were separated using 2% agarose gels and subsequent electrophoresis. The PCR products of the DNA fingerprinting PCR used for characterisation of iPSC (hMSC, 74y, viral) were separated in 3.5% agarose gels. Isolated RNA was quality-checked using 1.5% agarose gels. The PCR products of the fingerprinting PCR of all other hMSC-iPS cell lines were separated in 4% acrylamide gels.

Agarose gels were prepared using 200ml 1 x SB buffer (1:10 dilution of 10 x SB buffer in $_{dd}H_2O$, 7.1.2.3) with the appropriate amount of Agarose (Sigma-Aldrich, A9539). The mixture was heated until clear using a microwave oven. After letting the mixture cool for a short amount of time 5µl of Ethidium Bromide solution (Sigma-Aldrich, E1510) was added. The solution was mixed thoroughly, cast in a casting chamber and left to polymerise. The polymerised gel was used for electrophoresis employing 1 x SB buffer as running buffer.

For electrophoresis 12µl of each sample were mixed with 6 x loading buffer (7.1.2.2) and the agarose gel was loaded with the mix. 1 x SB buffer was used as separation buffer. The electrophoresis was carried out at 100 V for 20-30min or longer, depending on the gel concentration. Perfect Plus 1 kb DNA ladder (Roboklon) was used as a marker of amplicon length.
4% polyacrylamid gels were prepared using the following recipe:

13.4ml	30% acrylamide:bis-acrylamide (29:1)
20ml	5 x TBE (7.1.2.4)
56ml	$_{dd}H_2O$
750ul	10% ammonium persulfate
85ul	TEMED

The solution was mixed thoroughly and the gels were cast using a hand cast system. After the comb was put, the gel was left to polymerase for 1h. The polymerised gel was used in a Mini-PROTEAN® II electrophoresis cell (Biorad) using 1 x TBE buffer (1:5 dilution of 5 x TBE buffer in $_{dd}H_2O$) for separation. The samples were mixed with 6 x loading buffer and then loaded into the samples slots. The electrophoresis was carried out using 100V for 2h. For visualisation of the PCR product fragments, the gel was stained in 100ml distilled water containing 15µl of a 10mg/ml ethidium bromide solution. The DNA in agarose and polyacrylamide gels was visualised under UV light using AlphaImager™ (Alpha Innotech).

2.3.4 RNA isolation

The RNeasy® Mini Kit (Qiagen) was used to isolate RNA for qRT PCR and microarray-based gene expression analysis. The RNA was isolated following the instructions of the manufacturer. In addition, the optional on-column DNAse treatment using the RNase-Free DNAse Set (Quiagen) was carried out. The medium of the cells was aspirated and the cells were washed with 37°C warm PBS. The cells were lysed with RLT buffer containing 10µl per 1ml β-mercaptoethanol and the lysate was transferred to a 1.5ml micro centrifuge tube. The lysate was vortexted for 1min and passed through a 20-gauge (0.9mm) BD Microlance™ 3 injection needle (Becton Dickinson) attached to a sterile plastic syringe for 10 times. As a next step, the lysates were transferred to RNeasy®-columns and 80µl DNAse I mix (70µl Buffer RDD mixed with 10µl DNAse I stock solution) of the RNase-free DNAse Set were used to perform on-column DNA digestion for 15min at RT. The following steps were carried out exactly following the manufacturer´s instructions. However, the RNA was eluted using two times 15µl of DEPC treated water followed by a 1-min-centrifugation at full speed. The isolated RNA was quality-checked on a 1.5% agarose gel loading 200ng onto the gel for separation. In addition, the

concentration and quality parameters of the RNA were measured using spectrophotometer type NanoDrop® ND-1.000.

2.3.5 Reverse transcription

When the RNA sample could not be used for qRT PCR due to a too low concentration, it was concentrated by SpeedVac centrifugation using a Savant SPD131DDA SpeedVac concentrator.
0.5-2µg of RNA were transcribed to cDNA, depending on the sample with the lowest concentration. The RNA samples isolated after the osteoblast, adipocyte and chondrocyte differentiation of hMCSs were merged from three wells of a six well plate or three cell pellets respectively. The primers used for real-time PCR in this work are listed in Table 2.
The RNA was mixed with 0.05µl of a 1µg/µl oligo dT primer solution (Invitek) and with $_{dd}H_2O$ to a final volume of 15µl. The sample mixes were incubated for 3min at 70°C in a Thermocycler PTC100 (MJ Research Inc.). Subsequently, the samples were cooled on ice and a master mix was added with the following components per sample:

5µl	5 x-reaction buffer (Promega)
0.5µl	dNTP-Mix (dATP, dCTP, dGTP, dTTP each 25mM)
0.1µl	MMLV (Moloney Murine Leukemia Virus) reverse transcriptase (200U/µl, USB)
9.4µl	$_{dd}H_2O$

The solution was incubated in a thermocycler of the model PTC100 (MJ Research Inc.) for 1h at 42°C. The reaction was stopped by an incubation at 65°C for 10min. The cDNA samples were stored at -80°C until they were used for real-time PCR.

2.3.6 Real-time PCR

Determination of gene expression by real-time PCR was carried out using technical triplicates and a control in which $_{dd}H_2O$ is used instead of the template (NTC, no template control). The cDNA was diluted in $_{dd}H_2O$ before use with a ratio of 1:8 for 2µg of input RNA. The real-time PCR was carried out in 384-well Optical Reaction Plates (Applied Biosystems).
The following target gene-related reaction mix was transferred to one well per reaction:

3µl	SYBR®Green PCR Master Mix (Applied Biosystems)
1µl	mix of 5µM forward and 5µM reverse primer
2µl	$_{dd}H_2O$

6µl of the reaction mix was mixed with 2µl of diluted cDNA. A reaction mix specific for the amplification of GAPDH served as endogenous control for normalisation of the samples. After the

reaction mixed were added the reaction plate was sealed and the real-time PCR reactions were conducted in an ABI PRISM 7900HT Sequence Detection System (Applied Biosystems).

The following program was used for all real-time PCR reactions:

stage 1: 50°C for 2min
stage 2: 95°C for 10min
stage 3: 95°C for 15s and 60°C for 1min, for 40 cycles
stage 4: 95°C for 15s, 60°C for 15s and 95°C for 15s

Stage 4 was carried out using a ramp rate of 2% in order to generate a dissociation curve of the products of the real-time PCR reactions.
The measured data were analysed using the software SDS 2.2 (Life Technologies). The data were exported to Excel (Microsoft) and analysed according to the ΔΔCt method (Livak and Schmittgen 2001). The measured mRNA expression was normalised against the mRNA expression of GAPDH. The data were presented as log2 ratio of the mRNA level measured in the sample over the value measured in untreated hMSCs with respect to standard deviation.

2.3.7 Primers

The primers used in this work for PCR and real-time PCR are listed in Table 2.

Table 2 Primer sequences used in PCR and real-time PCR reactions.

Gene	forward primer sequence (5´-3´)	reverse primer sequence (5´-3´)
PCR: DNA fingerprinting		
D7S796	TTTTGGTATTGGCCATCCTA	GAAAGGAACAGAGAGACAGGG
D10S1214	ATTGCCCCAAAACTTTTTTG	TTGAAGACCAGTCTGGGAAG
PCR: episomal plasmid detection		
OriP	TTCCACGAGGGTAGTGAACC	TCGGGGGTGTTAGAGACAAC
EBNA	ATCGTCAAAGCTGCACACAG	CCCAGGAGTCCCAGTAGTCA
SV40LT	AGTTTGTGCCAGGGTTTTTG	ACTTCACCTTCCCTCCAACC
qRT-PCR		
GAPDH	GTGGACCTGACCTGCCGTCT	GGAGGAGTGGGTGTCGCTGT
COL1A1	GGTCAGATGGGCCCCCG	GCACCATCATTTCCACGAGC
PPARG	CGTGGCCGCAGAAATGAC	CACGGAGCTGATCCCAAAGT
LPL	AGTAGCAGAGTCCGTGGCTA	ATTCCTGTTACCGTCCAGCC
RUNX2	CTCGGGAACCCAGAAACCC	GGCTCAGGTAGGAGGGGTAA
ALPL	CTATCCTGGCTCCGTGCTC	ACTGATGTTCCAATCCTGCG
BGLAP	AAGGTGCAGCCTTTGTGTCC	GGCTCCCAGCCATTGATACA

2.3.8 Amplification of plasmid DNA

The plasmids used in this work are listed in Table 3.

Glycerol stocks of plasmid carrying E.coli JM109 were expanded selectively using LB medium (7.1.3.1) supplemented with 100µg/ml ampicillin. The isolation of the plasmids was carried out using NucleoBond Xtra Maxi EF Kit (MACHEREY-NAGEL) following the instructions of the manufacturer. The plasmid integrity was tested using a 1% agarose gel. The yield of the plasmids was measured using a spectrophotometer type NanoDrop® ND-1.000. The identity of the episomal plasmids was tested by digestion with restriction enzymes.

Table 3 Plasmids used for reprogramming experiments.

plasmid name	used for	transgenes	bacteria strain	company
pCMV-VSV-G	retrovirus generation	VSV-G envelope protein	E.Coli JM109	8454, Addgene
pUMVC3-gag-pol	retrovirus generation	gag, pol, viral packaging	E.Coli JM109	4561, Addgene
pMXs-hOCT3/4	viral reprogramming	OCT4	E.Coli JM109	17217, Addgene
pMXs-hSOX2	viral reprogramming	SOX2	E.Coli JM109	17218, Addgene
pMXs-hKLF4	viral reprogramming	KLF4	E.Coli JM109	17219, Addgene
pMXs-hc-MYC	viral reprogramming	c-MYC	E.Coli JM109	17220, Addgene
pLIB GFP	control of transduction	GFP	E.Coli JM110	PT3189-5, Clontech
pEP4 E02S EN2K	episomal plasmid based reprogramming	OCT4, SOX2, NANOG, KLF4	n/a	20925, Addgene
pCEP4-M2L	episomal plasmid based reprogramming	c-MYC, LIN28	n/a	20926, Addgene
pEP4 E02S ET2K	episomal plasmid based reprogramming	OCT4, SOX2, SV40LT, KLF4	n/a	20927, Addgene

2.4 Microarray-based gene expression profiling

2.4.1 Hybridisation on an Illumina Bead Chip

The Illumina platform was used for microarray-based gene expression analysis of fetal hMSC 1, fetal hMSC 2, aged hMSC (60y), aged hMSC (62y), aged hMSC (70y), aged hMSC (74y), iPSC (hMSC, fetal, line 1, viral), iPSC (hMSC, fetal, line 1, episomal 1), iPSC (hMSC, fetal, line 1, episomal 2), iPSC (hMSC, 62y, episomal), iPSC (hMSC, 74y, viral), hESC H1, iMSC (fetal, line 1, viral), iMSC (74y, viral) and iMSC (hESC H1). The RNA of one sample each was hybridised on an Illumina HumanHT-12 v3 Expression BeadChip.

500ng of high quality total RNA were amplified and used for the generation of cRNA and biotin labelling (Illumina TotalPrep RNA Amplification Kit, Ambion). The labelled cRNA was hybridised to an Illumina HumanHT-12 v3 Expression BeadChip, washed and stained with Cy3-streptavidin on an Illumina BeadStation 500 platform. The mRNA levels were detected quantitatively by scanning of the fluorescence signals on the array. The RNA preparation, hybridisation and scanning were carried out by the company Alacris Theranostics, Berlin.

2.5 Microarray data analysis

2.5.1 Normalisation and detection of expressed genes

The raw gene expression data were normalised and background-subtracted using the “rank invariant” algorithm of the Gene Expression Module, which is part of the GenomeStudio software (Illumina). To

exclude negative gene expression signals that may have been generated by background subtraction, a cut off was set. The software GenomeStudio compares the signal measured with negative control beads to calculate the probability that a gene is expressed. The result of this calculation is the "detection p-value". A gene was considered to be expressed when the expression p-value was below 0.01. The data were exported to Microsoft Excel (Microsoft) and the genes with a detection p-value below 0.01 were marked by conditional formatting to extract gene lists of expressed genes of each sample for further analysis.

2.5.2 Extraction of differentially expressed genes and up or down-regulated genes

The significance of differential gene expression was calculated using GenomeStudio based on an Illumina custom model (Kuhn et al. 2004). Doing this a "differential p-value" was computed describing the probability that average signal intensity measured for two samples or sample groups is significantly different. The "differential p-value" was adjusted in GenomeStudio using the Benjamini and Hochberg false discovery rate (FDR) correction algorithm (Benjamini and Hochberg 1995). Geneexpression values with a FDR-corrected differential p-value at least below 0.05 were considered significantly different in terms of expression. From these genes up- and down-regulation was determined by calculating ratios of the average signal. Genes with a ratio higher than 1.5 were considered up-regulated, whereas genes with an average signal that is at least 1.5-fold lower were considered to be down-regulated. Gene lists of FDR-corrected differentially expressed genes and of significantly down- or up-regulated genes were extracted using these thresholds in Microsoft Excel by conditional formatting.

2.5.3 Calculation of correlations and hierarchical clustering dendrograms

Correlations between the transcriptomes of the samples were calculated based on the Pearson correlation using the microarray-based transcriptome data and the software GenomeStudio.

2.5.4 Generation of Venn diagrams

Venn diagrams were generated using either expressed genes, differentially expressed genes or significantly up or down-regulated genes as input in the platform Venny 2.0 (http://bioinfogp.cnb.csic.es/tools/venny/).

2.5.5 Functional annotation of gene sets

Functional annotation of gene lists was carried out using the platform DAVID Bioinformatics resources 6.7 (http://david.abcc.ncifcrf.gov/, (Huang et al. 2009)). Lists of official gene symbols or

Illumina IDs were used as input against human background. The functional annotation was carried out using the default settings of DAVID Bioinformatics resources 6.7. Annotation of expressed or regulated genes extracted with GenomeStudio was carried out in DAVID Bioinformatics resources 6.7 by using the option pathways and the annotation to KEGG terms which are based on the database KEGG, by choosing the option general annotation to gene ontology (GO)-terms of biological processes named GO_BP_FAT, by choosing BIOCARTA, based on the database with the same name, or the option tissue-specific annotation with the category UNIGENE.

2.5.6 Hierarchical clustering analysis of gene sets

Lists of human gene sets annotated to the GO-terms osteoblast differentiation, cell cycle, senescence, response to oxidative stress, DNA-damage repair, ageing, regulation of senescence, oxidative phosphorylation, glutathione metabolism, glycolysis and insulin signalling were generated using AmiGO 2 version 2.3.1 (http://amigo2.berkeleybop.org/amigo, (Ashburner et al. 2000)). The average signals measured by microarray of the genes of these lists were extracted using Microsoft Excel. The extracted data were used for heat map generation and hierarchical clustering analysis based on the Pearson correlation or on the Euclidean distance of the gene expression patterns using TM4 Microarray Software Suite, Multiple Experiment Viewer version 4.9 (http://www.tm4.org/mev.html, (Saeed et al. 2006, Saeed et al. 2003))

2.5.7 *In silico* determination of pluripotency

In order to analyse whether hMSC-iPSCs are pluripotent based on the microarray gene expression data measured, the raw gene expression data (.idat files) were used as input for the platform PluriTest (www.pluritest.org, (Müller et al. 2011)) The similarity of the output based on Pearson correlation was used to generate a clustering dendrogram of the analysed samples.

2.6 Immunofluorescence labelling of proteins and surface epitopes

Before cells were subjected to immunofluorescence staining, they were fixed using 4% paraformaldehyde for 20min at RT. Subsequently, the cells were washed three times with PBS and the fixed cells were covered with fresh PBS and either stored at 4°C or stained immediately. To stain the fixed cells, they were permeabilised for 10min using 1% Triton X-100 in PBS. This was followed by a 45min blocking step using 10% chicken serum 0.1% Triton X-100 in PBS at RT and the incubation with the primary antibody which was diluted in 10% chicken serum, 0.1% Triton X-100 in PBS for 1 hour at RT or at 4°C overnight. The primary antibodies and dilutions that were used are listed in Table 4. 200µl of the primary antibody solution were used per well of a 12 well plate. This was followed by three washes with PBS for 5min each and subsequent incubation with the secondary antibody which was diluted in 10% chicken serum, 0.1% Triton X-100 in PBS for 1 hour at RT in the dark under mild

agitation. The secondary antibodies and dilutions used are listed in Table 4. Subsequently, the cells were washed another three times using PBS and incubated with 100ng/ml 4′,6-Diamidin-2-phenylindol (DAPI) in PBS for 20min at RT to visualise the nuclei. Finally, the cells were covered with PBS.

Table 4 Primary and secondary antibodies.

human antigen	dilution	species raised in	company	catalogue number
Primary Antibodies				
Vimentin (VIM)	1:80	mouse	Sigma-Aldrich	V6630
Confirmation of pluripotency marker				
OCT4 (C-10)	1:100	mouse	Santa Cruz	sc-5279
SOX2 (Y-17)	1:100	goat	Santa Cruz	sc-17320
NANOG	1:100	mouse	Abcam	ab62734
GKLF (H-180) (KLF-4)	1:100	rabbit	Santa Cruz	sc-20691
c-Myc (N-262)	1:100	rabbit	Santa Cruz	sc-764
SSEA-1	1:100	mouse	Millipore	SCR001
SSEA-4	1:100	mouse	Millipore	SCR001
TRA-1-60	1:100	mouse	Millipore	SCR001
TRA-1-81	1:100	mouse	Millipore	SCR001
Embryoid body based differentiation				
SOX17	1:50	goat	R&D	AF1924
AFP	1:300	mouse	Sigma-Aldrich	WH0000174M1
Smooth Muscle Actin (SMA)	1:100	mouse	Dako Cytomation	M0851
brachyury (T) (H-210)	1:300	rabbit	Santa Cruz	sc-20109
β-Tubulin III (TUJ1)	1:1000	mouse	Sigma-Aldrich	T8660
Nestin	1:200	mouse	Chemicon	MAB5326
Immunofluorescence labeling of ROS induced DNA damage				
8 Hydroxyguanosine (8-OHdG)	1:100	mouse	Abcam	ab48508
Immunofluorescence labeling DNA double strand breaks				
Phospho-Histone H2A.X (Ser139) (20E3)	1:400	rabbit	Cell Signalig Technology	#9718
Immunofluorescence labeling of DNA damage response signaling				
Phospho-p53 (Ser15) (16G8)	1:400	mouse	Cell Signalig Technology	#9286
Secondary antibodies				
Alexa Fluor 488 conjugated goat anti-mouse IgG	1:300	goat	Life Technologies	A10667
Alexa Fluor 594 conjugated goat anti-mouse IgG	1:300	goat	Life Technologies	A11013
Alexa Fluor 488 conjugated chicken anti-goat IgG	1:300	chicken	Life Technologies	A11006
Alexa Fluor 594 conjugated chicken anti-goat IgG	1:300	chicken	Life Technologies	A11013
Alexa Fluor 488 conjugated donkey anti-rabbit IgG	1:300	donkey	Life Technologies	A11015

2.7 Microscopy and quantitative image analysis

2.7.1 Bright-field microscopy

Frequent bright-field microscopy of cells in culture and reprogramming experiments was carried out using an inverted microscope model CK2 (Olympus). Bright-field pictures were taken by means of a digital camera Canon model Power shot A650IS through the ocular of the microscope.

2.7.2 Fluorescence microscopy

The fluorophores conjugated to the secondary antibodies were detected with a confocal microscope of the model LSM 510 Meta (Zeiss) with a camera of the model Axio-Cam ICc3 (Zeiss) using the software Axiovision 4.9 for image acquisition. Images were saved as .zvi files and processed using the softwares Axiovision 4.9 and Image J.

2.7.3 Quantification of ROS-induced DNA damage

Pictures of immunofluorescence-labelled 8-OHdG were opened in ImageJ as .zvi files. The threshold in the blue channel was set in a way that the blue nuclei could be marked as regions of interest using the option “analyse Particles”. The marked regions were saved as regions of interest (ROI) using the ROI manager of the program. The area of the nuclei was marked in the green channel picture and the mean colour intensity was measured in the area of the nuclei in the green channel, resulting in a list of mean intensities measured for each particle or area of the nucleus. Subsequently, the median of the mean intensities was calculated and plotted with the standard deviation. A two-tailed unpaired Student's t test was used to determine the significance of the differences between the samples. A p-value of <0.01 was considered significant.

2.8 Fluorescence-activated cell sorting and data analysis

2.8.1 Flow cytometry procedure

Fluorescence-labelled cells were kept on ice after the staining procedure. The samples were measured using a flow cytometer of the model FACSCalibur (Beckton Dickinson) following the manufacturer's instructions. Before multicolour acquisition, a fluorescence compensation was conducted using a stained positive control for each fluorophore. The Forward Scatter (FCS) and Side Scatter (SSC) were adjusted to the measured cell type, so single cells could be analysed. The program CellQuestPro was used for data acquisition. The software Cyflogic was used to analyse the measured data.

2.8.2 MSC surface marker staining

hMSCs and iMSCs were detached using 0.05% Trypsin (Life Technologies), were washed with PBS and stained with fluorophore labelled MSC marker gene-specific antibodies against CD73, CD90, CD105 and CD45, CD34, CD14 and CD20 using the MSC Phenotyping Kit (Miltenyi) following the instructions of the manufacturer. This was done using a cocktail of fluorochrome-conjugated antibodies consisting of CD14-PerCP (clone: TÜK4, isotype: mouse IgG2a), CD20-PerCP (clone: LT20.B4, isotype: mouse Ig G1), CD34-PerCP (clone: AC136, isotype: mouse IgG2a), CD45-PerCP (clone: 5B1, isotype: mouse IgG2a), CD73-APC (clone: AD2, isotype: mouse IgG1), CD90-FITC (clone: DG3, isotype: mouse IgG1) and CD105-PE (clone: 43A4E1, isotype: mouse IgG1). A cocktail

of the following antibodies was used as isotype control: Mouse IgG1-FITC (clone: IS5-21F5), Mouse IgG1-PE (clone: IS5-21F5), Mouse IgG1-APC (clone: IS5-21F5), Mouse IgG1-PerCP (clone: IS5-21F5) and Mouse IgG2a-PerCP (clone S43.10). The fluorophores were detected in the respective bandpass filter after compensation.

2.8.3 Propidium iodide staining

The cells were detached using 0.05% Trypsin (Life Technologies), were washed with PBS. Subsequently, the cell pellet was resuspended in 300µl cold PBS. The cells were fixed in cold 70% Ethanol in PBS using a vortexer with mild agitation, slowly adding 700µl of cold 100% Ethanol to the cell suspension. The cells were fixed for 30min in this solution and washed in PBS three times. The supernatant was discarded. Next, the cells were treated with Ribonuclease (RNase) by adding 50µl of a 100µg/ml stock solution of RNase to the cells, followed by 200µl of a 50µg/ml stock solution of propidium iodide. Subsequently, the stained cells were visualised using the filter FL-2. The gates to measure cells in the G1-phase, S-phase or G2-phase of the cell cycle were set in the histogram mode. The percentage of cells in the respective phase of the cell cycle was calculated based on the percentage of single cells visible in the red bandpass filter Fl-2.

2.8.4 Measurement of intracellular reactive oxygen species

The hMSCs and hMSC-iPSCs were washed with PBS twice and were subsequently incubated in medium supplemented with 15µM DCFDA for 30min at 37°C under normoxic conditions. ROS oxidise DCFDA to fluorescent DCF, which is measured. Subsequently, the cells were washed with PBS, trypsinised to detach them and resuspended in PBS. The fluorescent dye was measured in the green bandpass filter Fl-1. The samples of two groups were compared by unpaired Student´s t test.

2.8.5 Quantification of DNA double-strand breaks

The cells were trypsinised for detachment and washed with PBS twice. Subsequently the cells were fixed using with a solution containing 95% ethanol and 5% acetic acid for 10min. The cells were washed and resuspended in 1% formaldehyde, 0.25% Triton® X-100 in TBS for 5min. 2µg/ml Anti-γH2AX Antibody, clone JBW301, FITC conjugate (16-202A, Merck Millipore) was added and the cells were incubated in the solution for 1 h at RT. Subsequently, the stained cells were measured using the filter for green fluorescence Fl-1. The mean fluorescence intensity was calculated by gating the positively stained cells in a histogram using unstained cells as control.

2.8.6 Transduction and nucleofection efficiency

To calculate the transduction efficiency hMSCs were transduced with a GFP-carrying retrovirus that was produced along with retroviruses harbouring *OCT4*, *SOX2*, *KLF4* and *c-MYC*. The transduced cells were harvested by trypsinisation one day after transduction and the GFP-positive cells were

measured by FACS using the filter for green fluorescence Fl-1. The positive cells were determined by setting a gate that excluded unstained hMSCs, which were used as negative control. The potentially transduced cells showing a higher fluorescence than unstained cells were considered successfully transduced and GFP-positive. Likewise, to calculate the nucleofection efficiency hMSCs were nucleofected using the GFP carrying control plasmid pmaxGFP provided with the Human MSC Nucleofector® Kit (VPE-1001, LONZA) using the same nucleofection program that was used for the nucelofection of the episomal plasmids. The cells nucleofected with pmaxGFP were trypsinised one day after nucleofection and measured using the filter Fl-1. Non-nucleofected hMSCs were used as negative control. Cells with a higher fluorescence intensity than the negative control were considered GFP-positive. The percentage of GFP-positive cells was calculated by setting a respective gate.

2.9 Generation of iMSCs

hMSC-iPSCs and hESC H1 were differentiated into mesenchymal stem cells like cells (iMSCs) using a protocol as previously described (Yen Shun Chen et al. 2012). hMSC-iPSCs and hESC H1 were cultured under feeder free conditions until confluent. Subsequently, the medium was changed to unconditioned medium without FGF supplemented with 10µM SB-431542 in DMSO (Sigma-Aldrich). The medium was changed daily until the cells were trypsinised and passaged as single cells after 10 days. The cells were initially seeded at a density of $4x10^4$ cells per cm^2 in hMSC maintenance medium. In the next passaging the cells were seeded at a density of $2x10^4$ cells per cm^2 in hMSC maintenance medium, followed by a density of $1x10^4$ cells per cm^2 in the next passage. The seeding density of $1x10^4$ cells per cm^2 was maintained for every further passage.

2.10 Characterisation of hMSCs and iMSCs

2.10.1 *In vitro* osteoblast differentiation

The hMSCs or iMSCs were detached from the surface using trypsin and seeded in one six well plate and six wells of a twelve well plate at a density of $5x10^3$ cells per cm^2 in hMSC expansion medium. The cells were cultured until they reached 80% confluence. At this point the medium was changed to differentiation medium of the StemPro® Osteogenesis Differentiation Kit (Life Technologies, A10072-01) in three wells of the six well plate and three wells of the 12 well plate. The cells in the respective other three wells were cultured further in hMSC maintenance medium as negative control. The medium was changed every three days for 21 days. At day 21 RNA was isolated from the wells treated with osteogenic medium and from the control and analysed using real-time PCR-specific for *RUNX2*, *ALPL* and *BGLAP* was carried out. The cells in the 12 well format were stained using Alizarin Red. The osteoblast differentiation of aged hMSC (74y) was part of a previously published master thesis (Megges 2010).

Osteoblast differentiation of iPSC (hMSC, 74y, viral) and iPSC (hFF, viral) was carried out with a different protocol. The pluripotent cells were cultured in N2B27 medium (7.1.1.4) supplemented with 4ng/ml FGF2 in six wells of a 12 well cell culture plate. When the cells reached 80% confluence, three wells of the twelve well plate were cultured in osteogenic medium. In addition, three wells of a twelve well plate were cultured in DMEM supplemented with 10% FBS and 1% penicillin/streptomycin, which was used as a control. On day 11 RNA the cells cultured under osteogenic conditions and the cells cultured under control conditions were stained with Alizarin Red to visualise calcified bone matrix. The osteogenic induction, Alizarin Red staining and image acquisition was performed at Berlin-Brandenburger Centrum für Regenerative Therapien, Charité - Universitätsmedizin Berlin.

2.10.1.1 Alizarin Red S staining

After 21 days of culture under osteogenic conditions or in hMSC expansion medium, mineralised bone matrix was visualised by staining with the dye Alizarin Red S.

To stain the cells they were washed with PBS and fixed for 20min in 4% paraformaldehyde in PBS. Subsequently, the fixed cells were washed three times with PBS and the cells were incubated in 1ml of a 2% Alizarin Red S solution in $_{dd}H_2O$ (7.1.4.1) for 5min. The excess dye was washed away with water and the stained cells were covered with PBS and stored at 4°C until images were acquired.

2.10.2 *In vitro* adipocyte differentiation

To differentiate hMSCs and iMSC into adipocytes, $1x10^5$ cells were seeded per well of a six well plate and $0.5x10^5$ cells were seeded per well of a twelve well plate. The cells were seeded in six wells of a six well plate and six wells of a twelve well plate and cultured in hMSC maintenance medium until 80% confluence was reached. At this point half of the wells in six well and twelve well plate format were filled with adipogeneic medium using the StemPro® Adipogenesis Differentiation Kit (A10070-01, Life Technologies). The cells in the other wells were cultured in hMSC maintenance medium as control. The differentiation was carried out for 21 days with a medium change every three days. On day 21, cells in the twelve well plate format were fixed for staining with Oil Red O and the cells in the six well plate format were used for RNA isolation in order to measure the expression of the marker genes *PPARG* and *LPL*. Adipocyte differentiation of aged hMSC (74y) was carried out with a different protocol as part of a master thesis which was previously published (Megges 2010).

2.10.2.1 Oil Red staining

To visualise lipids in the vacuoles of differentiated adipocytes, the differentiated cells were stained with the lipophilic dye Oil Red O.

After 21 days of culture under adipogenic conditions or in hMSC maintenance medium the cells were washed with PBS and fixed for 20min in 4% paraformaldehyde in PBS. At this point, the fixed cells

were washed three times with PBS and the cells were covered with 100% propylene glycol for 5min at RT. Subsequently the polypropylene glycol was removed and replaced by a filtered Oil Red O staining solution diluted in water (7.1.4.2). The cells were left in the solution for four h at RT followed by a 5min incubation in 85% propylene glycol. The lipid vacuoles of adipocytes were now visible in red. After staining, the plates were left to dry and stored at 4ºC until images were acquired.

2.10.3 Chondrocyte differentiation

To differentiate hMSCs into chondrocytes the cells were harvested using trypsin, counted using a haemocytometer and $5x10^5$ cells were spun down to form a cell pellet. In order to differentiate iMSCs into chondrocytes, the cells were detached by trypsin, counted and a cell solution of $1.6x10^7$ cells per ml of hMSC maintenance medium was prepared. A 5µl drop of this solution was seeded per well of a 48 well plate to prepare micro mass cultures. The cell solution drops were incubated under high humidity at 37°C in an incubator. Subsequently, the micro mass cultures were cultured in chondrogenic medium using the StemPro® Chondrogenesis Differentiation Kit (A10071-01, Life Technologies). The hMSC cell pellets were cultured in 15ml centrifugation tubes in 1ml of the same chondrogenic medium after they were cultured in hMSCs maintenance medium for one day after the centrifugation step. For chondogenic differentiation of iMSCs, six wells of a 48 well plate were used and for chondrocyte differentiation of hMSCs, ten pellets were prepared per primary hMSC preparation. Half of the wells or pellets were cultured in hMSC maintenance medium as a control. The medium was changed every three days for 21 days. At day 21 successful chondrocyte differentiation of iMSCs was visualised using Alcian Blue staining of all micro mass culture wells. Two pellets cultured under chondrogenic conditions and two control pellets were stained with Alcian Blue at day 21 of the chondrocyte differentiation of hMSCs. In addition, RNA was isolated after 21 days of the chondrocyte differentiation of fetal hMSC 1 for expression analysis of the marker gene *COL1A1*.

2.10.3.1 Alcian blue staining

Successful chondrocyte differentiation was visualised by blue staining of proteoglycans produced by chondrocytes through Alician Blue staining. To do this, the micro mass cultures and cell pellets were washed with PBS and fixed with 4% paraformaldehyde in PBS. Subsequently, the fixed cells were washed with PBS and incubated in a 1% Alcian Blue solution in 0.1 N HCl for 30min, followed by three washes with 0.1N HCl and the addition of water to dilute the acidity. The micro mass cultures and pellets were stored at 4ºC after staining until bright-field images were acquired of the stained cells.

2.10.4 Visualisation of senescence – β-galactosidase staining

hMSCs were stained using the Senescence β-galactosidase Staining Kit (Cell Signaling Technology, #9860) following the instructions of the manufacturer. Briefly, the hMSCs maintenance medium was

removed and the cells were washed three times with PBS. The cells were cultured in one well of a 12 well plate each. Subsequently, 1x fixative solution consisting of 20% formaldehyde, 2% glutaraldehyde in 10 x PBS diluted 1:10 in $_{dd}H_2O$ was added, followed by incubation for 15min at RT. The cells were then rinsed with PBS for two times and incubated in β-galactosidase staining solution in a cell culture dish sealed with Para film at 37°C overnight in a dry incubator. The cells were checked on the next day under a bright-field microscope for the development of blue colour indicating senescence-associated β-galactosidase. For long-term storage, the stained cells were covered with 70% glycerol and stored at 4°C.

2.10.5 Colony-forming unit assay

hMSCs and iMSCs were analysed toward their numbers colony-of forming unit fibroblastoid cells as described previously (Colony Forming Unit Assays for MSCs - Springer 2008). hMSCs and iMSCs that were 80% confluent were detached from surface of the culture vessel using trypsin-EDTA and counted with a haemocytometer. 100 cells per 100mm^2 tissue culture dish were seeded in six wells of a six well plate and cultured in hMSC maintenance medium at 37°C in 5% CO_2 in a humidified atmosphere for ten days, with a media change every three days. Subsequently, the cells were washed with PBS and fixed in 4% paraformaldehyde in PBS for 20min at RT. Finally, the fixed cells were stained with 0.5% Crystal violet in methanol for 10min at RT. The excess dye was washed off and the stained cells were left to dry before image acquisition with a bright-field microscope.

2.11 Generation of induced pluripotent stem cells by retroviral transduction

2.11.1 Generation of retroviral particles

To generate retroviral particles for subsequent use in reprogramming experiments, 8x10^6 HEK293T cells were seeded per 150mm tissue culture dish. The cells were cultured in MEF maintenance medium for 24h. Two h before transfection the medium was changed to HEK293T medium (7.1.5.1). The cells were then transfected with a mix of plasmids consisting of

9µg of plasmid pCMV-VSV-G (harbouring a gene encoding a virus envelope protein)

20µg plasmid pUMVC3-gag-pol (harbouring a gene encoding proteins for viral packaging)

32µg of plasmid, either pMXs-hOCT4 or pMXs-hSOX2 or pMXs-hKLF4 or pMXs-hc-Myc or pLIB-GFP.

The plasmid mix was prepared with a final volume of 1125µl $_{dd}H_2O$. This was followed by addition of 125µl of 2.5M $CaCl_2$ to each plasmid DNA mix and an incubation of 5min at RT. While vortexing at full speed, 1250µl of a 2 x HBS (7.1.5.2) solution was added dropwise to the plasmid–$CaCl_2$ mixture to generate precipitates for transfection. This mixture was added to the HEK293T cell immediately by dropwise addition and distribution into the medium. HEK293T cells were incubated for 14 h with the plasmid DNA precipitates, followed by medium change. The retroviral particles produced by the transfected cells were harvested by collecting the medium 24 h and 48 h after transfection. The medium of the respective virus particle was pooled and filtered with a 0.45µm pore size syringe driven filter (Durapore). The filtered supernatant was centrifuged in Polyallomer centrifugation tubes using 20,000 rpm for 2h at 4°C in vacuum with a Beckman L7 Ultracentrifuge with a rotor type SW-28. After the centrifugation step, the supernatant was discarded and the pelleted retroviral particles were resuspended in 200-400µl Knock-out™ DMEM. The suspension was incubated at 4°C overnight, followed by careful mixing and subsequent aliquoting for storage at -80°C until use for transduction.

2.11.2 Calculation of the retrovirus titer

Fetal hMSC 1 were seeded with a density of $6x10^4$ cells per well of a twelve well plate in hMSC maintenance medium. After 24 h 1µl, 10µl and 100µl of the retrovirus suspension produced with the plasmid pLIB-GFP were added to 1ml hMSC maintenance medium in the well to the cells. In addition, 4µg/ml polybrene (Sigma-Aldrich, 107689-10G) were added per well and distributed by mild agitation. This was followed by a centrifugation of the culture plates at 2,000rpm, 37°C for 90min. After the centrifugation step, the medium was changed and the cells were left to grow for 48h in hMSC maintenance medium. Finally, the cells were trypsinised and the number of GFP-positive cells for each transduction was determined using FACS and used for the calculation of the virus-titer using the following equation:

$$TU/\mu l = (PxN / 100xV) \times 1/DF$$

TU = transducing units
P = % GFP positiv cells
N = number of cells at time of transduction in each well
V = volume of dilution added to each well
DF = dilution factor (1 = undiluted)

The retroviral particles harbouring *OCT4*, *SOX2*, *KLF4* and *c-MYC* were assumed to have the same titer as the particles harbouring *GFP*.

2.11.3 Verification of functionality of produced viral particles

Before being used in reprogramming experiments the retroviral particles harbouring *OCT4*, *SOX2*, *KLF4* and *c-MYC* were tested. Doing this, fetal hMSC 1 were seeded with a density of $6x10^4$ cell per well of a twelve well plate. Subsequently, the cells were transduced with the retroviral particles for the expression of OCT4 or SOX2 or KLF4 or c-MYC. Subsequently, the cells were fixed 48 hours after the transduction and stained for the respective protein encoded by the transgene using immunofluorescence staining and staining of the nuclei by DAPI. The staining results were monitored by confocal microscopy using a LSM510 meta confocal microscope.

2.11.4 Pluripotency induction in hMSCs mediated by retroviral transduction

2.11.4.1 Retrovirus transduction

Retroviral reprogramming of hMSCs was conducted using retrovirus-mediated expression of *OCT4*, *SOX2*, *KLF4* or *c-MYC*. The viral transduction was carried out in a laboratory of the security level S2. hMSCs were plated in six well plates with a seeding density of $2.5x10^5$ cells per well of a 6-well plate and cultured in hMSC maintenance medium overnight followed by a medium change. Subsequently, the equivalent volumes of 2.5 transduction units per cell for $2.5x10^5$ cells per well of a six well plate of retroviruses harbouring the genes *OCT4*, *SOX2*, *KLF4* or *c-MYC* were mixed. The mixed particles were added to each well followed by supplementation with 4µg/ml Polybrene (Sigma-Adrich) per well. This was followed by a centrifugation of the culture plates at 2,000rpm, 37°C for 90min. The cells were then incubated at 37°C and 5% CO_2 in humidified atmosphere for 24 hours. At this point the medium was changed and the cells were transduced a second time using the same amount of particles followed by a centrifugation of the culture plates at 2000rpm, 37°C for 90min. Subsequently, cell culture plates coated with Matrigel® (Corning) and $1.5x10^5$ feeder cells per well of a 6 well plate were prepared one day prior to splitting the transduced hMSCs. After a second incubation for 24h, the transduced cells were washed with PBS and harvested using trypsin. The cells were split with a ratio of 1:4 and seeded onto the previously prepared plates coated with Matrigel® and feeder cells and cultured in hMSC maintenance medium for two days. Subsequently, the medium was changed to the respective medium used for reprogramming specified in Table 5. The cells were either cultured under normoxia or und hypoxic conditions using a hypoxia incubator (C-200, LABOTECT) at 37°C, 5% CO_2 and 5% O_2. Retroviral transduction was carried out using fetal hMSC 1, fetal hMSC 2, aged hMSC (60y), aged hMSC (62y) and aged hMSC (70y) using the same batch of viral particles. Aged hMSC (74y) were transduced and reprogrammed as part of a previous master thesis using retroviral particles for overexpression of OCT4, SOX2, KLF4 and c-MYC produced with the same protocol (Megges 2010).

2.11.4.2 Reprogramming of transduced cells

The day when hMSCs were first transduced was defined as day zero of the respective reprogramming experiment. Throughout reprogramming 8ng/ml FGF2 were added to the reprogramming medium and the medium was changed every other day. The reprogramming conditions were adapted from a study in which they were used for episomal plasmid-based reprogramming (J. Yu et al. 2011) N2B27 medium (7.1.1.4) was used supplemented with 8ng/ml FGF2 as well as with and without a combination of 0.5µM MEK inhibitor PD0325901, 3µM GSK3β inhibitor CHIR99021, 0.5µM TGF-β/Activin/Nodal receptor inhibitor A-83-01 and 10µM ROCK inhibitor HA-100. [14] (smM, Table 5) The reprogramming of the transduced cells was conducted under normoxia or under hypoxia using a hypoxia incubator (C-200, LABOTECT) at 37°C, 5% CO_2 and 5% O_2. The treatment with inhibitors was started when the medium was changed to N2B27 medium. The inhibitors were stored according to the manufacturer´s instructions. In addition, one condition of viral reprogramming was a medium switch from N2B27 medium to mTeSR at day 14 of the reprogramming experiment (J. Yu et al. 2011) (Table 5). The medium was changed every other day until iPSC-like colonies were isolated. In the case of fetal hMSC 1 iPS-like colonies were isolated on day 55. The experiments were stopped at day 65 in case of fetal hMSC 2, aged hMSC (60y) and aged hMSC (62y) or on day 55 in the case of aged hMSC (70y). Aged hMSC (74y) were reprogrammed in my master thesis by being infected with retroviruses carrying *OCT4*, *SOX2*, *KLF4* or *c-MYC* and seeded onto six well plates coated with $2.5x10^5$ feeder cells per well. Until day seven the cells were cultured in unconditioned medium supplemented with 4ng/ml FGF2. At this point, the cells were cultured in conditioned medium with a supplementation of 4ng/ml FGF2. Furthermore, during the course of reprogramming the medium was supplemented with 0.5µM MEK inhibitor PD325901, 2µM inhibitor of the TGFβ receptors ALK4, ALK 5 and ALK 7 SB-431542 and 10µM P53 inhibitor pifithrin α. The medium was changed every other day until iPSCs could be isolated at day 40 after the transduced cells were seeded (Megges 2010).

Table 5 Reprogramming conditions used for retroviral reprogramming of hMSCs.

H: Hypoxia, cell culture in 5% oxygen; N: normoxia, cell culture under normoxic conditions; smM: cocktail of MEK inhibitor 0,5µM PD0325901, 3µM GSK3β inhibitor CHIR99021, 0.5µM TGF-β/Activin/Nodal receptor inhibitor A-83-01 and 10µM ROCK inhibitor HA-100. PD: 0.5µM MEK inhibitor PD0325901, SB: 2µM TGFβ receptor inhibitor SB-431542, p53i: 10µM P53 inhibitor pifithrin α. The reprogramming experiment of aged hMSC (74y) was part of a previously published master thesis (Megges 2010). mTeSR= culture in mTeSR 1 from day 14 post transduction.

primary hMSC	passage at transduction	Hypoxia (H)/ Normoxia(N)	addtion of small molecules (smM)	additional conditions	iPS cell lines established
fetal hMSC 1	2	N			
fetal hMSC 1	2	H			iPSC (hMSC, fetal line 1, viral)
fetal hMSC 1	2	H		mTeSR	
fetal hMSC 1	2	H	smM		
fetal hMSC 1	2	H	smM	mTeSR	
fetal hMSC 2	2	N			
fetal hMSC 2	2	H			
fetal hMSC 2	2	H		mTeSR	
fetal hMSC 2	2	H	smM		
fetal hMSC 2	2	H	smM	mTeSR	
aged hMSC (60y)	2	N			
aged hMSC (60y)	2	H			
aged hMSC (60y)	2	H		mTeSR	
aged hMSC (60y)	2	H	smM		
aged hMSC (60y)	2	H	smM	mTeSR	
aged hMSC (62y)	2	N			
aged hMSC (62y)	2	H			
aged hMSC (62y)	2	H		mTeSR	
aged hMSC (62y)	2	H	smM		
aged hMSC (62y)	2	H	smM	mTeSR	
aged hMSC (70y)	2	N			
aged hMSC (70y)	2	H			
aged hMSC (70y)	2	H	smM		
aged hMSC (74y)	2	N		SB, PD, p53i	iPSC (hMSC, 74y, viral)

2.11.5 Monitoring of transduction efficiency

hMSCs that were transduced with *OCT4*, *SOX2*, *KLF4* and *c-MYC* carrying viruses were transduced only with a *GFP*-carrying retrovirus in parallel as described in the section 'retroviral transduction'. The transduced cells were washed with PBS and detached using trypsin on the next day. The cells were resuspended in PBS and GFP-positive cells were measured for calculation of the transduction efficiency using a flow cytometer as described in the section 'fluorescence-activated cell sorting' and pictures were taken using a LSM510 meta confocal microscope.

2.12 Reprogramming using episomal plasmids

2.12.1 Plasmid amplification and verification

The episomal plasmids pEP4 E02S EN2K, pCEP4-M2L and pEP4 E02S ET2K (vector maps see 7.1.6.1) were received as glycerol stocks of already transformed bacteria. The bacteria were expanded in LB medium (7.1.3.1) and the plasmids were isolated and quality-checked as described in the section 'amplification of plasmid DNA'.

2.12.2 Nucleofection of hMSCs to deliver episomal plasmids

The primary hMSCs fetal hMSC 1, fetal hMSC 2, aged hMSC (60y) and aged hMSC (62y) were cultured in hMSC maintenance medium until they reached 80% confluence. At this point the cells were washed with PBS and detached from the surface using trypsin. The cells were then counted using a haemocytometer. To deliver the episomal plasmids to the cells the Human MSC (Mesenchymal Stem Cell) Nucleofector® Kit (Lonza, VPE-1001) and the Amaxa Nucleofector II® Device (Lonza) were used following the protocol of the manufacturer and by using the episomal plasmid combination 7F2 which was described in a recent study (J. Yu et al. 2011).
$1x10^6$ hMSCs were mixed with the plasmid DNA by combining:

-3µg of pEP4 EO2S EN2K
-3.2µg of pEP4 EO2S ET2K
-2.4µg of pCEP4-M2L
-100µl Human MSC Nucleofactor solution warmed to RT
-the respective volume of $1x10^6$ hMSCs

The solution was mixed under aseptic conditions and transferred to an Amaxa-certified cuvette delivered with the kit used. The lid was closed and the cuvette was placed in the nucleofector device after the absence of air bubbles was confirmed. All hMSCs were nucleofected with the program U-23 for high nucleofection efficiency. The nucleofected cell suspension was immediately transferred to a $150cm^2$ cell culture dish containing pre-warmed hMSC maintenance media. The nucleofected cells were cultured for 6 days with a media change every other day and subsequently shared to Matrigel® and feeder cell-coated 6 well plates with a seeding density of $6x10^4$ per well of a 6 well plate. The same nucleofection was carried out using the control plasmid pmax-GFP which is part of the the Human MSC (Mesenchymal Stem Cell) Nucleofector® Kit instead of the episomal plasmids. The nucleofection efficiency was monitored subsequently using either a flow cytometer as described in the section 'fluorescence-activated cell sorting' or by confocal microscopy using a microscope of the model LSM510 Meta (Zeiss).

2.12.3 Pluripotency induction in hMSCs by means of nucleofection with episomal plasmids

The day the nucleofected hMSCs were seeded onto feeder-coated cell culture dishes was defined as day zero of the reprogramming experiment. The nucleofected hMSCs were immediately cultured in N2B27 medium (7.1.1.4) supplemented with 4ng/ml FGF2 with and without the addition of the small molecule inhibitor cocktail smM (Table 6) and in case of aged hMSC (62y) with addition of 50µg/ml vitamin c, as previously described (Gao et al. 2013), as well as a medium switch to mTeSR 1 from day 14. In addition, the nucleofected cells were cultured under normoxia or under hypoxic conditions in 5% oxygen. The medium was changed every other day. All experimental conditions used for episomal plasmid-based reprogramming are listed in Table 6. The reprogramming experiment was stopped at day 41 or 45 when iPS colonies were isolated from fetal hMSC 1 or on day 54 in the reprogramming experiments of fetal hMSC 2, aged hMSC (60y) and aged hMSC (62y).

Table 6 Experimental conditions used for episomal plasmid-based reprogramming of hMSCs. Reprogramming conditions used for episomal plasmid-based reprogramming of hMSCs. H: hypoxia, cell culture in 5% oxygen; N: normoxia, cell culture under normoxic conditions; smM: cocktail of MEK inhibitor 0.5µM PD0325901, 3µM GSK3β inhibitor CHIR99021, 0.5µM TGF-β/Activin/Nodal receptor inhibitor A-83-01 and 10µM ROCK inhibitor HA-100. mTeSR= culture in mTeSR 1 from day 14 post-nucleofection. vitamin c= 50µg/ml vitamin c

primary hMSC	passage at nucleofection	Hypoxia (H)/ Normoxia(N)	addtion of small molecules (smM)	additional conditions	iPS cell lines established
fetal hMSC 1	2	N			iPSC (hMSC, fetal, line 1, episomal 3)
fetal hMSC 1	2	N	smM		iPSC (hMSC, fetal, line 1, episomal 1) iPSC (hMSC, fetal, line 1, episomal 2)
fetal hMSC 1	2	H			
fetal hMSC 1	2	H	smM		
fetal hMSC 2	2	N			
fetal hMSC 2	2	H			
fetal hMSC 2	2	H	smM		
aged hMSC (60y)	2	N			
aged hMSC (60y)	2	H			
aged hMSC (60y)	2	H	smM		
aged hMSC (62y)	2	N			
aged hMSC (62y)	2	H		Vitamin C from day14 mTesR	iPSC (hMSC, 62y, episomal)
aged hMSC (62y)	2	H	smM		

2.13 Isolation of iPS clones and establishment of iPS cell lines

The morphological changes of the hMSCs during the reprogramming experiments were monitored by bright-field microscopy. The colony-like structures containing cells with a high nucleus to cytoplasm

ratio and a high similarity to human embryonic stem cells were chosen for isolation. The iPS clones were cut manually into four pieces using a sterile BD Microlance™ 3 injection needle (Becton Dickinson) and transferred to a well of a twelve well plate coated with Matrigel® and feeders and containing fresh unconditioned medium supplemented with 4ng/ml FGF2 and 10µM ROCK inhibitor as previously described (Watanabe et al. 2007). The attached colonies were cultured further and passaged every seven days with a ratio of 1:1 onto new feeders. The medium was changed every day. The iPS clones were cultured until passage six to obtain stable iPS cell lines. After passage six the characterisation of the iPS cell lines was started.

2.14 Experimental conditions used for modulation of reprogramming efficiency in aged hMSCs

hMSCs were transduced or nucleofected as described in the respective section. After being seeded onto feeder-coated cell culture plates the cells were cultured under conditions potentially modulating age-related obstacles of hMSC reprogramming using conditioned medium supplemented with 4ng/ml FGF2, N2B27 medium with and without the inhibitor cocktail smM described for the viral and non-viral reprogramming, N2B27 medium supplemented with 2mM valproic acid (Stemgent, 04-0007) (Huangfu et al. 2008a) and smM, N2B27 medium supplemented with 50µg/ml L-ascorbic acid (Sigma-Aldrich, 57803) (Tao Wang et al. 2011) with and without smM, N2B27 medium with a combination of 2µM valproic acid (Stemgent, 04-0007), 10µM P53 inhibitor pifithrin α and 25µg/ml vitamin c (Yulin et al. 2012), N2B27 medium supplemented with 10µM P53 inhibitor pifithrin α and smM, N2B27 medium supplemented with 10µM of the insulin-like growth factor receptor (IGF1R) inhibitor PQ401 (Sivakumar et al. 2009) (Tocris Biosciences, 2768) and N2B27 medium supplemented with 10µg/ml of the Toll-like receptor 3 agonist Polyinosinic-polycytidylic acid poly (I:C) (Tocris Biosciences, 4287) (West et al. 2011). In addition, all conditions were carried out with an additional switch to mTeSR 1 (Stemcell Technologies) at day 14 after the start of the reprogramming experiments. These conditions were tested for fetal hMSC 1, fetal hMSC 2, aged hMSC (60y) and aged hMSC (62y). All conditions tested are listed in Table 7. The medium was changed every other day and the reprogramming efficiency was calculated based on the count of the colonies of embryonic stem cell-like morphology after 45 days.

Table 7 Overview of experimental conditions used to modulate reprogramming efficiency in hMSCs derived from fetal and aged origin.

smM: cocktail of MEK inhibitor 0.5µM PD0325901, 3µM GSK3β inhibitor CHIR99021, 0.5µM TGF-β/Activin/Nodal receptor inhibitor A-83-01 and 10µM ROCK inhibitor HA-100. mTeSR: culture in mTeSR 1 from day 14 post-transduction/nucleofection. CM: conditioned medium, VPA: 2mM in the condition VPA smM and 2µM valproic acid in condition VPA P53 VitC, VitC: 50µg/ml vitamin c in combination VitC smM and 25µg/ml vitamin c in combination VPA P53 VitC; P53=10µM of P53 inhibitor pifithrin α, IGF Inh: 10µM insulin-like growth factor receptor (IGF1R) inhibitor PQ401; TLR3 Agon: 10µg/ml Toll-like receptor 3 agonist Polyinosinic-polycytidylic acid poly (I:C). All experiments were carried out under hypoxic conditions in 5% oxygen.

condition	medium	modulation
normal	N2B27	
mTeSR	N2B27, from day 14 mTeSR 1	
smM	N2B27	inhibition of MEK, TGFβ receptor, GSK3β, Rho associated kinase
mTeSR	N2B27+smM, from day 14 mTeSR 1	
CM	conditioned medium	
mTeSR	CM, from day 14 TeSR 1	
smM VPA	N2B27	inhibiton of MEK, TGFβ receptor, GSK3β, Rho associated kinase, histone deacetylase
mTeSR	N2B27+smM VPA, from day 14 mTeSR 1	
VitC	N2B27	antioxidant
mTeSR	N2B27+VitC, from day 14 mTeSR 1	
smM VitC	N2B27	antioxidant and inhibition of MEK, TGFβ receptor, GSK3β, Rho associated kinase
mTeSR	N2B27+smM VitC, from day 14 mTeSR 1	
VPA p53 VitC	N2B27	antioxidant, inhibition of histone deacetylase, p53
mTeSR	N2B27+VPA p53 Vit C, from day 14 mTeSR 1	
smM p53	N2B27	inhibiton of MEK, TGFβ receptor, GSK3β, Rho associated kinase, p53
mTeSR	N2B27+smM p53 , from day 14 mTeSR 1	
IGF Inh	N2B27	insulin-like growth factor receptor (IGF1R)
mTeSR	N2B27+IGF Inh , from day 14 mTeSR 1	
TLR3 Agon	N2B27	stimulation of Toll-like receptor 3 (TLR3)
mTeSR	N2B27+TLR3 Agon , from day 14 mTeSR 1	

2.15 Characterisation of induced pluripotent stem cells

2.15.1 Alkaline phosphatase staining

The pluripotency marker Alkaline Phosphatase was visualised in hMSC-iPSCs using Alkaline Phosphatase Live Stain (Life Technologies, A14353) following the instructions of the manufacturer. Doing this, iPSCs were cultured under iPSC maintenance conditions using feeders until 50% confluence was reached. The unconditioned medium was aspirated and the cells were washed with Knock Out™ DMEM warmed to 37°C. The 500 x AP live stain stock solution was diluted in pre-warmed Knock Out™ DMEM to 1:500. The resulting 1 x AP live staining solution was applied to the

cells after removal of the previous medium, followed by an incubation at 37°C for 20min in the dark. Subsequently, the 1 x AP live staining solution was removed and the cells were washed with PBS and covered with unconditioned medium with FGF. The positive staining result was visualised using a confocal microscope.

2.15.2 Confirmation of pluripotency markers

To confirm the presence of the pluripotency markers OCT4 SOX2, KLF4, c-MYC, SSEA4, TRA-1-60 and TRA-1-81 as well as absence of SSEA1, hMSC-iPSCs were cultured with feeder cells and unconditioned medium supplemented with FGF2 until 50-70% confluence were reached. Subsequently, immunofluorescence staining was performed as described in the respective section using the primary antibodies against OCT4 (Santa Cruz, sc-5279), SOX2 (Santa Cruz, sc-17320), KLF-4 (Santa Cruz, sc-20691), c-MYC (Santa Cruz, sc-764), NANOG (Abcam, ab62734) and SSEA1, SSEA4, TRA-1-60, as well as TRA-1-81 (all Merck Millipore, #SCR004) in combination with the respective fluorophore-conjugated secondary antibodies for visualisation. Subsequently, images were acquired using a confocal microscope. The dilutions used for the respective primary and secondary antibodies are listed in Table 4.

2.15.3 *In vitro* confirmation of pluripotency by embryoid body-based differentiation

hMSC-iPSCs were grown until confluence was reached in three wells of a six well plate. Subsequently, the colonies were cut in equally sized pieces using a BD MicrolanceTM 3 injection needle (Becton Dickinson), followed by a medium change to 1ml unconditioned medium without FGF per well, and scraping of the iPSC colony pieces using a cell scraper. 60mm ultra-low attachment culture dishes (Corning) were filled with 5ml unconditioned medium without FGF and the suspension containing the scraped cells from three well of a 6 well plate was transferred to these dishes. The formation of embryoid bodies was monitored using bright-field microscopy. The medium was changed every other day by transferring the embryoid body medium suspension in a sterile 15ml plastic tube and letting the embryoid bodies settle on the bottom for 5min. The supernatant was removed and fresh medium was added, followed by a transfer back to the low attachment culture dish. After seven days of suspension culture in low attachment dishes, the embryoid bodies were transferred and distributed to 12 wells of a 24 well plate coated with 0.1% gelatine, culturing them further in the same medium without FGF. The medium was again changed every other day for 7 and for 14 days. At day 7 and day 14, the embryoid bodies and outgrowing cells on gelatine were fixed using 4% paraformaldehyde in PBS. The differentiation of the embryoid bodies into derivatives of ectoderm, endoderm and mesoderm was confirmed by immunofluorescence staining using antibodies against the mesodermal marker Brachyury (T) (Santa Cruz, sc-20109) to stain the embryoid bodies and outgrowth

that were fixed on day 7. The embryoid bodies and outgrowth that was fixed after 14 days was stained using antibodies against the mesodermal marker Smooth-Muscle-Actin (SMA) (Dako, M0851), against the endodermal markers Alpha-Fetoprotein (AFP) (Sigma-Aldrich, WH0000174M1), SOX17 (R&D, AF1924) and against the ectodermal markers Nestin (Chemicon, MAB5326) and β-TubulinIII (Sigma-Aldrich, T8660). The immunofluorescence staining was carried out as described in the respective section above. Images of the staining were acquired using a confocal microscope. The dilutions of the primary and secondary antibodies used in these experiments are listed in Table 4.

2.15.4 *In vivo* pluripotency test – teratoma assay

The confirmation of pluripotency of iPSC (hMSC, 74y, viral) by the teratoma formation assay was carried out by EPO Berlin GmbH. iPSC (hMSC, 74y, viral) were grown under feeder free conditions using conditioned medium until confluent. The cells were washed, treated with trypsin for 2min, where after the trypsin was washed away using conditioned medium. Approximately $2x10^6$ iPS cells were resuspended in Matrigel® and injected subcutaneously into NOD.Cg-Prkdcscid Il2rgtm1Wjl/SzJ mice (NOD scid gamma (NSG) mice). The experiment was carried out in duplicate. Mice that developed tumours at the site of injection were sacrificed at day 72 after injection. The tumour tissue was isolated and embedded in paraffin. Tissue sections were analysed by a pathologist after haematoxylin and eosin staining for presence of structures of mesoderm, ectoderm or endoderm.

2.15.5 DNA fingerprinting

Genomic DNA was isolated from hMSC-iPSCs, which were grown under feeder free conditions, from parental hMSCs and from hESC H1 and hESC H9 as described in the section isolation of DNA. 50ng of the genomic DNA were used as template in a PCR using primers amplifying the variable numbers of tandem repeats (VNTR) across the whole genome, resulting in a specific mixture of amplicons with different sizes enabling the distinction between cell lines. The amplicon size patterns of the parental hMSCs were compared to the patterns of the corresponding iPSCs and hESC H1 as well as hESC H9 to rule out cross-contamination and to confirm the somatic origin of the iPS cell lines generated. The PCR products were resolved using agarose or acrylamide gel electrophoresis and visualised using Ethidiumbromid. The details of PCR and primer sequences are explained in the sections polymerase chain reaction and gel electrophoresis. The primer sequences are listed in Table 2.

2.15.6 Karyotyping

Chromosomal analysis by GTG banding was performed to detect karyotypical abnormalities in hMSCs of fetal and aged background as well as in corresponding iPSCs. The karyotyping analysis was performed by Human Genetic Center of Berlin. 10 karyograms were generated and 20 metaphases were analysed of fetal hMSC 1, fetal hMSC 2, aged hMSC (60y), aged hMSC (70y), aged hMSC

(74y), iPSC (hMSC, fetal, line 1, episomal 1), iPSC (hMSC, fetal, line 1, episomal 2), iPSC (hMSC, fetal, line 1, episomal 3) and iPSC (hMSC, 74y, viral).

2.15.7 Confirmation of absence of episomal plasmids

To confirm that episomal plasmids were lost in iPSC (hMSC, fetal, line 1, episomal 1), iPSC (hMSC, fetal, line 1, episomal 2), iPSC (hMSC, fetal, line 1, episomal 3) and iPSC (hMSC, 62y, episomal), genomic DNA was isolated from these cells and 100ng of these were used as template in a PCR using primers specific for the OriP sequence and the transgenes EBNA1 and SV40LT which are not present in the human genome. The same PCR was carried out using the episomal plasmid pEP4 E02S ET2K as template, using it as positive control. The absence of a PCR product in gDNA from episomal plasmid-derived iPSCs and presence of a PCR product when pEP4 E02S ET2K was used, was interpreted as absence of the episomal plasmids in the respective iPS cells. The details of the PCR reaction and the primer secquences are explained in the section polymerase chain reaction. The primer sequences are listed in Table 2.

3 Results

In the following section bone marrow-derived mesenchymal stem cells will be referred to as hMSCs. Bone marrow-derived mesenchymal stem cells isolated from fetal femur at day 55 post-conception will be named fetal hMSCs. Two primary cell preparations of fetal hMSCs, fetal hMSC 1 and fetal hMSC 2 were used in this study. hMSCs isolated from the bone marrow of aged donors will be referred to as aged hMSCs. The age of the respective donor can be found in brackets behind the name. The letter 'y' stands for years in this case. Four aged hMSC preparations were used in the course of this study: aged hMSC (60y) derived from a 60-year-old donor, aged hMSC (62y) derived from a 62-year-old donor, aged hMSC (70y) derived from a 70-year-old donor and aged hMSC (74y) derived from the bone marrow of a 74-year-old-donor. Moreover, human fetal foreskin fibroblasts will be named hFF. Induced pluripotent stem cells will be named iPSCs or iPS cells in the following section. The iPS cell line derived from fetal hMSC 1 using retroviral reprogramming will be named iPSC (hMSC, fetal, line 1, viral). The three iPS cell lines derived from fetal hMSC 1 using episomal plasmid-based reprogramming will be named iPSC(hMSC, fetal, line 1, episomal 1), iPSC (hMSC, fetal, line 1, episomal 2) and iPSC (hMSC, fetal, line 1, episomal 3). The iPS cell line derived from aged hMSC (62y) using episomal plasmid-based reprogramming will be called iPSC (hMSC, 62y, episomal). The iPS cell line derived from aged hMSC (74y) by means of retroviral reprogramming will be named iPSC (hMSC, 74y, viral). iPSCs derived from hFF by retroviral reprogramming will be named iPSC (hFF, viral). Human embryonic stem cells will be referred to as hESCs. In addition, mesenchymal stem cell-like cells derived from hESC H1 and hMSC-iPSCs will be referred to as iMSCs. iMSCs derived from hESC H1 will be referred to as iMSC (hESC H1). iMSCs derived from iPSC (hMSC, fetal, line 1, viral) will be named iMSC (fetal, line 1, viral). iMSCs differentiated from iPSC (hMSC, 74y, viral) will be named iMSC (74y, viral).

The two primary hMSC preparations isolated from fetal femur and the four primary hMSC preparations isolated from the bone marrow of 60-year-old, 62-year-old, 70-year-old and 74-year-old donors were used in this study to compare age-related changes between these two age groups and to analyse the effect of the age-related differences between these two age groups on the induction of pluripotency, on the features of iPSCs and on the features of iMSCs from hMSC-iPSCs with different age backgrounds.

3.1 Characterisation of fetal hMSCs and hMSCs of aged donors used for pluripotency induction

Before the hMSCs, that were used in this study, were employed to characterise the effect of age-related differences on pluripotency induction and on the features of iPSCs and iMSCs, a confirmation of typical hMSC features was carried out. Doing this, the fulfilment of the criteria for mesenchymal

stem cells set by the International Society for Cellular Therapy (Dominici et al. 2006), such as morphology, surface marker expression and ability to differentiatiate into osteoblasts, chondrocytes and adipocytes, was analysed.

3.1.1 Confirmation of MSC-specific features in hMSCs of fetal and aged background

Both fetal hMSCs and hMSCs of aged donors showed a fibroblast-like morphology, whereas hMSCs from aged donors were bigger in size than fetal hMSCs (Figure 4 A). The pictures shown in Figure 4 A are representative of the morphology of the other primary hMSCs used in this study. Fetal hMSC 2 showed a morphology similar to the morphology of fetal hMSC 1, whereas the morphology of aged hMSC (70y) was similar to the morphology of aged hMSC (62y), aged hMSC (70y) and aged hMSC (74y). In addition, fetal hMSCs proliferated faster than hMSCs of aged donors. This led to confluence within two days after fetal hMSCs were seeded at a density of $1x10^3$ cells per cm^2. hMSCs of aged donors reached confluence within 5 to 8 days after being seeded at the same initial density (data not shown). Moreover, using microarray-based gene expression profiling, the expression of MSC marker genes *CD90*, *CD73* and *CD105* could be confirmed in the two fetal hMSC preparations as well as in hMSCs from older donors with 60, 62, 70 or 74 years of age. In contrast to that, expression of the hematopoietic marker genes *CD14*, *CD45* and *CD34* could not be detected. However, hESC H1 were found to express only the marker gene *CD90* (Figure 4 B). Moreover, the presence of hMSC surface markers *CD90*, *CD73* and *CD105* and the absence of hematopoietic markers *CD14*, *CD20*, *CD34* and *CD45* could be confirmed using flow cytometry-based detection of these markers for fetal hMSC 1, aged hMSC (62y) and aged hMSC (74y) against an isotype control (Figure 4 C).

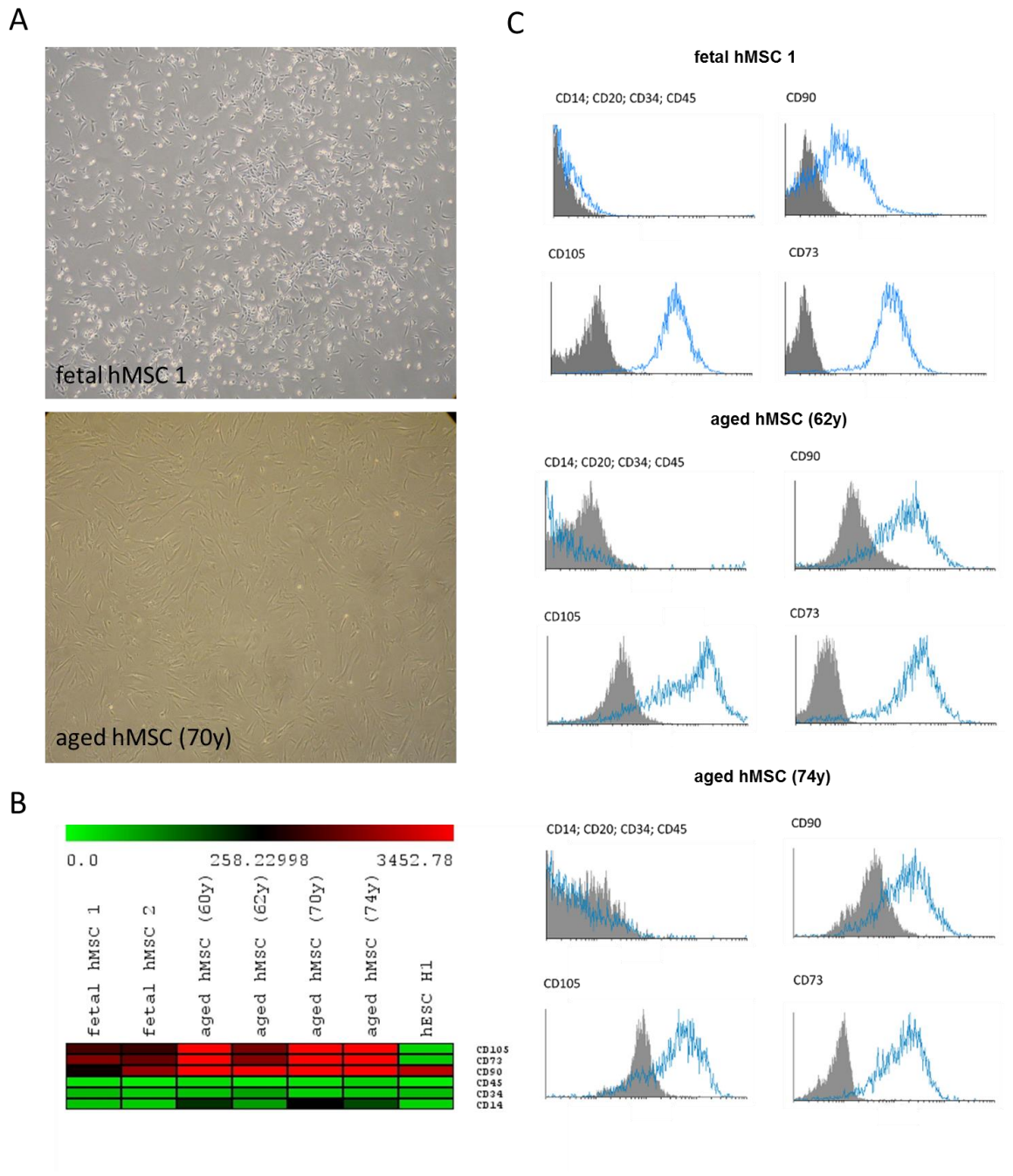

Figure 4 Morphology of fetal hMSCs and hMSCs of elderly donors and expression MCS surface markers.

(A) The cells of fetal hMSC 1 are smaller in size compared to the cells of aged hMSC (70y). Bright-field microscopy. 10 x magnification. Both cell preparations were in passage 2. (B) hMSCs of fetal and aged background were found to express typical MSC surface marker genes but no hematopoietic marker genes. hESC H1 did not show the same gene expression pattern. Heatmap based on average signal of gene expression values detected using an Illumina Bead Chip microarray. (C) Fetal hMSC 1, aged hMSC (62y) and aged hMSC (74y) showed MSC-typic surface marker expression detected by FACS. Hematopoietic markers were not detected by this method. Blue: fluorophore-conjugated antibody against surface antigen. Grey: isotype control.

As a next step, the differentiation capacity of the primary hMSCs of both age groups used in this study was tested. After 21 days of *in vitro* differentiation into osteoblasts, fetal hMSC 1 as well as aged hMSC (62y) and aged hMSC (74y) displayed calcified bone matrix indicated by red colour after Alizarin Red staining. Moreover, fat vacuoles were indicated by red colour through Oil Red O staining after *in vitro* adipocyte differentiation, and acidic mucosubstances were indicated by blue colour after staining with Alcian Blue after *in vitro* chondrogenesis. The osteoblast and adipocyte differentiation of aged hMSC (74y) was part of my master thesis and is shown here for comparison (Megges 2010) (Figure 5 A). Moreover, at day 21 of each differentiation RNA was isolated to confirm the expression of lineage-specific marker genes. RNA lysates of aged hMSC (74y) after osteoblast and adipocyte differentiation were prepared as part of my master thesis (Megges 2010). The isolation of RNA and analysis of marker gene expression by qRT-PCR and microarray were conducted as part of this thesis. The ability to differentiate into adipocytes could be confirmed by the expression of the marker genes *PPARγ* and *LPL* after 21 days of culture in adipogenic medium in fetal hMSC 1, aged hMSC (62y) and aged hMSC (74y) compared to low expression of the markers after 21 days in expansion medium. The expression of *PPARγ* was lower in fetal hMSCs compared to the detected expression in hMSCs derived from aged donors (Figure 5 B). Likewise, the chondrocyte differentiation marker gene *COL1A1* was found to be expressed in fetal hMSC 1 compared to low expression after 21 days of culture in expansion medium (Figure 5 C). Finally, the expression of osteoblast differentiation marker genes *RUNX2*, *ALPL*, *BGLAP* could be detected in aged hMSC (62y) and aged hMSC (74y) after 21 days of culture in osteoblast differentiation medium. The expression of *RUNX2*, *ALPL* and *BGLAP* was lower in fetal hMSC 1 compared to aged hMSC (62y) and aged hMSC (74y) (Figure 5 D). In addition to that, higher expression of genes related to bone cell differentiation could be confirmed comparing undifferentiated aged hMSC (74) and aged hMSC (74) after 21 days of culture in osteoblast differentiation medium by microarray-based gene expression profiling. In particular, genes such as *BMP6* or *SMOC1* were found to be upregulated in aged hMSC (74) after 21 days of culture in osteoblast differentiation medium compared to undifferentiated aged hMSC (74y) (Figure 5 E).

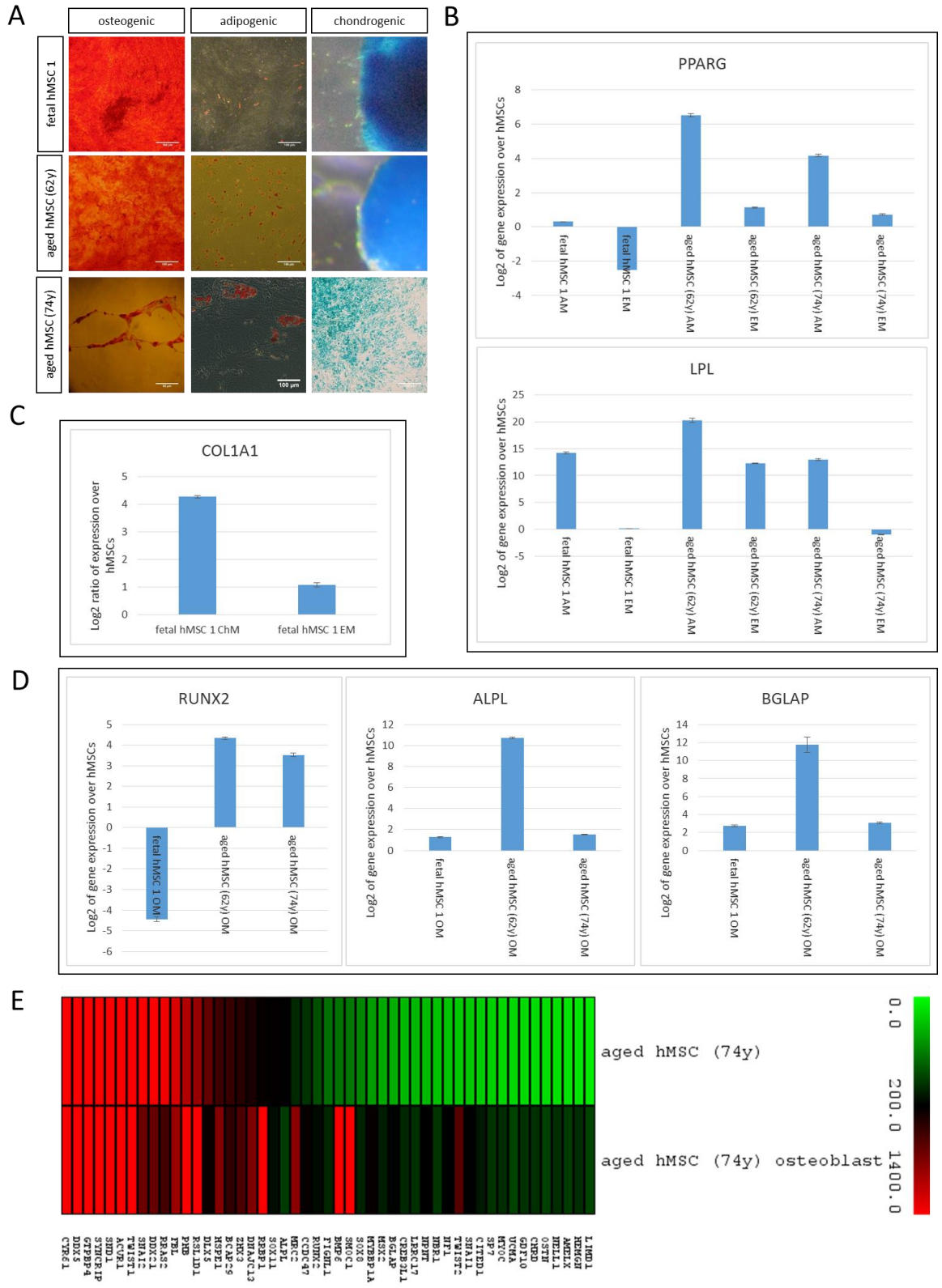

Figure 5 Trilineage differentiation potential of hMSCs of fetal and aged background.

(A) Confirmation of typical MSC lineage differentiation potential in fetal hMSC 1, aged hMSC (62y) and aged hMSC (74y). Osteogenic: hMSCs after 21 days of culture in osteogenic medium. Alizarin Red staining visualised the calcified matrix in red. Bright-field microscopy. 10 x

magnification. Adipogenic: hMSCs after 21 days of culture in adipogenic medium. Oil Red O staining was used to visualise fat vacuoles of adipocytes in red. Bright-field microscopy. 10 x magnification. Chondogenic: hMSCs after 21 days of culture in chondrogenic medium and subsequent stain with Alcian blue to visualise acidic mucosubstances in blue. Fetal hMSC 1 and aged hMSC (62y): pellet culture. Pictures were taken using a stereo microscope. Aged hMSC (74y): micro mass culture. Bright-field microscopy. 10 x magnification. Osteoblast and adipocyte differentiation of hMSC (74y) were performed and previously described as part of my master thesis. The images of osteogenic differentiation and adipogenic differentiation of aged hMSC (74y) were published in this work (Megges 2010) (B) Real-time PCR-based confirmation of adipocyte differentiation marker expression (*PPARγ, LPL*) after 21 days of culture in adipogenic medium (AM) in fetal hMSC 1, aged hMSC (62y) and aged hMSC (74y) compared to 21 days of culture in expansion medium (EM). (C) Real-time PCR-based confirmation of chondrocyte differentiation marker expression (*COL1A1*) after 21 days of culture in chondrogenic medium (ChM) in fetal hMSC 1 compared to 21 days of culture in expansion medium (EM). (D) Real-time PCR-based confirmation of osteoblast differentiation marker expression (*RUNX2, ALPL, BGLAP*) after 21 days of culture in osteogenic medium (OM) in fetal hMSC1, aged hMSC (62y) and aged hMSC (74y). The bars represent the mean of n=3, error bars represent the standard deviation. Data were plotted as log2 ratio of the differentiated sample or control over hMSCs of the same source that were cultured under standard conditions. (E) Expression of genes related to bone cell differentiation in aged hMSC (74y) cultured in osteogenic medium for 21 days compared to undifferentiated hMSCs of the same source under normal culture conditions. Heatmap based on average signal detected using an Illumina Bead Chip microarray. Gene description see Table 17.

3.1.2 Age-related differences present between fetal hMSCs and hMSCs of elderly donors before induction of pluripotency

In order to be able to narrow down whether age-related differences between fetal hMSCs and hMSCs of aged donors have an impact on the induction of pluripotency or on the features of iPS cells with different age background and cells differentiated from them, hMSCs of fetal and age background were compared towards the presence of such features. The focus of this characterisation of ageing-related features were (i) the effect on genomic stability, (ii) the effect on transcriptional patterns of genes involved in cell cycle regulation, senescence and response to oxidative stress as well as (iii) measurement of intracellular reactive oxygen species (ROS). Furthermore, the expression of pluripotency-associated genes and marker-proteins, the similarities of the transcriptomes as well as significantly up- and down-regulated genes were characterised comparing primary hMSCs of fetal and high age background.

The effect of age in primary hMSCs on genomic stability was analysed by karyotyping. In this karyotype analysis by GTG banding revealed a normal male karyotype for fetal hMSC 1 and hMSC 2. Furthermore, aged hMSC (60y), aged hMSC (62y) and aged hMSC (70y) were found to have a normal female karyotype. However, a female karyotype with two aberrant cell lines, both a distinct derivative chromosome 11 could be detected in aged hMSC (74y). More specifically, 14 mitoses out of 23 revealed an unbalanced translocation between chromosome 5 and 11 resulting trisomy 5q. Two mitoses showed no aberration whereas chromosome 11 contained additional of unknown origin in seven mitoses in aged hMSC (74y) (
Figure 6).

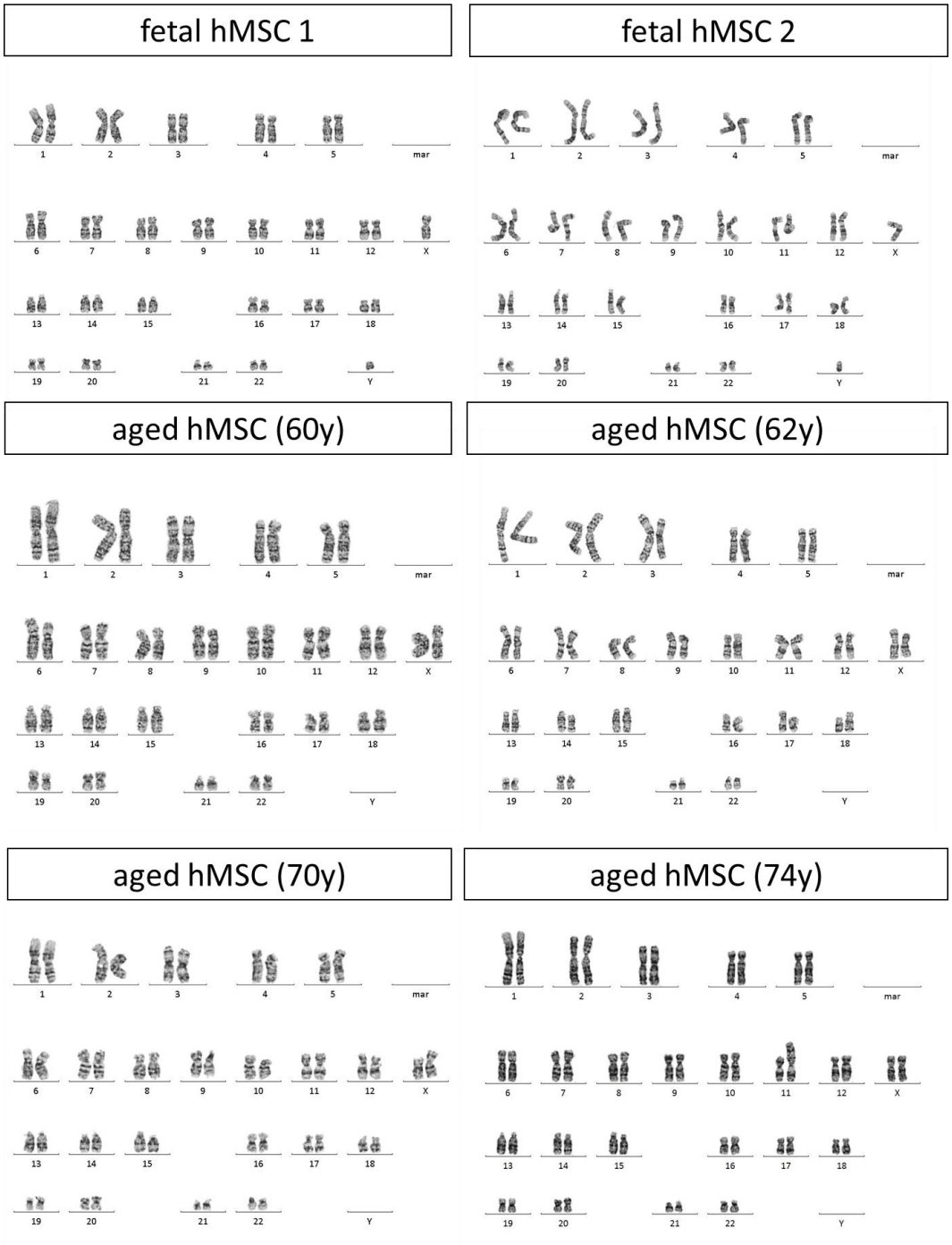

Figure 6 Karyotype of fetal and hMSCs of elderly donors.

A normal male karyotype was revealed for fetal hMSC 1 and fetal hMSC 2 by chromosomal analysis using GTG-banding. A normal female karyotype was revealed for aged hMSC (60y), aged hMSC (62y) and aged hMSC (70y). In aged hMSC (74y), a female karyotype with two aberrant cell lines, both with a distinct derivative chromosome 11, was detected. In 14 of 23 mitoses, an unbalanced translocation between chromosome 5 and 11 resulting in trisomy 5q

could be detected. In seven mitosis chromosome 11 contained additional material of unknown origin. Two mitoses showed no aberrations.

Moreover, the age-related changes of the cell cycle during proliferation were analysed by propidium iodide staining and FACS in fetal hMSC 1 and fetal hMSC 2 as well as in aged hMSC (60y), aged hMSC (62y) and aged hMSC (70y). The data were pooled according to age into two groups: fetal hMSCs consisting of the data measured for fetal hMSC 1 and fetal hMSC 2 and the second group aged hMSCs consisting of the merged sample data of hMSC (60y), aged hMSC (62y) and aged hMSC (70y). The average of the sample groups was calculated and compared. The comparison revealed that on average more cells were in the G2 phase of the cell cycle in aged hMSCs compared to the average measured for fetal hMSCs. In addition, fewer cells were detected to be in the G1-phase and the S-phase of the cell cycle in hMSCs of aged origin compared to fetal hMSCs (Figure 7 A). To analyse differences related to cell cycle regulation on the gene expression level, a hierarchical clustering analysis of fetal hMSCs and aged hMSCs based on gene expression related to cell cycle regulation was carried out. Moreover, the differences of the hMSC samples compared to hESC H1 was included by calculating the ratio of the hMSC samples over hESC H1. Interestingly, based on the expression of this gene set in this analysis, fetal hMSC 1 and fetal hMSC 2 were more similar to each other than to all samples derived from hMSCs of aged donors. Likewise, aged hMSC (60y), aged hMSC (62y), aged hMSC (70y) and aged hMSC (74y) were more similar to each other than to the samples derived from fetal hMSCs (Figure 7 B). In addition, it was tested whether genes of this gene set were significantly up-or down-regulated in fetal or aged hMSC samples compared to hESC H1. A gene that was found to be significantly up-regulated only in samples derived from age hMSCs but not from fetal hMSCs compared to hESC H1 with a p-value below 0.01 is *CCNDBP1*. Genes which were found to be significantly up-regulated with a p-value below 0.01 only in fetal hMSCs compared to hESC H1 but not in aged hMSCs are *JUN* and *SON*. In addition, the genes *PRR11* and *BOP1* were found to be significantly down-regulated in aged hMSCs but not in fetal hMSCs compared to hESC H1 (data not shown) In order to analyse whether there are age-related differences between hMSCs of fetal origin and hMSCs derived from elderly donors which are associated with senescence, a β-galactosidase staining visualising senescent cells and a comparative analysis of senescence-associated gene expression patterns was carried out. Doing this, a hierarchical clustering analysis based on the similarity of the ratios of the expression of senescence-associated genes in fetal hMSCs and hMSCs of aged donors over the expression in hESC H1 was conducted. The results revealed that similar to cell cycle-associated genes, fetal hMSC 1 and fetal hMSC 2 were more similar to each other based on the expression of this gene set than to all samples derived from hMSCs of aged donors. Likewise, the hybridised samples from aged hMSCs were more similar to each other than to fetal hMSC samples. Moreover, aged hMSC (60y) and aged hMSC (70y) formed one similarity cluster, whereas aged

hMSC (62y) formed a cluster with hMSC (74y) (Figure 7 C). In order to find significant up or down-regulated genes hMSC samples of both age groups were compared to hESC H1 using the software GenomeStudio. This analysis revealed that the genes *CDKN1C*, *ETS2*, *CDK4* and *NOX4* were significantly down-regulated with a p-value below 0.01 in all aged hMSC samples but not in fetal hMSC samples compared to hESC H1. Moreover, the genes *CCND1* and *SERPINB2* were found to be significantly up-regulated in aged hMSCs but not in fetal hMSCs with a p-value below 0.01 compared to hESC H1. In addition the genes *CDK6* and *ID1* were significantly up-regulated with a p-value below 0.01 in fetal hMSC 1 but not in aged hMSCs compared to hESC H1 (data not shown). To compare the level of senescence between fetal and aged hMSCs, β-galactosidase staining was performed. Aged hMSC (62y) displayed more cells positive for the senescence marker β-galactosidase in blue compared to cells of fetal hMSC 1 stained with the same protocol (Figure 7 D).

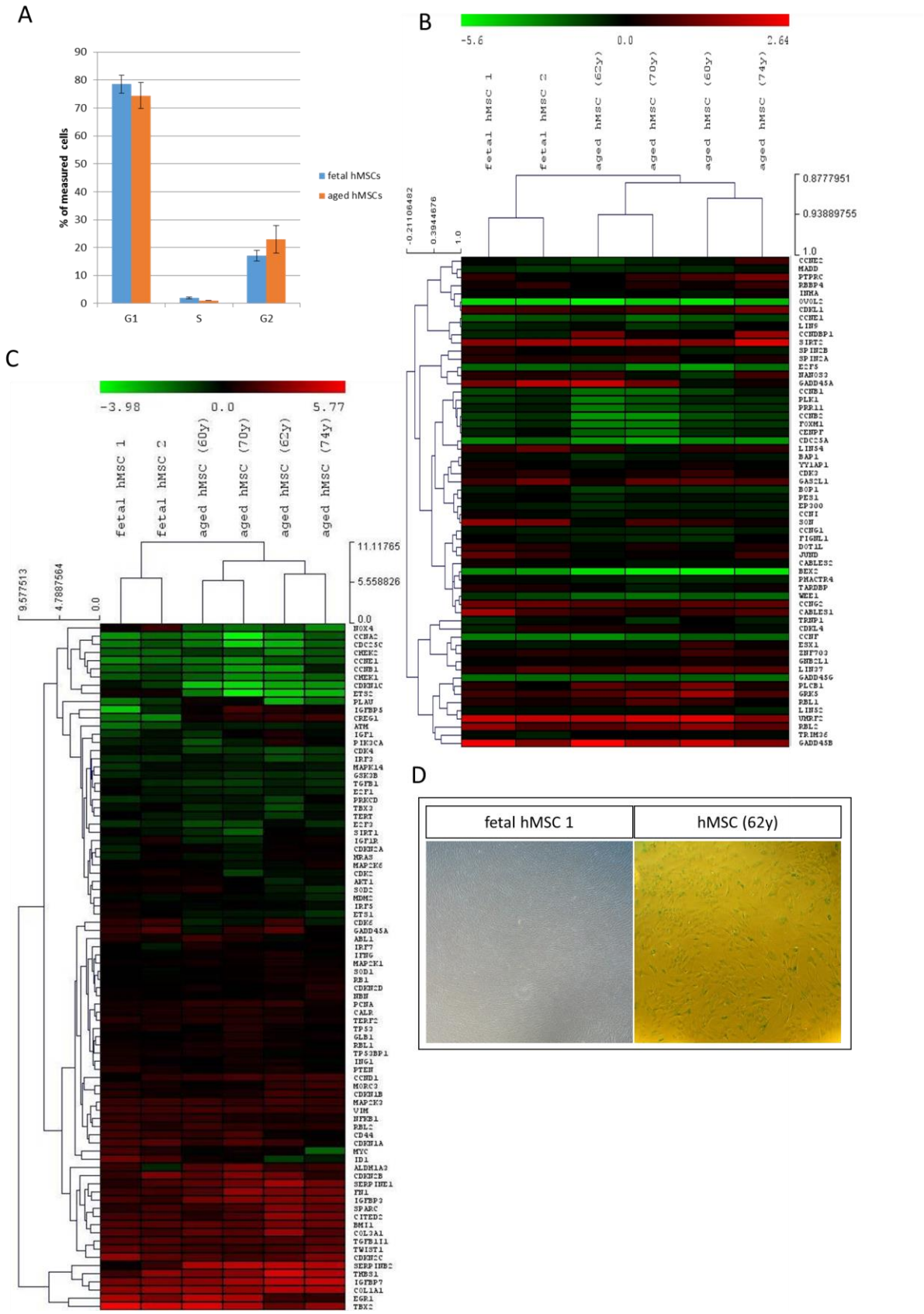

Figure 7 Differences in cell cycle regulation, senescence and associated gene expression between fetal hMSCs and hMSCs from elderly donors.

(A) Quantitative comparison of cell cycle stages of fetal hMSCs (pooled data of fetal hMSC 1and fetal hMSC 2) and aged hMSCs (pooled data of aged hMSC (60y), aged hMSC (62y), aged hMSC (70y)). Propidium iodide staining and analysis via FACS and software Cyflogic. The bars represent the mean of the pooled samples of n=6 for fetal hMSCs (n=3 per measured hMSCs preparation) and n=9 for aged hMSCs (n=3 per measured hMSC preparation). The standard deviation is represented by error bars. (B) Hierarchical clustering analysis of gene expression related to cell cycle regulation in fetal and aged hMSCs compared to hESC H1 detected using Illumina Bead Chip microarray. Heatmap based on log 2 ratio of average signal of the respective sample over average signal in hESC H1. Hierarchical clustering based on Pearson correlation. Gene description see Table 18. (C) Hierarchical cluster analysis comparing the expression of senescence associated genes in fetal and aged hMSCs detected by means of microarray (Illumina Bead Chip technology). Heatmap based on the log 2 ratio of the average signal in the respective sample over the average signal in hESC H1. Hierarchical clustering based on Euclidean distance. Gene description see Table 19. (D) Expression of senescence marker β-galactosidase in aged hMSC (62y) compared to the expression in fetal hMSC 1. Blue: β-galactosidase positive cells. Bright-field microscopy. 10 x magnification.

A further aspect of ageing is the deregulation of the redox homeostasis, a process that is important during reprogramming and could have an impact on pluripotency induction in these cells. In order to analyse whether this feature can be found in hMSCs derived from elderly donors, intracellular ROS measurement and analysis of age-related differences in gene expression related to the response to oxidative stress were carried out. Interestingly, the measurement of intracellular ROS using the fluorescent dye DCFDA and flow cytometry revealed significantly higher ROS levels in aged hMSC (60y) and hMSC (62y) but not in aged hMSC (70y) compared to fetal hMSC 1 and fetal hMSC 2 (Figure 8 A and B). A hierarchical clustering analysis of genes associated to the response to oxidative stress revealed no particular age-related regulation of gene expression as fetal hMSC 2 and aged hMSC (74y) displayed high similarity to each other but low similarity to the other samples which formed a cluster based on the similarity of the gene expression patterns of this category (Figure 8 C). However, an additionally performed microarray data analysis of differentially expressed genes comparing fetal hMSC 1 and hMSCs of aged background revealed, a significant up-regulation (p-value below 0.01) of the genes *PDLIM1*, *GPX3*, *MSRB2* in aged hMSC (60y) and a significant (p-value below 0.01) down-regulation of *RCAN* in the same sample. In addition, *PDLIM* and *MSRB3* were significantly up-regulated whereas *SCARA3* was significantly down-regulated in aged hMSC (62y) compare to fetal hMSC 1 both with a p-value below 0.01. Likewise, *GPX3*, *PDLIM1* and *MSRB2* displayed significant up-regulation whereas *OXR1* was down-regulated in aged hMSC (70y). Finally, *PDLIM1*, *MSRB3*, *MSRA* and *RCAN* were significantly up-regulated whereas *DUSP1*,

SCARA3 and *ORX1* were significantly down-regulated in aged hMSC (74y) compare to fetal hMSC 1 (data not shown).

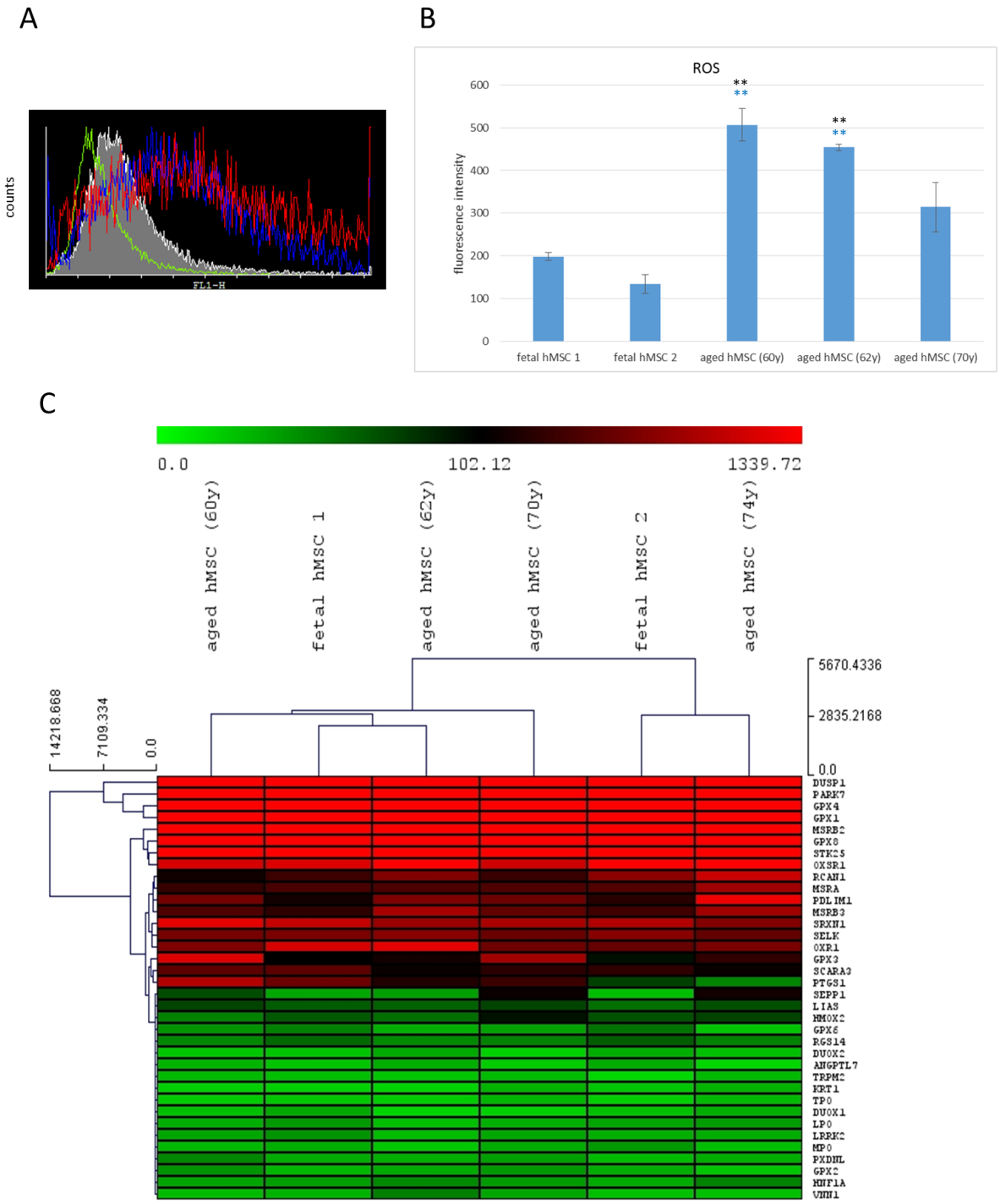

Figure 8 Age-related changes of reactive oxygen species (ROS) levels and gene expression related to response to oxidative stress in fetal hMSCs and hMSCs of elderly donors.

(A) Measurement of reactive oxygen species in fetal hMSC 1 (grey), fetal hMSC 2 (green), aged hMSC (60y) (red) and aged hMSC (70y) (blue). DCFDA and FACS-based measurement of reactive oxygen species in living hMSCs. Histogram was prepared using software Cyflogic. (B) Quantification of reactive oxygen species in fetal hMSCs and hMSCs of elderly donors. DCFDA-

based measurement of reactive oxygen species in living cells using FACS. Data analysis with software Cyflogic and Excel. The bars represent the mean of n=4 measurements. Error bars represent the standard deviation. Black asterisks: significant difference to fetal hMSC 1 (p-value<0.05). Blue asterisks: significant difference to fetal hMSC 2 (p-value<0.05). (C) Hierarchical cluster analysis of the expression values of genes involved in response to oxidative stress in fetal hMSCs and hMSCs of aged donors. Heatmap based on average signal detected using Illumina Bead Chip microarray technology. Hierarchical clustering based on Euclidean distance. Gene description see Table 20.

To test the notion that fetal hMSCs might express more pluripotency related genes than their counterparts derived from aged donors, the expression of pluripotency markers was analysed on the protein level and on the level of gene expression in hMSCs of both age groups. Immunofluorescence-based detection of pluripotency markers in fetal hMSC 1 resulted in positive staining for SSEA4, KLF4 and c-MYC, whereas the detected staining signals for OCT4 and SOX2 were very faint. In contrast to that, no signal was detected when fetal hMSC 1 were stained for SSEA1, TRA1-60 and TRA-81 as well as NANOG (Figure 9 A). Likewise, aged hMSC (74y), when analysed towards expression of pluripotency markers, displayed positive expression for KLF4. In addition, OCT4 and SOX2 could not be detected (Figure 9 B). To analyse the expression of pluripotency markers on the mRNA level, a hierarchical clustering analysis based on the expression of pluripotency marker genes in hESC H1 compared to the expression in fetal hMSCs and aged hMSCs was conducted. All hMSC samples shared a low similarity with the sample derived from pluripotent hESC H1. More specifically, fetal hMSCs formed a similarity cluster with aged hMSC (74y) whereas aged hMSC (60y), aged hMSC (62y) and aged hMSC (70y) formed a separate cluster. Pluripotency-related genes expressed in all hMSC samples and hESC H1 were *ALPL*, *CD9*, *PODXL*, *c-MYC* and *KLF4*. In contrast to that, all other pluripotency-associated genes displayed low expression compared to the expression hESC H1 (Figure 9 C).

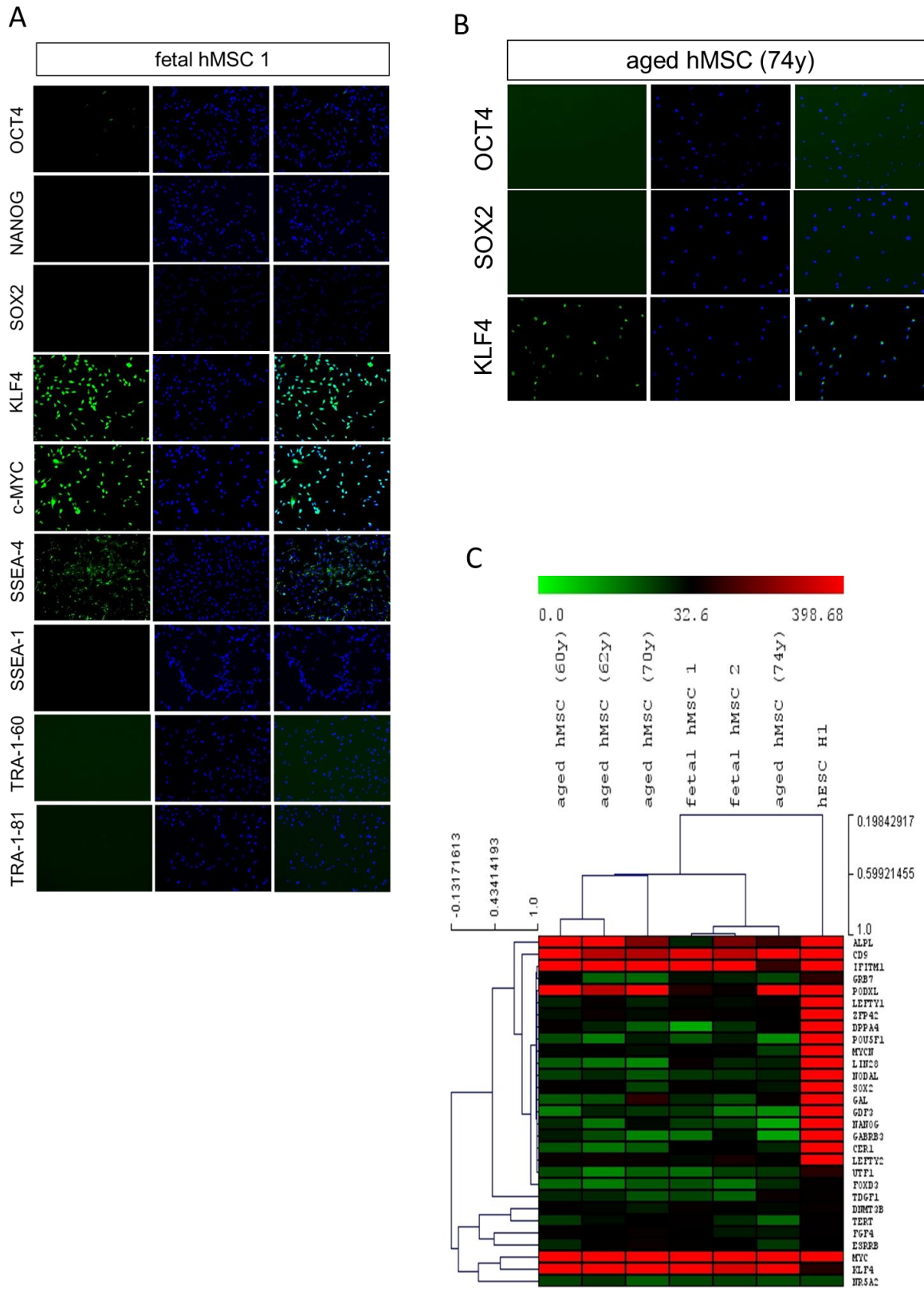

Figure 9 Expression of pluripotency markers in fetal hMSCs and hMSCs of elderly donors.

(A) Expression of pluripotency markers KLF4, c-MYC and SSEA4 in fetal hMSC 1. Immunofluorescence staining. Green: fluorescence signal of marker. Blue: nuclei visualised by DAPI. Both: merge of blue and green channel. Confocal microscopy. 10 x magnification. (B)

Expression of KLF4 in aged hMSC (74y). Immunofluorescence staining. Green: fluorescence signal of maker, blue: nuclei visualised by DAPI. Both: merge of green and blue channel. (C) Hierarchical clustering analysis comparing the expression of pluripotency marker genes in hESC H1 with the expression in fetal hMSCs and aged hMSCs. Heatmap based on average signal detected using an Illumina Bead Chip microarray. Hierarchical clustering based on Pearson correlation. Gene description see Table 21.

In order to characterise the similarities and differences of the transcriptomes of hMSCs of fetal and aged background that were used to study the effect of biological age on pluripotency induction, a microarray-based gene expression analysis was performed using RNA samples isolated from fetal hMSC 1, fetal hMSC 2, aged hMSC (60y), aged hMSC (62y), aged hMSC (70y), aged hMSC (74y) as well as from hESC H1 and hESC H9. To compare the similarities of the transcriptomes, a clustering dendrogram was generated based on the Pearson correlation between the transcriptomes. A higher similarity between the transcriptomes of the hMSC samples compared to a low similarity between the transcriptomes of the hMSC samples and hESC H1 was revealed. Surprisingly, the transcriptomes of fetal hMSCs, while most similar to each other, formed a cluster with aged hMSC (60y) and aged hMSC (70y). These samples were in turn less similar to aged hMSC (62y) and aged hMSC (74y) whose transcriptomes were most similar to each other (Figure 10 A). The exact values of the Pearson correlations between detected transcriptomes of the samples are listed in Figure 10 B. To better visualise the similarities and differences between the samples, a colour code was used. The colour green stands for high similarity, whereas red represents lower similarity comparing only the correlation values of the respective column of the table. According to the results, the correlation between the samples of aged hMSCs was above 0.9. More specifically, the correlation between the transcriptomes of aged hMSC (74y) and aged hMSC (62y) has the second highest value (0.97), whereas the transcriptomes of aged hMSC (60y) and aged hMSC (70y) had a correlation of 0.99, which was the highest correlation between aged hMSC samples. In contrast to that, the correlations of the transcriptomes of aged hMSC (62y), of aged hMSC (60y) and aged hMSC (70y) had a value of 0.93 and 0.94 respectively. Moreover, the correlation between the transcriptome of aged hMSC (74y), the transcriptome of hMSC (60y) and aged hMSC (70y) was measured with a value of 0.95 and 0.94 respectively. However, the correlations between aged hMSC (60) and hMSC (70) was measured with a value of above 0.96 and was therefore higher than the correlation between fetal hMSC samples, aged hMSC (62y) and aged hMSC (74y), which were measured with values between 0.93 and 0.94. Interestingly, the correlations between the transcriptomes of fetal hMSCs and hESCs was 0.9 and therefore higher than the correlations between the transcriptomes of aged hMSC samples and the transcriptome of hESC H1 and hESC H9 which had a value below 0.9 (Figure 10 B). To characterise the differences between fetal hMSC 1 and all aged hMSC samples of 60-74 year old donors, a Venn

diagram of the differentially expressed genes with a p-value below 0.01 comparing fetal hMSC 1 and all aged hMSC samples was generated using the platform VENNY. The genes that were differentially expressed according to a statistical test of the software GenomeStudio and had a p-value of 0.01 and below were used as input. According to this analysis, all samples of aged hMSC share 888 genes, which are differentially expressed in fetal hMSC 1. The highest number of differentially expressed genes only measured in one sample but not in the other three samples was detected for the sample of aged hMSC (62y) with 1276 genes that are differentially expressed. This was followed by aged hMSC (70y) with 488 genes, aged hMSC (74y) with 390 genes and finally aged hMSC (60y) with 285 genes, which were differentially expressed between fetal hMSC 1, and the respective samples. In addition to that, the differentially expressed genes commonly present in two samples of aged hMSCs were detected. The highest number of overlapping gene expression was detected for the samples aged hMSC (62y) and hMSC (74y) with 847 genes which are common in the two samples. This was followed by 390 common genes in aged hMSC (70y) and aged hMSC (60y), 261 common genes in aged hMSC (62y) and aged hMSC (70y), 117 common genes in aged hMSC (70y) and aged hMSC (74y) and the lowest number of common genes in the samples aged hMSC (74y) and aged hMSC (60y) with 51 genes (Figure 10 C).

A

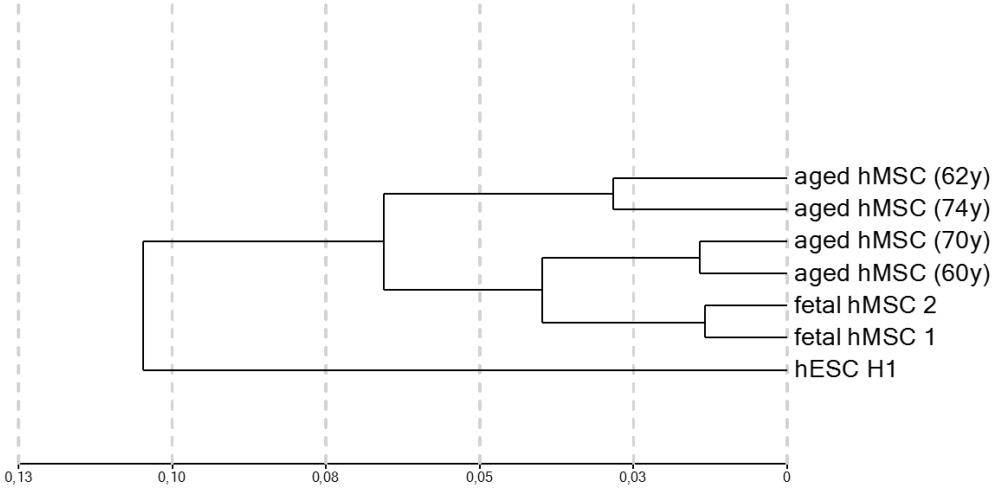

B

sample	aged hMSC (74y)	aged hMSC (62y)	aged hMSC (60y)	aged hMSC (70y)	fetal hMSC 1	fetal hMSC 2	hESC H1	hESC H9
aged hMSC (74y)	1.000	0.972	0.944	0.951	0.933	0.943	0.869	0.855
aged hMSC (62y)	0.972	1.000	0.929	0.939	0.924	0.937	0.869	0.857
aged hMSC (60y)	0.944	0.929	1.000	0.986	0.961	0.964	0.885	0.874
aged hMSC (70y)	0.951	0.939	0.986	1.000	0.957	0.962	0.877	0.865
fetal hMSC 1	0.933	0.924	0.961	0.957	1.000	0.987	0.931	0.923
fetal hMSC 2	0.943	0.937	0.964	0.962	0.987	1.000	0.939	0.925
hESC H1	0.869	0.869	0.885	0.877	0.931	0.939	1.000	0.983
hESC H9	0.855	0.857	0.874	0.865	0.923	0.925	0.983	1.000

C

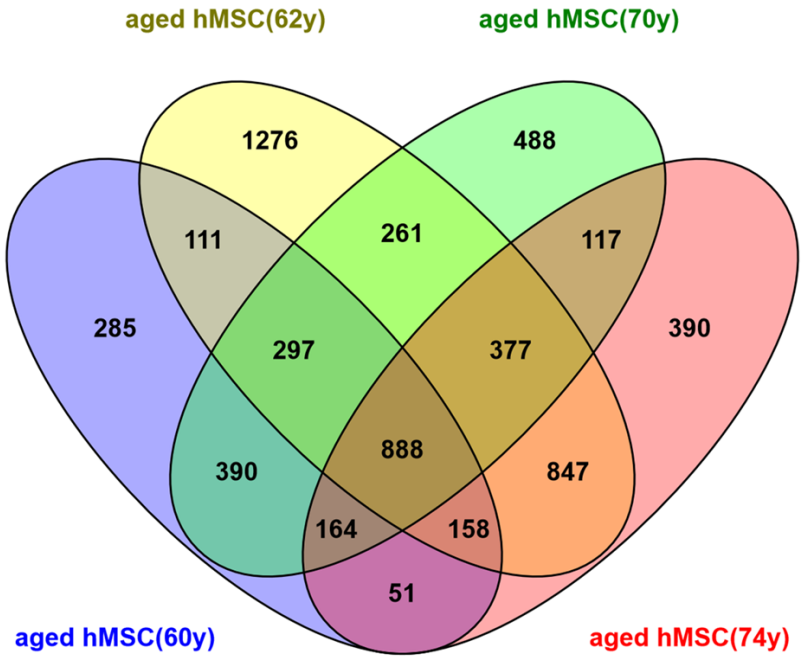

Figure 10 Microarray-based gene expression analysis comparing fetal hMSCs and hMSCs of aged individuals.

(A) Hierarchical clustering dendrogram comparing the transcriptomes of fetal hMSC 1, fetal hMSC 2, aged hMSC (60y), aged hMSC (62y), aged hMSC (70y), aged hMSC (74y) and hESC H1 based on Pearson correlation generated using the software GenomeStudio. (B) Table of Pearson correlation values between all fetal hMSC and aged hMSC samples as well as hESC H1 and hESC H9. Correlations were calculated using the software GenomeStudio. The similarity of the samples is coded by colour of the cell starting from green representing the highest similarity to strong red representing the lowest similarity. (C) Venn diagram showing overlaps of genes differentially expressed (p-value of 0.01 and below) in aged hMSCs derived from 60, 62, 70 and 74-year-old donors compared to fetal hMSC 1. Venn diagram created with the platform VENNY. A statistical test towards differential expression was performed using software GenomeStudio.

In order to characterise the processes which are differentially regulated between fetal hMSCs and hMSCs derived from older donors, the transcriptome data measured by microarray-based transcriptome profiling was grouped according to the age of the samples. In this way the average gene expression of the merged samples was calculated. The samples fetal hMSC 1 and fetal hMSC 2 were grouped and the grouped sample was called fetal hMSCs. Likewise, the samples aged hMSC (60y), aged hMSC (62y), aged hMSC (70y) and aged hMSC (74y) were grouped and the merged samples were called aged hMSCs. Subsequently, a statistical test using the software GenomeStudio was performed to narrow down the genes, which are differentially expressed between the grouped, samples fetal hMSCs and aged hMSCs. The genes, which were detected to be different with a p-value of below 0.05, were used in the next step. At this point, the ratio of the average signals of the grouped sample aged hMSCs over fetal hMSC was calculated and the genes with a 1.5-fold lower average signal in aged hMSC compared to fetal hMSCs were considered to be down-regulated. The results of the functional annotation of these genes using the DAVID functional annotation database are listed in Table 8 and Table 9. The down-regulated genes in aged hMSCs compared to fetal hMSCs were annotated to the processes Cell cycle, Notch signalling pathway and Axon guidance of the category KEGG with a p-value of below 0.05, whereas the further annotations of the category KEGG with p-values between 0.06 and 0.086 were Pathways in Cancer, Spliceosome and P53 signalling pathway. In addition, genes down-regulated in aged hMSCs were annotated to the BIOCARTA-processe Role of MEF2D in T-cell Apoptosis, whereas the down-regulated gene ontology terms (GO-terms) with the ten lowest p-values below 0.01 were related to cell cycle and cell cycle regulation processes, such as M-Phase except for the annotations regulation of transcription from RNA polymerase II promoter and amine biosynthetic process (Table 8).

Table 8 Significantly down-regulated processes in hMSCs of aged individuals compared to fetal hMSCs.

Functional annotation of genes, which were differentially expressed between fetal hMSCs (merged samples of fetal hMSC 1 and fetal hMSC 2) and aged hMSCs (merged samples of aged hMSC (60y), aged hMSC (62y) and aged hMSC (70y)) with a p-value below 0.05 and at least 1.5-fold lower average signal. The average signal was detected using an Illumina Bead Chip microarray. The genes were annotated using the DAVID functional annotation database. A p-value of 0.05 and below was considered significant but all results are listed for categories KEGG and BIOCARTA. In addition, the first ten annotations of the category GO-TERM_BP_FAT are listed.

Down-regulated in aged hMSCs compared to fetal hMSCs				
Category	Term	Count	%	PValue
KEGG_PATHWAY	hsa04110:Cell cycle	17	2.773	4.95E-06
KEGG_PATHWAY	hsa04330:Notch signaling pathway	6	0.979	2.22E-02
KEGG_PATHWAY	hsa04360:Axon guidance	10	1.631	3.39E-02
KEGG_PATHWAY	hsa05200:Pathways in cancer	18	2.936	6.00E-02
KEGG_PATHWAY	hsa03040:Spliceosome	9	1.468	6.96E-02
KEGG_PATHWAY	hsa04115:p53 signaling pathway	6	0.979	8.52E-02
Category	Term	Count	%	PValue
BIOCARTA	h_mef2dPathway:Role of MEF2D in T-cell Apoptosis	4	0.653	9.98E-03
BIOCARTA	h_s1pPathway:SREBP control of lipid synthesis	3	0.489	5.28E-02
Category	Term	Count	%	PValue
GOTERM_BP_FAT	GO:0051726~regulation of cell cycle	36	5.873	1.39E-09
GOTERM_BP_FAT	GO:0007049~cell cycle	60	9.788	1.87E-09
GOTERM_BP_FAT	GO:0022403~cell cycle phase	40	6.525	4.36E-09
GOTERM_BP_FAT	GO:0000278~mitotic cell cycle	36	5.873	2.53E-08
GOTERM_BP_FAT	GO:0022402~cell cycle process	45	7.341	1.31E-07
GOTERM_BP_FAT	GO:0008284~positive regulation of cell proliferation	35	5.710	1.14E-06
GOTERM_BP_FAT	GO:0000279~M phase	30	4.894	1.76E-06
GOTERM_BP_FAT	GO:0006357~regulation of transcription from RNA polymerase II promoter	48	7.830	9.24E-06
GOTERM_BP_FAT	GO:0009309~amine biosynthetic process	13	2.121	1.40E-05
GOTERM_BP_FAT	GO:0007067~mitosis	22	3.589	1.44E-05

In contrast to that, the genes with a 1.5-fold higher average signal in the grouped sample aged hMSCs compare to the grouped sample fetal hMSCs were considered to be up-regulated and were further characterised using the DAVID gene annotation database to find the processes these genes are part of. The ten gene annotations of the category KEGG with the lowest p-values below 0.05 in aged hMSCs were ECM-receptor interaction, Focal adhesion, Graft-versus-host disease, Antigen processing and presentation, Lysosome, Viral myocarditis, Type I diabetes mellitus, Complement and coagulation cascades, Allograft rejection and Cell adhesion molecules (CAMs). Furthermore, the up-regulated genes in aged hMSCs compared to fetal hMSCs were annotated to Antigen Processing and Presentation as well as to Ghrelin: Regulation of Food Intake and Energy Homeostasis in the category BIOCARTA. In addition, among the ten GO-term-based annotations with the lowest p-value below 0.01 for the up-regulated genes, were the annotations to extracellular matrix organisation, response to

wounding, wound healing, cell adhesion, antigen processing and presentation of peptide antigen as well as the GO-term immune response (Table 9).

Table 9 Up-regulated processes in hMSCs of aged individuals compared to fetal hMSCs. Functional annotation of genes, which are differentially expressed (p-value of 0.05 and below) between fetal hMSCs (merged samples of fetal hMSC 1 and fetal hMSC 2) and hMSCs of aged donors (merged samples of aged hMSC (60y), aged hMSC (62y) and aged hMSC (70y)) that had an at least 1.5-fold higher average signal detected by an Illumina Bead Chip microarray. The genes were annotated using DAVID functional annotation platform. A p-value of 0.05 and below was considered significant. The first ten annotations with the lowest p-values below 0.01 are listed for the category KEGG. All results are shown for the category BIOCARTA. The first ten annotations for the category GO-TERM_BP_FAT are listed.

Up-regulated in aged hMSCs compared to fetal hMSCs				
Category	Term	Count	%	PValue
KEGG_PATHWAY	hsa04512:ECM-receptor interaction	18	2.378	2.06E-06
KEGG_PATHWAY	hsa04510:Focal adhesion	29	3.831	3.51E-06
KEGG_PATHWAY	hsa05332:Graft-versus-host disease	12	1.585	4.71E-06
KEGG_PATHWAY	hsa04612:Antigen processing and presentation	17	2.246	8.06E-06
KEGG_PATHWAY	hsa04142:Lysosome	20	2.642	1.58E-05
KEGG_PATHWAY	hsa05416:Viral myocarditis	15	1.982	2.29E-05
KEGG_PATHWAY	hsa04940:Type I diabetes mellitus	11	1.453	6.46E-05
KEGG_PATHWAY	hsa04610:Complement and coagulation cascades	14	1.849	7.44E-05
KEGG_PATHWAY	hsa05330:Allograft rejection	10	1.321	1.00E-04
KEGG_PATHWAY	hsa04514:Cell adhesion molecules (CAMs)	18	2.378	7.89E-04
Category	Term	Count	%	PValue
BIOCARTA	h_mhcPathway:Antigen Processing and Presentation	6	0.793	3.10E-04
BIOCARTA	h_ghrelinPathway:Ghrelin: Regulation of Food Intake and Energy Homeostasis	6	0.793	1.33E-03
BIOCARTA	h_fibrinolysisPathway:Fibrinolysis Pathway	5	0.661	5.36E-03
BIOCARTA	h_ifnaPathway:IFN alpha signaling pathway	4	0.528	2.13E-02
BIOCARTA	h_compPathway:Complement Pathway	5	0.661	2.78E-02
BIOCARTA	h_il5Pathway:IL 5 Signaling Pathway	4	0.528	2.89E-02
BIOCARTA	h_amiPathway:Acute Myocardial Infarction	4	0.528	5.89E-02
BIOCARTA	h_tsp1Pathway:TSP-1 Induced Apoptosis in Microvascular Endothelial Cell	3	0.396	8.29E-02
Category	Term	Count	%	PValue
GOTERM_BP_FAT	GO:0009611~response to wounding	64	8.454	3.55E-14
GOTERM_BP_FAT	GO:0042060~wound healing	33	4.359	1.41E-11
GOTERM_BP_FAT	GO:0007155~cell adhesion	68	8.983	1.24E-10
GOTERM_BP_FAT	GO:0022610~biological adhesion	68	8.983	1.28E-10
GOTERM_BP_FAT	GO:0048002~antigen processing and presentation of peptide antigen	12	1.585	6.76E-09
GOTERM_BP_FAT	GO:0019882~antigen processing and presentation	18	2.378	4.3E-08
GOTERM_BP_FAT	GO:0006955~immune response	61	8.058	4.48E-08
GOTERM_BP_FAT	GO:0030198~extracellular matrix organization	20	2.642	4.91E-08
GOTERM_BP_FAT	GO:0010033~response to organic substance	62	8.190	9.24E-08
GOTERM_BP_FAT	GO:0009719~response to endogenous stimulus	40	5.284	9.73E-07

A recent study that compared gene expression between different aged mice in various organs confirmed the metabolic stability theory of ageing (Brink et al. 2009). In addition, the senescence-related mitochondrial oxidative stress pathway very likely plays a role during reprogramming of somatic cells to iPSCs (Prigione et al. 2011b). Therefore, genes, which were found to be significantly

up-or down-regulated with age in hMSCs in this study were annotated to biological processes using the database DAVID and as additional step screened for annotations confirming differentially gene expression of processes and gene ontologies related to metabolic stability as well as the mitochondrial oxidative stress pathway including the categories KEGG, BIOCARTA, GOTERM_MF_FAT, GOTERM_BP_FAT and GOTERM_CC_FAT in the functional annotation platform DAVID. Doing this, the genes found to be up-regulated by microarray in aged hMSCs (merged sample of aged hMSC (60y), aged hMSC (62y) and aged hMSC (70y)) compared to fetal hMSCs (merged samples of fetal hMSC 1 and fetal hMSC 2) showed annotations to response to oxidative stress (p-value 0.004), glutathione metabolism (p-value: 0.19), antioxidant activity (p-value 0.280) and mitochondrion (p-value 0.880). However, the genes detected as significantly down-regulated in aged hMSCs compared to fetal hMSCs were annotated to response to insulin stimulus (p-value: 0.009), insulin receptor signalling pathway (p-value: 0.14) and glucose metabolic process (p-value: 0.763 (Table 10).

Table 10 Differential expression of genes related to processes associated to the metabolic stability theory of ageing.

Functional annotation of genes, which were differentially expressed (p-value of 0.05 and below) between fetal hMSCs (merged samples of fetal hMSC 1 and fetal hMSC 2) and hMSCs of aged donors (merged samples of aged hMSC (60y), aged hMSC (62y) and aged hMSC (70y)). Genes with a 1.5-fold higher (up-regulation) or 1.5-fold lower (down-regulation) average signal in fetal hMSCs compared to the average signal in aged hMSCs measured using Illumina Bead Chip microarray. The up- or down-regulated genes were annotated using the DAVID functional annotation platform. Results related to oxidative phosphorylation, citric acid cycle, oxidative stress, glutathione metabolism, glycolysis and insulin signalling are shown. A p-value of 0.5 and below was considered significant but all results are listed.

down-regulated in aged hMSCs against fetal hMSCs					
Category	**Term**	**Count**	**%**	**PValue**	**Genes**
GOTERM_BP_FAT	GO:0032868~response to insulin stimulus	7	2.053	9.078E-03	IRS2, ADM, FADS1, BAIAP2, BCAR1, VGF, ABCC5
GOTERM_BP_FAT	GO:0008286~insulin receptor signaling pathway	3	0.880	1.414E-01	IRS2, BAIAP2, BCAR1
GOTERM_BP_FAT	GO:0006006~glucose metabolic process	3	0.880	7.625E-01	IRS2, ATF3, PGM2L1
up-regulated in aged hMSCs against fetal hMSCs					
Category	**Term**	**Count**	**%**	**PValue**	**Genes**
GOTERM_BP_FAT	GO:0006979~response to oxidative stress	11	2.657	3.962E-03	TXNIP, EPAS1, CRYAB, HMOX1, GPX3, CYGB, PDLIM1, BCL2L1, GPX7, STAT1, GCLM
KEGG_PATHWAY	hsa00480:Glutathione metabolism	4	0.966	1.922E-01	GPX3, GPX7, GCLM, MGST1
GOTERM_MF_FAT	GO:0016209~antioxidant activity	3	0.725	2.814E-01	GPX3, CYGB, GPX7
GOTERM_CC_FAT	GO:0005739~mitochondrion	23	5.556	8.758E-01	TXNIP, SQRDL, COX7A1, TDRD7, AK1, STXBP1, NLRX1, BCL2L1, OAS2, MAPK10, MSRB2, STARD13, ACADVL, SLC1A3, FYN, HEBP1, CTSB, XAF1, SLC27A3, SLC25A43, IFI6, MGST1, PC

Interestingly, a recent study confirmed the age-related regulation of a set of genes in human fibroblasts (Hashizume et al. 2015). To reveal whether these genes are regulated with age in hMSCs, the average

signal detected by microarray was plotted comparing the expression of the genes *COX7A1*, *MRPL28*, *CAPRIN2*, *GCAT*, *EHHADH*, *ALDH5A1* and *SHMT2* between the samples of fetal hMSCs and aged hMSCs. The analysis revealed a higher average signal for the gene *COX7A1* in aged hMSC samples but not in fetal hMSCs. In addition, the signal intensity of the gene *SHMT2* was higher than the signal intensity of *MRPL28*, *CAPRIN2*, *GCAT*, *EHHADH* and *ALDH5A1* in fetal and aged hMSCs. Moreover, a slightly lower average signal was detected for the gene *GCAT* in aged hMSCs compared to fetal hMSCs (Figure 11 A). In addition to that, gene lists based on the GO-terms oxidative phosphorylation, citric acid cycle, glycolysis, glutathione metabolism and insulin signalling that were differentially expressed in fetal hMSCs (merged samples of fetal hMSC 1 and fetal hMSC 2) compared to aged hMSCs (merged samples of aged hMSC (60y), aged hMSC (62y) and aged hMSC (70y)) were extracted using microarray-based gene expression analysis. Genes involved in glycolysis were found to be significantly up-regulated (*ALDOC*, *PFKFB3*) and down-regulated (*GPI*) in fetal hMSCs compared to aged hMSCs. In addition, the gene *IRS2* involved in insulin signalling was found to be up-regulated, whereas the gene *GCLM*, which is involved in glutathione metabolism was down-regulated in fetal hMSCs compared to aged hMSCs (Figure 11 B).

A

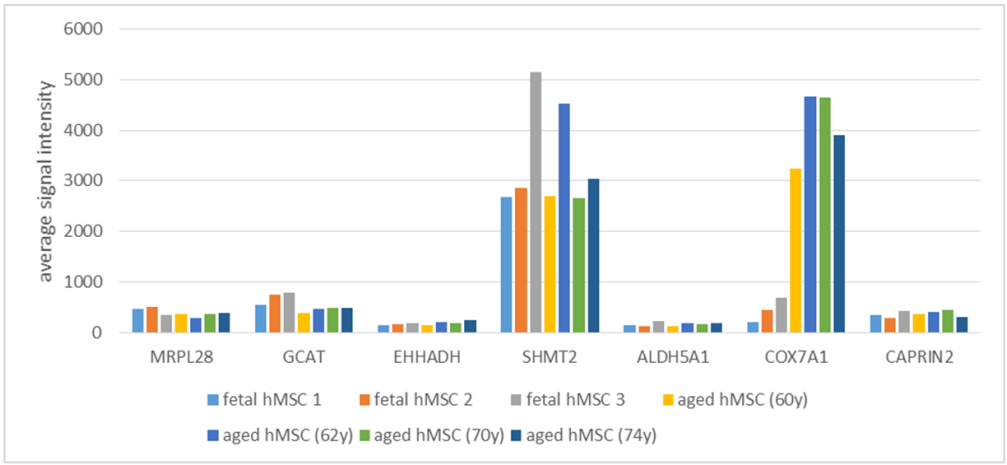

B

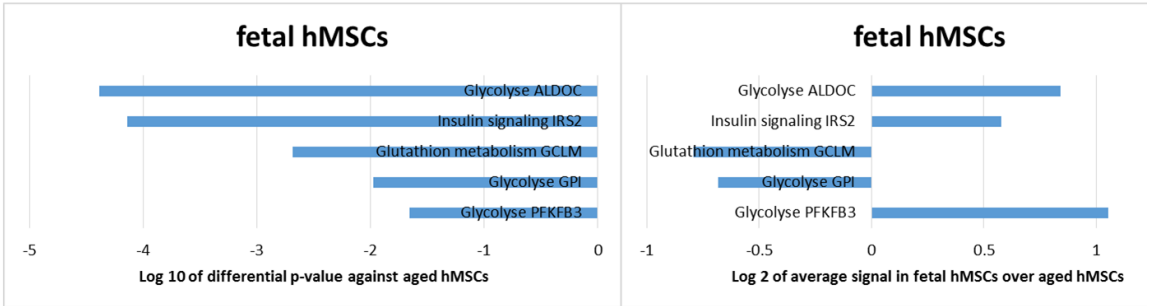

Figure 11 Expression of genes regulated with age and with implications in the metabolic stability theory of ageing in fetal hMSCs compared to hMSCs of aged donors.

(A) Histogram plot of the average signal of expression of genes described to be regulated with age in a recent study (Hashizume et al. 2015). Compared are fetal hMSC 1, fetal hMSC 2, fetal hMSC 3, aged hMSC (60y), aged hMSC (62y), aged hMSC (70y) and aged hMSC (74y). Gene expression was measured using an Illumina Bead Chip. (B) Genes of gene lists based on the GO-terms oxidative phosphorylation, TCA cycle, glycolysis, glutathione metabolism and insulin signalling that were differentially expressed in fetal hMSCs (merged samples of fetal hMSC 1 and fetal hMSC 2) compared to aged hMSCs (merged samples of aged hMSC (60y), aged hMSC (62y) and aged hMSC (70y)). Left: Log 10 of the differential p-values below 0.05 of differentially expressed genes calculated by the software GenomeStudio. Right: Log 2 of the ratios of the average signals in fetal hMSCs over aged hMSCs of the differentially expressed genes sorted according to the differential p-value. Gene expression was measured using an Illumina Bead Chip.

In addition to that, the results of recent studies suggest that the cytoskeleton dynamics change in aged hMSCs compared to hMSCs of young background and that stem cells in aged individuals interact differently with their surrounding extracellular matrix (Geissler et al. 2012, Rando and Wyss-Coray 2014). Therefore, genes that were significantly up- or down-regulated in aged hMSCs compared to fetal hMSCs were extracted and annotated to pathways and gene ontologies using DAVID functional annotation database. The results of the analysis revealed an up-regulation of genes annotated to the gene ontologies and processes proteinaceous extracellular matrix, extracellular matrix, cell adhesion, biological adhesion, extracellular matrix part, extracellular matrix organisation, ECM-receptor interaction, Focal adhesion, cell migration and Cell adhesion molecules (CAMs) in aged hMSCs compared to fetal hMSCs. In contrast to that, the comparison revealed that genes annotated to the processes and gene ontologies microtubule cytoskeleton, cytoskeleton organisation, extracellular matrix, cytoskeleton, proteinaceous extracellular matrix, cytoskeletal part, microtubule cytoskeleton organisation, cell adhesion and actin cytoskeleton were down-regulated in aged hMSCs compared to fetal hMSCs (Table 11).

Table 11 Differential expression of genes related to processes associated to the cytoskeleton and to the interaction with the extracellular matrix.

Functional annotation of genes, which were differentially, expressed (p-value of 0.05 and below) between fetal hMSCs (merged samples of fetal hMSC 1 and fetal hMSC 2) and hMSCs of aged donors (merged samples of aged hMSC (60y), aged hMSC (62y) and aged hMSC (70y)). Genes with a 1.5-fold higher (up-regulation) or 1.5-fold lower (down-regulation) average signal in fetal hMSCs compared to the average signal in aged hMSCs measured using Illumina Bead Chip Microarray. The up or down-regulated genes were annotated using the DAVID functional annotation platform. Results related to cell adhesion, extracellular matrix interaction and the cytoskeleton are shown. A p-value of 0.5 and below was considered significant but the ten most significant annotations with the lowest differential p-value are listed.

down-regulated in aged hMSCs against fetal hMSCs				
Category	**Term**	**Count**	**%**	**PValue**
GOTERM_CC_FAT	GO:0015630~microtubule cytoskeleton	31	5.057	9.377E-04
GOTERM_BP_FAT	GO:0007010~cytoskeleton organization	27	4.405	2.971E-03
GOTERM_CC_FAT	GO:0031012~extracellular matrix	20	3.263	7.175E-03
GOTERM_CC_FAT	GO:0005856~cytoskeleton	56	9.135	1.380E-02
GOTERM_CC_FAT	GO:0005578~proteinaceous extracellular matrix	18	2.936	1.479E-02
GOTERM_CC_FAT	GO:0044430~cytoskeletal part	41	6.688	1.582E-02
GOTERM_BP_FAT	GO:0000226~microtubule cytoskeleton organizatio	11	1.794	2.504E-02
GOTERM_BP_FAT	GO:0007155~cell adhesion	34	5.546	2.781E-02
GOTERM_BP_FAT	GO:0022610~biological adhesion	34	5.546	2.788E-02
GOTERM_CC_FAT	GO:0015629~actin cytoskeleton	15	2.447	2.977E-02
up-regulated in aged hMSCs against fetal hMSCs				
Category	**Term**	**Count**	**%**	**PValue**
GOTERM_CC_FAT	GO:0005578~proteinaceous extracellular matrix	49	6.473	3.69E-13
GOTERM_CC_FAT	GO:0031012~extracellular matrix	50	6.605	1.68E-12
GOTERM_BP_FAT	GO:0007155~cell adhesion	68	8.983	1.24E-10
GOTERM_BP_FAT	GO:0022610~biological adhesion	68	8.983	1.28E-10
GOTERM_CC_FAT	GO:0044420~extracellular matrix part	24	3.170	3.06E-09
GOTERM_BP_FAT	GO:0030198~extracellular matrix organization	20	2.642	4.91E-08
KEGG_PATHWAY	hsa04512:ECM-receptor interaction	18	2.378	2.06E-06
KEGG_PATHWAY	hsa04510:Focal adhesion	29	3.831	3.51E-06
GOTERM_BP_FAT	GO:0016477~cell migration	26	3.435	2.29E-04
KEGG_PATHWAY	hsa04514:Cell adhesion molecules (CAMs)	18	2.378	7.89E-04

3.2 iPS generation and characterisation

In order to analyse the effect of age-related differences between fetal hMSCs and hMSCs of aged donors on the induction of pluripotency and on the features of induced pluripotent stem cells derived from hMSCs of fetal and high age background, hMSCs of both age groups were reprogrammed to iPS

cells using retroviral and episomal plasmid-based, non-viral methods. Table 12 gives an overview of the reprogramming experiments conducted.

3.2.1 Reprogramming of hMSCs of fetal and aged background to induced pluripotent stem cells

Retroviral reprogramming

Retroviral iPS cell generation from hMSCs was carried out by means of pMX vector-based retrovirus generation and subsequent transduction and overexpression of the so called Yamanaka factors OCT4, SOX2, KLF4 and c-MYC based on a previously described protocol that was modified (Takahashi et al. 2007). The reprogramming protocol was modified according to a protocol described for episomal plasmid-based reprogramming (Yu et al. 2011). Reprogramming was conducted using N2B27 medium with and without addition of an inhibitor cocktail consisting of MEK inhibitor PD0325901, GSK3β inhibitor CHIR99021, TGF-β/Activin/Nodal receptor inhibitor A-83-01 and ROCK inhibitor HA-100 (Yu et al. 2011) (smM) and under hypoxia (5% oxygen) as well as normoxia. Moreover, the reprogramming was conducted with and without switch of the initial medium to mTeSR 1 14 days after viral transduction. In addition, the viral reprogramming of hMSC (74y) was carried out as part of my master thesis. The further characterisation and comparison to other hMSC-iPSCs was conducted in this PhD thesis. In contrast to the other hMSCs, aged hMSC (74y) was reprogrammed using hESC maintenance medium followed by conditioned medium and addition of an inhibitor cocktail consisting of MEK inhibitor PD0325901, TGFβ receptor inhibitor SB-431542 and P53 inhibitor pifithrin α (Megges 2010). All reprogramming experiments conducted are listed in Table 12.

The retroviruses harbouring the open reading frames of *OCT4*, *SOX2*, *KLF4* and *c-MYC* were generated using HEK293T cells. Subsequently, the functionality of the viruses was assessed by a test-transduction of fetal hMSC 1. Immunofluorescence staining after the viral transduction revealed OCT4-positive cells, SOX2-positive cells, KLF4-positive and c-MYC-positive cells after transduction with the retrovirus harbouring the respective transgene (Figure 12 A). In addition to the viruses used for reprogramming, GFP-carrying viruses were produced and used to test the functionality of the approach as well as to calculate the virus titer and transduction efficiency. Fetal hMSC 1 transduced with a GFP-carrying virus-based on the plasmid pLIB GFP revealed a total of 16.1% GFP-positive cells when analysed using FACS compared to the same cells without transduction which showed 0.13% GFP positivity. In addition to that, fetal hMSC 1 transduced with a GFP harbouring retrovirus displayed a positive fluorescence signal in the green channel of a fluorescence microscope (Figure 12 B and C).

Fetal hMSC 1 could be reprogrammed to induced pluripotent cells by all conditions used. Reprogramming in N2B27 medium and normoxia resulted in a reprogramming efficiency of 0.03%

whereas hypoxia (5% oxygen) enhanced the efficiency to 0.04% under the same conditions. Hypoxia and addition of mTeSR 1 after 14 days resulted in an efficiency of 0.04%. In contrast to that, hypoxia and addition of the inhibitor cocktail smM resulted in a reprogramming efficiency of 0.02%, whereas addition of mTeSR 1 enhanced the efficiency to 0.06% in fetal hMSC 1. One stable iPS cell line was isolated from fetal hMSC 1 by retroviral reprogramming under hypoxia in N2B27 medium named iPSC (hMSC, fetal, line 1, viral). In contrast to that, aged hMSC (74y) were reprogrammed with an efficiency of 0.0005% as part of my master thesis (Megges 2010). The generated iPS cell line was further characterised in this work. However, fetal hMSC 2, aged hMSC (60y), aged hMSC (62y) and aged hMSC (70y) could not be reprogrammed with any of the conditions used. The reprogramming experiments were stopped 65 days after viral transduction (Table 12).

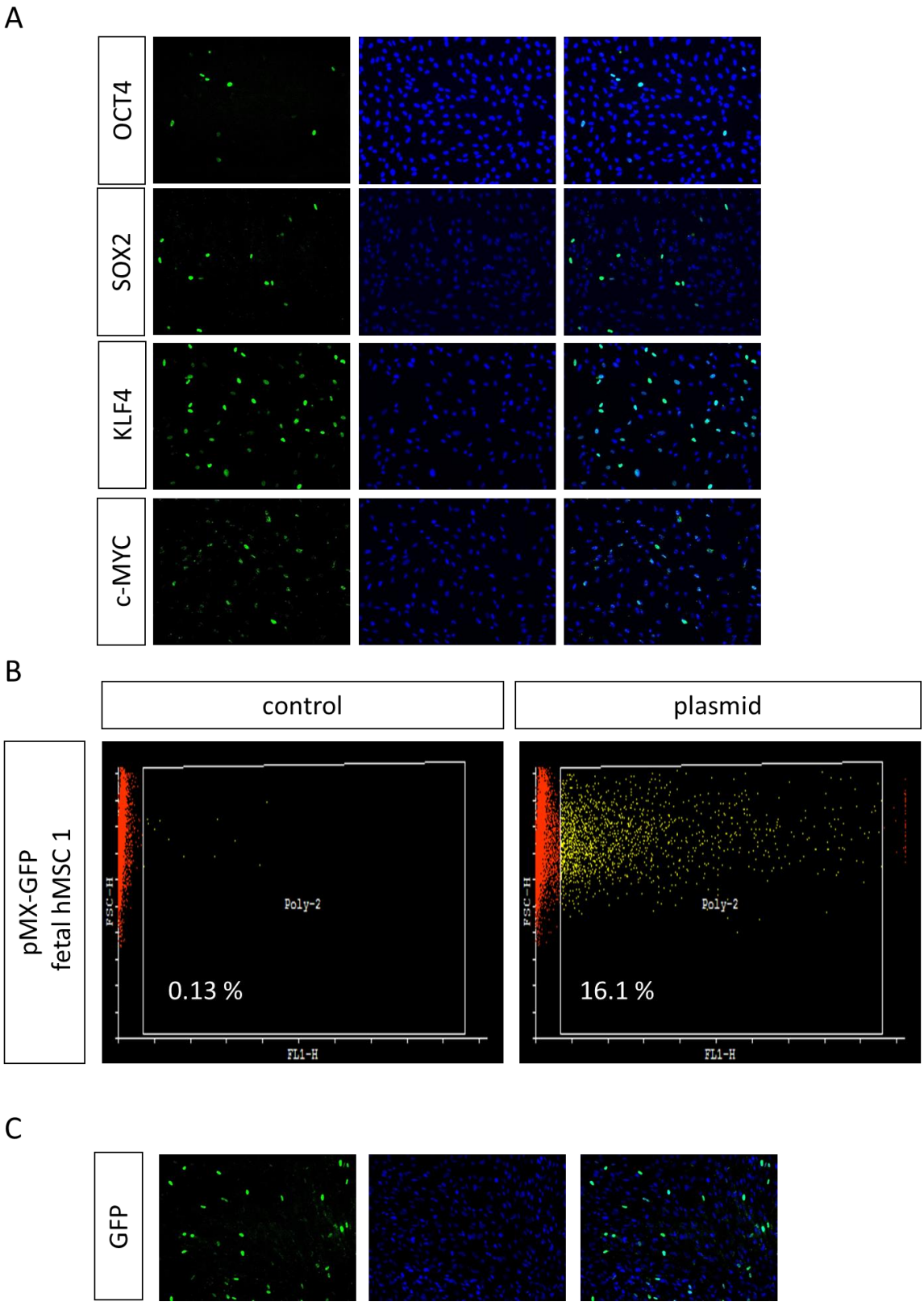

Figure 12 Confirmation of functionality of retroviruses used for reprogramming of hMSCs into iPS cells.

(A) Example of a functionality test of the generated retroviruses used for reprogramming. OCT4: fetal hMSC 1 infected with *OCT4*-harbouring retrovirus. SOX2: fetal hMSC 1 infected

with *SOX2*-harbouring retrovirus. KLF4: fetal hMSC 1 infected with *KLF4*-harbouring retrovirus. c-MYC: fetal hMSC 1 infected with c-*MYC*-harbouring retrovirus. The correct expression of the transgene was visualised by immunofluorescence staining employing primary antibodies specific for the respective transgene. Green: fluorescence signal visualising transgene expression. Blue: nuclei visualised by DAPI. Both: merge of green and blue channel. Confocal microscopy. 10 x magnification. (B) FACS-based quantification of infection efficiency. Example of fetal hMSC 1 infected with a retrovirus harbouring *GFP* (plasmid) compared to fetal hMSC 1 without infection (control). FACS analysis carried out one day after transduction. Shown are percentages of GFP-positive cells of cells measured. (C) Example of fetal hMSC 1 infected with a *GFP*-carrying retrovirus produced in parallel to *OCT4, SOX2, KLF4* and *c-MYC*-harbouring retroviruses. Picture taken 1 day after viral transduction. Green: expressed GFP. Blue: nuclei stained with DAPI. Confocal microscopy. 10 x magnification.

Reprogramming using episomal plasmids

Non-viral reprogramming based on episomal plasmids was conducted according to a protocol that was previously described (Yu et al. 2011). The plasmid combination 7F-2 was used employing the same amounts of plasmids for nucleofection. All reprogramming experiments were conducted on feeder cells (inactivated mouse embryonic fibroblasts). hMSCs were cultured for five days in hMSC medium before they were plated for reprogramming in N2B27 medium with FGF2. The same reprogramming conditions as described for viral reprogramming were used for episomal reprogramming: hypoxia or normoxia and addition of the inhibitor cocktail smM as well as medium switch to mTeSR 1 after 14 days (Yu et al. 2011). The addition of vitamin c to the reprogramming medium using a previously described concentration (Gao et al. 2013) was a modification yielded episomal iPSCs from aged hMSC (62y).

All hMSCs used in this study were nucleofected with the plasmid combination 7-F2. In order to analyse whether the nucleofection was successful, hMSCs were nucleofected with pmax-GFP, a control plasmid delivered as part of the Human MSC Nucleofector® Kit (LONZA), which was for all episomal plasmid-based reprogramming experiments. The nucleofection of fetal hMSC 1 pmax-GFP resulted in 30.1% GFP-positive cells measured using FACS compared to 0.4% cells measured as positive using FACS in non-nucleofected fetal hMSC 1. Moreover, 31.45% cells measured as GFP-positive cells by FACS compared to 1.34% cells detected as GFP-positive in nucleofected cells after the nucleofection of aged hMSC (62y) with pmax-GFP (

Figure 13 A). In addition to that, fetal hMSC 1 and aged hMSC (62y) nucleofected with pmax-GFP according to the manufacturer's instructions displayed a fluorescence signal in the green channel of a fluorescence microscope indicating the presence of GFP and successful nucleofection (

Figure 13 B and C).

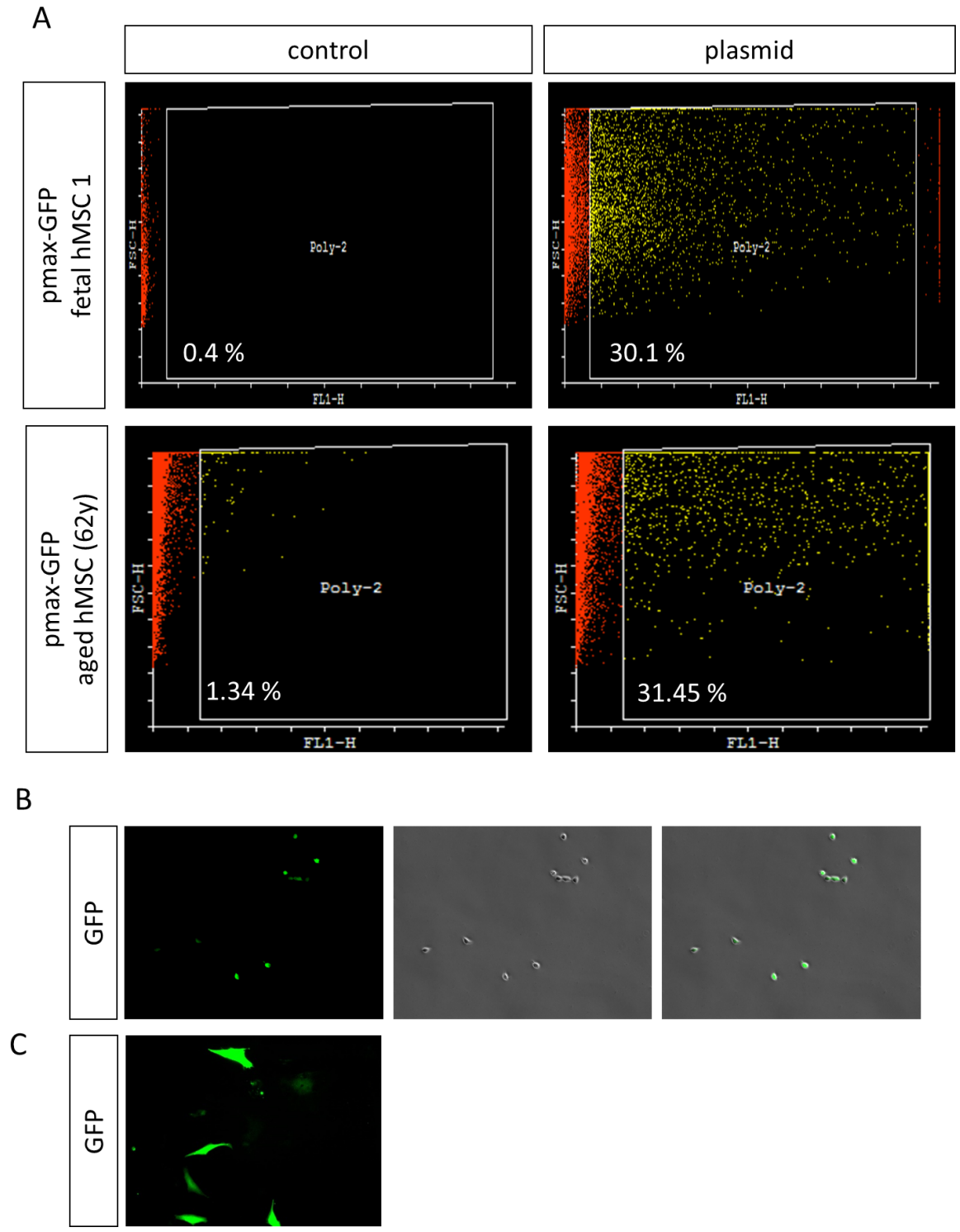

Figure 13 Confirmation of successful nucleofection in episomal plasmid-based reprogramming of fetal hMSCs and hMSCs of aged donors.

(A) FACS-based measurement of nucleofection efficiency. Shown are fetal hMSC 1 and aged hMSC (62y) nucleofected with the control plasmid pmax–GFP (plasmid) of the Human MSC Nucleofector® Kit (LONZA) used for reprogramming against non-nucleofected cells of the same type (control). The same nucleofection parameters as for the nucleofection of the episomal

plasmid combination for reprogramming were used. The cells measured as GFP-positive with this method of all measured cells are shown in percent. (B) Fetal hMSC 1 nucleofected with plasmid pmax-GFP of the Human MSC Nucleofector® Kit (LONZA) using the same conditions as for the nucleofection of episomal plasmid combination for reprogramming. Green: GFP-positive cells, Grey: bright-field recorded with a confocal microscope. 10 x magnification (C) Aged hMSC (62y) nucleofected with plasmid pmax-GFP using the same conditions that were used for the nucleofection of the episomal plasmid combination during reprogramming. Green: GFP-positive cells.

Fetal hMSC 1 could be reprogrammed using episomal plasmids with efficiencies of 0.01% to 0.05%. Reprogramming under normoxia in N2B27 medium resulted in a reprogramming efficiency of 0.01% with and without the inhibitor cocktail smM. In contrast to that, the reprogramming efficiency was 0.04% with N2B27 medium and 0.05% with N2B27 medium and switch to mTeSR 1 after 14 days, whereas hypoxic conditions and N2B27 medium with smM and with smM and medium switch to mTeSR 1 lead to a reprogramming efficiency of 0.01%. Interestingly, fetal hMSC 2 could be induced to derived iPS cell colonies under hypoxia, N2B27 medium, addition of smM and switch to mTeSR 14 days after the cells were plated for reprogramming with an efficiency of 0.02%. Under all other conditions used no pluripotent stem cell colonies could be detected during reprogramming of fetal hMSCs. Moreover, aged hMSC (62y) could be reprogrammed to iPSCs under hypoxia using the condition N2B27 medium and medium switch to mTeSR 1 14 days after seeding on feeder cells and addition of vitamin c. All other conditions tested to reprogram aged hMSC (62y) did not result in visible iPS cell colonies. In addition to that, aged hMSC (60y) and aged hMSC (70y) could not be reprogrammed to iPS cells by any of the tested conditions. (Table 12)
Four iPS cell lines were isolated and established using episomal plasmid-based reprogramming in this study. iPSC (hMSC, fetal, line 1, episomal 3) was derived from fetal hMSC 1 using N2B27 medium under normoxia, whereas iPSC (hMSC, fetal, line 1, episomal 1) and iPSC (hMSC, fetal, line 1, episomal 2) were derived from fetal hMSC 1 using N2B27 medium and the addition of the inhibitor cocktail smM under normoxia. Moreover, the iPS cell line iPSC (hMSC, 62y, episomal) was derived from aged hMSC (62y) under hypoxia N2B27 medium, addition of vitamin c and switch to mTeSR 1 14 days after seeding of the nucleofected cells on feeders (Table 12).

Isolation and expansion of iPS clones

During the course of all reprogramming experiments, morphological changes occurred, which resulted in the case of successful reprogramming into clusters of small cells that developed further into cells with a morphology similar to hESCs. These colony-like cell clusters were picked by hand using a pipette and seeded onto feeder cells using addition of ROCK inhibitor. When the picked colonies showed a stable hESC-like morphology, they were passaged further every seven days until the

characterisation was started at passage six. Figure 14 A shows an example of morphological changes that occurred during viral reprogramming of fetal hMSC 1 during the reprogramming experiment Fetal 1.8 described in Table 12 14 days after viral transduction. All iPS cell lines derived from fetal hMSC 1, aged hMSC (62y) and aged hMSC (74y) showed a morphology similar to human embryonic stem cells. The hMSC-iPSCs displayed a high nucleus to cytoplasm ratio and grew in colonies with smooth edges. Figure 14 B shows examples of the hESC-like morphology of iPSC (hMSC, fetal, line 1, episomal 1), iPSC (hMSC, 62y, episomal) and iPSC (hMSC, 74y, viral).

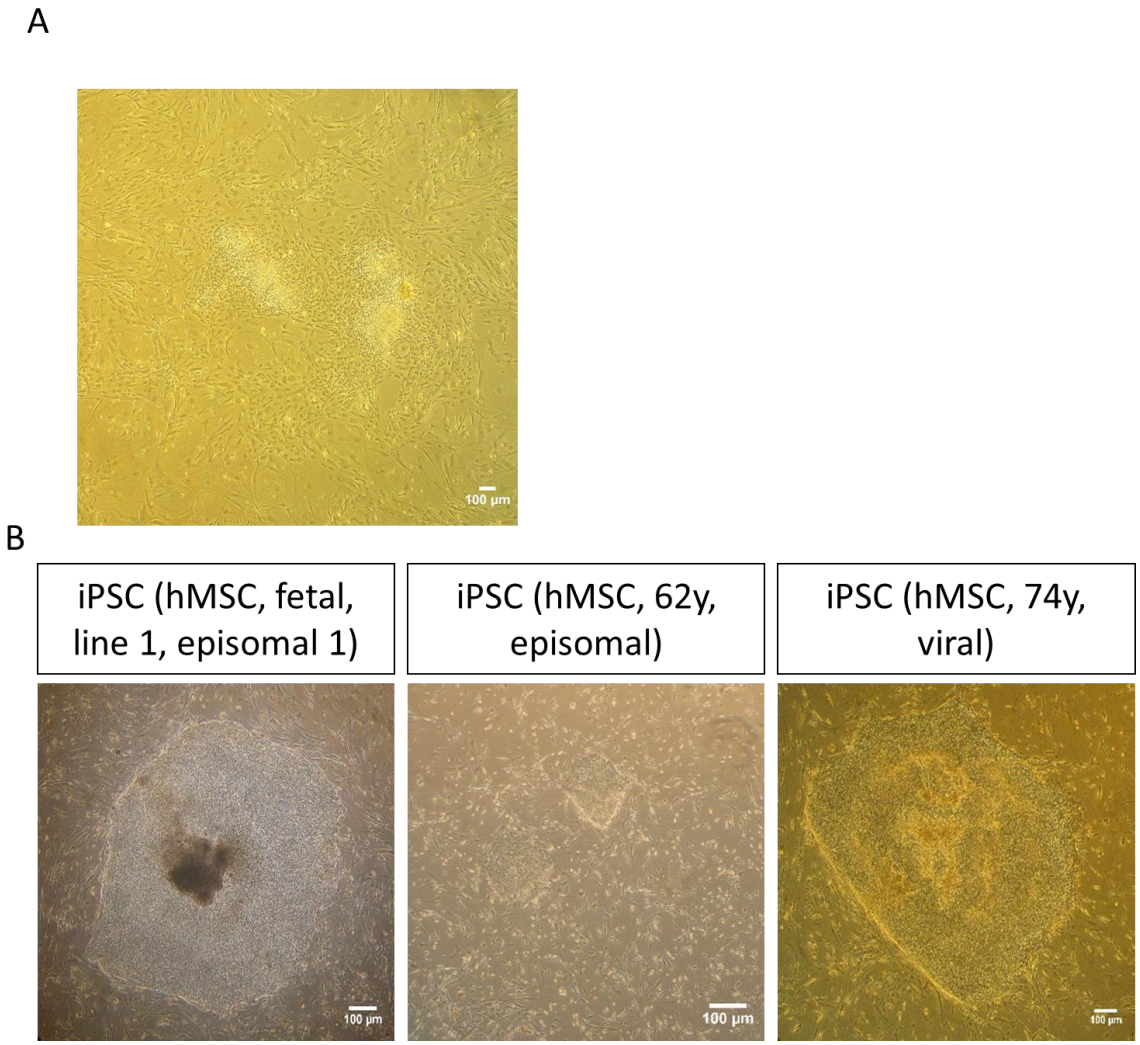

Figure 14 Morphological changes during reprogramming and morphology of generated hMSC-iPS cells.

(A) Representative picture of morphology changes observed during viral reprogramming of fetal hMSC 1 (reprogramming experiment Fetal 1.8) Picture taken at day 14 after viral transduction (B) Morphologies of generated hMSC-iPS cells. Pictures taken at passage 11: iPSC (hMSC, fetal, line 1, episomal 1), passage 8: iPSC (hMSC, 62y, episomal) and passage 18: iPSC (hMSC, 74y, viral). All iPS cell lines showed typical small cell size, colony-like growth and high

nucleus to cytosol ratio. Bright-field microscopy. Pictures were taken with a digital camera and processed using the software ImageJ.

Comparison of retroviral and episomal plasmid-based reprogramming efficiencies

As fetal hMSC 1 could be reprogrammed with all conditions tested, a comparison between the reprogramming techniques could be made. Viral reprogramming of fetal hMSC 1 under normoxia resulted in an efficiency of 0.03% compared to 0.01% when episomal plasmids were used. Moreover, viral reprogramming under hypoxia led to an efficiency of 0.04% and 0.04% when mTeSR 1 was added 14 days after viral transduction compared to efficiencies of 0.04% and 0.05% with mTeSR 1 addition after 14 days when episomal plasmid-based reprogramming was used. In addition to that, hypoxia and addition to the inhibitor cocktail smM resulted in an efficiency of 0.02% using viral reprogramming, whereas the efficiency was 0.01% when episomal plasmid-based reprogramming was used (Table 12).

Table 12 Overview of conducted viral and episomal plasmid-based reprogramming experiments. M: male, F: female; s: addition of small molecules: MEK inhibitor PD0325901, GSK3β inhibitor CHIR99021, TGF-β/Activin/Nodal receptor inhibitor A-83-01 and ROCK inhibitor HA-100. PD: MEK inhibitor PD0325901, SB: TGFβ receptor inhibitor SB-431542, p53i: P53 inhibitor pifithrin α. The reprogramming experiment of aged hMSC (74y) was part of a previously published master thesis (Megges 2010). Episomal: reprogramming based on episomal plasmids with the plasmid combination 7F-2 previously described. (Yu et al. 2011). Viral: reprogramming using retroviruses harbouring *OCT4, SOX2, KLF4* and *c-MYC*, N: normoxia, H: hypoxia, 5% oxygen. mTeSR: from day 14 post-transduction / post-nucleofection cells were cultured in mTeSR 1. Table see next page.

Reprogramming experiment	parental cell	age	sex	passage at infection/ nucleofection	reprogramming method	Hypoxia (H)/ Normoxia(N)	addtion of small molecules (s)	additional conditions	number of input cell	number of colonies visible (days post transduction/ nucleofection)	efficiency	iPS cell lines established
Fetal 1.1	fetal hMSC 1	day 55 post conception	M	2	episomal	N			3.3E+04	29(41)	0.01%	iPSC (hMSC, fetal, line 1, episomal 3)
Fetal 1.2	fetal hMSC 1			2	episomal	N	s		3.3E+04	28(41)	0.01%	iPSC (hMSC, fetal, line 1, episomal 1) iPSC (hMSC, fetal, line 1, episomal 2)
Fetal 1.3	fetal hMSC 1			2	episomal	H			8.0E+04	35(45)	0.04%	
Fetal 1.4	fetal hMSC 1			2	episomal	H		mTeSR	8.0E+04	36(45)	0.05%	
Fetal 1.5	fetal hMSC 1			2	episomal	H	s		2.0E+04	2(45)	0.01%	
Fetal 1.6	fetal hMSC 1			2	episomal	H	s	mTeSR	2.0E+04	2(45)	0.01%	
Fetal 1.7	fetal hMSC 1			2	viral	N			6.0E+04	18(55)	0.03%	
Fetal 1.8	fetal hMSC 1			2	viral	H			2.4E+05	101(55)	0.04%	iPSC (hMSC, fetal line 1, viral)
Fetal 1.9	fetal hMSC 1			2	viral	H		mTeSR	2.4E+05	150(55)	0.04%	
Fetal 1.10	fetal hMSC 1			2	viral	H	s		8.0E+04	17(55)	0.02%	
Fetal 1.11	fetal hMSC 1			2	viral	H	s	mTeSR	8.0E+04	50(55)	0.06%	
Fetal 2.1	fetal hMSC 2	day 55 post conception	M	2	episomal	N			4.0E+04	0(54)	n.a	
Fetal 2.2	fetal hMSC 2			2	episomal	H			2.0E+04	0(54)	n.a	
Fetal 2.3	fetal hMSC 2			2	episomal	H		mTeSR	2.0E+04	0(54)	n.a	
Fetal 2.4	fetal hMSC 2			2	episomal	H	s		4.0E+04	0(54)	n.a	
Fetal 2.5	fetal hMSC 2			2	episomal	H	s	mTeSR	4.0E+04	9(54)	0.02%	
Fetal 2.6	fetal hMSC 2			2	viral	N			6.0E+04	0(65)	n.a	
Fetal 2.7	fetal hMSC 2			2	viral	H			2.4E+05	0(65)	n.a	
Fetal 2.8	fetal hMSC 2			2	viral	H		mTeSR	2.4E+05	0(65)	n.a	
Fetal 2.9	fetal hMSC 2			2	viral	H	s		8.0E+04	0(65)	n.a	
Fetal 2.10	fetal hMSC 2			2	viral	H	s	mTeSR	8.0E+04	0(65)	n.a	
(60y).1	aged hMSC (60y)	60 years	F	2	episomal	N			4.0E+04	0(54)	n.a	
(60y).2	aged hMSC (60y)			2	episomal	H			2.0E+04	0(54)	n.a	
(60y).3	aged hMSC (60y)			2	episomal	H		mTeSR	2.0E+04	0(54)		
(60y).4	aged hMSC (60y)			2	episomal	H	s		4.0E+04	0(54)	n.a.	
(60y).5	aged hMSC (60y)			2	episomal	H	s	mTeSR	4.0E+04	0(54)		
(60y).6	aged hMSC (60y)			2	viral	N			6.0E+04	0(65)	n.a	
(60y).7	aged hMSC (60y)			2	viral	H			2.4E+05	0(65)	n.a	
(60y).8	aged hMSC (60y)			2	viral	H		mTeSR	2.4E+05	0(65)		
(60y).9	aged hMSC (60y)			2	viral	H	s		8.0E+04	0(65)	n.a	
(60y).10	aged hMSC (60y)			2	viral	H	s	mTeSR	8.0E+04	0(65)		
(62y).1	aged hMSC (62y)	62 years	F	2	episomal	N			4.0E+04	0(54)	n.a	
(62y).2	aged hMSC (62y)			2	episomal	H			2.0E+04	0(54)	n.a	
(62y).3	aged hMSC (62y)			2	episomal	H		mTeSR	2.0E+04	0(54)		
(62y).4	aged hMSC (62y)			2	episomal	H		mTesR+ Vitamin C	2.0E+04	8(54)	0.04%	iPSC (hMSC, 62y, episomal)
(62y).5	aged hMSC (62y)			2	episomal	H	s		4.0E+04	0(54)	n.a.	
(62y).6	aged hMSC (62y)			2	episomal	H	s	mTeSR	4.0E+04	0(54)		
(62y).7	aged hMSC (62y)			2	viral	N			6.0E+04	0(65)	n.a	
(62y).8	aged hMSC (62y)			2	viral	H			2.4E+05	0(65)	n.a	
(62y).9	aged hMSC (62y)			2	viral	H		mTeSR	2.4E+05	0(65)		
(62y).10	aged hMSC (62y)			2	viral	H	s		8.0E+04	0(65)	n.a	
(62y).11	aged hMSC (62y)			2	viral	H	s	mTeSR	8.0E+04	0(65)		
(70y).1	aged hMSC (70y)	70 years	F	2	viral	N			6.0E+04	0(55)	n.a	
(70y).2	aged hMSC (70y)			2	viral	H			6.0E+04	0(55)	n.a	
(70y).3	aged hMSC (70y)			2	viral	H	s		6.0E+04	0(55)	n.a	
(74y).1	aged hMSC (74y)	74 years	F	2	viral	N		SB, PD, p53i	2.0E+05	1(40)	0.0005%	iPSC (hMSC, 74y, viral)

3.2.2 Characterisation of hMSC-iPSCs

In order to confirm pluripotency, the iPS cells derived from hMSCs of fetal and high age background were tested towards expression of pluripotency markers.

A green fluorescence signal indicating the expression of the pluripotency marker alkaline phosphatase could be detected in iPSC (hMSC, fetal, line 1, viral), iPSC (hMSC, fetal, line 1, episomal 1), iPSC (hMSC, fetal, line 1, episomal 2), iPSC (hMSC, fetal, line 1, episomal 3), iPSC (hMSC, 62y, episomal) and iPSC (hMSC, 74y, viral) (Figure 15).

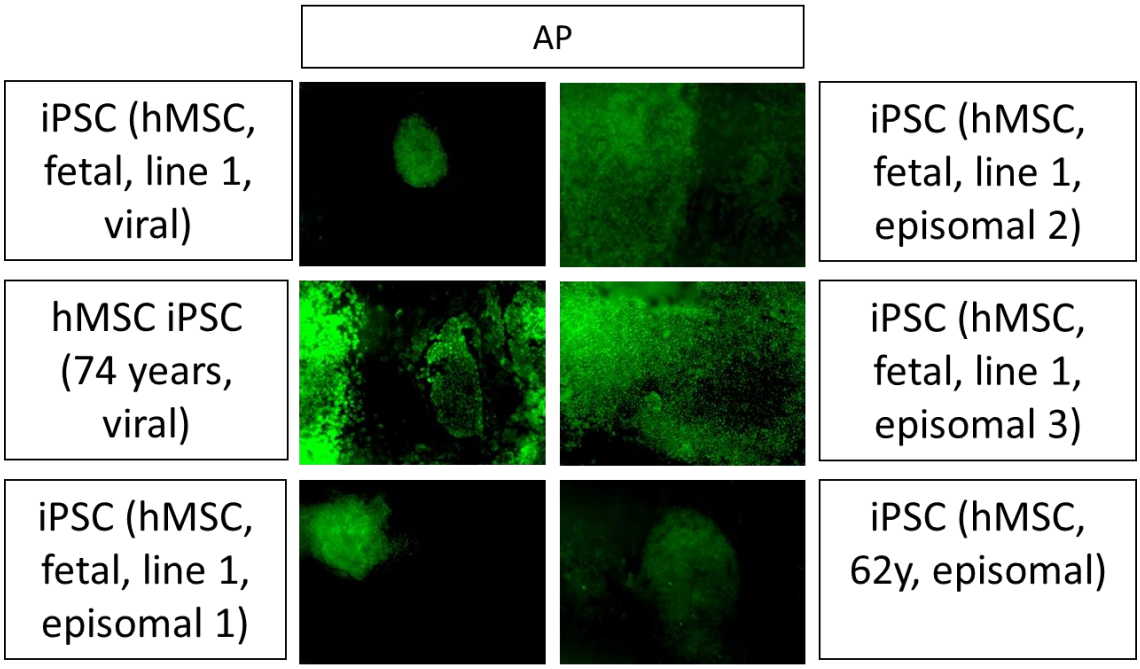

Figure 15 Expression of pluripotency marker alkaline phosphatase in hMSC-iPSCs of different age and reprogramming backgrounds.
iPSCs were stained with Alkaline Phosphatase Live Stain (Life Technologies). Green: alkaline phosphatase positive cells. Confocal microscopy. 10 x magnification. AP: alkaline phosphatase.

In addition to that, microarray-based gene expression profiling and subsequent comparison of measured expression of pluripotency marker genes in the derived hMSC-iPSCs of different age background revealed the induction pluripotency-related genes in fetal hMSC 1 using viral and episomal plasmid-based reprogramming, in aged hMSC (74y) with viral reprogramming and in aged hMSC (62y) with episomal plasmid-based reprogramming. The pluripotency-related genes were detected as expressed in iPSC (hMSC, fetal, line 1, episomal 1), iPSC (hMSC, fetal, line 1, episomal 2) and iPSC (hMSC, 74y, viral) in a similar manner to the expression in hESC H1. In contrast to that, iPSC (hMSC, fetal, line 1, viral) and iPSC (hMSC, 62y, episomal) were found to express fewer pluripotency-related genes compared to hESCs and the other hMSC-iPSCs. However more pluripotency-related genes were expressed than in the parental hMSCs, fetal hMSC 1 and aged hMSC (62y). The pluripotency marker gene *NANOG* was expressed in hESC H1 as well as in hMSC-iPSCs except iPSC (hMSC, fetal, line 1, viral) in which a very low expression of this gene was detected. Furthermore, *LIN28* and *LEFTY1* displayed a high expression in iPSC (hMSC, fetal, line 1, episomal

1), iPSC (hMSC, fetal, line 1, episomal 2) and iPSC (hMSC, 74y, viral) but a low expression in iPSC (hMSC, fetal, line 1, viral) and iPSC (hMSC, 62y, episomal). In contrast to that, the pluripotency marker genes *KLF4*, *SOX2*, *POU5F1* (*OCT4*), *c-MYC* and *DPPA4* showed high expression levels in all iPS cell lines similar to the expression in hESC H1. However, genes like *FGF4* and *TERT* were detected with a low expression in all samples (Figure 16 A). Subsequently, the expression of pluripotency markers was tested on the protein level using immunofluorescence staining. The set of antibodies used for this purpose was tested using hESC H1 as positive control. Indeed, the expression of OCT4, NANOG, SOX2, KLF4, SSEA4, TRA1-60, TRA1-81 and absence of SSEA1 could be confirmed in hESCs (Figure 16 B). Moreover, the expression of the pluripotency markers OCT4, NANOG, SOX2, KLF4, c-MYC, SSEA4, TRA1-60, TRA1-81 and absence of SSEA1 expression could be confirmed in iPSC (hMSC, 74y, viral) and iPSC (hMSC, fetal, line 1, viral). However, iPSC (hMSC, fetal, line 1, viral) were not stained for c-MYC and SSEA1 (Figure 16 C and D). In addition to that, iPSC (hMSC, fetal, line 1, episomal 1), iPSC (hMSC, fetal, line 1, episomal 2) and iPSC (hMSC, fetal, line 1, episomal 3) showed positive staining results for the pluripotency markers OCT4, NANOG, SOX2, SSEA4 and TRA1-60, whereas iPSC (hMSC, 62y, episomal) displayed positive immunofluorescence staining results for OCT4, NANOG, SSEA4, TRA1-60, TRA1-81 (Figure 17).

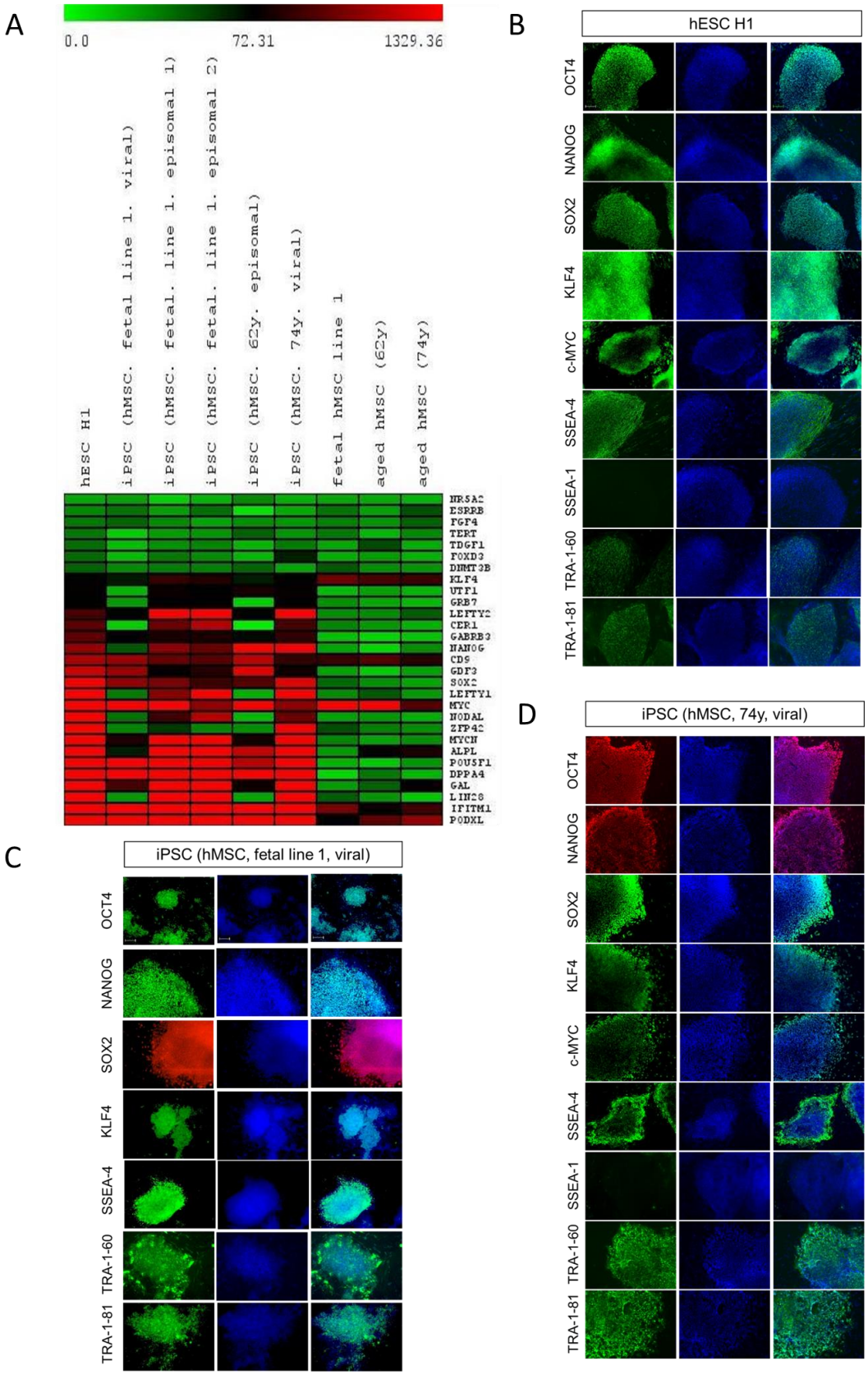

Figure 16 Analysis of pluripotency maker gene expression in hMSCs of fetal and aged background and immunofluorescence-based pluripotency marker detection in iPS cells derived with retrovirus-mediated reprogramming.

(A) Heatmap based on average signal intensities of pluripotency-related genes detected using an Illumina Bead Chip microarray in samples isolated from iPSCs derived from fetal hMSC 1, aged hMSC (62y) and aged hMSC (74y) by viral and episomal plasmid based methods. Parental hMSCs and hESC H1 are shown for comparison. Gene description see Table 21. (B) Pluripotency marker expression in hESC H1 cultured in unconditioned medium. (C) Expression of pluripotency markers detected in iPSCs derived from fetal hMSC 1 by retroviral reprogramming. (D) Expression of pluripotency markers detected in iPSCs derived from aged hMSC (74y) (taken from (Megges et al. 2015)) by means of retroviral reprogramming. The marker expression was comparable to the expression in hESC H1 shown in B. (B, C, D): Immunofluorescence. Green/red: fluorescence signal indicating marker expression. Blue: Nuclei visualised by DAPI. Confocal microscopy. 10 x magnification. Scale bar=100µm.

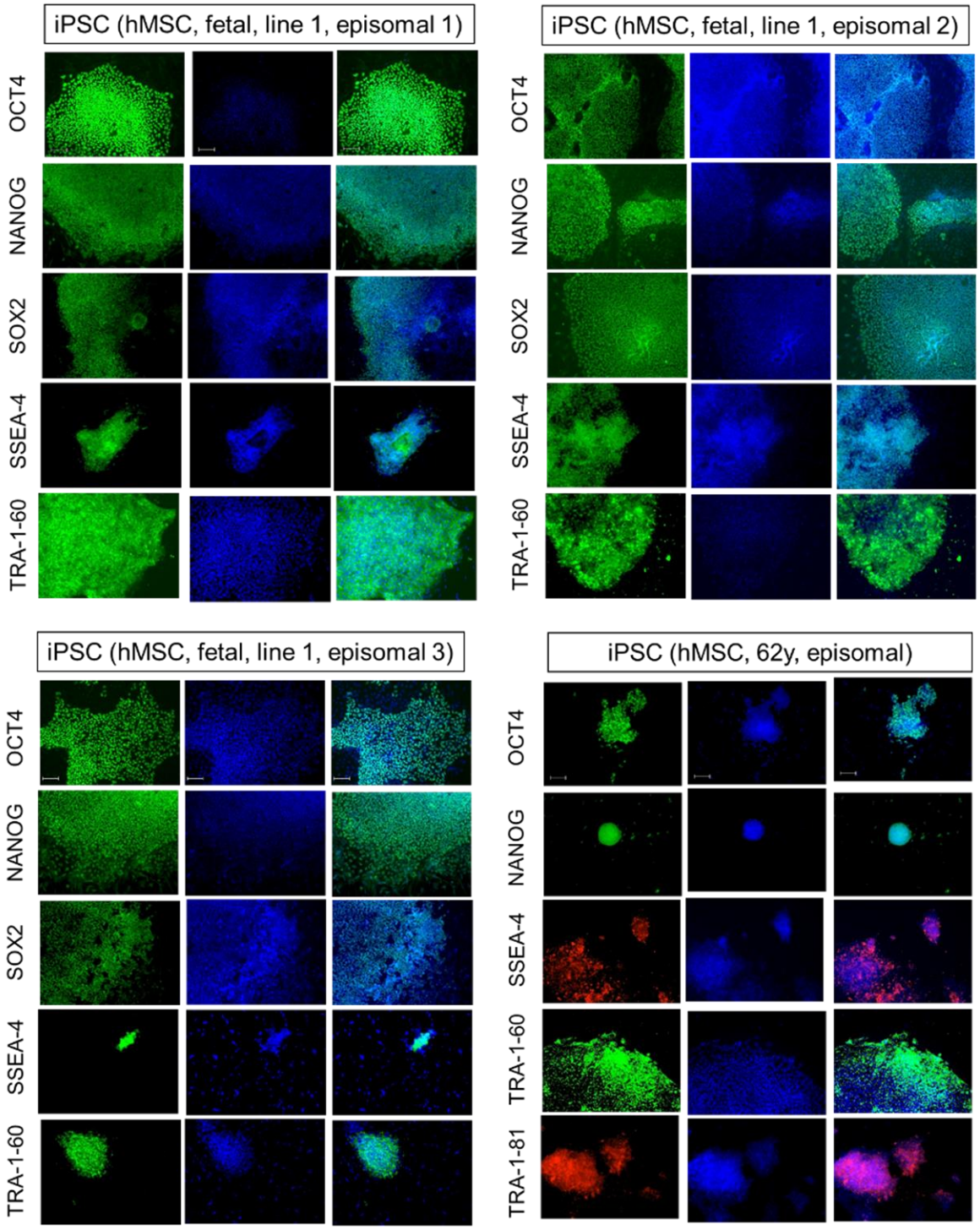

Figure 17 Immunofluorescence-based pluripotency marker detection in iPS cells derived with episomal plasmid-based reprogramming methods.

Episomal plasmid-based reprogramming resulted in iPSCs derived from fetal hMSC 1 and aged hMSC (62y) that express pluripotency markers in a manner similar to hESC H1 shown in Figure 16 B. Immunofluorescence-based visualisation. Green/red: fluorescence signal indicating marker expression. Blue: Nuclei visualised by DAPI. Confocal microscopy. 10 x magnification. Scale bar=100µm.

In order to confirm the somatic origin of the derived hMSC-iPS cell lines DNA fingerprinting was performed. iPSC (hMSC, fetal, line 1, viral), iPSC (hMSC, fetal, line 1, episomal 1), iPSC (hMSC, fetal, line 1, episomal 2), iPSC (hMSC, fetal, line 1, episomal 3), iPSC (hMSC, 62y, episomal) and iPSC (hMSC, 74y, viral) showed the same size distribution of PCR products as their parental cells. In addition, cross contamination with the embryonic stem cell lines H1 and H9 could be ruled out as none of the iPS cell lines had the same pattern of PCR product sizes (Figure 18 A, B, C and D).

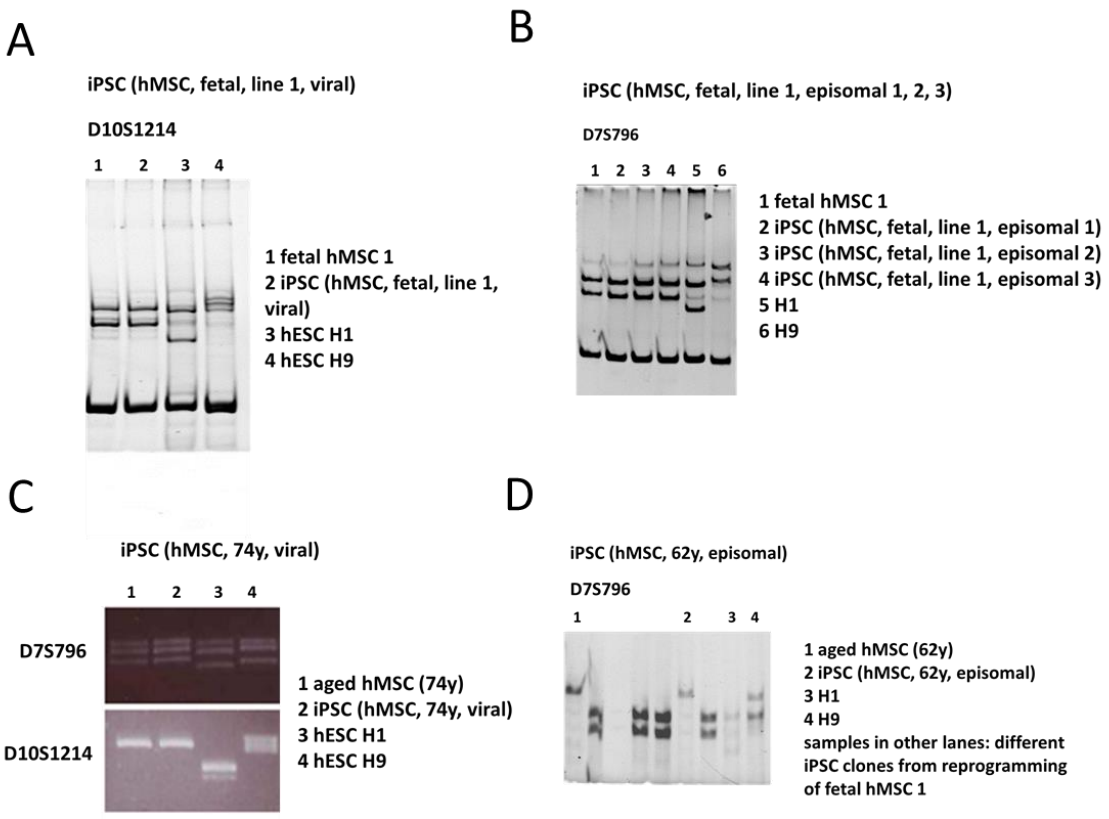

Figure 18 Confirmation of the somatic origin of generated hMSC-iPSCs.

DNA fingerprinting was used to confirm the original parental primary hMSC population of the respective iPSCs using microsattelite-specific primers in a PCR with genomic DNA of (A) iPSC (hMSC, fetal, line 1, viral) with a primer for the microsattelite marker D10S1214, (B) iPSC (hMSC, fetal, line 1, episomal 1), iPSC (hMSC, fetal, line 1, episomal 2) and iPSC (hMSC, fetal, line 1, episomal 3) using a primer for D7S796, (C) iPSC (hMSC, 74y, viral) using primers for D7S796 and D101214 (taken from (Megges et al. 2015)) and (D) iPSC (hMSC, 62y, episomal) using primers for D7S796. The PCR products were separated using agaraose gel electrophoresis in 4% agarose gels the case of (C) or in 4% acrylamide gels using electrophoresis in (A), (B) and (D). Genomic DNA of hESC H1 and H9 was used in all experiments to exclude cross-contamination with these pluripotent cell lines during reprogramming.

Moreover, the iPS cell lines derived from hMSCs using episomal plasmid-based reprogramming were tested towards the presence of the episomal plasmid using PCR and transgene-specific primers. iPSC (hMSC, fetal, line 1, episomal 1), iPSC (hMSC, fetal, line 1, episomal 2), iPSC (hMSC, fetal, line 1, episomal 3) as well as iPSC (hMSC, 62y, episomal) derived genomic DNA was used in the PCR reaction. No PCR product was generated in all samples of the episomal plasmid derived iPS cell lines, which were derived from fetal hMSC 1 and from aged hMSC (62y). However, a PCR product was generated when the episomal plasmid pEP4 E02S ET2K was used (Figure 19 A and B).

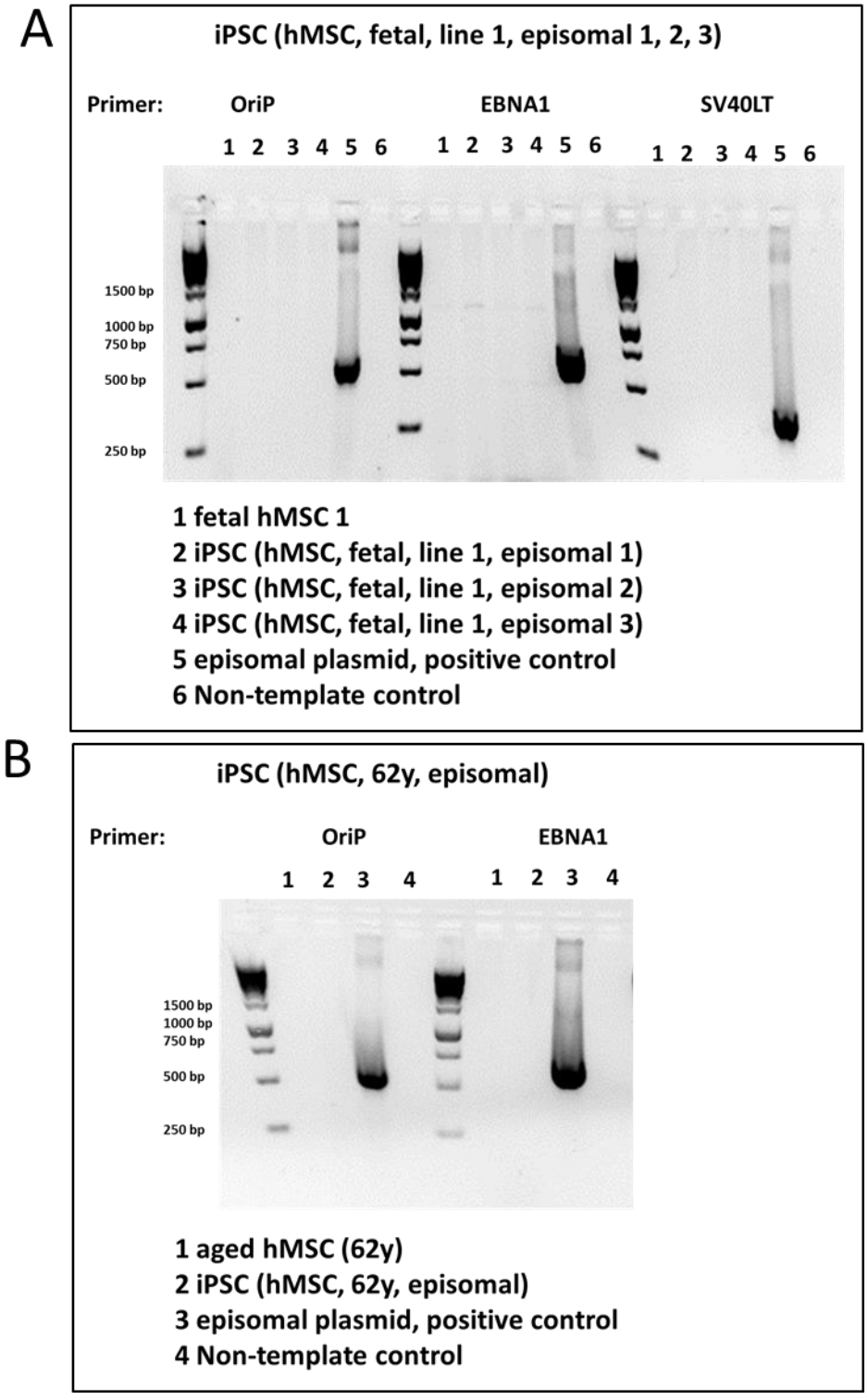

Figure 19 Episomal plasmids are not present in hMSC-iPSCs derived with episomal plasmid-based reprogramming.

The absence of episomal plasmids in hMSC-iPSCs could be confirmed with PCR using genomic DNA of iPS cells as template and primers specific for sequences within *OriP*, *EBNA1* or *SV40LT* on the episomal plasmids. (A) Sequences within *OriP*, *EBNA1* and *SV40LT* on the episomal plasmids could not be detected in genomic DNA samples of iPSC (hMSC, fetal, line 1, episomal

1), iPSC (hMSC, fetal, line 1, episomal 2) and iPSC (hMSC, fetal, line 1, episomal 3) compared to the positive control, 50ng of the episomal plasmid pEP4 E02S ET2K, and negative control, gDNA of parental fetal hMSC 1. gDNA was isolated at passage 26 after iPS cell isolation. (B) Sequences within *OriP*, *EBNA1* and *SV40LT* on the episomal plasmids could not be detected in the genomic DNA sample of iPSC (hMSC, 62y, episomal) compared to the positive control, 50ng of the episomal plasmid pEP4 E02S ET2K and negative control parental aged hMSC (62y). Size marker: GeneRuler 1 kb DNA Ladder (Life Technologies). Maps of the episomal plasmids can be found in the appendix.

As a next step, all derived hMSC-iPS cell lines were analysed towards their pluripotency using an embryoid body based *in vitro* differentiation assay testing the ability to give rise to derivatives of all three germ layers expressing the respective marker proteins. The embryonic stem cell line H1 served as positive control. The expression of mesodermal marker smooth muscle actin (SMA), the ectodermal markers nestin (NES), β-III tubulin (TUJ1) and the endodermal markers α fetoprotein (AFP) and SOX17 could be detected via immunofluorescence staining in hESC H1 after embryoid body-based differentiation (Figure 20 A). Likewise, all derived hMSC-iPS cell lines expressed markers of endoderm, mesoderm and ectoderm after embryoid body-based differentiation. The expression of smooth muscle actin (SMA), the ectodermal markers nestin (NES), β-III tubulin (TUJ1) and the endodermal markers α fetoprotein (AFP) and SOX17 could be detected via immunofluorescence staining in hMSC-iPSCs derived using viral and episomal plasmid-based reprogramming. In addition to that, all derived iPS cell lines expressed brachiury at day 7 after being plated as embryoid bodies onto gelatine-coated cell culture dishes and cultured without FGF2 (Figure 20 B, Figure 21).

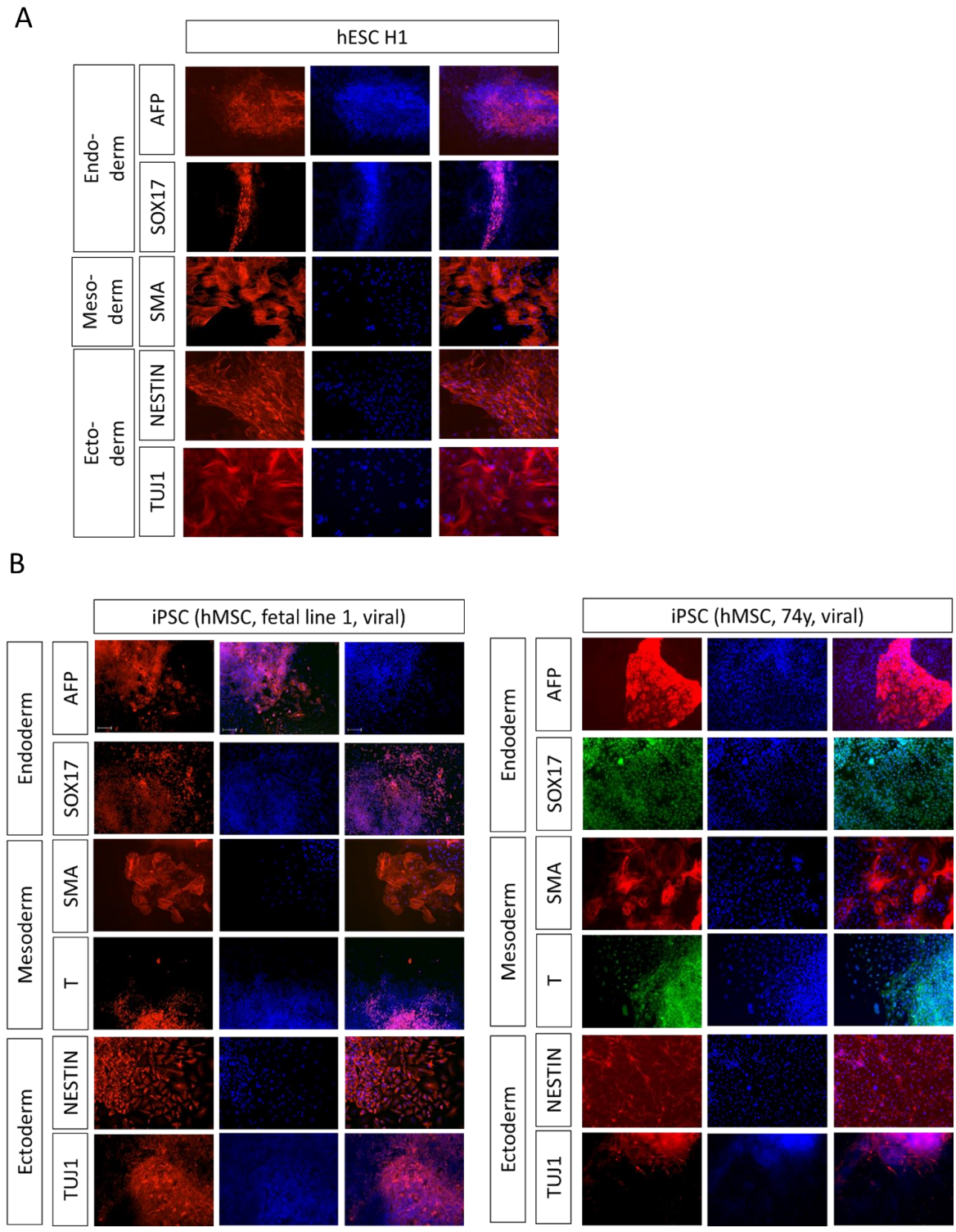

Figure 20 *In vitro* pluripotency confirmation for iPSCs derived from fetal hMSCs and elderly donors by viral reprogramming.

Embryoid body-based differentiation was performed to test the ability of the generated hMSC-iPSCs to generate derivatives of all three germ layers. Derivatives of mesoderm, ectoderm or endoderm were identified by immunofluorescence staining using germ layer-specific markers. (A) hESCs H1 served as positive control and expressed markers of all three germ layers upon

embryoid body-based differentiation. (B) iPSCs derived from fetal hMSC 1 and aged hMSC (74y) (taken from (Megges et al. 2015)) by retroviral reprogramming expressed markers of the three germ layers after embryoid body-based differentiation. Immunofluorescence staining using primary antibodies against mesodermal markers brachiury (T), smooth muscle actin (SMA), ectodermal markers nestin (NES), β-III tubulin (TUJ1) and endodermal markers α fetoprotein (AFP) and SOX17. Green/red: fluorescence signal of marker protein detected by immunofluorescence. Blue: nuclei visualised by DAPI. Confocal microscopy. 10 x magnification. Scale bar=100µm.

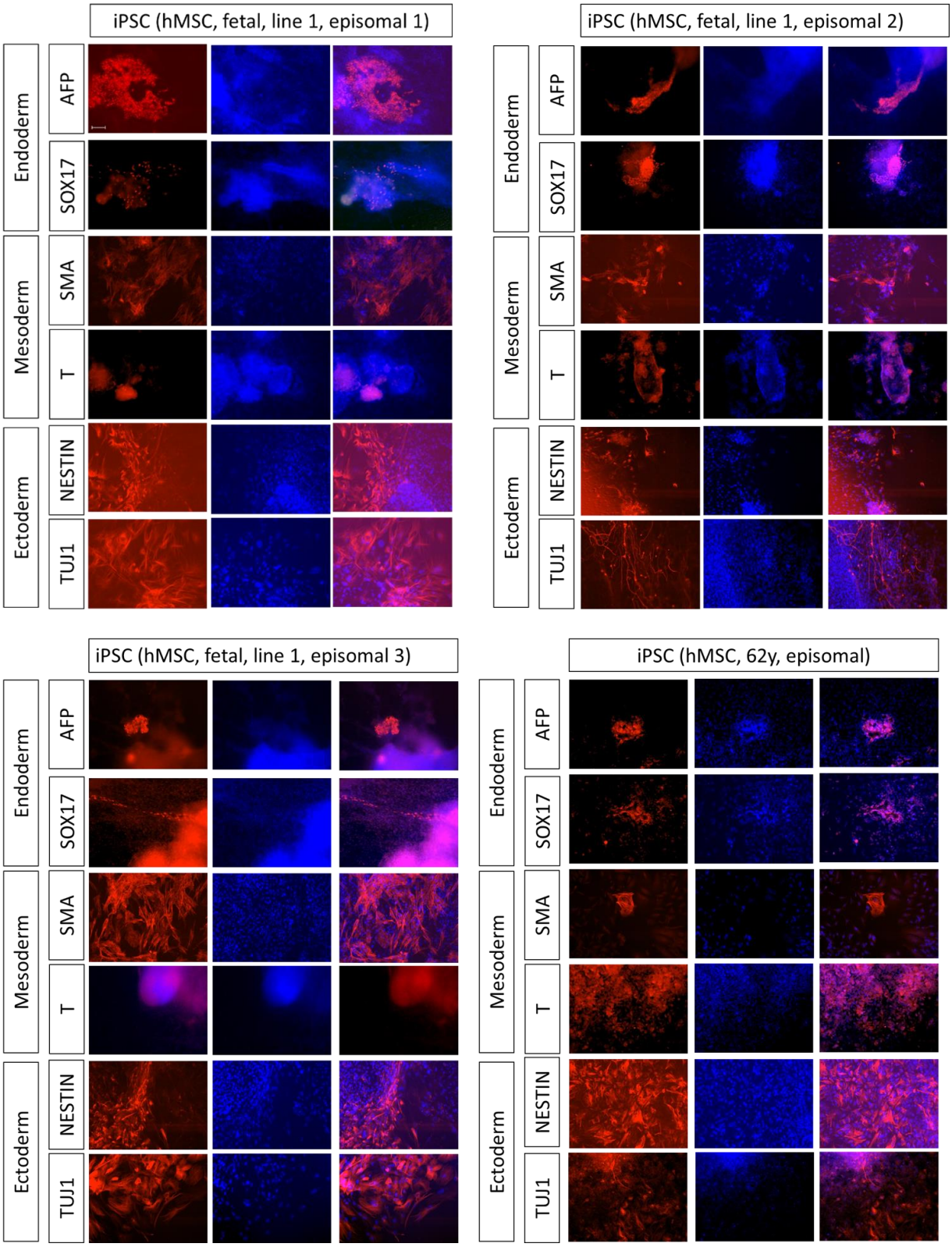

Figure 21 *In vitro* pluripotency confirmation for iPSCs derived from fetal hMSCs and elderly donors by episomal plasmid-based reprogramming.

Embryoid body-based differentiation was performed to test the ability of the generated hMSC-iPSCs to generate derivatives of all three germ layers. Derivatives of mesoderm, ectoderm or endoderm were identified by immunofluorescence staining using germ layer-specific markers.

iPSCs derived from fetal hMSC 1 and aged hMSC (62y) by episomal plasmid-based reprogramming were able to undergo differentiation into lineages of the three germ layers as confirmed by expression of markers for mesoderm, ectoderm and endoderm. Immunofluorescence staining using primary antibodies against mesodermal markers brachiury (T), smooth muscle actin (SMA), ectodermal markers nestin (NES), β-III tubulin (TUJ1) and endodermal markers α fetoprotein (AFP) and SOX17. Green/red: fluorescence signal of marker protein detected by immunofluorescence. Blue: nuclei visualised by DAPI. Confocal microscopy. 10 x magnification. Scale bar=100µm.

In order to test the genomic stability of the iPS cell lines derived from fetal hMSCs and hMSC of older donors, GTG banding-based karyotyping was performed. iPSC (hMSC, fetal, line 1, episomal 1) and iPSC (hMSC, fetal, line 1, episomal 2) revealed a normal male karyotype in 20 metaphases that were analysed. In contrast to that, iPSC (hMSC, fetal, line 1, episomal 3) showed an aberrant male karyotype with a derivative chromosome 15 containing additional material with the size of a D group chromosome in all metaphases (46,XY,add(15)(q24[20]) in 20 analysed metaphases. In addition, iPSC (hMSC, 74y, viral) revealed a normal female karyotype in 25 of 33 analysed metaphases. However, 8 of 33 metaphases showed a tetraploid female karyotype (46,XX[25]/92,XXXX[8]) (Figure 22). The karyotype of iPSC (hMSC, fetal, line 1, viral) and iPSC (hMSC, 62y, episomal) needs to be analysed to confirm absence of aberrations.

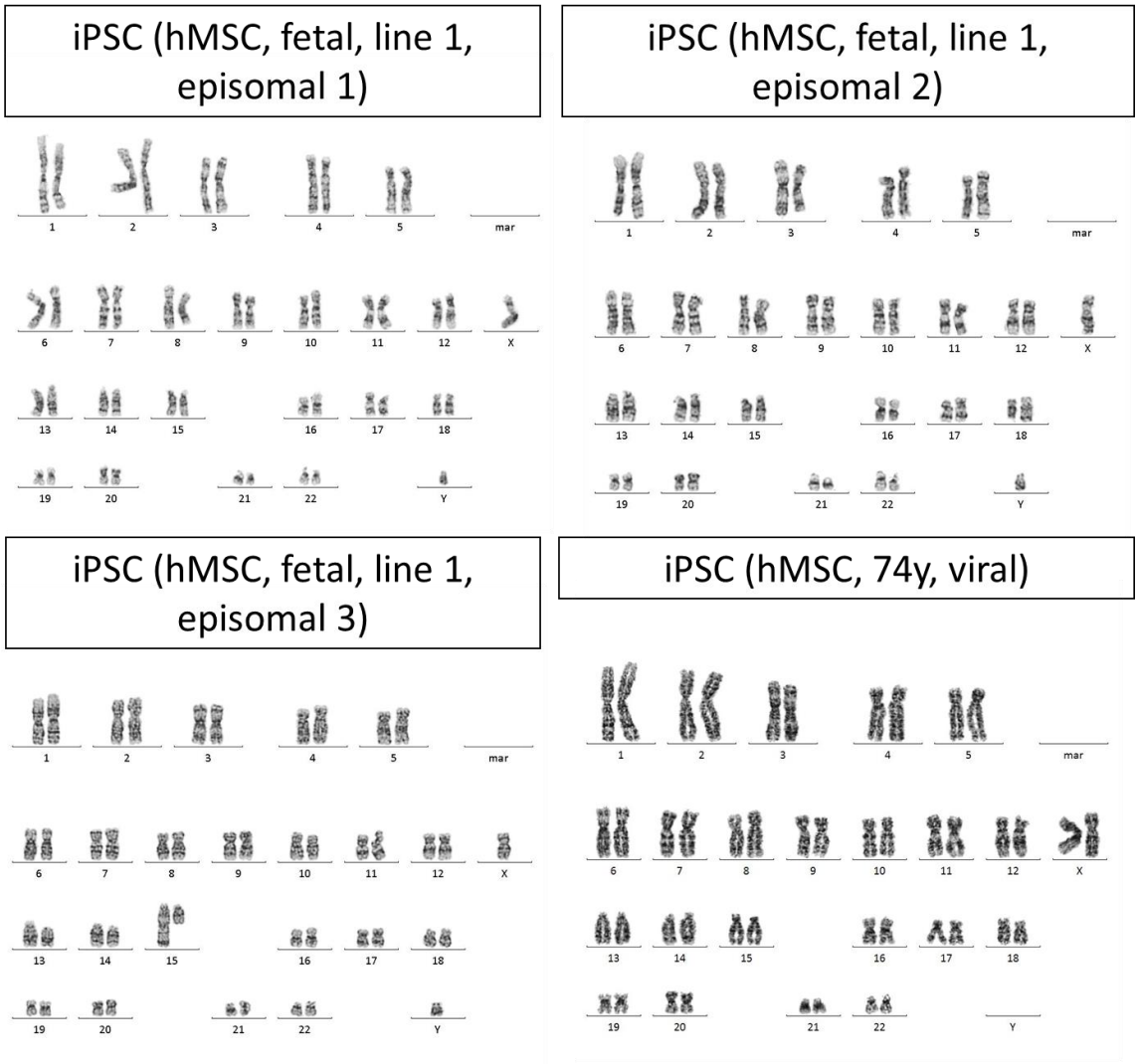

Figure 22 Karyotype of generated hMSC-iPSCs.

Chromosomal analysis by GTG banding was used to characterise the karyotype of the derived hMSC-iPSCs. A normal male karyotype was found in 20 metaphases in iPSC (hMSC, fetal, line 1, episomal 1) and iPSC (hMSC, fetal, line 1, episomal 2). An aberrant male karyotype with a derivative chromosome 15 containing additional material with the size of a D group chromosome in all metaphases (46,XY,add(15)(q24[20]) was found in iPSC(hMSC, fetal, line 1, episomal 3). The chromosomal analysis of iPSC (hMSC, 74y, viral) revealed a normal female karyotype in 25 of 33 analysed metaphases. 8 of 33 metaphases revealed a tetraploid female karyotype (46,XX[25]/92,XXXX[8]). Chromosomal analysis of iPSC (hMSC, 74y, viral) taken from (Megges et al. 2015).

After confirmation of pluripotency using embryoid body-based differentiation, further pluripotency tests were performed. iPSC (hMSC, 74y, viral) were tested towards their ability to differentiate into lineages of all three germ layers in an *in vivo* teratoma test. To do this, iPSC (hMSC, 74y, viral) cells were injected subcutaneously in a NOD scid gamma mouse. Using this method the formation of

endodermal, mesodermal and ectodermal tissue structures in the derived teratoma could be confirmed in two experiments (Figure 23 A). The *in vivo* confirmation of pluripotency using this test was not performed for iPSC (hMSC, fetal, line 1, viral), iPSC (hMSC, fetal, line 1, episomal 1), iPSC (hMSC, fetal, line 1, episomal 2), iPSC (hMSC, fetal, line 1, episomal 3) and iPSC (hMSC, 62y, episomal). However, all derived hMSC-iPS cell lines were tested using the *in silico* transcriptome-based test towards pluripotency called PluriTest which was recently described (Müller et al. 2011). According to the results of this test, hESCs H1 and H9 as well as all iPS cell lines derived from hMSCs in this study are similar. Interestingly, iPSC (hMSC, fetal, line 1, viral) and iPSC (hMSC, 62y, episomal) are more similar to each other than to the other iPS and hESC samples whereas iPSC (hMSC, fetal, line 1, episomal 1), iPSC (hMSC, fetal, line 1, episomal 2) and hESC H1 and H9 samples were more similar to each other than to the other samples. However, the outcome in hMSCs derived from fetal and aged donors is not similar to the hESC and iPSC samples. In addition, the hMSC samples are similar among each other based on the results of PluriTest (Figure 23 B).

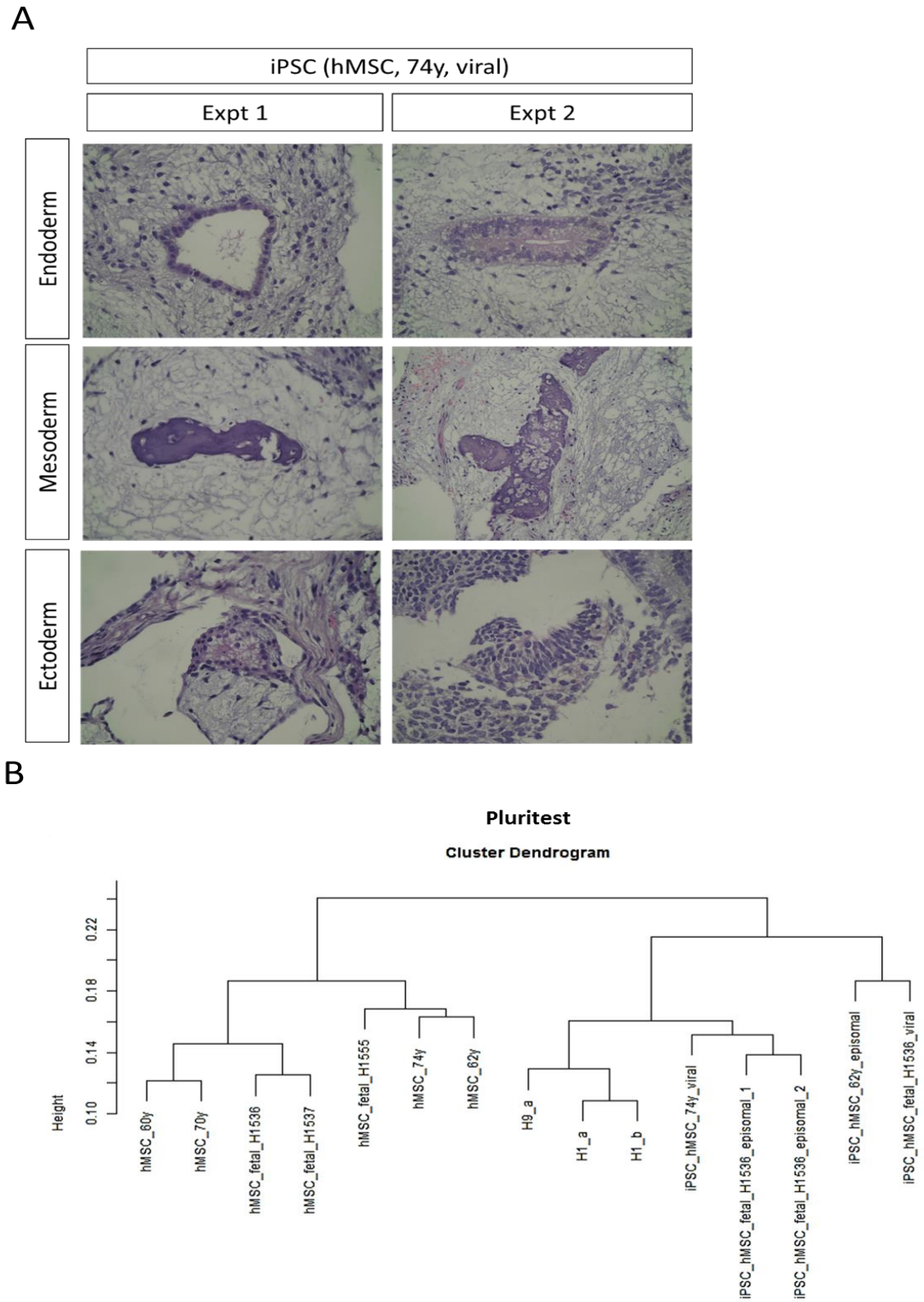

Figure 23 *In vivo* confirmation of pluripotency in iPSC (hMSC, 74y, viral) and transcriptome-based confirmation of pluripotency in generated hMSC-iPSCs.

(A) iPSC (hMSC, 74y, viral) was able to differentiate into derivatives of the three germ layers in two experiments after subcutaneous injection in a NOD scid gamma mouse: Expt 1: endoderm:

tublar gland-like structure; mesoderm: bone; ectoderm: mucous gland. Expt 2: endoderm: gut-like epithelium; mesoderm: bone; ectoderm: neuroepithelial structure. Haematoxylin and eosin stained teratoma tissue sections of each experiment. Bright-field microscopy. Taken from (Megges et al. 2015) (B) Hierarchical clustering dendrogram of generated hMSC-iPS cells, hESCs H1 and H9 and hMSCs of fetal and aged origin based on the results of the transcriptome-based *in silico* pluripotency test PluriTest (Müller et al. 2011). hMSC_fetal_H1536: fetal hMSC 1, hMSC_fetal_H1537: fetal hMSC 2, hMSC_60y: aged hMSC (60y), hMSC_62y: aged hMSC (62y), hMSC_70y: aged hMSC (70y), hMSC_74y: aged hMSC (74y), iPSC_hMSC_fetal_H1536_viral: iPSC (hMSC, fetal, line 1, viral), iPSC_hMSC_fetal_H1536_episomal_1: iPSC (hMSC, fetal, line 1, episomal 1), iPSC_hMSC_fetal_H1536_episomal_2: iPSC (hMSC, fetal, line 1, episomal 2), iPSC_hMSC_62y_episomal: iPSC (hMSC, 62y, episomal), iPSC_hMSC_74y_viral: iPSC (hMSC, 74y, viral), H1_a, H1_b: hESC H1, H9_a: hESC H9.

In order to characterise the commonalities and differences of the transcriptomes of hMSCs of different age background with the transcriptomes of corresponding hMSC-iPSCs and with the transcriptomes of hESCs H1 and H9, a microarray-based gene expression analysis was performed using RNA samples isolated from the respective cells. To visualise the similarities between the samples, a clustering dendrogram was generated based on the Pearson correlation of the transcriptomes using GenomeStudio. Interestingly, iPS cell samples and hESC samples formed one cluster, which is separate from all hMSC samples, which in turn formed a second cluster based on the correlations of the transcriptomes of the samples. More specifically, the transcriptomes of hESC H1 and H9 were most similar to each other, whereas the transcriptome of iPSC (hMSC, 74y, viral) was most similar to the transcriptomes of the hESC samples. However, the transcriptomes of iPSC (hMSC, fetal, line 1, viral) and hESCs displayed the lowest correlation of all pluripotent cell samples of this cluster. In addition, the transcriptomes of iPSC (hMSC, fetal, line 1, episomal 1), iPSC (hMSC, fetal, line 1 and iPSC (hMSC, 62y, episomal) were more similar to each other than to all other iPSC or hESC samples, whereas they were more similar to the transcriptomes of hESCs than iPSC (hMSC, fetal, line 1, viral) (Figure 24 A). The measured correlation values between hMSCs, iPSCs and hESCs are listed in Figure 24 B. The correlation between the transcriptomes of hMSC (74y) and iPSC (hMSC, 74y, viral) was detected to be 0.89 whereas there is a lower similarity to the transcriptomes of hESCs. A similar result could be detected for the transcriptomes of hMSC (62y) as well as iPSC (hMSC, 62y, episomal) and the transcriptomes of hESC H1 and H9. In contrast to that, there is a correlation of 0.87 to 0.88 between the transcriptomes of hMSC (60y) and hMSC (70y) and the transcriptomes of hMSC-iPSCs derived from aged donors. Moreover, the correlation of the transcriptomes of fetal hMSCs and iPSCs derived from aged donors was measured to be between 0.91 and 0.93, whereas the correlation between

the transcriptomes of fetal hMSCs and the transcriptomes of iPSC (hMSC, fetal, line 1, episomal 1) and iPSC (hMSC, fetal, line 1, episomal 2) were detected to be 0.93. In addition to that, the correlations between the transcriptomes of fetal hMSCs and iPSC (hMSC, fetal, line 1, viral) were measured with values of 0.90 to 0.92. Interestingly, the correlation of the transcriptomes of the iPS cell lines derived from aged donors was 0.95, whereas the correlation between the transcriptomes of iPSC (hMSC, 74y, viral) and iPSC (hMSC, fetal, line 1, viral) was 0.92. In addition, the correlation between the samples of the iPS cell lines derived from aged hMSC (62y) and from fetal hMSC 1 was 0.96. However, the similarity between the samples iPSC (hMSC, fetal, line 1, viral) and hESC H1 was 0.89 (Figure 24 B).

A

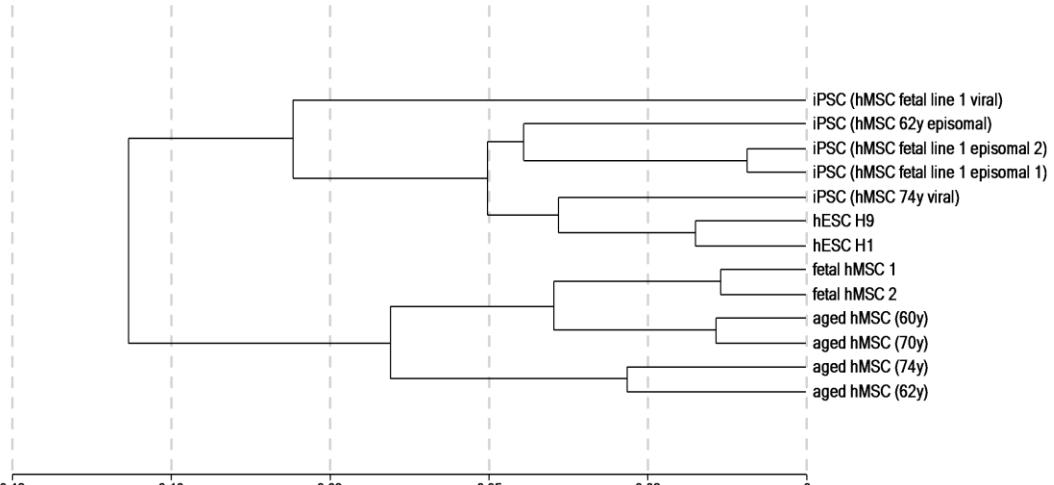

B

sample	aged hMSC (74y)	aged hMSC (62y)	aged hMSC (60y)	aged hMSC (70y)	fetal hMSC 1	fetal hMSC 2	iPSC (hMSC, 62y, episomal)	iPSC (hMSC, 74y, viral)	iPSC (hMSC, fetal, line 1, viral)	iPSC (hMSC, fetal, line 1, episomal 1)	iPSC (hMSC, fetal, line 1, episomal 2)	hESC H1	hESC H9
aged hMSC (74y)	1.000	0.972	0.944	0.951	0.933	0.943	0.868	0.897	0.862	0.880	0.884	0.869	0.855
aged hMSC (62y)	0.972	1.000	0.929	0.939	0.924	0.937	0.868	0.896	0.862	0.878	0.880	0.869	0.857
aged hMSC (60y)	0.944	0.929	1.000	0.986	0.961	0.964	0.881	0.887	0.884	0.891	0.902	0.885	0.874
aged hMSC (70y)	0.951	0.939	0.986	1.000	0.957	0.962	0.872	0.883	0.881	0.884	0.893	0.877	0.865
fetal hMSC 1	0.933	0.924	0.961	0.957	1.000	0.987	0.925	0.933	0.918	0.932	0.938	0.931	0.923
fetal hMSC 2	0.943	0.937	0.964	0.962	0.987	1.000	0.914	0.931	0.903	0.926	0.932	0.939	0.925
iPSC (hMSC, 62y, episomal)	0.868	0.868	0.881	0.872	0.925	0.914	1.000	0.954	0.947	0.958	0.958	0.935	0.943
iPSC (hMSC, 74y, viral)	0.897	0.896	0.887	0.883	0.933	0.931	0.954	1.000	0.923	0.962	0.958	0.962	0.967
iPSC (hMSC, fetal, line 1, viral)	0.862	0.862	0.884	0.881	0.918	0.903	0.947	0.923	1.000	0.927	0.930	0.899	0.906
iPSC (hMSC, fetal, line 1, episomal 1)	0.880	0.878	0.891	0.884	0.932	0.926	0.958	0.962	0.927	1.000	0.991	0.953	0.956
iPSC (hMSC, fetal, line 1, episomal 2)	0.884	0.880	0.902	0.893	0.938	0.932	0.958	0.958	0.930	0.991	1.000	0.952	0.953
hESC H1	0.869	0.869	0.885	0.877	0.931	0.939	0.935	0.962	0.899	0.953	0.952	1.000	0.983
hESC H9	0.855	0.857	0.874	0.865	0.923	0.925	0.943	0.967	0.906	0.956	0.953	0.983	1.000

Figure 24 Microarray-based comparison of the transcriptomes of generated hMSC-iPSCs, hESCs and hMSCs of fetal and aged background.

(A) Hierarchical clustering dendrogram showing the similarities between hESCs H1 and H9, aged hMSCs derived from 60, 62, 70 and 74-year-old donors, fetal hMSC 1 and 2 as well as iPSCs derived from fetal hMSC 1, aged hMSC (62y) and aged hMSC (74y) by viral and episomal plasmid-based methods. The dendrogram was generated using the software GenomeStudio (Illumina) and is based on the Pearson correlation between the transcriptomes. (B) Table listing the Pearson correlations between the samples shown in A. The colour of each cell of the table is coded according to the correlation value. Starting from the highest similarity represented by green colouring to red representing the least similar transcriptome samples in one column. The less similar the transcriptomes are, the stronger is the red colouring. The correlation values were calculated using the software GenomeStudio. The shown transcriptome data were generated using an Illumina Bead Chip microarray.

3.3 Effect of age-related differences in hMSCs on the reprogramming process

In order to analyse the effect of the age-related differences between fetal hMSCs and hMSC derived from aged donors on the reprogramming process and to elucidate whether and how these differences change during reprogramming, the up-and down-regulated genes of iPSCs compared to the parental hMSCs of different age backgrounds were analysed in detail. In addition, the change of ageing related features after pluripotency induction was tested.

3.3.1 Donor age-dependent changes of ageing features during reprogramming of hMSCs

To find out whether age-related features found in hMSCs change in the first six days after viral transduction during reprogramming and to analyse whether this change depends on the age, fetal hMSC 1, fetal hMSC 2, aged hMSC (60y), aged hMSC (62y) were transduced with the same retroviruses used to generate hMSC-iPSCs in this study. Retroviruses harbouring the transgenes *OCT4*, *SOX2*, *KLF4* and c-*MYC* were used in combination. On day six, after viral transduction hMSCs were stained using immunofluorescence to visualise ROS-induced DNA damage and DNA double-strand breaks. The results revealed that fetal hMSC 1 and cells of aged hMSC (62y) showed a positive staining signal visualising ROS-induced DNA damage employing 8-OHdG. In addition, γH2AX, a marker of DNA double-strand breaks, was found in both fetal hMSC 1 and nuclei of aged hMSC (62y) at day six after retroviral transduction (Figure 25 A) Moreover, the fluorescence signal in the nuclei after staining for ROS-induced DNA damage was measured using the software ImageJ comparing fetal hMSC 1, aged hMSC (62y) as well as fetal hMSC 1, aged hMSC (60y) and aged hMSC (62y) at day 6 after retroviral transduction. Interestingly, fetal hMSC 1 and aged hMSC (62y) transduced six days before showed a significantly lower fluorescence signal compared to hMSCs that were not transduced. However, there was no obvious difference between the fluorescence signals for 8-OHdG between the different age groups of fetal hMSCs and aged hMSC derived from a 60 and 62-year-old donor (Figure 25 B).

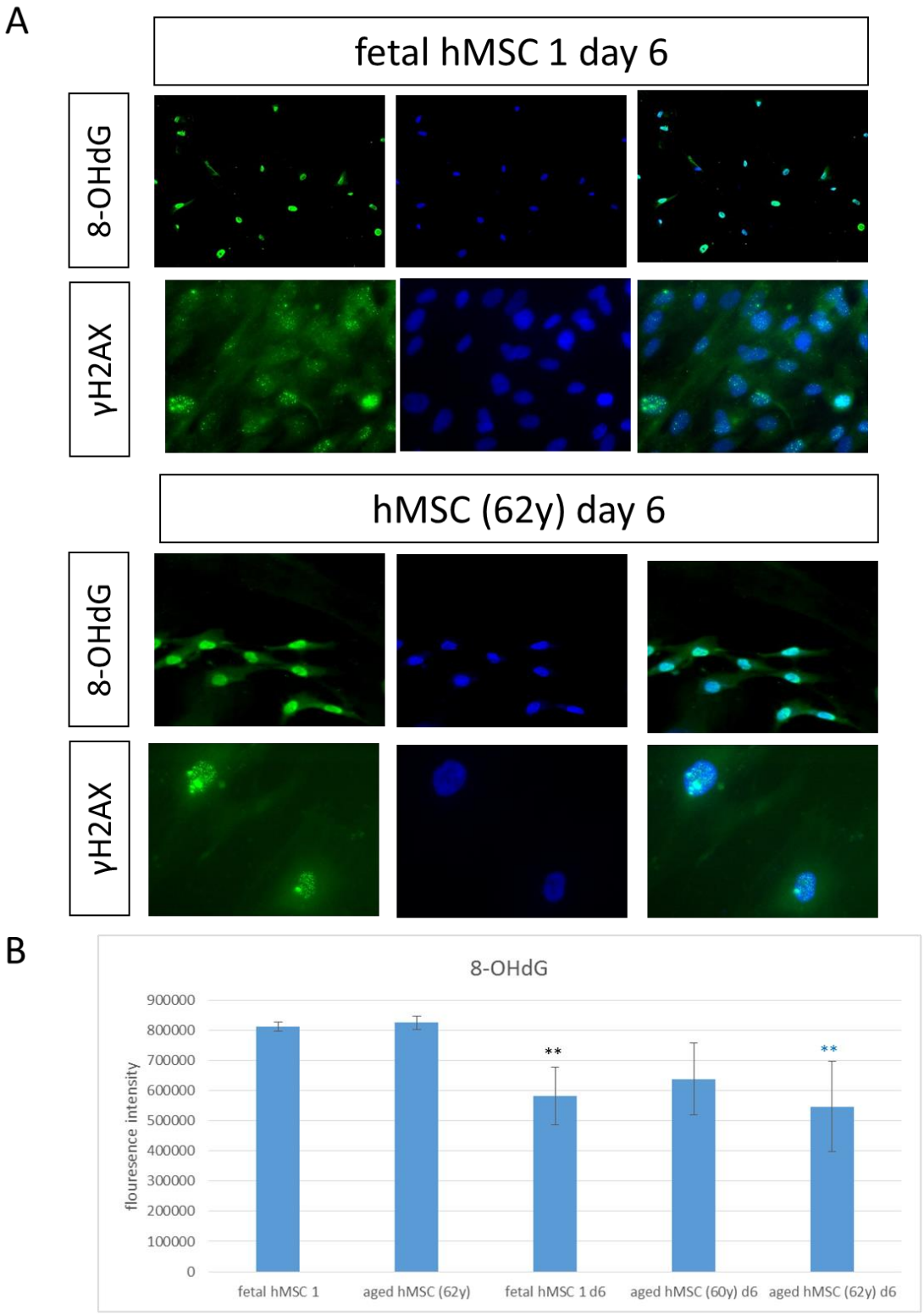

Figure 25 Age-dependent changes of reactive oxygen species (ROS)-induced DNA damage and DNA double-strand breaks upon viral reprogramming in fetal hMSC 1, aged hMSC (60y) and aged hMSC (62y).

(A) ROS-induced DNA damage was visualised by 8-OHdG-specific immunofluorescence staining. DNA double-strand breaks visualised by γH2AX-specific antibodies. Depicted are fetal

hMSC 1 and aged hMSC (62y) at day 6 after viral transduction with retroviruses harbouring open reading frames of *OCT4, SOX2, KLF4* and *c-MYC*. The combination was used in all viral reprogramming experiments. No obvious differences between the two samples could be detected. Green: fluorescence signal indicating the marker staining. Blue: nuclei visualised by DAPI. (B) Quantification of immunofluorescence staining of ROS-induced DNA damage marker 8-OHdG comparing non-transduced fetal hMSC 1 and aged hMSC (62y) with fetal hMSC 1, aged hMSC (60y) and aged hMSC (62y) at day 6 after transduction with retroviruses harbouring *OCT4, SOX2, KLF4* and *c-MYC*. The quantification was carried out using the software ImageJ. Plotted are the median fluorescence intensities measured in 20 nuclei. Error bars represent the standard deviation. Black asterisks: significant difference to fetal hMSC 1 (p-value<0.01). Blue asterisks: significant difference to aged hMSC (62y) (p-value<0.01).

3.3.2 Transcriptional changes in fetal and aged hMSCs upon induction of pluripotency

To understand the effect of the age-related differences between fetal hMSCs and hMSCs of aged donors on the processes taking place during reprogramming, a more detailed comparative analysis of the microarray-based transcriptome data was carried out.

For this purpose, two Venn diagrams were generated using the platform VENNY. The first Venn diagram was prepared using genes that were differentially regulated compared to their parental hMSCs with a p-value below 0.01 and were up-regulated (more than 1.5-fold higher average signal in iPSCs). The second Venn diagram was prepared using genes that were differentially regulated compared to their parental hMSCs with a p-value below 0.01 and were down-regulated (less than 1.5-fold lower average signal in iPSCs). Comparisons were between samples iPSC (hMSC, fetal, line 1, viral), iPSC (hMSC, fetal, line 1, episomal 1), iPSC (hMSC, 62y, episomal) and iPSC (hMSC, 74y, viral) in both Venn diagrams. Subsequently the genes that were common to all four samples were annotated to biological processes using the functional annotation database DAVID. Interestingly, 384 genes were found to be up-regulated, whereas less than half as many genes were detected as down-regulated. The genes commonly down-regulated in all hMSC-iPSC samples were annotated to glycine, serine and threonine metabolism and alanine, aspartate and glutamate metabolism with a p-value below 0.05. In contrast to that, the commonly up-regulated genes were annotated to the processes focal adhesion, ECM-receptor interaction, regulation of actin cytoskeleton, hypertrophic cardiomyopathy (HCM), hematopoietic cell lineage, TGFβsignalling pathway, dilated cardiomyopathy, MAPK signalling pathway, Fc gamma R-mediated phagocytosis, arrhythmogenic right ventricular cardiomyopathy (ARVC) and pathways in cancer with a p-value below 0.05. In order to elucidate processes only changing in aged hMSCs or only in fetal hMSCs during reprogramming, the overlapping genes of the iPS samples derived from fetal hMSCs and the iPS samples derived from aged hMSC (62y) and aged

hMSC (74y) were analysed using functional annotation. 360 up-regulated genes were common to iPSC (hMSC, 62y, episomal) and iPSC (hMSC, 74y, viral) whereas only 187 up-regulated genes were common to the iPS samples derived from fetal hMSC 1. The up-regulated genes common to hMSC-iPSCs of aged origin were annotated to antigen processing and presentation, systemic lupus erythematosus, lysosome, viral myocarditis, allograft rejection, graft-versus-host disease, type I diabetes mellitus, autoimmune thyroid disease, asthma, metabolism of xenobiotics by cytochrome P450 drug metabolism and cell adhesion molecules (CAMs) with a p-value of below 0.05. However, the up-regulated genes common to iPSCsderived from fetal hMSC 1 were annotated to melanogenesis, endocytosis and MAPK signalling pathway. Interestingly, the significantly down-regulated genes compared to the parental hMSC differed between iPSCs derived from fetal hMSC 1 and iPSCs derived from hMSCs of aged background. 229 down-regulated genes were found to be common to iPSCs derived from hMSCs of aged background, whereas only 74 down-regulated genes were common between iPSCs derived from fetal hMSC 1. The genes commonly down-regulated compared to the parental hMSCs in iPSCs derived from hMSCs of aged background were annotated to aminoacyl-tRNA biosynthesis and mismatch repair with a p-value below 0.05. The genes commonly down-regulated in iPSCs derived from fetal hMSC 1 with viral and non-viral approaches were annotated to GO-terms, such as cellular lipid catabolic process, response to wounding, positive regulation of neurological system process with a p-value below 0.05 and could not be annotated to any KEGG terms using the DAVID functional annotation (Figure 26).

Term	PValue
hsa04612:Antigen processing and presentation	1.10E-04
hsa05322:Systemic lupus erythematosus	3.76E-04
hsa04142:Lysosome	0.001
hsa05416:Viral myocarditis	0.002
hsa05330:Allograft rejection	0.004
hsa05332:Graft-versus-host disease	0.005
hsa04940:Type I diabetes mellitus	0.007
hsa05320:Autoimmune thyroid disease	0.013
hsa05310:Asthma	0.015
hsa00980:Metabolism of xenobiotics by cytochrome P450	0.023
hsa00982:Drug metabolism	0.025
hsa04514:Cell adhesion molecules (CAMs)	0.032
hsa04672:Intestinal immune network for IgA production	0.058
hsa00760:Nicotinate and nicotinamide metabolism	0.069

Term	PValue
GO:0044242~cellular lipid catabolic process	0.005
GO:0009611~response to wounding	0.010
GO:0031646~positive regulation of neurological system process	0.013
GO:0051240~positive regulation of multicellular organismal process	0.024
GO:0001525~angiogenesis	0.029
GO:0022904~respiratory electron transport chain	0.034
GO:0048754~branching morphogenesis of a tube	0.035
GO:0030334~regulation of cell migration	0.041
GO:0016042~lipid catabolic process	0.043

Term	PValue
hsa04144:Endocytosis	0.018
hsa04916:Melanogenesis	0.026
hsa04010:MAPK signaling pathway	0.031

Term	PValue
hsa00970:Aminoacyl-tRNA biosynthesis	0.001
hsa03430:Mismatch repair	0.002
hsa03030:DNA replication	0.061

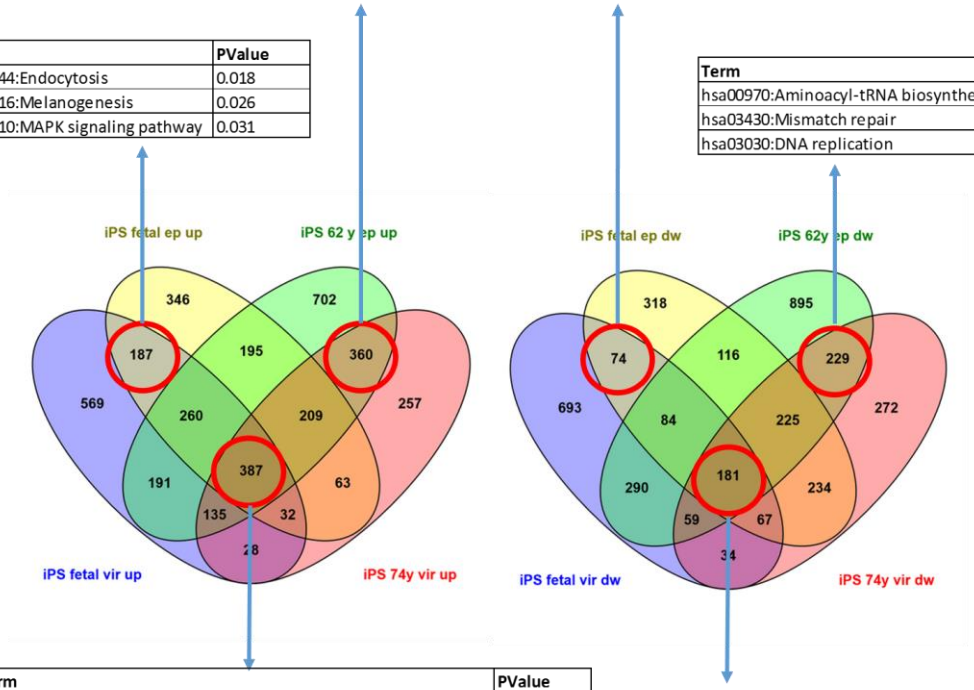

Term	PValue
hsa04510:Focal adhesion	9.15E-10
hsa04512:ECM-receptor interaction	3.46E-06
hsa04810:Regulation of actin cytoskeleton	1.38E-04
hsa05410:Hypertrophic cardiomyopathy (HCM)	1.53E-04
hsa04640:Hematopoietic cell lineage	0.004
hsa04350:TGF-beta signaling pathway	0.004
hsa05414:Dilated cardiomyopathy	0.006
hsa04010:MAPK signaling pathway	0.023
hsa04666:Fc gamma R-mediated phagocytosis	0.024
hsa05412:Arrhythmogenic right ventricular cardiomyopathy (ARVC)	0.033
hsa05200:Pathways in cancer	0.044
hsa05130:Pathogenic Escherichia coli infection	0.045
hsa04142:Lysosome	0.057
hsa00600:Sphingolipid metabolism	0.063
hsa04060:Cytokine-cytokine receptor interaction	0.089
hsa05212:Pancreatic cancer	0.089

Term	PValue
hsa00260:Glycine, serine and threonine metabolism	0.003
hsa00250:Alanine, aspartate and glutamate metabolism	0.034

Figure 26 Age-related transcriptional changes during viral and episomal plasmid based reprogramming of hMSCs of fetal and aged origin.

Shown are two Venn diagrams of genes that are differentially regulated compared to their parental hMSCs with a p-value below 0.01 and are up-regulated (more than 1.5-fold higher average signal in iPSCs) or down-regulated (less than 1.5-fold lower average signal in iPSCs). The gene lists were detected and generated using an Illumina Bead Chip microarray and the software GenomeStudio. Genes common between all samples and common between iPSCs derived from fetal hMSC 1 or between iPSCs derived from aged hMSC (62y) and hMSC (74y)

were annotated to pathways using the gene annotation platform DAVID, the option pathways and the category KEGG or GO-terms of biological processes. P-values of less or equal to 0.05 were considered significant but the full results are shown in the tables. Ep: episomal, Vir: retroviral.

3.4 Effect of age on reprogramming efficiency in hMSCs and possible modulation

Comparative reprogramming of fetal hMSCs and hMSCs of aged donors revealed a negative effect of hMSC donor age on the reprogramming efficiency (Table 12). To optimise the reprogramming protocol for hMSCs of aged donors and to find out whether it is possible to compensate the negative effect on the reprogramming efficiency, reprogramming experiments were performed in which pathways implicated in ageing were inhibited and in which inhibitor combinations were used that are known to enhance reprogramming efficiency.

Following a previously described protocol reprogramming was performed using N2B27 medium or N2B27 medium followed by culture in mTeSR 1 14 days after the start of the reprogramming experiment. In addition, a combination of inhibitors consisting of MEK inhibitor PD0325901, GSK3β inhibitor CHIR99021, TGF-β/Activin/Nodal receptor inhibitor A-83-01 and ROCK inhibitor HA-100 (smM) described in the same study was used (Yu et al. 2011). Furthermore, the culture in conditioned medium was used in the reprogramming experiments. In addition, valproic acid, which is known to enhance the reprogramming efficiency (Wang and Adjaye 2011), was used together with the inhibitor combination smM. Moreover, the insulin-like growth factor receptor (IGF1R) inhibitor PQ401 was used as IGF-1 signalling has implications for longevity in humans and has a putative enhancing role during reprogramming (Li and Geng 2010, Vitale et al. 2012). In addition, the possibility to modulate the reprogramming efficiency of hMSCs derived from aged donors was tested using vitamin c as an enhancer during cell reprogramming as previously described (Tao Wang et al. 2011). Moreover, the P53 inhibitor pifithrin α was used to modulate age-dependent impairment of reprogramming efficiency in hMSCs as the limiting role of P53 during reprogramming was described before (Takenaka et al. 2010). In this work a combination of pifithrin α and smM was used as experimental condition for reprogramming. Apart from that, the combination of VPA, P53 inhibition and vitamin c was described to increase reprogramming efficiencies in hMSCs (Yulin et al. 2012). This combination was used in this work. Finally, the toll-like receptor 3 agonist Polyinosinic-polycytidylic acid (poly(I:C)) was used to find out whether the enhancing effect of the activation of the innate immune system could be used to compensate the low reprogramming efficiency of hMSCs derived from aged donors (Lee et al. 2012).

Out of all reprogramming conditions used, none could enhance viral reprogramming of aged hMSC (60y) and aged hMSC (62y). Likewise, none of the experimental conditions tested led to enhanced efficiency of iPS cell generation with episomal plasmids in hMSC (60y). However, aged hMSC (62y) could be reprogrammed using episomal plasmids in the condition culture in mTeSR 1 from day 14 and addition of vitamin c as well as using the combination of smM and vitamin c and by using a combination of P53 inhibition and smM. Interestingly, the first condition yielded an almost threefold higher reprogramming efficiency in aged hMSC (62y). All other reprogramming conditions did not result in induction of pluripotency of aged hMSC (62y) (Figure 27 A).

In contrast to that, fetal hMSC 2 could only be reprogrammed using episomal plasmids and the condition N2B27 medium and culture in mTeSR 1 from day 14 after start of the reprogramming experiment. Viral reprogramming of fetal hMSC 2 could not be achieved with any of the used experimental conditions (Figure 27 A).

This is in contrast to the second fetal hMSC preparation fetal hMSC 1, which could be reprogrammed using retroviral reprogramming in all experimental conditions that were tested. In addition, the reprogramming efficiency was found to be higher than the reprogramming efficiencies of fetal hMSC 2 and aged hMSC (62y) when episomal plasmids were used. However, fetal hMSC 1 revealed a lower reprogramming efficiency when episomal plasmids were used compared to viral reprogramming. Interestingly, fetal hMSC 1 could not be reprogrammed using episomal plasmids in conditioned medium; in the condition combination of smM and VPA, in the condition vitamin c, in the condition combination of VPA, P53 inhibition and vitamin c as well as when the combination of P53 inhibition and smM was used (Figure 27 A and B).

Moreover, the addition of mTeSR 1 at day 14 after the start of the reprogramming experiment enhanced the reprogramming efficiency of fetal hMSC 1 in the case of viral reprogramming. More specifically the highest enhancement could be detected for the combination smM and VPA with a four-fold higher reprogramming efficiency when mTeSR 1 was used as culture medium from day 14 compared to all other tested conditions. Out of these conditions, the combination smM; the combination of VPA, P53 inhibition and vitamin c and the combination of P53 inhibition and smM showed the highest fold change when mTeSR 1 was used (Figure 27 C).

The enhancing effect of the experimental conditions used was much lower when fetal hMSC 1 were reprogrammed using episomal plasmids. Fetal hMSC 1 could not be reprogrammed when conditioned medium was used as well as when the combination VPA, P53 and vitamin c was used. In addition, fetal hMSC 1 could only be reprogrammed when mTeSR 1 was not added in the conditions smM and VPA, smM and vitamin c as well as when the agonist of TLR3 was used. In contrast to that, fetal hMSC 1 could only be reprogrammed when mTeSR 1 was used as culture medium from day 14 after the start of the pluripotency induction when vitamin c was used and when smM and P53 inhibition was employed (Figure 27 C).

A

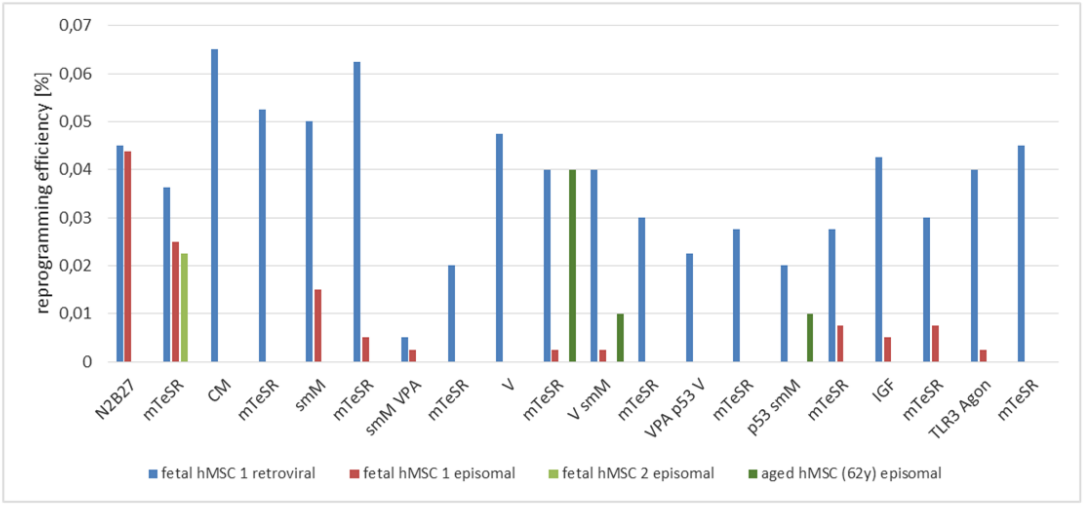

B

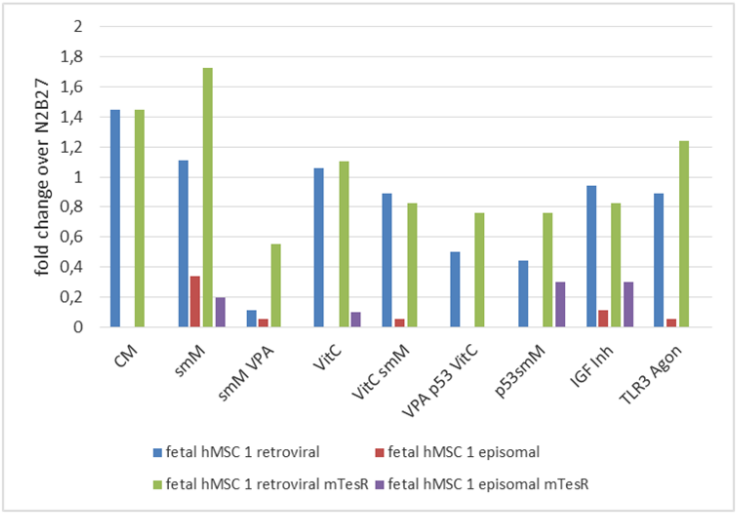

C

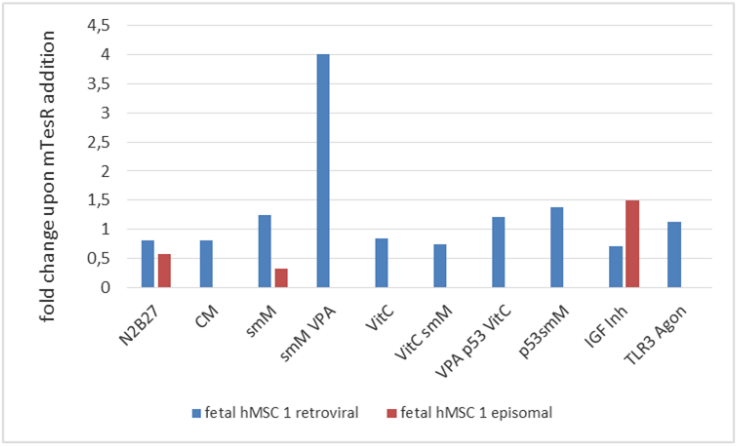

Figure 27 Enhancement of the reprogramming efficiency in fetal hMSC 1, fetal hMSC 2 and aged hMSC (62y) using conditions modulating age-related processes.

(A) Effect of reprogramming conditions used in reprogramming of hMSC 1 by means of viral and episomal plasmid-based reprogramming techniques and of fetal hMSC 2 and aged hMSC (62y) using episomal plasmid-based iPS generation. Depicted is the calculated reprogramming efficiency in per cent based on counted colonies. (B) Effect of used reprogramming conditions and of the addition of mTeSR 1 at day 14 post-nucleofection/post-transduction on the reprogramming efficiency compared to N2B27 medium in retroviral and episomal plasmid-based reprogramming of fetal hMSC 1. (C) Effect of addition of mTeSR 1 at day 14 post-nucleofection/post-transduction on the reprogramming efficiency in fetal hMSC 1 comparing retroviral and episomal reprogramming. Colonies were counted at day 55 post-transduction (fetal hMSC 1 retroviral), day 45 post-nucleofection (fetal hMSC 1 episomal), day 54 post-nucleofection (fetal hMSC 2 episomal) and day 54 post-nucleofection (aged hMSC (62y). CM: unconditioned medium conditioned with inactivated mouse embryonic fibroblasts; smM: combination of MEK inhibitor PD0325901, GSK3β inhibitor CHIR99021, TGF-β/Activin/Nodal receptor inhibitor A-83-01 and ROCK inhibitor HA-100; VPA: valproic acid; V: vitamin c; P53: P53 inhibitor pifithrin α, IGF Inh: IGF receptor inhibitor PQ401; TLR3 Agon: toll-like receptor 3 agonist polyinosinic-polycytidylic acid (poly(I:C); mTeSR: switch to medium mTeSR 1 from day 14 post-transfection/post-nucleofection. Depicted are the results of one experiment each.

3.5 Effect of age of hMSCs on the features of iPSCs derived from them

In order to clarify whether differences of ageing-related features have an effect on the features of hMSC-iPSCs, features such as intracellular ROS, oxidative DNA damage as well as integrity of the DNA were measured comparatively. In addition, the effect of biological age of the parental hMSCs on the transcriptome of hMSC-iPSCs was analysed in detail to find potential residual donor age-specific transcriptional patterns that might have an influence on the characteristics of the respective iPS cell line.

3.5.1 Ageing-related features in hMSC-iPSCs of different age background

Age-related features, such as ROS-induced DNA damage and DNA double-strand breaks were measured in hMSC-iPSCs of both fetal and aged background. Doing this, immunofluorescence staining specific for 8-OHdG, a DNA damage induced by intracellular ROS, resulted in positive staining signals for iPSC (hMSC, fetal, line 1, episomal 1), iPSC (hMSC, fetal, line 1, episomal 2), iPSC (hMSC, fetal, line 1, episomal 3) and iPSC (hMSC, 74y, viral). Furthermore, positive immunofluorescence staining signals could be measured using an antibody specific for the DNA double-strand break marker γH2AX in iPSC (hMSC, fetal, line 1, episomal 1) and iPSC (hMSC, 62y,

episomal). Interestingly, the measured immunofluorescence signal for γH2AX was much lower in iPSC (hMSC, 74y, viral). In addition, positive immunofluorescence staining signals were measured in iPSC (hMSC, 62y, episomal) after staining with an antibody specific for the phosphorylation of P53 during DNA damage response signalling (Figure 28).

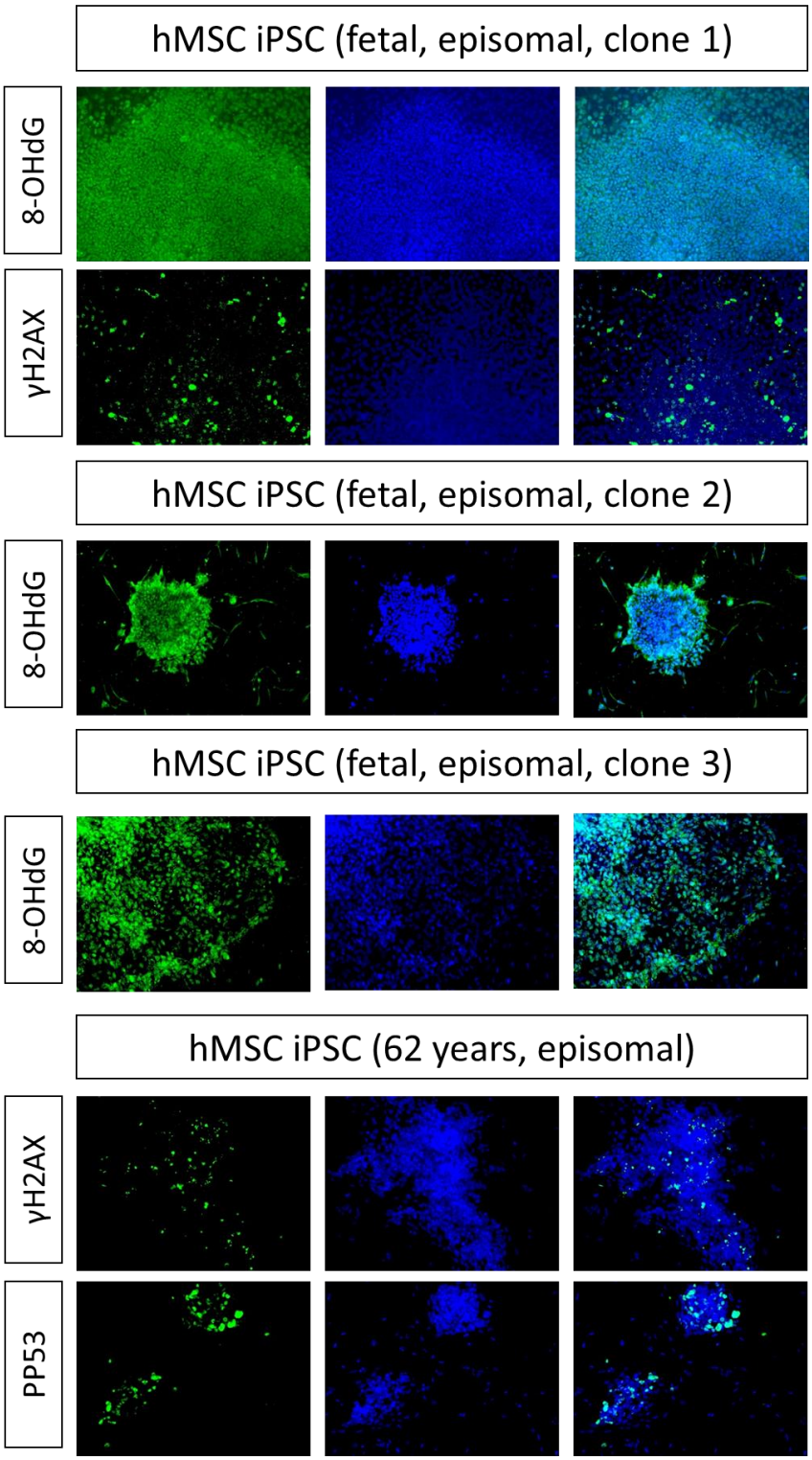

Figure 28 Age-related DNA damage, ROS-induced DNA lesions and DNA damage response in hMSC-iPSCs of fetal and higher donor age origin.

ROS-induced DNA damage was visualised using immunofluorescence staining of the marker 8-OHdG. DNA double-strand breaks were visualised by immunostaining using an antibody specific for the marker γH2AX. P53-mediated DNA damage response was visualised using immunofluorescence staining with an antibody against phosphorylated P53 (PP53), specific for DNA damage response. Confocal microscopy. Green: marker visualised by immunofluorescence. Blue: nuclei visualised by DAPI. 10 x magnification.

In order to elucidate whether donor age of hMSC has an effect on intracellular ROS levels and expression of genes related to the response to oxidative stress, age-related changes of intracellular ROS levels were measured by FACS in hMSCs of fetal and high age background and corresponding iPSCs. In addition to that, the gene expression related to oxidative stress was measured using microarray-based gene expression profiling and subsequent extraction of the expression of genes, which are annotated to the GO-term response to oxidative stress. For comparison, a hierarchical clustering of the expression of this gene set was carried out.

The results of the FACS-based quantification of intracellular ROS levels by means of DCFDA revealed significantly lower fluorescence levels in fetal hMSC 1 compared to iPSCs derived from fetal hMSC 1. Significantly higher fluorescence signals were measured in iPSC (hMSC, fetal, line 1, episomal 1) compared to iPSC (hMSC, fetal, line 1, episomal 2), iPSC (hMSC, fetal, line 1, episomal 3) and iPSC (hMSC, fetal, line 1, viral). The measured fluorescence levels indicating intracellular ROS in aged hMSCs varied depending on the donor. Among the fluorescence signals measured for aged hMSCs the signal measured in aged hMSC (60y) was higher than the signal measured in aged hMSC (62y) and aged hMSC (70y) whereas the signal measured in aged hMSC (62y) was higher than the signal measured in aged hMSC (70y). However, similar to fetal hMSCs and respective iPSCs the fluorescence signal indicating intracellular ROS was significantly higher in iPSC (hMSC, 62y, episomal) and iPSC (hMSC, 74y, viral) than in aged hMSC (62y). In addition, there were no obvious differences in measured fluorescence signals between iPSCs derived from fetal hMSC 1 and iPSCs derived from hMSCs of aged donors (Figure 29 A). In order to analyse the impact of age of hMSCs on the expression of genes related to the response to oxidative stress in hMSC-iPSCs, a hierarchical clustering analysis was carried out based on the log2 ratio of the average signal of the gene of the respective sample over the average signal detected in hESC H1. The Pearson correlation-based clustering revealed high similarity of iPSC (hMSC, fetal, line 1, episomal 1) and iPSC (hMSC, fetal, line 1, episomal 2). In addition, a high similarity between iPSC (hMSC, fetal, line 1, viral), iPSC (hMSC, 62y, episomal) and iPSC (hMSC, 74y, viral) could be detected. However, gene expression pattern related to the response to oxidative stress showed a low similarity between the cluster of the samples iPSC (hMSC, fetal, line 1, episomal 1) and iPSC (hMSC, fetal, line 1, episomal 2) and the

similarity cluster of iPSC (hMSC, fetal, line 1, viral), iPSC (hMSC, 62y, episomal) and iPSC (hMSC, 74y, viral) (Figure 29 B).

A

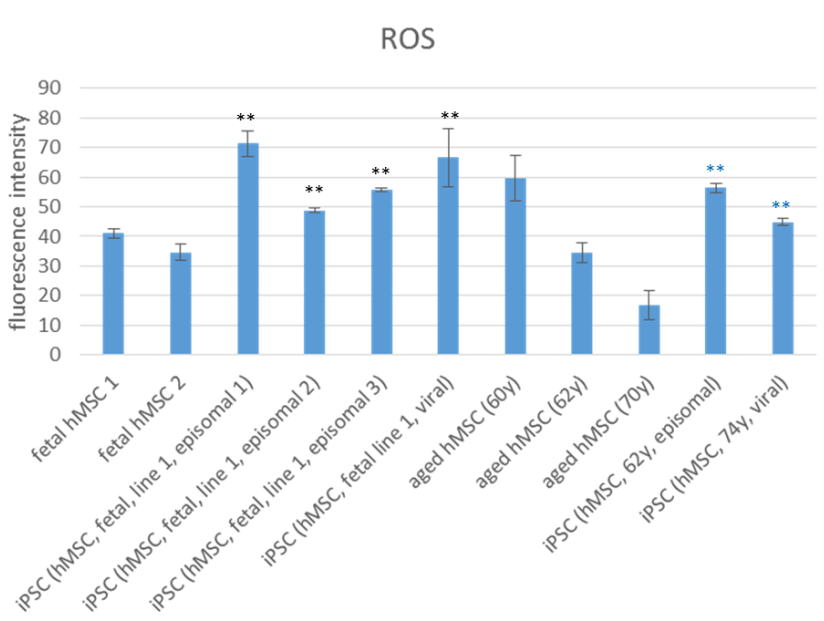

B

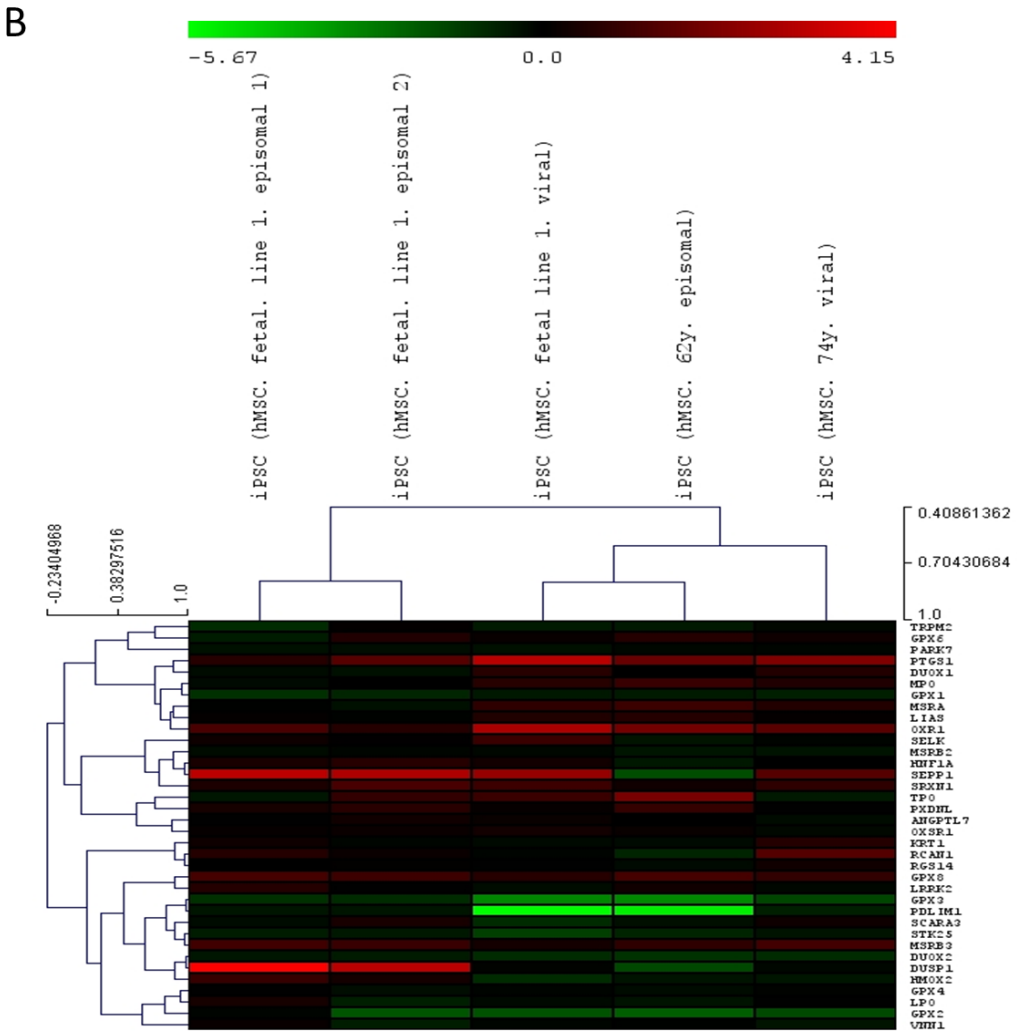

Figure 29 Age-related changes of intracellular ROS levels and gene expression related to oxidative stress in hMSCs of fetal and high age background and corresponding iPSCs.
(A) FACS-based quantification of intracellular reactive oxygen species by means of DCFDA treatment and flow cytometry-based measurement. FACS data were quantified using the software Cyflogic. Plottet is the mean value of n=4. The error bars represent the standard deviation. Black asterisks: significant difference to fetal hMSC 1 (p-value<0.05). Blues asterisks: significant difference to aged hMSC(62y) (p-value<0.05). (B) Hierarchical clustering analysis of gene expression related to the response to oxidative stress. Heatmap based on the log 2 ratio of the average signal of the respective sample over the average signal detected in hESC H1. The average signal intensities were detected using an Illumina Bead Chip microarray. The hierarchical clustering is based on Pearson correlation of the samples and genes. Gene description see Table 20.

As mentioned above, a recent study confirmed the regulation of the genes *COX7A1*, *MRPL28*, *CAPRIN2*, *GCAT*, *EHHADH*, *ALDH5A1* and *SHMT2* through biological age (Hashizume et al. 2015). A hierarchical clustering analysis based on these genes comparing iPSCs derived in this study with hESC H1 revealed a higher similarity between the samples iPSC (hMSC, fetal, line 1, episomal 1), iPSC (hMSC, fetal, line 1, episomal 2) and iPSC (hMSC, 74y, viral) which formed a cluster separating these samples from iPSC (hMSC, fetal, line 1, viral) and iPSC (hMSC, 62y, episomal). In addition, iPSC (hMSC, 62y) was more similar to the samples of this cluster than to iPSC (hMSC, fetal, line 1, viral), which showed the lowest similarity compared to all other samples (Figure 30 A). To further look into the changes of genes involved in processes implicated in the metabolic stability theory of ageing (Brink et al. 2009) during reprogramming of aged hMSCs to iPSCs, genes of gene lists based on the GO-terms oxidative phosphorylation, TCA cycle, glycolysis, glutathione metabolism and insulin signalling that were differentially expressed in iPSC (hMSC aged) (merged samples of iPSC (hMSC, 62y, episomal) and iPSC (hMSC, 74y, viral)) against aged hMSCs (merged samples of aged hMSC (60y), aged hMSC (62y) and aged hMSC (70y)) and up or down-regulated were extracted from microarray data generated with an Illumina Bead Chip microarray. The analysis showed that the gene *OGDHL*, which is involved in the citric acid cycle, was found to be up-regulated in iPSC (hMSC aged) compared to the merged samples of aged hMSCs with a p-value of 9.258E-36. In addition to that, the genes *GAPDH* and *PFKP*, which are part of the glycolysis, were down-regulated in iPSC (hMSC aged) compared to the merged samples of aged hMSCs. Moreover, genes involved in glutathione metabolism were found to up-regulated (*GGCT*, *CNDP2*) and down-regulated (*GCCM*) in iPSC (hMSC aged) compared to aged hMSCs. Finally, the genes *MAP2K1* and *IRS1*, which are involved in insulin signalling, were down-regulated in iPSC (hMSC aged) compared to aged hMSCs (Figure 30 B).

A

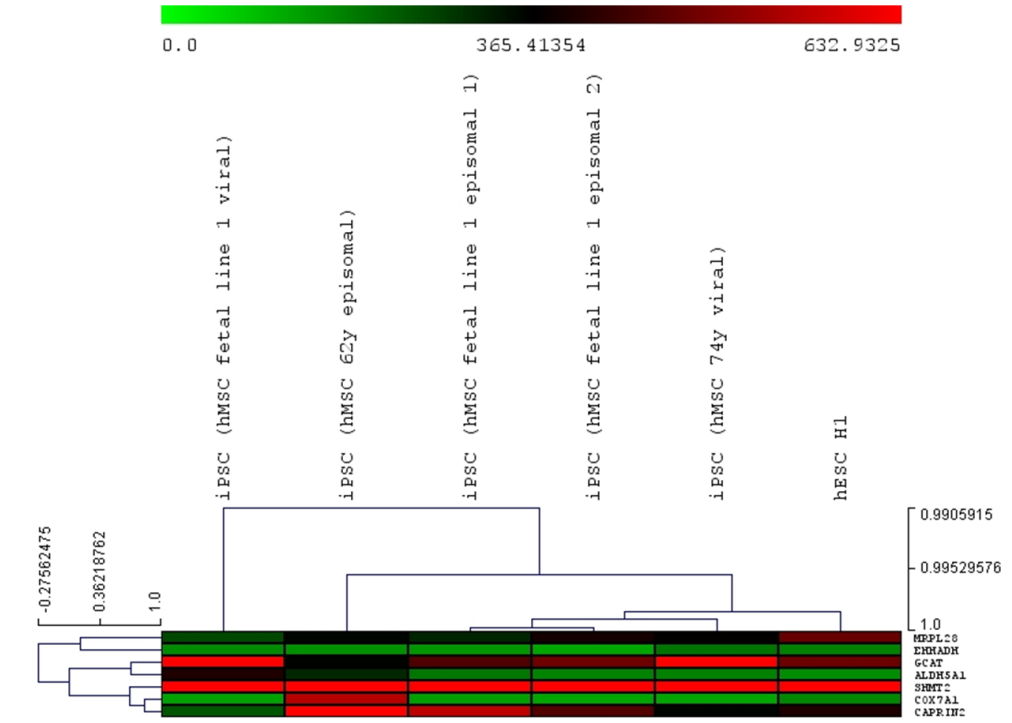

B

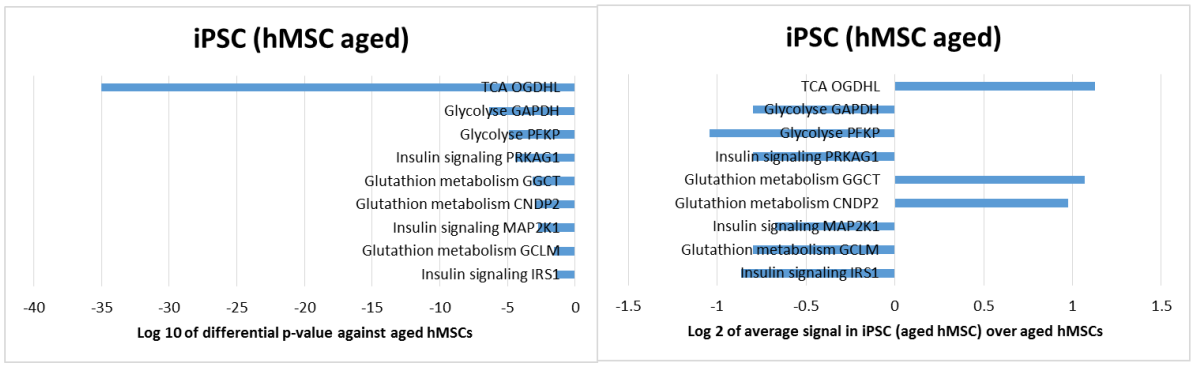

Figure 30 Expression patterns of genes regulated with age and with implications in the metabolic stability theory of ageing comparing hMSC-iPSCs derived aged hMSCs and corresponding parental hMSCs.

(A) Hierarchical clustering analysis based on the Pearson correlation of the average signal of the expression of genes described to be regulated with age in a recent study (Hashizume et al. 2015). Compared are hMSC-iPSCs derived from fetal and aged hMSCs with hESC H1. Gene expression was measured using an Illumina Bead Chip. (B) Genes of gene lists based on the GO-terms oxdative phosphorylation, TCA cycle, glycolysis, glutathione metabolism and insulin signalling that are differentially expressed in iPSC (hMSC aged) (merged samples of iPSC (hMSC, 62y, episomal) and iPSC (hMSC, 74y, viral)) against aged hMSCs (merged samples of aged hMSC (60y), aged hMSC (62y) and aged hMSC (70y)). Left: log 10 of the differential p-

values below 0.01 calculated by GenomeStudio of differentially expressed genes in iPSC (hMSC aged) (merged samples of iPSC (hMSC, 62y, episomal) and iPSC (hMSC, 74y, viral)) against aged hMSCs (merged samples of aged hMSC (60y), aged hMSC (62y) and aged hMSC (70y)). Right: log 2 of the ratios of the average signals in in iPSC (hMSC aged) over aged hMSCs of the differentially expressed genes sorted according to the differential p-value. Gene expression was measured using an Illumina Bead Chip microarray.

3.5.2 Age-related and cell type-specific transcriptional memory in iPS cells compared to parental hMSCs

Several studies describe that after reprogramming a donor cell-specific transcriptional memory can be detected in iPSCs (Bar-Nur et al. 2011, Kim et al. 2011). Following the notion that age-related transcriptional signatures might be still present in hMSC-iPSCs of fetal and high age background, Venn diagrams were prepared consisting of genes detected as expressed in parental hMSCs and the corresponding iPS cell line. To rule out a potential influence of gene expression patterns generally present in pluripotent cells compared to somatic cells, the expressed genes detected in hESC H1 were included in each Venn diagram. In the next step, the overlapping genes between the parental hMSC sample and the corresponding iPS cell sample were analysed by functional annotation using the database DAVID. The genes expressed in fetal hMSC 1 and iPSC (hMSC, fetal, line 1, viral) were annotated to the KEGG terms Axon guidance, Circadian rhythm with a p-value below 0.05 and to Apoptosis with a p-value of 0.09. Moreover, the genes expressed in fetal hMSC 1 and iPSC (hMSC, fetal, line 1, episomal 1) were annotated to the KEGG terms Axon guidance and Renin-angiotensin system with a p-value below 0.01. In contrast to that, the genes expressed in aged hMSC (62y) and iPSC (hMSC, 62y, episomal) were annotated to the KEGG term Vascular smooth muscle contraction with a p-value below 0.05 and to the KEGG terms Renin-angiotensin system, Purine metabolism, GnRH signalling pathway, Systemic lupus erythematosus, Viral myocarditis, Alzheimer's disease, Natural killer cell mediated cytotoxicity and Phosphatidylinositol signalling system with p-values between 0.06 and 0.09. In addition, the genes present in aged hMSC (74y) and iPSC (hMSC, 74y, viral) were annotated to the KEGG terms Pentose and glucoronate interconversions, Calcium signalling pathway and MAPK signalling pathway with p-value below 0.01 and to the KEGG terms Hematopoietic cell lineage and Neurotrophin signalling pathway with p-values between 0.07 and 0.1 (Figure 31).

Term	PValue	Genes
hsa04360:Axon guidance	0.012	UNC5B, CFL2, SRGAP3, NTN4, NTNG1, SEMA3C, SEMA3B, NFATC4
hsa04710:Circadian rhythm	0.025	NPAS2, PER1, CLOCK
hsa04210:Apoptosis	0.089	IRAK4, IRAK2, IL1RAP, IL1B, FAS

Term	PValue	Genes
hsa04360:Axon guidance	0.029	UNC5B, CFL2, SRGAP3, NTN4, NTNG1, SEMA3C, SEMA3B
hsa04614:Renin-angiotensin system	0.037	LNPEP, AGTR1, ANPEP

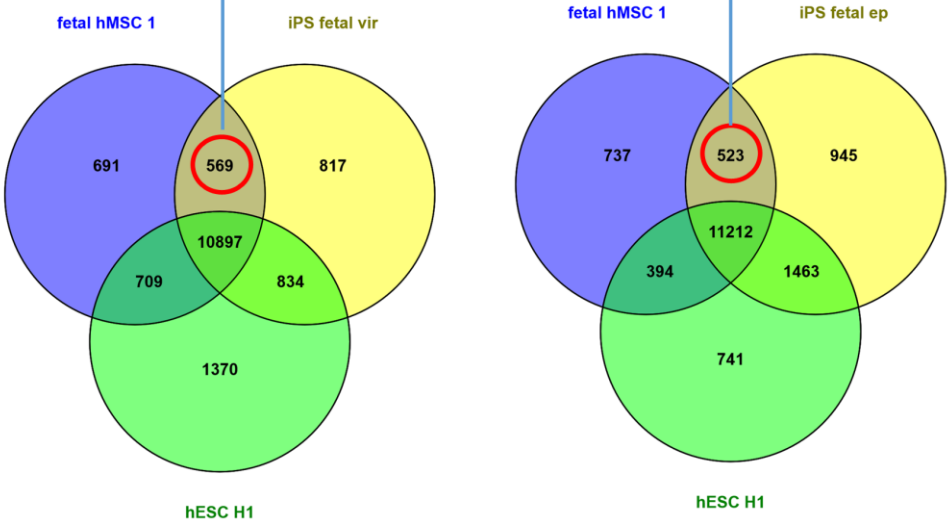

Term	PValue	Genes
hsa04270:Vascular smooth muscle contraction	0.015	AGTR1, ADCY4, PLCB4, PLA2G12A, NPR1, CACNA1C, PRKCE, ITPR1
hsa04614:Renin-angiotensin system	0.059	LNPEP, AGTR1, ANPEP
hsa00230:Purine metabolism	0.066	ADCY4, NME5, PDE7B, PDE1A, ENTPD5, NPR1, PDE8A, NT5E
hsa04912:GnRH signaling pathway	0.079	ADCY4, PLCB4, PLA2G12A, MAPK11, CACNA1C, ITPR1
hsa05322:Systemic lupus erythematosus	0.081	CD86, H2AFV, HIST1H2BJ, C1R, C1S, FCGR3A
hsa05416:Viral myocarditis	0.084	LAMA2, CD86, MYH3, SGCD, ABL2
hsa05010:Alzheimer's disease	0.086	NDUFA5, PLCB4, NDUFA4L2, BACE1, LOC727947, FAS, CACNA1C, ITPR1
hsa04650:Natural killer cell mediated cytotoxicity	0.091	LAT, ICAM2, ULBP2, FAS, PIK3R3, FCGR3A, SHC4
hsa04070:Phosphatidylinositol signaling system	0.094	PLCE1, PLCB4, INPP4B, PIK3R3, ITPR1

Term	PValue	Genes
hsa00040:Pentose and glucuronate interconversions	0.010	CRYL1, UGT1A3, LOC729020, XYLB
hsa04020:Calcium signaling pathway	0.035	AGTR1, PTGER1, HRH1, PLCE1, P2RX6, BDKRB2, PTGFR, CACNA1C, ITPR1, MYLK
hsa04010:MAPK signaling pathway	0.039	HSPA1L, MAP3K5, IL1R1, PLA2G12A, MAPK8IP2, MOS, CACNB1, RAP1A, MAPK11, FAS, CACNA1C, DUSP8, CD14
hsa04640:Hematopoietic cell lineage	0.068	IL1R1, ITGA1, ANPEP, IL7R, CD14, CSF1R
hsa04722:Neurotrophin signaling pathway	0.097	IRAK4, IRAK2, MAP3K5, BCL2, RAP1A, MAPK11, SHC4

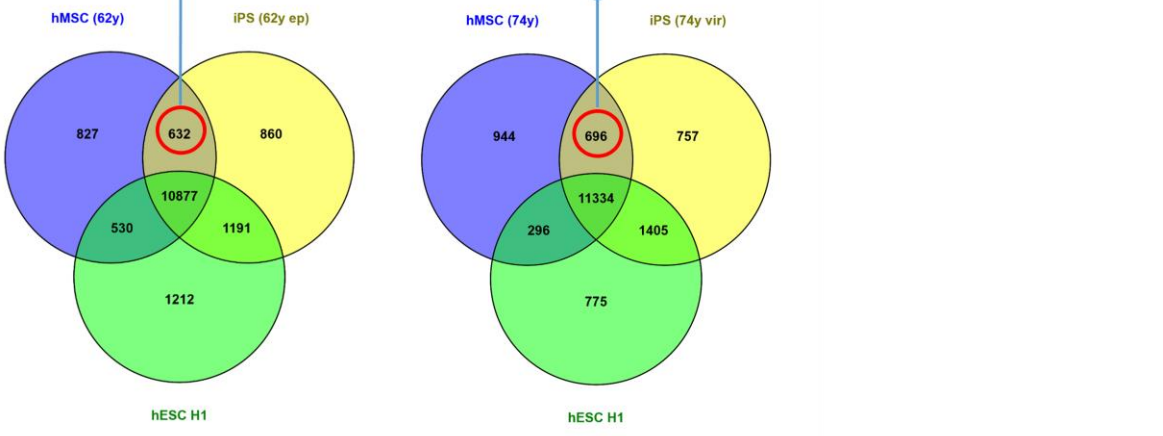

Figure 31 Age-and parental cell type-specific transcriptional memory in hMSC-iPSCs derived from hMSCs with fetal and high age background.

The Venn diagrams were prepared with lists of genes detected as expressed (expression p-value below or equal to 0.01) in fetal hMSC 1, aged hMSC (62y), aged hMSC (74y), corresponding

iPSCs and hESC H1 using an Illumina Bead Chip microarray and the platform Venny. The inclusion of the sample hESC H1 served to filter out genes of the iPS gene lists which are related to the pluripotent state. The genes expressed exclusively in parental hMSCs and corresponding iPSCs but not in hESC H1 (red circle) were considered to be the parental cell type specific retained genes in hMSC-iPSCs. The list was annotated to pathways using DAVID gene annotation database, the option pathways and the category KEGG. A p-value of 0.05 and below was considered significant. The complete list of results is shown. See also Table 13.

To further elucidate whether the gene expression patterns measured in hMSC-iPSCs reveal an age or cell type-specific transcriptional memory. The functional annotation of the genes expressed in iPSCs and parental hMSCs but not in hESCs highlighted by the red circles in Figure 31 was repeated using DAVID functional annotation database and the category GO-BP-FAT, which is based on Go-terms of biological processes. More specifically, annotations to processes related to ageing, mesenchymal stem cells, osteoblast differentiation, adipocyte differentiation or chondrocyte differentiation and related processes were highlighted after scanning the the resulting list of annotations. The analysis revealed that the functional annotation of genes expressed in fetal hMSC 1 and iPSC (hMSC, fetal, line 1, viral) resulted in annotation to the GO-terms skeletal system development (p-value: 7.79E-07), skeletal system morphogenesis (p-value: 7.42E-06), embryonic skeletal system morphogenesis (p-value: 3.59E-05), embryonic skeletal system development (p-value: 5.21E-05), cartilage development (p-value: 2.36E-04), aging (p-value: 0.037) and cell aging (p-value: 0.037). In addition, the functional annotation of genes expressed in fetal hMSC 1 and iPSC (hMSC, fetal, line 1, episomal 1) were annotated to the GO-terms skeletal system development (p-value: 1,380E-05), skeletal system morphogenesis (p-value: 3.14E-04), ossification (p-value: 3.82E-04), bone development (p-value: 6.26E-04), regulation of ossification (p-value: 0.0173) and osteoblast differentiation (p-value: 0.047). In contrast to that, the functional annotation of genes expressed in aged hMSC (62y) and iPSC (hMSC, 62y, episomal) were annotated to the GO-terms skeletal system development (p-value: 0.0003), skeletal system morphogenesis (p-value: 0.001), cell aging (p-value: 0.0082, genes: *CDKN2A*, *TBX2*, *MORC3*, *PML*) and cartilage development (p-value: 0.0094). Finally, the functional annotation of genes expressed in aged hMSC (74y) and iPSC (hMSC, 74y, viral) were annotated to the GO-terms skeletal system development (p-value: 0.0001), skeletal system morphogenesis (p-value: 0.0017), cartilage development (p-value: 0.006), bone development (p-value: 0.011), cell aging (p-value: 0.015, genes: *CDKN2A*, *TBX2*, *MORC3*, *BCL2*), mesenchyme development (p-value: 0.017) and ossification (p-value: 0.020) (Table 13).

Table 13 Ageing- and parental-cell type-specific retained processes in hMSC-iPSCs of fetal and high age background.

Listed are the results of the functional annotation of the list of genes expressed in parental hMSCs and corresponding iPSCs but not in hESC H1 (red circle in Figure 31). Genes that were found to be expressed by Illumina Bead Chip microarray with an expression p-value of 0.01 and below were used as input. The gene lists were generated using the software GenomeStudio. The overlapping gene expression was found using Venn diagrams. The functional annotation was carried out using DAVID functional annotation database and the option general annotation with the category GOTERM_BP_FAT. A p-value of 0.05 and below was considered significant. Listed are only results with a p-value below 0.05. Processes related to MSC-specific differentiation were marked yellow. Processes related to ageing were marked green. Table see next page.

overlap fetal hMSC 1 and iPSC (hMSC, fetal line 1, viral)		overlap aged hMSC (74y) and iPSC (hMSC, 74y, viral)	
Term	PValue	Term	PValue
GO:0006355~regulation of transcription, DNA-dependent	4.43E-07	GO:0001501~skeletal system development	1.88E-04
GO:0001501~skeletal system development	7.79E-07	GO:0032835~glomerulus development	2.40E-04
GO:0051252~regulation of RNA metabolic process	1.03E-06	GO:0006355~regulation of transcription, DNA-dependent	0.002
GO:0045449~regulation of transcription	5.27E-06	GO:0048705~skeletal system morphogenesis	0.002
GO:0048705~skeletal system morphogenesis	7.42E-06	GO:0051252~regulation of RNA metabolic process	0.003
GO:0007389~pattern specification process	3.15E-05	GO:0043392~negative regulation of DNA binding	0.004
GO:0048704~embryonic skeletal system morphogenesis	3.59E-05	GO:0051216~cartilage development	0.006
GO:0003002~regionalization	3.62E-05	GO:0030155~regulation of cell adhesion	0.007
GO:0048562~embryonic organ morphogenesis	4.25E-05	GO:0051100~negative regulation of binding	0.007
GO:0006350~transcription	5.06E-05	GO:0045449~regulation of transcription	0.008
GO:0048706~embryonic skeletal system development	5.21E-05	GO:0003014~renal system process	0.009
GO:0048598~embryonic morphogenesis	6.13E-05	GO:0043433~negative regulation of transcription factor activity	0.010
GO:0051216~cartilage development	2.36E-04	GO:0060348~bone development	0.010
GO:0009952~anterior/posterior pattern formation	3.02E-04	GO:0001558~regulation of cell growth	0.012
GO:0048568~embryonic organ development	4.84E-04	GO:0010033~response to organic substance	0.013
GO:0009954~proximal/distal pattern formation	0.002	GO:0007169~transmembrane receptor protein tyrosine kinase signaling pathway	0.015
GO:0006357~regulation of transcription from RNA polymerase II promoter	0.002	GO:0007569~cell aging	0.015
GO:0032835~glomerulus development	0.005	GO:0046903~secretion	0.016
GO:0001822~kidney development	0.006	GO:0060485~mesenchyme development	0.018
GO:0010033~response to organic substance	0.006	GO:0000902~cell morphogenesis	0.018
GO:0030182~neuron differentiation	0.010	GO:0008361~regulation of cell size	0.019
GO:0001655~urogenital system development	0.012	GO:0001503~ossification	0.020
GO:0006954~inflammatory response	0.014	GO:0032880~regulation of protein localization	0.020
GO:0009725~response to hormone stimulus	0.018	GO:0001822~kidney development	0.023
GO:0009719~response to endogenous stimulus	0.020	GO:0009408~response to heat	0.024
GO:0048858~cell projection morphogenesis	0.022	GO:0032989~cellular component morphogenesis	0.025
GO:0048511~rhythmic process	0.025	GO:0060416~response to growth hormone stimulus	0.027
GO:0030878~thyroid gland development	0.028	GO:0034097~response to cytokine stimulus	0.028
GO:0002675~positive regulation of acute inflammatory response	0.028	GO:0016049~cell growth	0.033
GO:0048545~response to steroid hormone stimulus	0.029	GO:0051149~positive regulation of muscle cell differentiation	0.033
GO:0032990~cell part morphogenesis	0.029	GO:0001649~osteoblast differentiation	0.034
GO:0051384~response to glucocorticoid stimulus	0.030	GO:0031647~regulation of protein stability	0.034
GO:0045995~regulation of embryonic development	0.033	GO:0051098~regulation of binding	0.037
GO:0030155~regulation of cell adhesion	0.034	GO:0006357~regulation of transcription from RNA polymerase II promoter	0.037
GO:0007568~aging	0.037	GO:0006350~transcription	0.038
GO:0007569~cell aging	0.037	GO:0022610~biological adhesion	0.039
GO:0045944~positive regulation of transcription from RNA polymerase II promoter	0.039	GO:0007155~cell adhesion	0.040
GO:0031960~response to corticosteroid stimulus	0.041	GO:0001655~urogenital system development	0.043
GO:0007517~muscle organ development	0.047	GO:0009725~response to hormone stimulus	0.043
		GO:0000165~MAPKKK cascade	0.045
		GO:0010810~regulation of cell-substrate adhesion	0.045
		GO:0051222~positive regulation of protein transport	0.047
		GO:0001934~positive regulation of protein amino acid phosphorylation	0.047
overlap fetal hMSC 1 and iPSC (hMSC, fetal, line 1, episomal 1)		**overlap aged hMSC (62y) and iPSC (hMSC, 62y, episomal)**	
Term	**PValue**	**Term**	**PValue**
GO:0001501~skeletal system development	1.38E-05	GO:0001501~skeletal system development	3.31E-04
GO:0006355~regulation of transcription, DNA-dependent	1.11E-04	GO:0048705~skeletal system morphogenesis	4.17E-04
GO:0030182~neuron differentiation	1.20E-04	GO:0006355~regulation of transcription, DNA-dependent	0.001
GO:0000902~cell morphogenesis	1.93E-04	GO:0045449~regulation of transcription	0.002
GO:0051252~regulation of RNA metabolic process	2.00E-04	GO:0051252~regulation of RNA metabolic process	0.002
GO:0032989~cellular component morphogenesis	2.60E-04	GO:0003014~renal system process	0.005
GO:0048705~skeletal system morphogenesis	3.14E-04	GO:0009952~anterior/posterior pattern formation	0.007
GO:0045449~regulation of transcription	3.48E-04	GO:0007569~cell aging	0.008
GO:0001503~ossification	3.82E-04	GO:0001558~regulation of cell growth	0.008
GO:0060348~bone development	6.26E-04	GO:0051216~cartilage development	0.009
GO:0006350~transcription	9.03E-04	GO:0048706~embryonic skeletal system development	0.011
GO:0048666~neuron development	9.14E-04	GO:0048704~embryonic skeletal system morphogenesis	0.013
GO:0048858~cell projection morphogenesis	9.57E-04	GO:0008361~regulation of cell size	0.013
GO:0007409~axonogenesis	0.001	GO:0034097~response to cytokine stimulus	0.013
GO:0032990~cell part morphogenesis	0.001	GO:0007588~excretion	0.014
GO:0006357~regulation of transcription from RNA polymerase II promoter	0.002	GO:0007389~pattern specification process	0.015
GO:0048667~cell morphogenesis involved in neuron differentiation	0.002	GO:0007517~muscle organ development	0.015
GO:0000904~cell morphogenesis involved in differentiation	0.003	GO:0032387~negative regulation of intracellular transport	0.016
GO:0048812~neuron projection morphogenesis	0.003	GO:0048562~embryonic organ morphogenesis	0.017
GO:0043392~negative regulation of DNA binding	0.003	GO:0032507~maintenance of protein location in cell	0.017
GO:0031175~neuron projection development	0.004	GO:0016481~negative regulation of transcription	0.018
GO:0030030~cell projection organization	0.005	GO:0030155~regulation of cell adhesion	0.019
GO:0051100~negative regulation of binding	0.006	GO:0007010~cytoskeleton organization	0.022
GO:0051173~positive regulation of nitrogen compound metabolic process	0.007	GO:0003002~regionalization	0.023
GO:0007517~muscle organ development	0.008	GO:0043433~negative regulation of transcription factor activity	0.024
GO:0009891~positive regulation of biosynthetic process	0.008	GO:0006350~transcription	0.025
GO:0007507~heart development	0.009	GO:0048568~embryonic organ development	0.026
GO:0001822~kidney development	0.011	GO:0006952~defense response	0.029
GO:0043433~negative regulation of transcription factor activity	0.011	GO:0051651~maintenance of location in cell	0.029
GO:0031328~positive regulation of cellular biosynthetic process	0.013	GO:0045185~maintenance of protein location	0.029
GO:0021700~developmental maturation	0.013	GO:0032386~regulation of intracellular transport	0.030
GO:0003002~regionalization	0.014	GO:0007173~epidermal growth factor receptor signaling pathway	0.030
GO:0048562~embryonic organ morphogenesis	0.015	GO:0006955~immune response	0.032
GO:0010604~positive regulation of macromolecule metabolic process	0.015	GO:0030878~thyroid gland development	0.034
GO:0048469~cell maturation	0.015	GO:0046903~secretion	0.034
GO:0034341~response to interferon-gamma	0.015	GO:0045792~negative regulation of cell size	0.035
GO:0048598~embryonic morphogenesis	0.016	GO:0032535~regulation of cellular component size	0.035
GO:0030155~regulation of cell adhesion	0.017	GO:0030029~actin filament-based process	0.035
GO:0030278~regulation of ossification	0.017	GO:0043392~negative regulation of DNA binding	0.036
GO:0045935~positive regulation of nucleobase, nucleoside, nucleotide and nucleic acid metabolic process	0.018	GO:0008217~regulation of blood pressure	0.036
GO:0048568~embryonic organ development	0.019	GO:0048598~embryonic morphogenesis	0.040
GO:0001655~urogenital system development	0.020	GO:0010629~negative regulation of gene expression	0.041
GO:0045893~positive regulation of transcription, DNA-dependent	0.023	GO:0040008~regulation of growth	0.041
GO:0008285~negative regulation of cell proliferation	0.023	GO:0042992~negative regulation of transcription factor import into nucleus	0.045
GO:0006954~inflammatory response	0.024	GO:0043526~neuroprotection	0.045
GO:0051254~positive regulation of RNA metabolic process	0.025	GO:0045934~negative regulation of nucleobase, nucleoside, nucleotide and nucleic	0.047
GO:0009719~response to endogenous stimulus	0.026	GO:0010558~negative regulation of macromolecule biosynthetic process	0.048
GO:0009725~response to hormone stimulus	0.026	GO:0051725~protein amino acid de-ADP-ribosylation	0.048

In order to elucidate whether genes related to processes associated with extracellular matrix interaction or the cytoskeleton as well as related to the metabolic instability theory of ageing are changed in hMSC-iPSCs of different age backgrounds upon reprogramming, differentially expressed genes that are up-or downregulated in iPSCs derived from fetal hMSCs or from aged hMSCs compared to aged hMSCs were extracted from microarray data. Subsequently the genes were annotated to processes using DAVID functional annotation database and screened for annotations related to extracellular matrix interaction or the cytoskeleton as well as related to the metabolic instability theory of ageing. The analysis revealed that genes down-regulated in iPSCs derived from aged hMSCs compared to aged hMSCs were annotated to the processes and gene ontologies actin cytoskeleton organisation, actin cytoskeleton, extracellular matrix and antioxidant activity with a p-value below 0.01, whereas the genes up-regulated in iPSCs derived from aged hMSCs compared to aged hMSCs were annotated to the gene ontology term mitochondrion with a p-value below 0.01. In contrast to that, genes down-regulated in iPSCs derived from fetal hMSCs compared to aged hMSCs were annotated to the processes and gene ontologies focal adhesion, insulin-like growth factor binding, positive regulation of cell-substrate adhesion, extracellular matrix and mitochondrion with a p-value below 0.05. Moreover, the genes up-regulated between iPSCs derived from fetal hMSCs compared to aged hMSCs could not be annotated to processes or gene ontologies with a p-value below 0.05 (Table 14).

Table 14 Differential expression of genes related to processes associated to the cytoskeleton, interaction with the extracellular matrix and to the metabolic instability theory of ageing.
Functional annotation of genes which were differentially expressed (p-value of 0.01 and below) between iPSC (hMSC aged) (merged samples of iPSC (hMSC, 62y, episomal) and iPSC (hMSC, 74y, viral)) or iPSC (hMSC fetal) (merged samples of iPSC (hMSC, fetal, line 1, viral), iPSC (hMSC, fetal, line 1, episomal 1) and iPSC (hMSC, fetal, line 1, episomal 2)) and hMSCs of aged donors (merged samples of aged hMSC (60y), aged hMSC (62y) and aged hMSC (70y)). Genes with a 1.5-fold higher (up-regulation) or 1.5-fold lower (down-regulation) average signal in iPSC (hMSC aged) or iPSC (hMSC fetal) compared to the average signal in aged hMSCs were measured using an Illumina Bead Chip microarray. The up or down-regulated genes were annotated using DAVID functional annotation platform. Results related to cell adhesion, extracellular matrix interaction, cytoskeleton, oxidative phosphorylation, insulin signalling, glycolysis and glutathione metabolism are shown. A p-value of 0.5 and below was considered significant. Table see next page.

down-regulated in iPSC (hMSC aged) against aged hMSC				
Category	**Term**	**Count**	**%**	**PValue**
GOTERM_BP_FAT	GO:0030036~actin cytoskeleton organization	37	3.144	1.950E-07
GOTERM_CC_FAT	GO:0015629~actin cytoskeleton	38	3.229	3.115E-05
GOTERM_CC_FAT	GO:0031012~extracellular matrix	39	3.314	2.176E-03
GOTERM_MF_FAT	GO:0016209~antioxidant activity	8	0.680	2.240E-02
KEGG_PATHWAY	hsa00010:Glycolysis / Gluconeogenesis	8	0.680	1.251E-01
GOTERM_MF_FAT	GO:0004602~glutathione peroxidase activity	3	0.255	1.411E-01
GOTERM_BP_FAT	GO:0006119~oxidative phosphorylation	9	0.765	2.704E-01
KEGG_PATHWAY	hsa04910:Insulin signaling pathway	11	0.935	4.783E-01
GOTERM_BP_FAT	GO:0006006~glucose metabolic process	11	0.935	4.913E-01
GOTERM_CC_FAT	GO:0005739~mitochondrion	59	5.013	9.831E-01
up-regulated in iPSC (hMSC aged) against aged hMSC				
Category	**Term**	**Count**	**%**	**PValue**
GOTERM_CC_FAT	GO:0005739~mitochondrion	50	7.974	6.776E-03
GOTERM_BP_FAT	GO:0007010~cytoskeleton organization	20	3.190	1.256E-01
GOTERM_CC_FAT	GO:0005856~cytoskeleton	49	7.815	2.556E-01
GOTERM_BP_FAT	GO:0032869~cellular response to insulin stimulus	4	0.638	3.842E-01
GOTERM_CC_FAT	GO:0031012~extracellular matrix	10	1.595	7.648E-01
down-regulated in iPSC (hMSC fetal) against aged hMSC				
Category	**Term**	**Count**	**%**	**PValue**
GOTERM_CC_FAT	GO:0005925~focal adhesion	21	1.878	8.587E-06
GOTERM_MF_FAT	GO:0005520~insulin-like growth factor binding	9	0.805	4.776E-05
GOTERM_BP_FAT	GO:0010811~positive regulation of cell-substrate adhesion	7	0.626	4.967E-03
GOTERM_CC_FAT	GO:0031012~extracellular matrix	35	3.131	1.162E-02
GOTERM_CC_FAT	GO:0005739~mitochondrion	86	7.692	4.866E-02
GOTERM_BP_FAT	GO:0006749~glutathione metabolic process	5	0.447	7.875E-02
GOTERM_BP_FAT	GO:0006750~glutathione biosynthetic process	3	0.268	1.133E-01
KEGG_PATHWAY	hsa00480:Glutathione metabolism	6	0.537	2.403E-01
KEGG_PATHWAY	hsa04910:Insulin signaling pathway	12	1.073	2.913E-01
KEGG_PATHWAY	hsa00190:Oxidative phosphorylation	8	0.716	7.766E-01
GOTERM_CC_FAT	GO:0070469~respiratory chain	4	0.358	8.780E-01
GOTERM_CC_FAT	GO:0005746~mitochondrial respiratory chain	3	0.268	9.292E-01
up-regulated in iPSC (hMSC aged) against aged hMSC				
Category	**Term**	**Count**	**%**	**PValue**
GOTERM_CC_FAT	GO:0005925~focal adhesion	5	0.711	0.409
GOTERM_BP_FAT	GO:0032869~cellular response to insulin stimulus	4	0.569	0.442
GOTERM_BP_FAT	GO:0016337~cell-cell adhesion	11	1.565	0.531
GOTERM_BP_FAT	GO:0030155~regulation of cell adhesion	6	0.853	0.548
GOTERM_CC_FAT	GO:0005741~mitochondrial outer membrane	4	0.569	0.550
KEGG_PATHWAY	hsa04512:ECM-receptor interaction	3	0.427	0.767

In order to analyse in more detail, whether the age of the parental hMSCs influences the expression of ageing-related genes in hMSC-iPSCs, a hierarchical clustering analysis based on Pearson correlation of average signal values measured for genes of the GO- term ageing was performed comparing the expression signatures of fetal hMSCs and hMSCs of aged background with the corresponding iPS cell lines and hESC H1. Interestingly, based on the clustering analysis, the hMSC samples formed one cluster based on similarity, whereas iPSCs and hESC H1 formed a separate cluster. Within the cluster consisting of hESC H1 and the iPS cell samples, iPSC (hMSC, fetal, line 1, episomal 1), iPSC (hMSC, fetal, line 1, episomal 2) and iPSC (hMSC, 74y, viral) formed one cluster based on the similarity of the gene expression patterns. iPSC (hMSC, fetal, line 1, viral) and iPSC (hMSC, 62y, episomal) formed a separate similarity cluster. All hMSC-iPSC samples formed a cluster that separated them from hESC

H1 (Figure 32). A statistical test toward differential expression of genes of the GO-term ageing comparing the respective iPS cell sample to hESC H1 revealed a down-regulation of *ROMO1*, *ID2*, *FADS1* and *IDE* and an up-regulation of *TBX2*, *MIF*, *PDCD4*, *PNPT1*, *ATM*, *ZNF277*, *VASH1*, *APOD*, *TWIST1*, *C2orf40* and *TSPO* of more than 1.5-fold with a p-value below 0,01 in iPSC (hMSC, fetal, line 1, viral). Moreover, *ROMO1* and *FADS1* were down-regulated and *CITED2*, *TBX3*, *PNPT1* and *ID2* were detected as up-regulated in iPSC (hMSC, fetal, line 1, episomal 1). In addition, *ROMO1* was down-regulated in iPSC (hMSC, fetal, line 1, episomal 2), whereas *PDCD4*, *CITED2*, *TBX3*, *ID2*, *TSPO* and *PNPT1* were up-regulated compared to the gene expression in hESC H1. Interestingly, *ROMO1*, *FADS1* and *TWIST1* were detected to be down-regulated significantly in iPSC (hMSC, 62y, episomal) whereas *VASH1*, *KRT25*, *PDCD4*, *PNPT1*, *ATM* and *TSPO* were up-regulated. Moreover, *ROMO1* was detected to be down-regulated in iPSC (hMSC, 74y, viral) and *ID2*, *TSPO*, *CITED2* and *TBX2* were detected to be up-regulated.

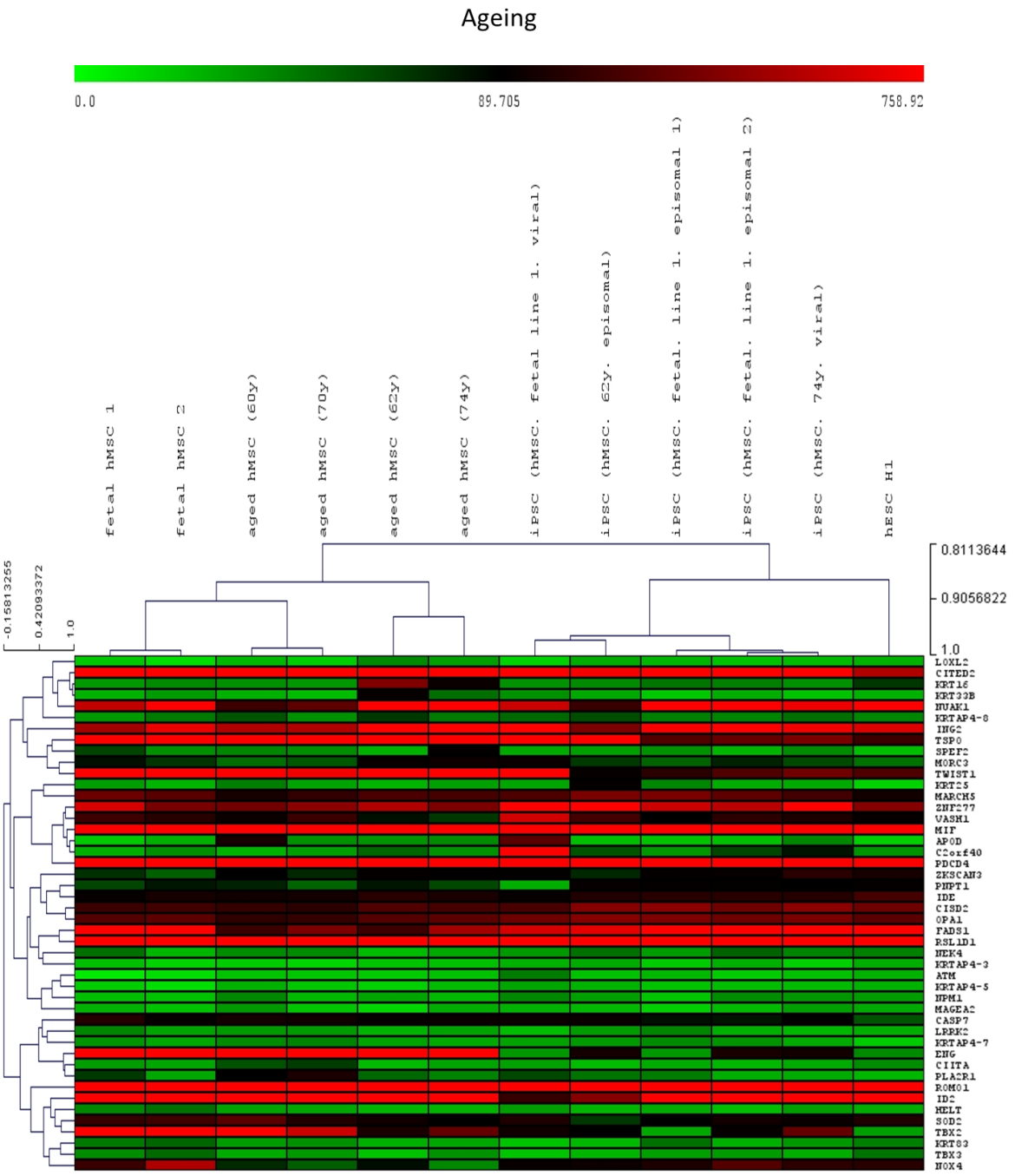

Figure 32 Gene expression changes related to ageing-associated processes in fetal and aged hMSCs upon induction of pluripotency with viral and episomal plasmid-based methods.

Hierarchical clustering analysis of gene expression related to ageing (GO-term: ageing) detected using an Illumina Bead Chip microarray and extracted using the software GenomeStudio. Heatmap based on the average signal. Hierarchical clustering based on Pearson correlation between the samples and genes. Gene description see Table 22.

3.5.3 Influence of parental cell type on differentiation propensity and cell fate-specific transcriptional memory in hMSC-iPSCs

To further analyse the donor cell-specific memory and to find out whether it influences the functionality and differentiation propensity of hMSC-iPSCs, a comparative microarray-based gene expression analysis was carried out comparing the transcriptomes of iPSC (hMSC, 74y, viral) with an iPS cell line derived from human foreskin fibroblasts using retroviral reprogramming (iPS (hFF, viral)). Furthermore, *in vitro* osteoblast differentiation was carried out to test the influence of the somatic origin of hMSCs as parental cell type has an effect on the efficiency of osteoblast differentiation in iPSC (hMSC, 74y, viral) compared to iPS (hFF, viral). More Alizarin Red positive calcified matrix was detected when iPSC (hMSC, 74y, viral) were cultured in osteogenic medium for 11 days compared to iPS (hFF, viral) differentiated under the same conditions (Figure 33 A). Comparing iPSCs derived from aged hMSC (74y) and derived from hFF a statistical test was used to extract differentially expressed genes between the two samples. The genes differentially expressed with a p-value below 0.01 and a 1.5-fold higher average signal in iPSC (hMSC, 74y, viral) were considered to be up-regulated. These genes were analysed using functional annotation with the database DAVID. Interestingly, the up-regulated genes in iPSC (hMSC, 74y, viral) were annotated to the UNIGENE terms bone_normal_3rd (p-value: 5.267E-06, 161 genes), connective tissue_normal_3rd (p-value: 7,343E-05, 162 genes), chondrosarcoma_disease_3rd (p-value: 0.0001, 122 genes), adipose tissue_normal_3rd (p-value: 0.0004, 110 genes) and to bone marrow_normal_3rd (p-value: 0.002, 101 genes) (Figure 33 B). Moreover, a hierarchical clustering analysis based on the Euclidean distance between the gene expression values measured by microarray in iPSC (hMSC, 74y, viral), iPSC (hFF, viral) and hESC H1 with the genes annotated to the UNIGENE term bone_normal_3rd revealed a higher similarity between iPSC (hFF, viral) and hESC H1 than between iPSC (hMSC, 74y, viral) and hESC H1 (Figure 33 C).

A

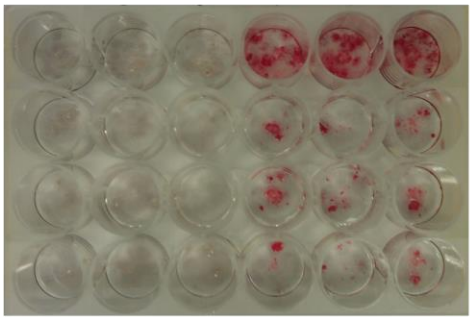

B

Term	Count	%	PValue
embryonic tissue_normal_3rd	98	35.636	1.264E-10
neonate (< 4 weeks old)_development_3rd	70	25.455	2.693E-10
ear_normal_3rd	68	24.727	6.630E-09
vascular_normal_3rd	76	27.636	1.839E-08
umbilical cord_normal_3rd	55	20.000	2.862E-08
bladder_normal_3rd	75	27.273	9.936E-08
soft tissue/muscle tissue tumor_disease_3rd	78	28.364	1.312E-06
urinary bladder tumor_disease_3rd	70	25.455	1.620E-06
bone_normal_3rd	89	32.364	5.267E-06
esophageal tumor_disease_3rd	62	22.545	1.529E-05
infant (< 3 years old)_development_3rd	57	20.727	3.684E-05
connective tissue_normal_3rd	66	24.000	7.343E-05
chondrosarcoma_disease_3rd	88	32.000	1.161E-04
esophagus_normal_3rd	56	20.364	2.319E-04
adrenal tumor_disease_3rd	70	25.455	2.389E-04
uterine tumor_disease_3rd	81	29.455	4.198E-04
adipose tissue_normal_3rd	65	23.636	4.207E-04
kidney tumor_disease_3rd	72	26.182	6.034E-04
skin_normal_3rd	72	26.182	6.688E-04
mixed (normal and tumor)_disease_3rd	58	21.091	7.394E-04
juvenile (< 17 years old)_development_3rd	65	23.636	8.741E-04
small intestine_normal_3rd	67	24.364	1.099E-03
bone marrow_normal_3rd	61	22.182	1.660E-03
cervical tumor_disease_3rd	56	20.364	2.551E-03
salivary gland_normal_3rd	48	17.455	3.359E-03
oral tumor_disease_3rd	54	19.636	5.650E-03

C

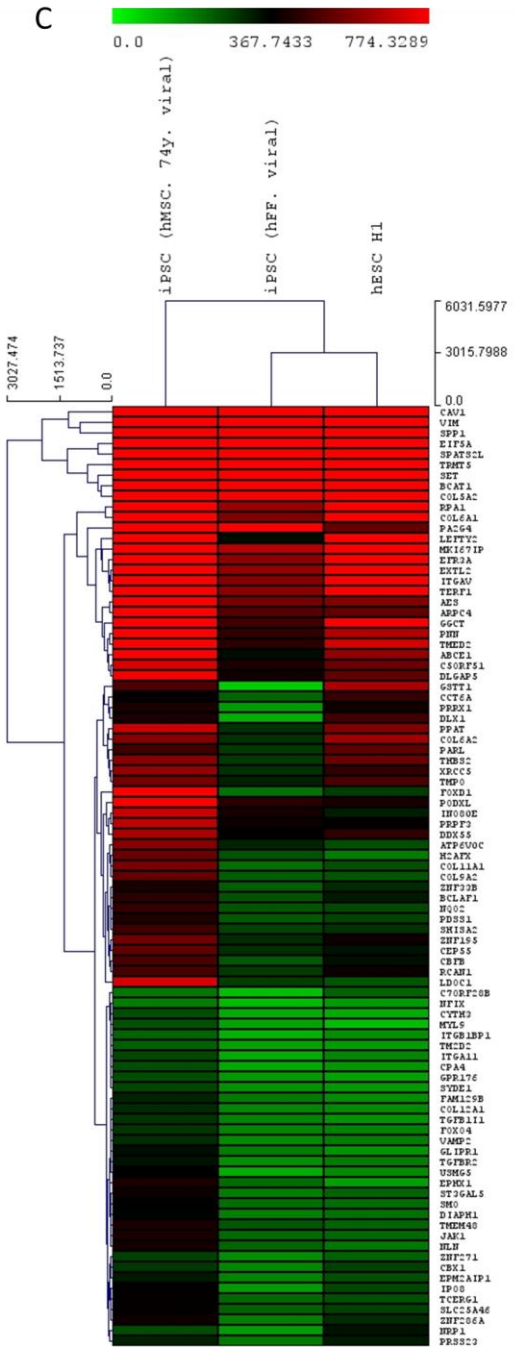

Figure 33 Retained parental cell type-specific functional properties in iPSCs derived from aged hMSC (74y) compared to hFF-derived iPSCs.

(A) Enhanced osteoblast differentiation of iPSC (hMSC, 74y, viral) compared to iPS (hFF, viral) after 11 days of treatment with osteoblast differentiation medium (OM) compared to 11 days of culture in expansion medium (EM). Alizarin Red S staining was used to visualise calcified matrix in red. (B) Functional annotation of differentially expressed (p-value of 0.01 and below) and up-regulated genes (1.5-fold higher average signal in iPSC (hMSC, 74y, viral)) detected using an Illumina Bead Chip microarray. The genes were used as input for functional annotation by the tool DAVID. The option tissue-specific annotation and the category UNIGENE were used. P-values of 0.05 and below were considered as significant. Listed are the first 26 annotations. (C) Hierarchical clustering analysis of the up-regulated genes annotated to bone_normal_3d in B comparing iPSC (hMSC, 74y, viral), iPS (hFF, viral) and hESC H1. Heat map based on average signal detected by microarray-based transcriptome profiling. The hierarchical clustering is based on Euclidean distance. Gene description see Table 23.

3.6 Directed differentiation of iPS cells derived from hMSCs of different biological age into mesenchymal stem cell-like cells

The fast *in vitro* senescence of primary hMSCs derived from aged donors might be circumvented by generation of mesenchymal stem cell-like cells from iPS cells. A recent study described the a rejuvenation of ageing-related features in cell differentiated from iPS cell of aged donors (Miller and Studer 2014). However, the effect of the donor age of the parental hMSCs and the potential effect of the somatic cell type of the parental cells on the features of mesenchymal stem cell-like cells (iMSCs) is not clear. Therefore, hMSC-iPSCs derived from fetal hMSC 1 and from aged hMSC (74y) as well as from hESC H1 were differentiated into iMSCs. Subsequently, the MSC phenotype as well as the differentiation potential were analysed. The effect of age of the parental hMSCs of the generated iPS cell lines and the effect of the pluripotent parental cell type of iMSCs was analysed by microarray-based comparative gene expression profiling.

3.6.1 Generation and characterisation of iMSCs

To analyse the potential effect of the biological age of parental hMSCs and of the type of cell on the features of iMSCs, mesenchymal stem cell-like cells were generated using a previously published protocol (Yen Shun Chen et al. 2012). iMSCs were generated from iPSC (hMSC, fetal, 1, viral) and will be called iMSC (fetal, line 1, viral), from iPSC (hMSC, 74y, viral) which will be called iMSC (74y, viral), from iPSC (hMSC, fetal, line 1, episomal 1) named iMSC (fetal, line 1, episomal 1) and from hESC H1 named iMSC (hESC H1). The iPS cells were treated for one with the inhibitor of the TGFβ receptor SB-431542. Subsequently, the cells were split and seeded normal cell culture dishes in hMSC maintenance medium. After three more passages, the iMSCs

tested for their ability to differentiate into osteoblasts, adipocytes and chondrocytes in *in vitro* differentiation experiments. After being treated with osteogenic medium for 21 days iMSC 1, viral) and iMSC (74y, viral) showed more Alizarin Red positive areas compared to iMSC H1) the staining colour intensity of which was similar to the control condition, 21 days in hMSC expansion medium. In contrast to that, after 21 days of culture in adipocyte differentiation iMSC (fetal, line 1, viral), iMSC (74y, viral) and iMSC (hESC H1) showed few Oil Red O cells after the respective staining. Moreover, the chondrogenic potential of iMSC (fetal, line 1, iMSC (74y, viral) and iMSC (hESC H1) was tested in micro mass culture. After 21 days of chondrogenic medium and subsequent Alcian Blue staining to visualise acidic mucosubstances (74y, viral) and iMSC (hESC H1) showed Alcian Blue positive blue staining compared to the However, iMSC (fetal, line 1, viral) did not show a clear blue staining after Alcian Blue was used compared to the control culture in expansion medium for 21 days (
Figure 34 A). Subsequently, an immunofluorescence-based detection of MSC-specific surface markers was carried out. The results of the analysis revealed that iMSC (fetal, line 1, viral), iMSC (74y, viral) and iMSC (hESC H1) showed no expression of the hematopoietic markers CD14, CD20, CD34 and CD45, whereas CD105 and CD73 were detected in all three iMSC preparations. Interestingly, CD90 could not be detected in iMSC (hESC H1) whereas this marker was detected on the surface of iMSC (fetal, line 1, viral) and iMSC (74y, viral) cells (
Figure 34 B). To further confirm the MSC phenotype of the generated iMSCs the average signal of the gene expression measured by microarray was compared for MSC marker genes *CD90, CD73* and *CD105* as well as for genes encoding hematopoietic markers comparing hMSCs and iMSC samples. The expression of the genes *CD90, CD73* and *CD105* encoding the respective marker proteins was detected in all iMSC preparations and the expression levels were similar to the levels detected in hMSCs of fetal and aged background. Moreover, the genes *CD45, CD34* and *CD14* encoding hematopoietic markers were not detected as expressed (
Figure 34 C).

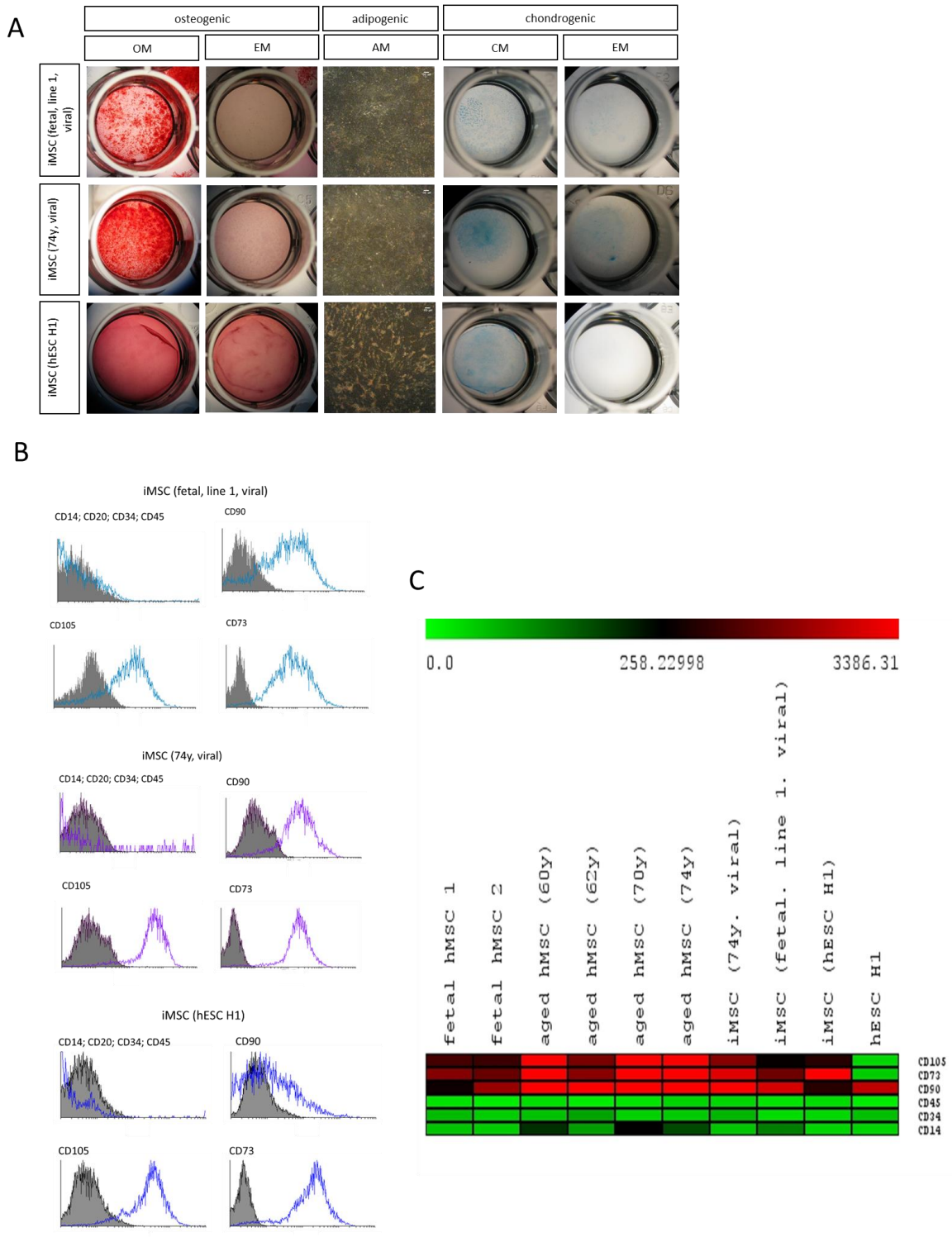

Figure 34 Characterisation of mesenchymal stem cell-like cells (iMSC) derived from hMSC-iPSCs of different age and reprogramming background.

(A) Trilineage potential of iMSCs. osteogenic: iMSCs were cultured for 21 days in osteoblast differentiation medium (OM) or in expansion medium (EM). The calcified matrix was visualised in red using Alizarin Red S staining. adipogenic: iMCs were cultured for 21 days in adipocyte differentiation medium (AM). Fat vacuoles were visualised in red using the dye Oil Red O.

Chondrogenic: iMSCs were cultured as micro mass culture for 21 days in chondrogenic differentiation medium (CM) and in hMSC expansion medium (EM). Acidic mucosubstances were visualised in blue using the dye Alcian Blue. (B) iMSC (fetal, line 1, viral), iMSC (74y, viral) and iMSC (hESC H1) were found to express typical MSC surface markers. The expression of hematopoietic markers could not be detected. FACS-based detection of typical MSC and hematopoietic marker antigens using fluorophore-conjugated antibodies. Grey: isotype control, Blue: cells stained with labelled marker-specific antibody. (C) Expression of MSC surface marker genes in iMSCs compared to fetal hMSCs and hMSCs of higher age as well as hESC H1. Heat map based on the average signal detected using an Illumina Bead Chip microarray.

3.7 Reflection of ageing features and pluripotent cell-specific features in iMSCs differentiated from hMSC-iPSCs of distinct biological age

3.7.1 Effect of hMSC donor age and parental pluripotent cell type on cellular and transcriptional features of iMSCs

In order to test a potential reflection of the age of the original parental hMSCs and of the parental pluripotent cell line in the morphology of the iMSC preparations generated, bright-field pictures were taken to compare iMSC (fetal, line 1, viral), iMSC (fetal, line 1, episomal 1), iMSC (74y, viral) and iMSC (hESC H1). The morphology of iMSC (fetal, line 1, viral), iMSC (74y, viral) and iMSC (hESC H1) was fibroblast-like with few elongated cells. In contrast to that, the morphology of iMSC (fetal, line 1, episomal 1) cell revealed a more elongated morphology, along with a bigger cell size (Figure 35 A). In order to test whether the age of the parental hMSCs influences the number of colony-forming unit fibroblastoid cells (CFU-f) in iMSCs, a CFU-f assay was performed comparing iMSC (fetal, line 1, viral), iMSC (74y, viral) with fetal hMSC 2. Doing this, iMSC (fetal, line 1, viral) showed a similar number of CFU-f compared to fetal hMSC 2, whereas the number of CFU-f detected in iMSC (74y, viral) was reduced (Figure 35 B).

A

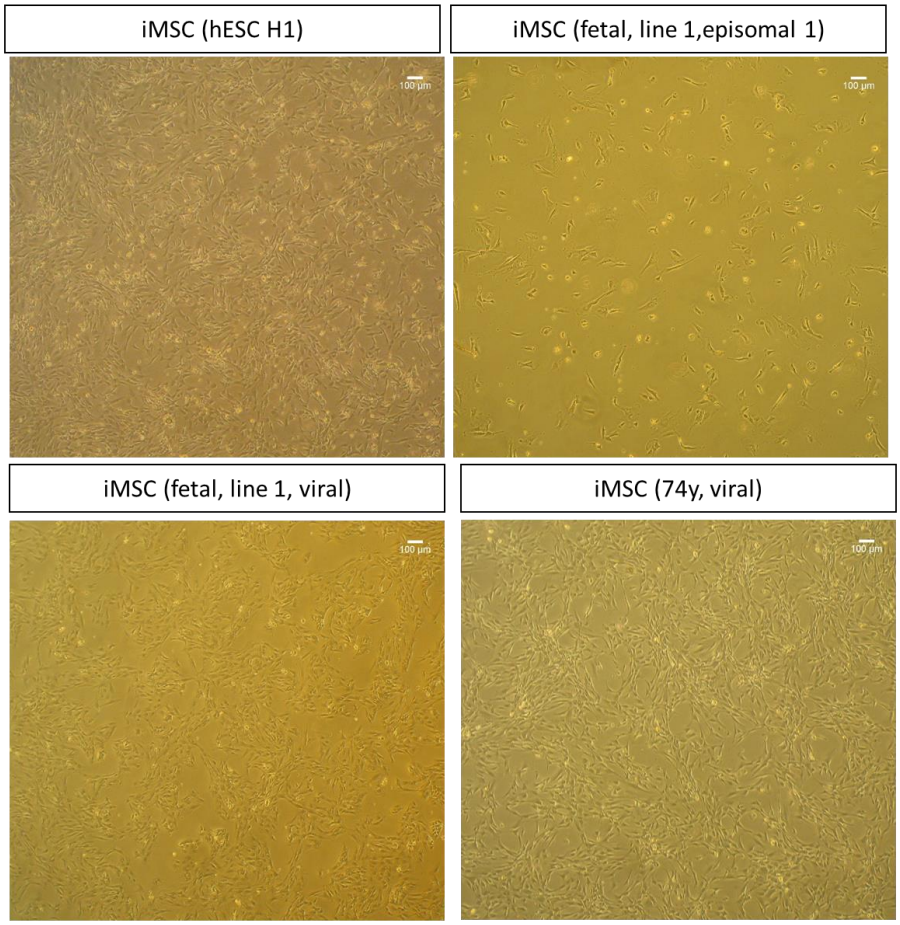

B

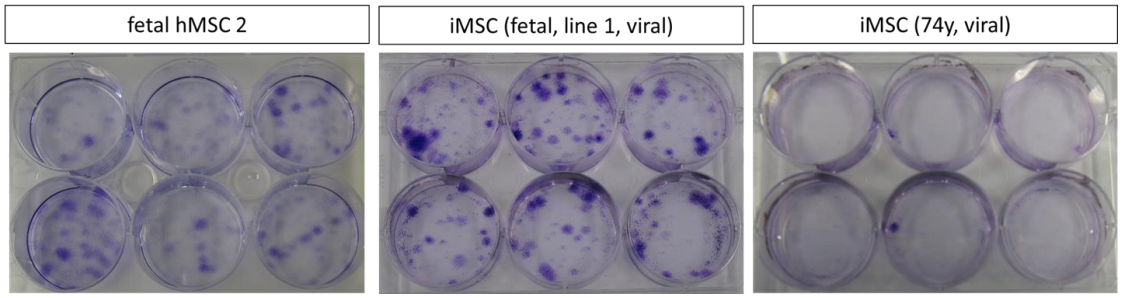

Figure 35 Morphology and colony forming unit fibroblastoid cells of iMSCs derived from fetal hMSC 1, aged hMSC (74y) and hESC H1.

(A) Morphology of iMSCs derived from hESC H1, iPSC (hMSC, fetal, line 1, episomal 1), iPSC (hMSC, fetal, line 1, viral) and iPSC (hMSC, 74y, viral). Bright-field microscopy. 10 x magnification. (B) CFU-f assay comparing fetal hMSC 2 to iMSCs derived from iPSC (hMSC, fetal, line 1, viral) and from iPSC (hMSC, 74y, viral). CFU-fs were visualised using Crystal violet staining.

Furthermore, a microarray-based gene expression analysis was conducted to compare and characterise transcriptional changes between hMSCs and iMSCs as well as between hMSC-iPSCs and iMSCs. To reach this goal, correlations of the transcriptomes of hMSCs, iMSC and hMSC-iPSCs were compared using the software GenomeStudio. The correlation values detected are listed in Figure 36 A. The similarity analysis between the transcriptomes revealed a correlation of 0.95 between fetal hMSC 1 and corresponding iMSCs. The correlation between the transcriptomes of aged hMSC (74y) and the corresponding iMSCs was 0.94. Comparing the transcriptomes of iMSCs and the corresponding pluripotent cell lines they originated from, the highest similarity could be found between the samples hESC H1 and iMSC (hESC H1) with a value of 0.92 followed by the similarity between iPSC (hMSC, fetal, line 1, viral) and iMSC (fetal, line 1, viral) with a value of 0.90. Interestingly, the correlation between iPSC (hMSC, 74y, viral) and iMSC (74y, viral) was the lowest with a value of 0.88. In addition, the transcriptomes of iMSCs were more similar to the transcriptome of fetal hMSC 2 than to fetal hMSC 1. The correlation between fetal hMSC 1 and iMSC (fetal, line 1, viral) was 0.93 like the correlation between fetal hMSC 1 and iMSC (hESC H1), whereas the correlation between fetal hMSC 1 and iMSC (74y, viral) was 0.92 and therefore the lowest of all three. In contrast to that, the correlation between fetal hMSC 2 and iMSC (fetal, line 1, viral) was 0.96 like the correlation between fetal hMSC 2 and iMSC (hESC H1) whereas the correlation between fetal hMSC 2 and iMSC (74y, viral) was 0.94. Interestingly, there was a higher similarity between aged hMSC (62y) and iMSC (74y, viral) with a value of 0.95 than between aged hMSC (74y) and iMSC (74y, viral) with a value of 0.94. Comparing hMSCs and iMSCs towards their similarity to the corresponding iPS cell line sample, iMSCs were less similar to the iPS cell than the corresponding hMSC samples. The correlation between iPSC (hMSC, fetal, line 1, viral) and fetal hMSC 1 was 0.92 whereas the corresponding correlation between iPSC (hMSC, fetal, line 1, viral) and iMSC (fetal, line 1, viral) was 0.89, which is lower than the correlation between iMSC (fetal, line 1, viral) and fetal hMSC1 with a value of 0.95. Likewise, the correlation between iPSC (hMSC, 74y, viral) and aged hMSC (74y) was 0.9, whereas the correlation between iPSC (hMSC, 74y, viral) and iMSC (74y, viral) was 0.87. In addition, the correlation between hMSC (74y) and iMSC (74y, viral) was higher with a value of 0.94 (Figure 36 A). Furthermore, a clustering dendrogram based on the Pearson correlation between the grouped transcriptome samples fetal hMSCs (fetal hMSC 1 and fetal hMSC 2), aged hMSCs (aged hMSC (60y), aged hMSC (62y), aged hMSC (70y), aged hMSC (74y)), iMSC. (iMSC (fetal, line 1, viral), iMSC (74y, viral) and iMSC (hESC H1)) and hESCs (hESC H1 and hESC H9 grouped) revealed the highest similarities between the grouped transcriptomes fetal hMSCs and aged hMSCs. The grouped transcriptome data sample iMSC was more similar to the grouped samples fetal hMSCs and aged hMSCs than to hESC H1 (Figure 36 B). Moreover, a hierarchical clustering dendrogram comparing the grouped samples fetal hMSCs and aged hMSCs with iMSC (74y, viral) and iMSC (fetal, line 1, viral) revealed a higher similarity between iMSC (fetal, line 1, viral) and the grouped samples fetal

hMSCs and aged hMSCs than between iMSC (74y, viral) and the grouped samples fetal hMSCs and aged hMSCs (Figure 36 C). A further hierarchical clustering dendrogram comparing all hMSC-iPSCs, hESC H1, hMSCs of fetal and aged background with the generated iMSCs revealed a separate similarity-based clustering of all pluripotent cell samples and the samples of hMSCs and iMSCs. In addition, iMSC (74y, viral) and iMSC (hESC H1) were more similar to aged hMSC (62y) and aged hMSC (74y) than to all other samples. In contrast to that, iMSC (fetal, line 1, viral) were more similar to fetal hMSC 1 and 2 as well as to aged hMSC (60y) and aged hMSC (70y) (Figure 36 D).

A

sample	aged hMSC (74y)	aged hMSC (62y)	aged hMSC (60y)	aged hMSC (70y)	fetal hMSC 1	fetal hMSC 2	iMSC (74y, viral)	iMSC (fetal, line 1, viral)	iMSC (hESC H1)	iPSC (hMSC, 74y, viral)	iPSC (hMSC, fetal line 1, viral)	hESC H1
aged hMSC (74y)	1.000	0.972	0.944	0.951	0.933	0.943	0.940	0.940	0.948	0.897	0.862	0.869
aged hMSC (62y)	0.972	1.000	0.929	0.939	0.924	0.937	0.948	0.940	0.952	0.896	0.862	0.869
aged hMSC (60y)	0.944	0.929	1.000	0.986	0.961	0.964	0.917	0.935	0.928	0.887	0.884	0.885
aged hMSC (70y)	0.951	0.939	0.986	1.000	0.957	0.962	0.921	0.931	0.929	0.883	0.881	0.877
fetal hMSC 1	0.933	0.924	0.961	0.957	1.000	0.987	0.927	0.946	0.946	0.933	0.918	0.931
fetal hMSC 2	0.943	0.937	0.964	0.962	0.987	1.000	0.943	0.958	0.964	0.931	0.903	0.939
iMSC (74y, viral)	0.940	0.948	0.917	0.921	0.927	0.943	1.000	0.937	0.970	0.914	0.867	0.895
iMSC (fetal, line 1, viral)	0.940	0.940	0.935	0.931	0.946	0.958	0.937	1.000	0.957	0.919	0.891	0.915
iMSC (hESC H1)	0.948	0.952	0.928	0.929	0.946	0.964	0.970	0.957	1.000	0.934	0.879	0.921
iPSC (hMSC, 74y, viral)	0.897	0.896	0.887	0.883	0.933	0.931	0.914	0.919	0.934	1.000	0.923	0.962
iPSC (hMSC, fetal line 1, viral)	0.862	0.862	0.884	0.881	0.918	0.903	0.867	0.891	0.879	0.923	1.000	0.899
hESC H1	0.869	0.869	0.885	0.877	0.931	0.939	0.895	0.915	0.921	0.962	0.899	1.000

B

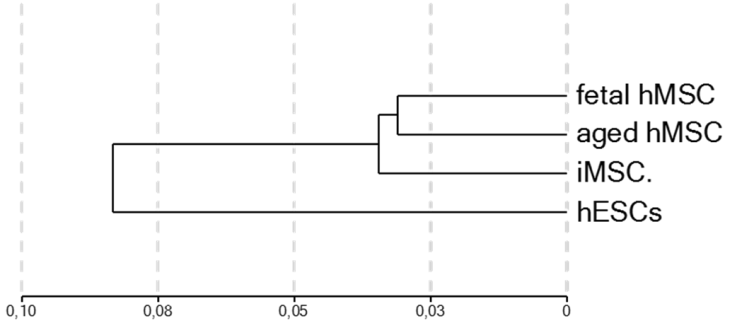

C

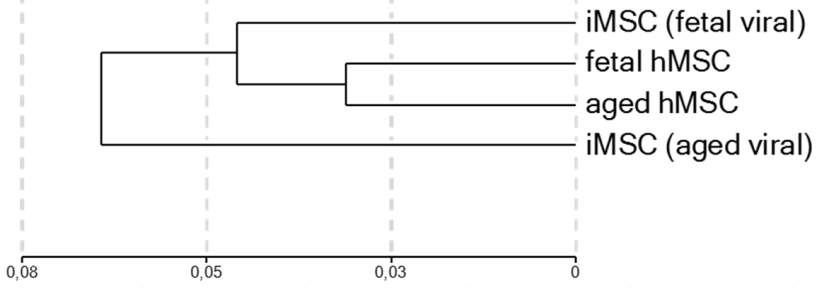

D

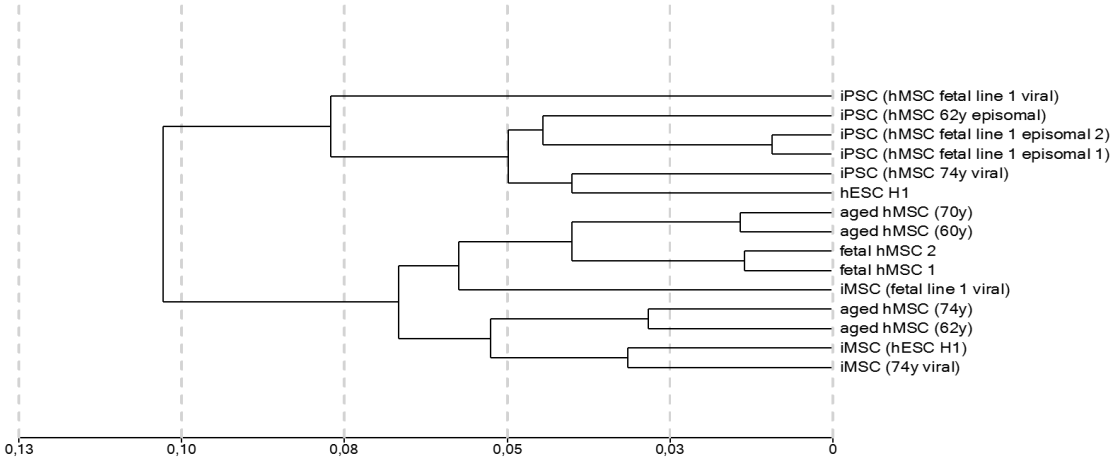

Figure 36 Microarray-based comparison of transcriptomes of iMSCs corresponding hMCSs and hMSC-iPSCs of fetal and high age background and hESCs.

(A) Table listing Pearson correlations between transcriptomes of iMSCs, fetal hMSCs and hMSCs of aged origin, corresponding iPSCs used for iMSC generation and hESCs. The similarity of the samples is colour coded starting with green representing the highest similarity to strong red representing the lowest similarity. (B) Hierarchical clustering dendrogram

representing the similarity of grouped transcriptomes based on Pearson correlation. Fetal hMSCs (fetal hMSC 1 and fetal hMSC 2 grouped), aged hMSCs (aged hMSC (60y), aged hMSC (62y), aged hMSC (70y), aged hMSC (74y) grouped), iMSC. (iMSC (fetal, line 1, viral), iMSC (74y, viral) and iMSC (hESC H1) grouped) and hESCs (hESC H1 and hESC H9 grouped). (C) Hierarchical clustering dendrogram based on the Pearson correlation of the transcriptomes of iMSC (fetal viral) (iMSC (fetal, line 1, viral)), iMSC (aged viral) (iMSC (74y, viral)), fetal hMSCs (fetal hMSC 1 and fetal hMSC 2 grouped) and aged hMSCs (aged hMSC (60y), aged hMSC (62y), aged hMSC (70y), aged hMSC (74y) grouped). (D) Hierarchical clustering dendrogram based on Pearson correlation of the transcriptomes of single samples including hESC H1, iPSCs of fetal and high age background, fetal hMSCs, hMSCs of aged donors and corresponding iMSCs. All clustering dendrograms were generated using the software GenomeStudio. The data were generated with an Illumina Bead Chip microarray.

In order to compare the transcriptional features of iMSCs derived from the hMSC-iPS cells and hESC H1, a Venn diagram based on genes found to be expressed by microarray in iMSC (fetal, line 1, viral), iMSC (74y, viral) and iMSC (hESC H1) was prepared. Among the genes commonly expressed in all three iMSC samples MSC-specific marker genes *ALCAM*, *ANPEP*, *BMP2*, *CASP3*, *CD44*, *ENG* (*CD105*), *ERBB2* (*HER2*), *FUT4*, *FZD9*, *ITGA6*, *ITGAV*, *MCAM*, *NT5E* (*CD73*), *PDGFRB* and *THY1* (*CD90*) were detected. Moreover, further genes associated with MSCs were detected as expressed in all derived iMSC preparations by microarray such as *ANXA5*, *COL1A1*, *CTNNB1*, *EGF*, *GTF3A*, *ICAM1*, *IL10*, *IL1B*, *IL6*, *ITGB1*, *KITLG*, *MMP2*, *NES*, *NUDT6*, *PIGS*, *TGFB3*, *VEGFA* and *VIM*. In addition, genes associated with osteogenesis, adipogenesis, chondrogenesis, myogenesis and tenogenesis were detected to be expressed in iMSC (fetal, line 1, viral), iMSC (74y, viral) and iMSC (hESC H1) (Figure 37 A). Furthermore, a Venn diagram consisting of genes found to be expressed by microarray in grouped samples of fetal hMSCs (fetal hMSC 1, fetal hMSC 2 and fetal hMSC 3), aged hMSCs (aged hMSC (60y), aged hMSC (62y), aged hMSC (70y), aged hMSC (74y)) and iMSCs (iMSC (fetal, line 1, viral), iMSC (74y, viral) and iMSC (hESC H1)) was prepared. Interestingly, the grouped sample iMSCs shared 534 genes with the group fetal hMSCs and only 398 genes with the group aged hMSCs. In order to characterise the processes the genes common to iMSCs and fetal hMSCs are involved in, a functional annotation of these genes was carried out. The commonly expressed genes were annotated to the KEGG terms Cell cycle (p-value: 0.046, genes: *CCNE2*, *CDKN1C*, *ORC4L*, *RBL1*, *CDC25C*, *TGFB2*), Prostate cancer (p-value: 0.051, genes: *CCNE2*, *IGF1R*, *AR*, *PDGFA*, *TCF7L2*) and Pathways in cancer (p-value: 0.071, genes: *TRAF1*, *CCNE2*, *FZD9*, *IGF1R*, *AR*, *PDGFA*, *PAX8*, *TCF7L2*, *DAPK1*, *TGFB2*) (Figure 37 B).

A

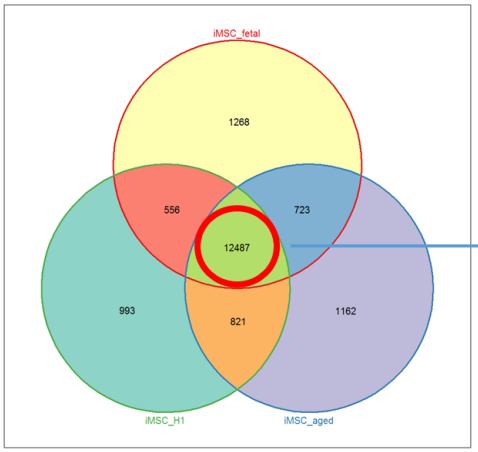

MSC-specific Markers	Other genes associated with MSCs	Differentiation Markers
ALCAM	ANXA5	Osteogenesis
ANPEP	COL1A1	HDAC1
BMP2	CTNNB1	PTK2
CASP3	GTF3A	RUNX2
CD44	IL10	SMURF1
ENG (CD105)	IL6	Adipogenesis
ERBB2 (HER2)	ITGB1	PPARG
FUT4	KITLG	RHOA
ITGAV	MMP2	RUNX2
NT5E (CD73)	NES	Chondrogenesis
PDGFRB	NUDT6	BMP4
THY1 (CD90)	PIGS	HAT1
VCAM1	TGFB3	KAT2B
	VEGFA	SOX9
	VIM	TGFB1
	SerpinE1	Myogenesis
	MIF	ACTA2
		JAG1
		NOTCH1
		Tenogenesis
		GDF15 (PLAB)

B

Term	Count	PValue	Genes
hsa04110:Cell cycle	6	4.610E-02	CCNE2, CDKN1C, ORC4L, RBL1, CDC25C, TGFB2
hsa05215:Prostate cancer	5	5.073E-02	CCNE2, IGF1R, AR, PDGFA, TCF7L2
hsa05200:Pathways in cancer	10	7.071E-02	TRAF1, CCNE2, FZD9, IGF1R, AR, PDGFA, PAX8, TCF7L2, DAPK1, TGFB2
hsa04114:Oocyte meiosis	5	9.412E-02	CCNE2, IGF1R, AR, SGOL1, CDC25C

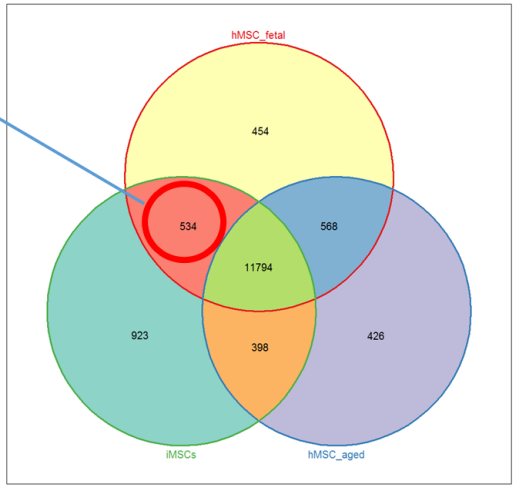

Figure 37 Transcriptional features of iMSCs derived from iPS cells and hESC H1.

(A) Venn diagram based on genes found to be expressed by microarray (detection p-value of 0.01 and below) in iMSC (fetal viral) (iMSC_fetal), iMSC (74y, viral) (iMSC_aged) and iMSC (hESC H1) (iMSC_H1). Expressed genes common to all three samples were found to contain genes related to MSCs and MSC differentiation as well as MSC marker genes. Gene description see Table 24 and Table 25. (B) Venn diagram consisting of genes found to be expressed by microarray (detection p-value 0.01 and below) in grouped samples of fetal hMSCs, aged hMSCs and iMSCs. Sample groups: hMSC_fetal: grouped fetal hMSC 1, fetal hMSC 2 and fetal hMSC 3. hMSC_aged: grouped aged hMSC (60y), aged hMSC (62y), aged hMSC (70y), aged hMSC (74y). iMSCs: grouped iMSC (fetal, line 1, viral), iMSC (74y, viral) and iMSC (hESC H1). The genes expressed in the groups hMSC_fetal and iMSCs (red circle) were annotated using DAVID functional annotation tool. Results are shown in the table. A p-value of 0.05 and below was considered significant. The table shows the complete list of results.

To analyse the potential effect of donor age of parental hMSCs on the transcriptional features of corresponding iMSCs, microarray based gene expression profiling followed by extraction of genes differentially expressed between iMSC (fetal, line 1, viral) and iMSC (74y, viral) with a p-value below 0.01 was carried out. The differentially expressed genes which were up-regulated (1.5-fold higher average signal) or down-regulated (1.5-fold lower average signal) were analysed by functional annotation using the database DAVID. The functional annotation of up-regulated genes in iMSC (74y, viral) against iMSC (fetal, line 1, viral) resulted in an annotation to the KEGG terms Cell cycle (p-value: 8.34E-11, genes: e.g. *CDC7*, *E2F2*) to DNA replication (p-value: 4.72E-07, genes: e.g. *RFC3*, *MCM7*), P53 signalling pathway (p-value: 0.005, genes: e.g. *CCNE2*), Oocyte meiosis (p-value: 0.015, genes: e.g. *CCNE2*, *CCNB1*), Mismatch repair (p-value: 0.022, genes: e.g. *RFC5*, *EXO1*), Pentose phosphate pathway (p-value: 0.029, genes: e.g. *GPI*, *ALDOC*) and Pyrimidine metabolism (p-value: 0.036, genes: *POLR2H*, *POLR3G*). In contrast to that, functional annotation of down-regulated genes in iMSC (74y, viral) compared to iMSC (fetal, line 1, viral) resulted in an annotation to the KEGG terms Pathways in cancer, Focal adhesion, Lysosome, ECM-receptor interaction, Pancreatic cancer, Colorectal cancer, Bladder cancer, Small cell lung cancer and Regulation of actin cytoskeleton with a p-value below 0.01 and to the KEGG terms Chronic myeloid leukemia, Leukocyte trans-endothelial migration, Axon guidance, TGF-beta signalling pathway, Epithelial cell signalling in Helicobacter pylori infection, Complement and coagulation cascades, Neurotrophin signalling pathway, Other glycan degradation, Endocytosis, Glioma, Adherens junction, P53 signalling pathway and Glycosaminoglycan degradation with p-values between 0.01 and 0.05. The corresponding genes which or the respective annotations of the up and down-regulated genes are listed in Table 15.

Table 15 The effect of donor age of hMSCs on the transcriptional features of corresponding iMSCs.

Genes that were differentially expressed (p-value 0.01 and below) and were up-regulated (1.5-fold higher average signal) or down-regulated (1.5-fold lower average signal) in iMSC (74y, viral) compared to iMSC (fetal, line 1, viral) were annotated using the DAVID functional annotation database employing the option pathway and the category KEGG. A p-value of 0.05 and below was considered significant. Listed are the results with a p-value below 0.05. See following page. Table see next page.

up-regulated in iMSC (74y, viral) against iMSC (fetal, line 1, viral)			
Term	Count	PValue	Genes
hsa04110:Cell cycle	27	8.342E-11	CDC7, E2F2, LOC100133012, TGFB3, PRKDC, TTK, PKMYT1, CDC20, MCM2, PTTG1, MCM3, CDC25C, MCM4, MCM5, CDC25A, MCM6, CCNB1, CCNE2, CCNE1, MAD2L1, MCM7, CCND3, ORC6L, BUB1, BUB1B, CCNA2
hsa03030:DNA replication	12	4.721E-07	RFC5, RFC3, MCM7, RFC4, POLA2, MCM2, MCM3, RNASEH2A, MCM4, FEN1, MCM5, MCM6
hsa04115:p53 signaling pathway	10	4.544E-03	CCNE2, CCNB1, CCNE1, LOC100133012, CCNB2, CCND3, RRM2, CYCS, RPRM, GTSE1
hsa04114:Oocyte meiosis	12	1.488E-02	CCNE2, CCNB1, CCNE1, MAD2L1, CCNB2, BUB1, PKMYT1, CDC20, AURKA, PTTG1, CDC25C, ITPR1
hsa03430:Mismatch repair	5	2.169E-02	RFC5, EXO1, RFC3, RFC4, MSH3
hsa00030:Pentose phosphate pathway	5	2.878E-02	GPI, ALDOC, PGM1, PRPS2, PRPS1
hsa00240:Pyrimidine metabolism	10	3.585E-02	POLR2H, POLR3G, TYMS, POLR1E, RRM2, PNPT1, RRM1, CTPS2, POLA2, TK1
down-regulated in iMSC (74y, viral) against iMSC (fetal, line 1, viral)			
Term	Count	PValue	Genes
hsa05200:Pathways in cancer	47	8.308E-07	BID, WNT5B, MMP9, PPARG, NFKBIA, KITLG, GLI2, ITGB1, MMP2, MMP1, LOC407835, CDC42, FOS, CDKN2A, CDKN2B, RAC2, RAC3, RALB, NKX3-1, RARA, LAMB1, MYC, FN1, EGFR, AR, PLD1, EPAS1, IL8, KLK3, TGFBR2, PIK3CD, SMAD3, ITGA2, CDK6, ITGA3, FZD2, FZD4, RALGDS, COL4A6, FZD6, JUP, LAMA1, CCND1, ETS1, MAPK3, PDGFRB, LAMC2
hsa04510:Focal adhesion	31	2.328E-05	CAV1, BCAR1, ITGA11, PIP5K1C, ITGB1, MYL9, CDC42, RAC2, RAC3, COL6A3, PDGFC, SHC1, LAMB1, SHC3, THBS2, FN1, SPP1, EGFR, PIK3CD, ITGA1, ITGA2, ITGA3, COL5A2, COL4A6, LAMA1, CCND1, CCND2, MAPK3, COL1A2, PDGFRB, LAMC2
hsa04142:Lysosome	22	2.611E-05	TCIRG1, CTSZ, NAGLU, PLA2G15, HEXB, FUCA1, MANBA, GLB1, SLC11A2, ATP6V0C, GNS, LAMP2, CD68, AP1S1, TPP1, AP3M1, CTSO, GAA, CTSD, CTSH, IDUA, GBA
hsa04512:ECM-receptor interaction	16	3.972E-04	ITGA11, ITGA1, ITGA2, ITGA3, COL5A2, ITGB1, COL4A6, LAMA1, COL6A3, COL1A2, LAMC2, AGRN, LAMB1, THBS2, FN1, SPP1
hsa05212:Pancreatic cancer	14	8.622E-04	EGFR, CDC42, PLD1, CCND1, CDKN2A, RAC2, RAC3, TGFBR2, MAPK3, PIK3CD, RALB, SMAD3, CDK6, RALGDS
hsa05210:Colorectal cancer	15	1.255E-03	EGFR, PIK3CD, TGFBR2, SMAD3, FZD2, FZD4, RALGDS, FZD6, FOS, CCND1, RAC2, RAC3, MAPK3, PDGFRB, MYC
hsa05219:Bladder cancer	10	1.553E-03	EGFR, LOC407835, CCND1, CDKN2A, IL8, MMP9, MAPK3, MYC, MMP2, MMP1
hsa05222:Small cell lung cancer	14	3.656E-03	PIK3CD, NFKBIA, ITGA2, CDK6, ITGA3, ITGB1, COL4A6, LAMA1, CCND1, CDKN2B, LAMC2, LAMB1, MYC, FN1
hsa04810:Regulation of actin cytoskeleton	25	9.071E-03	GNA13, EGFR, FGD1, SSH1, BAIAP2, BCAR1, PIK3CD, ITGA1, ITGA11, PIP5K1C, ITGA2, ITGA3, ITGB1, MYL9, LOC407835, CDC42, PFN2, RAC2, RAC3, MAPK3, RRAS, PDGFRB, PDGFC, FN1, F2R
hsa05220:Chronic myeloid leukemia	12	1.085E-02	LOC407835, CCND1, CDKN2A, MAPK3, PIK3CD, TGFBR2, SMAD3, NFKBIA, CDK6, SHC1, SHC3, MYC
hsa04670:Leukocyte transendothelial migration	16	1.203E-02	F11R, ICAM1, GNAI2, MMP9, BCAR1, PIK3CD, MMP2, CXCL12, ITGB1, MYL9, VCAM1, CDC42, CYBA, RAC2, CLDN1, JAM2
hsa04360:Axon guidance	17	1.211E-02	ABLIM1, GNAI2, ABLIM3, DPYSL2, CXCL12, ITGB1, SLIT2, EPHA2, EPHB2, SEMA5A, CDC42, UNC5B, RAC2, RAC3, MAPK3, SEMA3C, SEMA3A
hsa04350:TGF-beta signaling pathway	13	1.283E-02	PPP2R1A, ACVRL1, SMAD7, TGFBR2, GDF5, FST, SMAD3, DCN, ID2, CDKN2B, MAPK3, MYC, THBS2
hsa05120:Epithelial cell signaling in Helicobacter pylori	11	1.457E-02	EGFR, ATP6V0C, CXCL1, TCIRG1, F11R, CDC42, IL8, NFKBIA, HBEGF, ATP6V1G1, JAM2
hsa04610:Complement and coagulation cascades	11	1.605E-02	PLAT, LOC653879, CFB, SERPINE1, CFH, TFPI, C1S, PROS1, PLAU, F2R, PLAUR
hsa04722:Neurotrophin signaling pathway	16	1.840E-02	IRAK2, PIK3CD, NFKBIA, IRS1, MAGED1, LOC407835, CDC42, BDNF, PRDM4, MAPK3, SH2B3, SHC1, MAPK7, SHC3, ARHGDIA, ARHGDIB
hsa00511:Other glycan degradation	5	1.917E-02	HEXB, FUCA1, MANBA, GLB1, GBA
hsa04144:Endocytosis	21	2.148E-02	EGFR, FAM125B, PLD1, CHMP4B, RAB5C, TGFBR2, PSD3, ASAP2, ASAP1, PIP5K1C, CDC42, AP2B1, ADRB2, NEDD4, SH3KBP1, NEDD4L, PARD6G, ARAP3, EHD3, F2R, RNF41
hsa05214:Glioma	10	2.379E-02	EGFR, LOC407835, CCND1, CDKN2A, MAPK3, PIK3CD, PDGFRB, CDK6, SHC1, SHC3
hsa04520:Adherens junction	11	3.226E-02	EGFR, CDC42, CSNK2A1, RAC2, PTPRF, WASF3, RAC3, BAIAP2, MAPK3, TGFBR2, SMAD3
hsa04115:p53 signaling pathway	10	3.697E-02	BID, CCND1, CDKN2A, TNFRSF10B, CCND2, ZMAT3, CD82, SERPINE1, CDK6, IGFBP3
hsa00531:Glycosaminoglycan degradation	5	4.840E-02	GNS, NAGLU, HEXB, GLB1, IDUA

Having analysed the differences between iMSCs of fetal and aged background, further gene expression analysis was carried out to extract a list of genes, which show rejuvenated expression patterns. To do this, genes which were not expressed in all hMSC samples (detection p-value of 0.01 and above) and which were expressed in all iPSCs (detection p-value 0.001 and below) and in iMSCs derived from hMSC-iPSCs of fetal and aged background (detection p-value 0.001 and below) were extracted. The gene list was annotated to biological processes and gene ontologies using the DAVID database. The results of the functional annotation analysis are listed in Table 16. The rejuvenated genes were annotated to the KEGG term TGF-beta signalling pathway however with a p-value below 0.05. Moreover, the genes with a rejuvenated expression pattern were annotated to the gene ontologies neuron recognition, regulation of cell-substrate adhesion, negative regulation of cell proliferation, regulation of cyclin-dependent protein kinase activity, cell recognition, cell adhesion and biological adhesion with a p-value below 0.05 (Table 16).

Table 16 Functional annotation of rejuvenated gene expression signatures in iMSCs.
Genes which were not expressed in all hMSC samples (detection p-value of 0.01 and above) and which were expressed in all iPSCs (detection p-value 0.001 and below) and in iMSCs derived from hMSC-iPSCs of fetal and aged background (detection p-value 0.001 and below) were extracted. The gene list was annotated to biological processes and gene ontologies using DAVID database. A p-value of 0.05 and below was considered significant however the complete results are listed.

processes with rejuvenated gene expression signature			
Term	**Count**	**PValue**	**Genes**
hsa04350:TGF-beta signaling pathway	3	0.067	LTBP1, ACVRL1, INHBE
GO:0008038~neuron recognition	3	0.004	BDNF, EFNB3, NTM
GO:0010810~regulation of cell-substrate adhesion	3	0.017	ACVRL1, EDIL3, EMILIN1
GO:0008285~negative regulation of cell proliferation	6	0.020	CDKN1C, BDNF, ACVRL1, CDKN2C, CXADR, GAL
GO:0000079~regulation of cyclin-dependent protein kinase activity	3	0.023	CDKN1C, CDKN2C, HERC5
GO:0008037~cell recognition	3	0.024	BDNF, EFNB3, NTM
GO:0007155~cell adhesion	8	0.032	ISLR, HAPLN1, PCDHB2, IL32, EDIL3, CXADR, NTM, EMILIN1
GO:0022610~biological adhesion	8	0.032	ISLR, HAPLN1, PCDHB2, IL32, EDIL3, CXADR, NTM, EMILIN1
GO:0007186~G-protein coupled receptor protein signaling pathway	10	0.053	AGTR1, KIAA1324L, ENPP2, CXCR7, ELTD1, MRGPRF, GPR68, GAL, D4S234E, KCNK2
GO:0007166~cell surface receptor linked signal transduction	14	0.054	AGTR1, KIAA1324L, ACVRL1, EFNB3, HEY1, ENPP2, CXCR7, DLL3, ELTD1, MRGPRF, GPR68, D4S234E, GAL, KCNK2
GO:0042127~regulation of cell proliferation	8	0.054	CDKN1C, AGTR1, BDNF, ACVRL1, CDKN2C, HCLS1, CXADR, GAL
GO:0045597~positive regulation of cell differentiation	4	0.078	AGTR1, BDNF, DLL3, DNMT3B
GO:0006024~glycosaminoglycan biosynthetic process	2	0.088	GCNT2, XYLT1
GO:0006790~sulfur metabolic process	3	0.090	SULF2, ALDH5A1, DNMT3B
GO:0006023~aminoglycan biosynthetic process	2	0.096	GCNT2, XYLT1
GO:0045666~positive regulation of neuron differentiation	2	0.100	BDNF, DNMT3B

Subsequently, the effect of age of the parental hMSC and of hESCs as parental pluripotent cell line on senescence-related gene expression in iMSCs generated from hMSC-iPSCs and generated from hESC H1 were analysed by comparing gene expression patterns in the respective transcriptomes, which were

detected using microarray. First, a hierarchical clustering analysis of genes annotated to the GO-term regulation of senescence base on the Euclidean distance of the average signal of the genes was carried out comparing fetal hMSCs, hMSCs of aged donors, iMSCs and hESC H1. The clustering analysis revealed a high similarity between the samples aged hMSC (60y) and aged hMSC (70y) which formed a cluster separated from iMSCs, hESC h1 fetal hMSCs, aged hMSC (62y) and aged hMSC (74y) who in turn formed a similarity cluster. Within this cluster aged hMSC (62y), aged hMSC (74y) and iMSC (74y, viral) were most similar and formed a cluster which separates these samples from a cluster consisting of iMSC (fetal, line 1, viral), iMSC (hESC H1), fetal hMSC 1 and fetal hMSC 2. These two clusters were separated from hESC H1 which was more similar to the samples within the two clusters than to aged hMSC (60y) and aged hMSC (70y) (Figure 38 A). A statistical test was used in addition to find genes of the GO-term regulation of senescence, which were differentially regulated comparing iMSCs and fetal hMSC 1. In addition, *CDK6*, *VASH1* and *ZNF277* were down-regulated in iMSC (fetal, line 1, viral) and *NUAK1* was detected to be up-regulated compared to fetal hMSC 1. Finally, *TWIST1* was down-regulated in iMSC (74y, viral) while *NEK6*, *CDK6* and *NUAK1* were detected as up-regulated. Subsequently, a hierarchical clustering analysis based on a gene set annotated to the GO-term senescence and on the log 2 ratio of the average signal in iMSC (fetal, line 1, viral), iMSC (74y, viral) and the corresponding hMSCs over the average signal in hESC H1 was carried out. The Pearson correlation-based clustering revealed that aged hMSC (74y) and iMSC (74y, viral) were the most similar samples which in turn were more similar to iMSC (fetal, line 1, viral) than to the fetal hMSC 1 (Figure 38 B). In order to elucidate the differences in gene expression of senescence-related genes in aged hMSC (74y) and iMSC (74y, viral) compared to the corresponding iPS cell line named iPSC (hMSC, 74y, viral) and to analyse whether iMSC (74y, viral) share a similar expression pattern of senescence-related genes with fetal hMSC 1, the ratio of the expression levels in hMSCs and iMSCs over iPSC (hMSC, 74y, viral) was plotted. The fold changes are depicted in Figure 38 C showing the genes which were differentially expressed between fetal hMSC 1 and iPSC (hMSC, 74y, viral) and additionally were up-regulated (1.5-fold higher average signal) or down-regulated (average signal lower than 1.5-fold) in fetal hMSC 1 compared to iPSC (hMSC 74y viral). The respective ratios of hMSC (74y) and iMSC (74y viral) over iPSC (hMSC 74y viral) were plotted for comparison. The genes, which are differentially expressed in all samples but have a difference in regulation, were *CREG* which was significantly down-regulated in fetal hMSC 1 but up-regulated in aged hMSC (74y) and iMSC (74y viral). Moreover, *CDK6* was significantly down-regulated in aged hMSC (74y) but up-regulated in fetal hMSC 1 and iMSC (74y viral) and *ALDH1A3* was significantly up-regulated in both hMSC samples but down-regulated in iMSC (74y viral). Plotting of the ratios of gene expression signals revealed that *IGFBP5* is the most down-regulated senescence-associated gene in fetal hMSC 1 compared to iPSC (hMSC, 74y, viral) whereas *EGR1* is the most up-regulated gene. In addition, genes

with a higher expression ratio in fetal hMSC 1 than in aged hMSC (74y) and iMSC (74y viral) were *ID1*, *ETS2*, *TBX2* and *EGR1* (Figure 38 C).

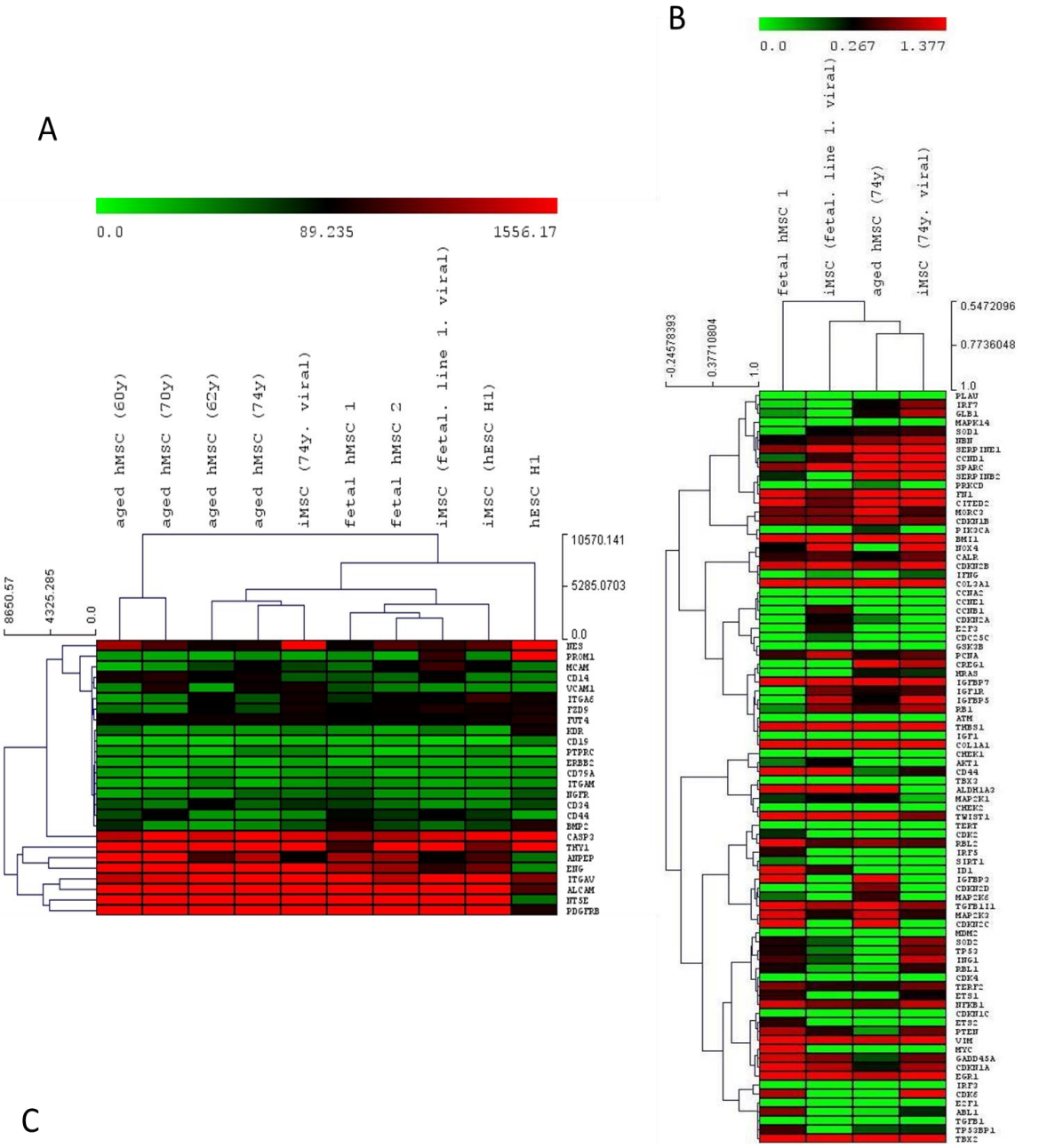

Figure 38 Effect of hMSC donor age on senescence-related gene expression in generated iMSCs. (A) Hierarchical clustering analysis of gene expression related to regulation of senescence in fetal hMSCs, hMSCs of aged donors, iMSCs and hESC H1. Heat map based on average signal detected using an Illumina Bead Chip microarray. Hierarchical clustering analysis based on Euclidean distance. Gene description see Table 26. (B) Hierarchical clustering analysis of senescence-related gene expression in fetal hMSC 1 and aged hMSC (74y) and corresponding iMSCs compared to hESC H1. Heat map based on log 2 ratio of average signal in hMSCs or iMSCs over the average signal in hESC H1. Hierarchical clustering analysis based on Pearson correlation. Gene description see Table 19. (C) Expression of senescence-related genes comparing fetal hMSC 1, aged hMSC (74y) and iMSC (74y viral) to iPSC (hMSC 74y viral). Bars represent log 2 ratios of the average signals. Depicted are genes that are differentially expressed (p-value 0.01 and below) between fetal hMSC 1 and iPSC (hMSC 74y viral) and are up-regulated (1.5-fold higher average signal) or down-regulated (average signal lower than 1.5-fold) in fetal hMSC 1 compared to iPSC (hMSC 74y viral). The respective ratios of hMSC (74y) and iMSC (74y viral) and iPSC (hMSC 74y viral) are shown for comparison.

Furthermore, to analyse the effect of hMSC age on gene expression related to ageing-associated processes in generated iMSCs, hierarchical clustering analyses were carried out comparing the similarity between the samples based on gene sets annotated to the GO-terms DNA damage repair, ageing, ageing and response to oxidative stress. The hierarchical clustering analysis based on the Euclidean distance of the average signal of genes related to DNA damage repair revealed that aged hMSCs were most similar to each other and formed a cluster that separated them from fetal hMSCs and iMSCs. Likewise, fetal hMSCs and iMSCs formed a similarity cluster that separated these samples from all aged hMSC samples. Within the cluster consisting of iMSCs and fetal hMSCs, iMSC (fetal, line 1, viral) showed the lowest similarity to fetal hMSCs (Figure 39).

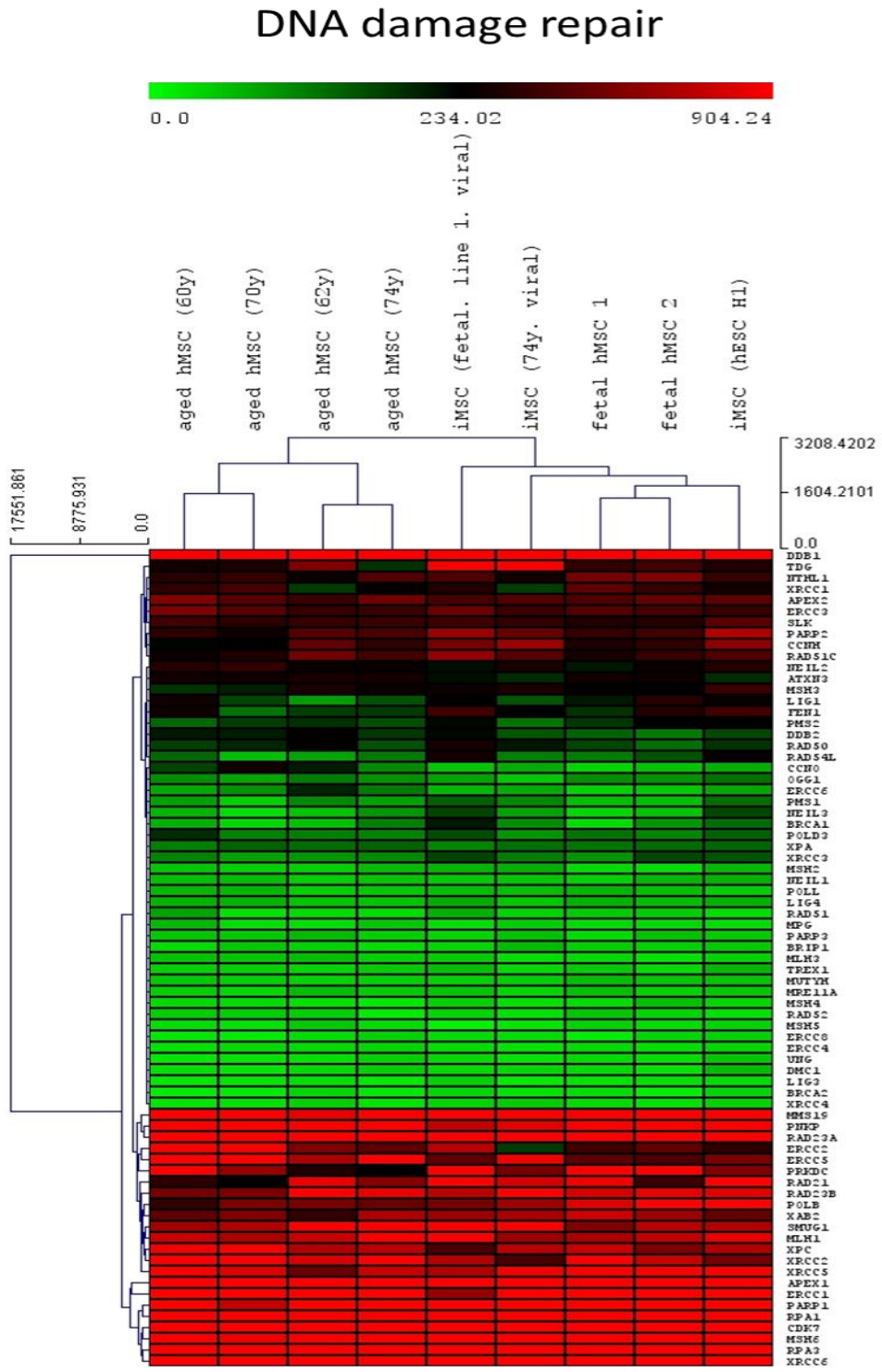

Figure 39 Effect of biological age of hMSCs on the gene expression related to DNA-damage repair in generated iMSCs.

Hierarchical clustering analysis showing similarities in gene expression related to DNA damage repair comparing hMSCs and iMSCs of fetal and aged genetic background. Heat map based on average signal detected using microarray-based gene expression profiling. Hierarchical clustering analysis based on Euclidean distance. Gene description see Table 27.

Moreover, the hierarchical clustering analysis based on the Pearson correlation of the average signal of genes related to ageing separated the samples into distinct similarity clusters. Aged hMSC (62y) and aged hMSC (74y) formed a cluster which showed the lowest similarity to all other samples followed by iMSC (fetal, line 1, viral), which formed a cluster with all samples except aged hMSC (62y) and aged hMSC (74y) but showed the lowest similarity to the samples in this cluster. Furthermore, iMSC (74y, viral) and iMSC (hESC H1) formed a cluster with fetal hMSC 1 and 2, which shared a low similarity to all other samples but the highest similarity to aged hMSC (60y) and aged hMSC (70y) (Figure 40). Subsequently, analysis of microarray data was carried out comparing fetal hMSC 1, iMSC (fetal, line 1, viral), iMSC (74y, viral) and iMSC (hESC H1) to aged hMSC (74y) towards differentially expressed genes related to ageing. The test revealed the significant down-regulation of *TSPO* in all iMSC samples and fetal hMSC 1. Furthermore, the genes *ATM* and *FADS1* were up-regulated in fetal hMSC 1 and iMSC (74y, viral) but not in the other iMSC samples. Finally, *RSL1D1* was up-regulated in fetal hMSC 1 and the corresponding iMSCs. A further hierarchical clustering analysis was carried out to compare the similarities of gene expression patterns of genes related to response to oxidative stress based on the Pearson correlation of the average signals between the samples comparing fetal hMSCs, hMSCs of elderly donors, iMSCs and hESC H1. Interestingly, all samples shared a low similarity to hESC H1 and formed a cluster. Within this cluster aged hMSC (74y) and iMSC (74y, viral) were most similar to each other but not to all other samples of the cluster. In addition, iMSC (fetal, line 1, viral) and iMSC (hESC H1) were most similar to fetal hMSC 2 and formed a cluster which was most similar to a cluster of the samples fetal hMSC 1, aged hMSC (60y), aged hMSC (62y) and aged hMSC (70y) (Figure 41). A statistical test toward differential expression compared to hESC H1 revealed the significant more than 1.5-fold down-regulation of *DUSP1*, *MSRB3*, *PTGS1*, *OXR1*, *PDLIM1*, *RCAN1*, *SRXN1* and *GPX8* in iMSC (fetal, line 1, viral), iMSC (74y, viral), iMSC (hESC H1) and fetal hMSC 1 compared to hESC H1. However, the gene *PDLIM1* was down-regulated with a p-value below 0.01.

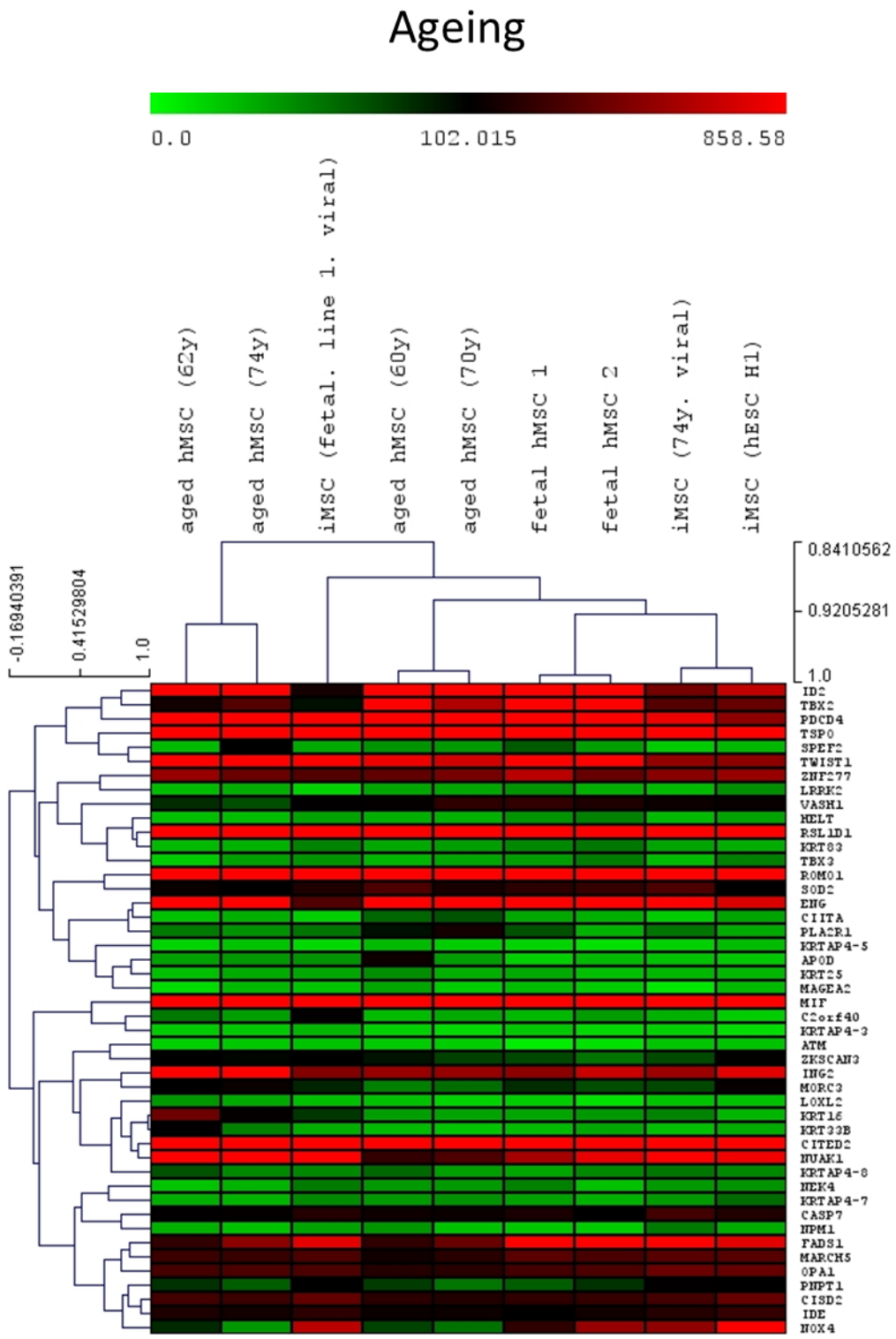

Figure 40 Effect of biological age of hMSCs on the gene expression annotated to ageing and to response to oxidative stress in generated iMSCs.

Hierarchical clustering analysis of gene expression related to ageing comparing hMSCs and iMSCs of fetal and aged genetic background. Heat map based on average signal detected by microarray. Hierarchical clustering analysis based on Pearson correlation. Gene description see Table 22.

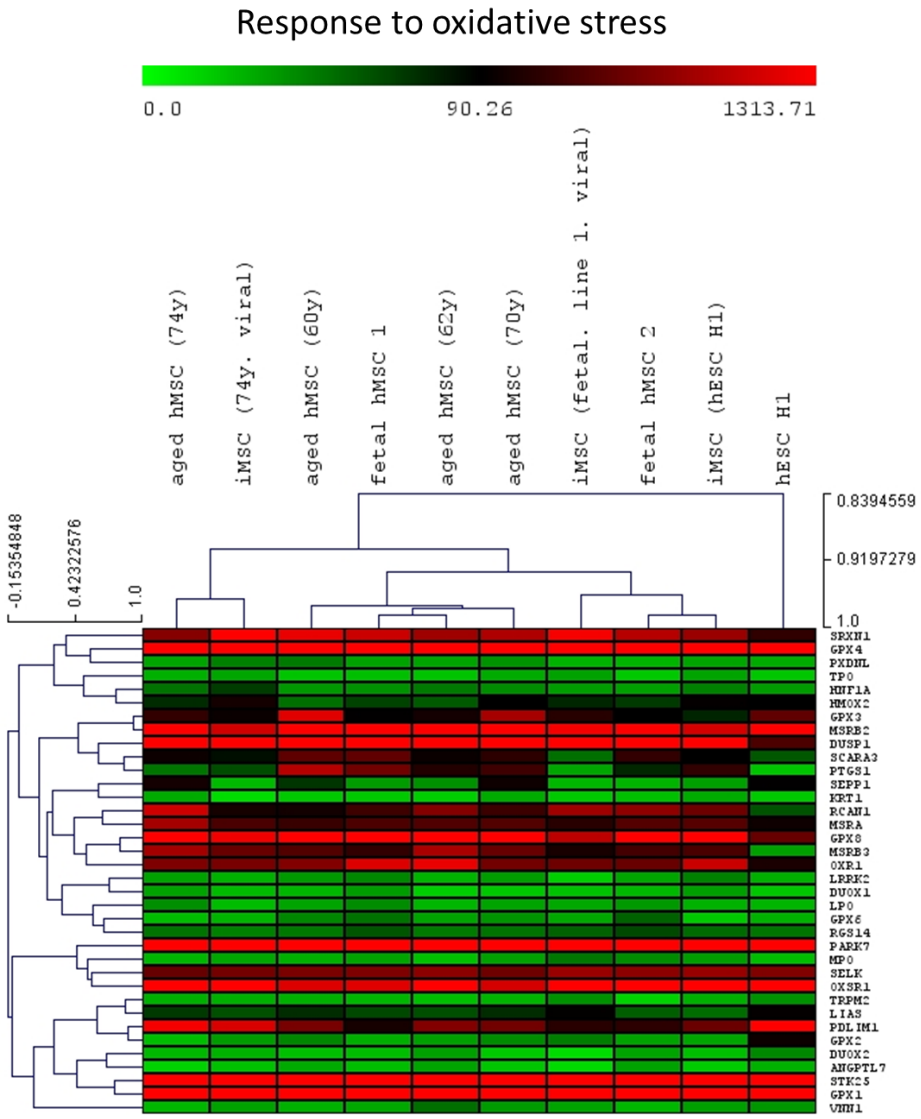

Figure 41 Effect of biological age of hMSCs on the gene expression annotated to response to oxidative stress in generated iMSCs.

Hierarchical clustering analysis based on genes related to the response to oxidative stress comparing fetal hMSCs, hMSCs of elderly donors, iMSCs and hESC H1. Heat map based on average signal measured by microarray gene expression profiling. The hierarchical clustering analysis was based on the Pearson correlation between the samples and genes. Gene description see Table 20.

To follow the notions that the expression patterns of ageing-related genes associated with the metabolic stability theory of ageing and the michondrial oxidative stress pathway (Brink et al. 2009, Prigione et al. 2010) in iMSCs are influenced by the biological age of parental hMSCs, hierarchical clustering analyses based on gene expression measured by microarray were carried out. Doing this, iMSCs were compared to hMSCs, iPSCs and hESCs. A hierarchical clustering analysis based on a gene list of the GO-term oxidative phosphorylation revealed, that a similarity cluster consisting of

fetal hMSC 1, fetal hMSC 2, aged hMSC (60y) and aged hMSC (70y) shared the least similarities with all other samples, whereas the samples were more similar to each other. Yet, the other samples formed one cluster in which iPSC (hMSC, fetal, line 1, viral) was least similar to all other samples that in turn formed three separate clusters. One cluster of these clusters consisted of iPSC (hMSC, fetal, line 1, episomal 1), iPSC (hMSC, fetal, line 1, episomal 2) and iPSC (hMSC, 74y, viral), a second cluster consisted of iPSC (hMSC, 62y, episomal), hESC H1 and iMSC (fetal, line 1, viral) and a third cluster consisted of aged hMSC (62y), aged hMSC (74y), iMSC (74y, viral) and iMSC (hESC H1) (Figure 42).

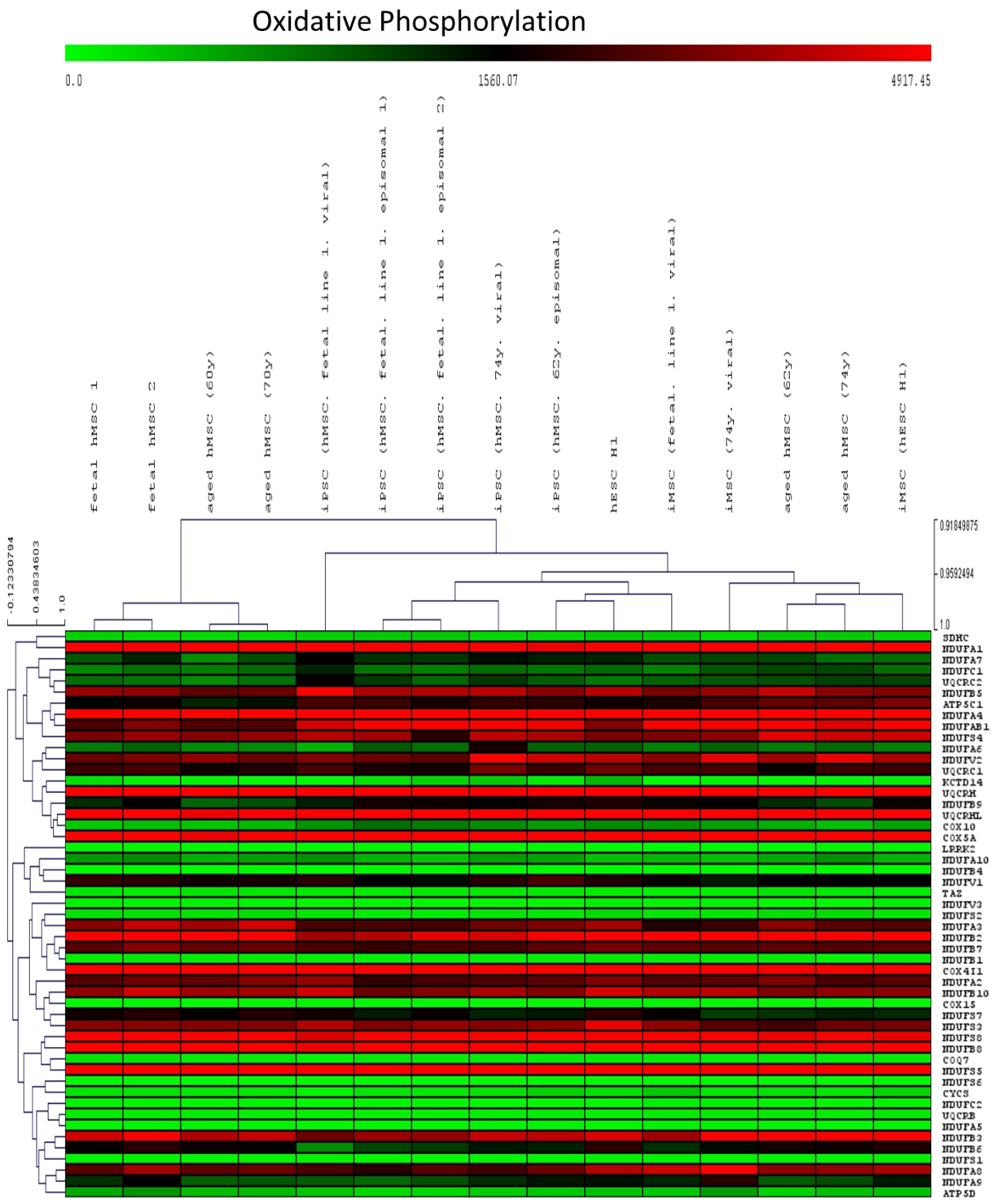

Figure 42 Effect of biological age of hMSCs on the gene expression related to oxidative phosphorylation in generated iMSCs compared hMSC-iPSCs and hMSCs.

Hierarchical clustering analysis showing similarities in gene expression related to oxidative phosphorylation comparing iMSCs of fetal and aged genetic background and derived from hESC H1 to hMSCs of different biological age, iPSCs and hESC H1. Heat map based on average signal detected using microarray-based gene expression profiling. Hierarchical clustering analysis based on Pearson correlation. Gene description Table 28.

In addition, a hierarchical clustering analysis based on genes of the GO-term glutathione metabolism was carried out. The experiment revealed two similarity clusters based on Pearson correlation between the samples. One cluster mainly consisted of all hMSC-iPSCs and hESC H1 as well as of iMSC (fetal, line 1, viral) and iMSC (74y, viral). The second cluster consisted of fetal hMSCs, aged hMSCs and iMSC (hESC H1), which was most similar to aged hMSC (62y) (Figure 43).

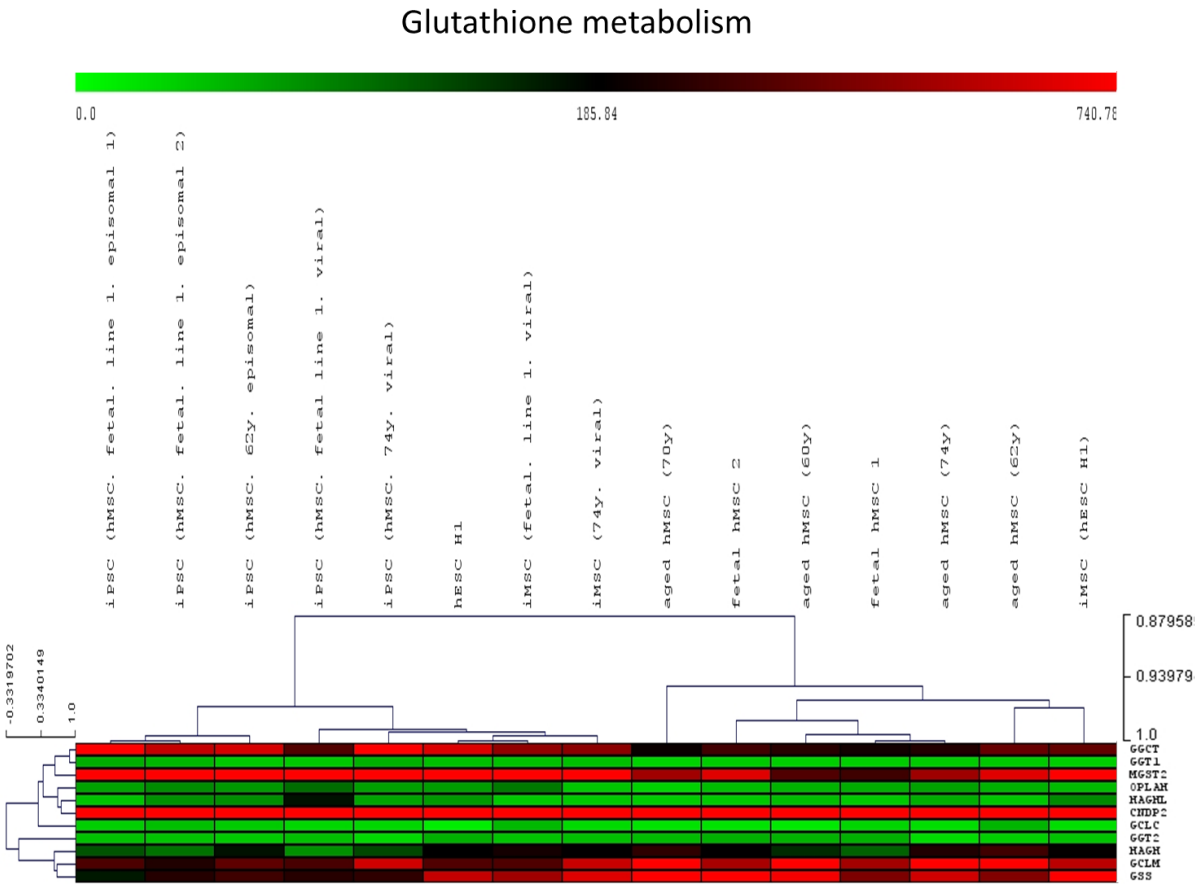

Figure 43 Effect of biological age of hMSCs on the gene expression related to glutathione metabolism in generated iMSCs compared hMSC-iPSCs and hMSCs.
Hierarchical clustering analysis showing similarities in gene expression related to glutathione metabolism comparing iMSCs of fetal and aged genetic background to hMSCs of different biological age, iPSCs and hESC H1. Heat map based on average signal detected using microarray-based gene expression profiling. Hierarchical clustering analysis based on Pearson correlation. Gene description see Table 29.

To further analyse the effect of biological age of parental hMSCs on processes related to the metabolic stability theory of ageing, hierarchical clustering analyses based on genes of the GO-terms glycolysis and insulin signalling were carried out. The hierarchical clustering analysis based on the genes

associated with glycolysis showed the lowest similarity between iPSC (hMSC, fetal, line 1, viral) and all other samples, which in turn formed two clusters. One of these clusters consisted of hMSCs of fetal and aged background as well as of iMSC (74y, viral), which in turn formed a cluster with aged hMSC (70y) and aged hMSC (74y). The second cluster consisted of hMSC-iPSCs, hESCs, iMSC (fetal, line 1, viral) and iMSC (hESC H1). Interestingly, iMSC (fetal, line 1, viral) and iMSC (hESC H1) formed a similarity cluster with iPSC (hMSC, fetal, line 1, episomal 2) and iPSC (hMSC, 62y) (Figure 44).

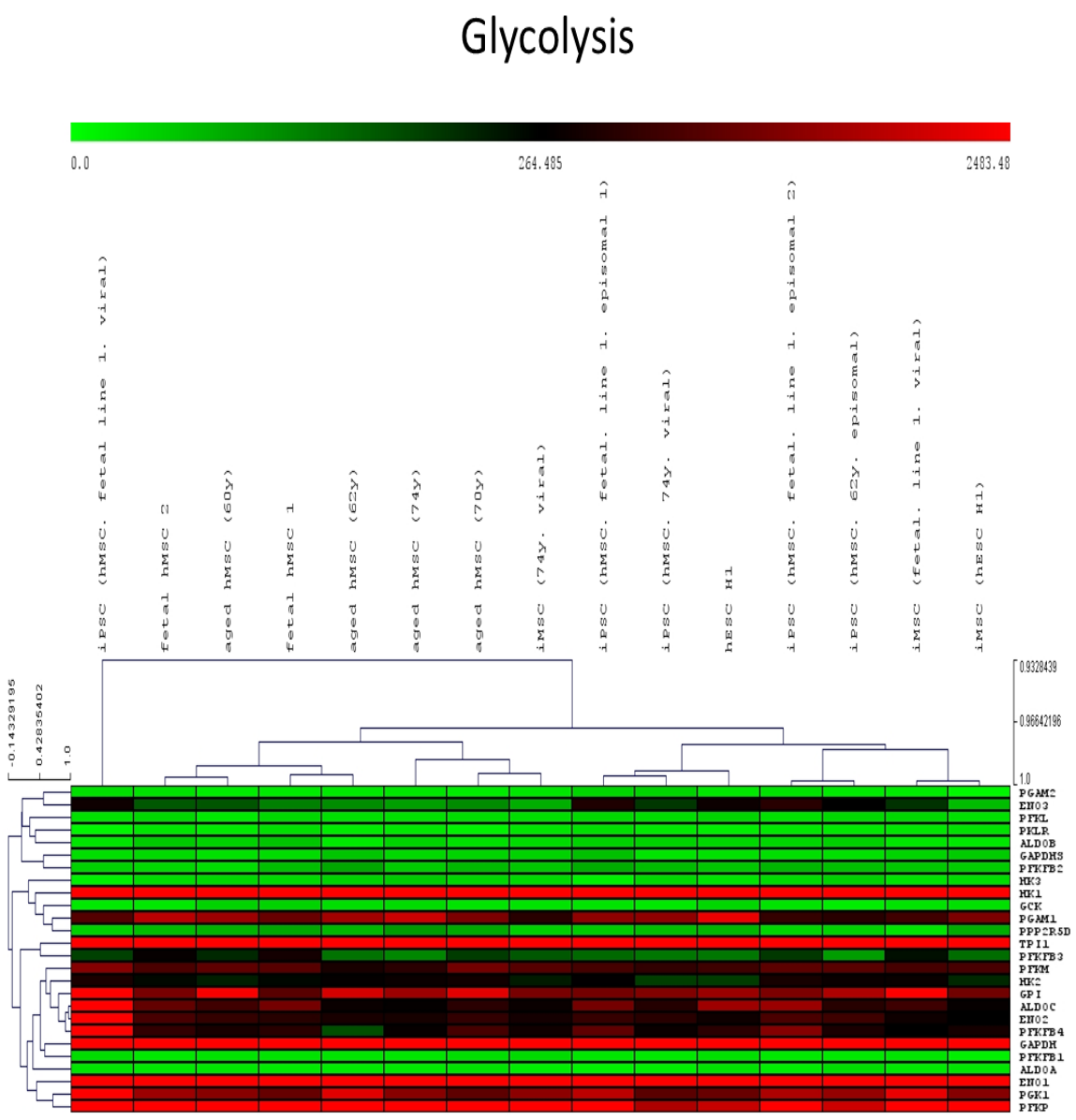

Figure 44 Effect of biological age of hMSCs on the gene expression related to glycolysis in generated iMSCs compared hMSC-iPSCs and hMSCs.

Hierarchical clustering analysis showing similarities in gene expression related to glycolysis comparing iMSCs of fetal and aged genetic background to hMSCs of different biological age, iPSCs and hESC H1. Heat map based on average signal detected using microarray-based gene

expression profiling. Hierarchical clustering analysis based on Pearson correlation. Gene description see Table 30.

A further hierarchical clustering analysis was performed to find the differences and similarities between iMSCs, iPSCs, hESC H1 and hMSCs of genes related to the GO-term insulin signalling. analysis revealed a high similarity between all iPSC samples except iPSC (hMSC, 74y, viral) and hESC H1 that were part of a separate cluster additionally consisting of hMSCs and iMSCs. cluster iMSC (fetal, line 1, viral) was detected to be the least similar sample compared to all samples of the cluster. In contrast to that, iMSC (hESC H1) showed the highest similarity to hMSC (74y) and formed a cluster with iPSC (hMSC, 74y, viral) and hESC H1 and fetal hMSC 1 fetal hMSC 2 which in turn formed a similarity cluster themselves. Moreover, iMSC (74y, viral) showed the highest similarity to aged hMSC (62y) (
Figure 45).

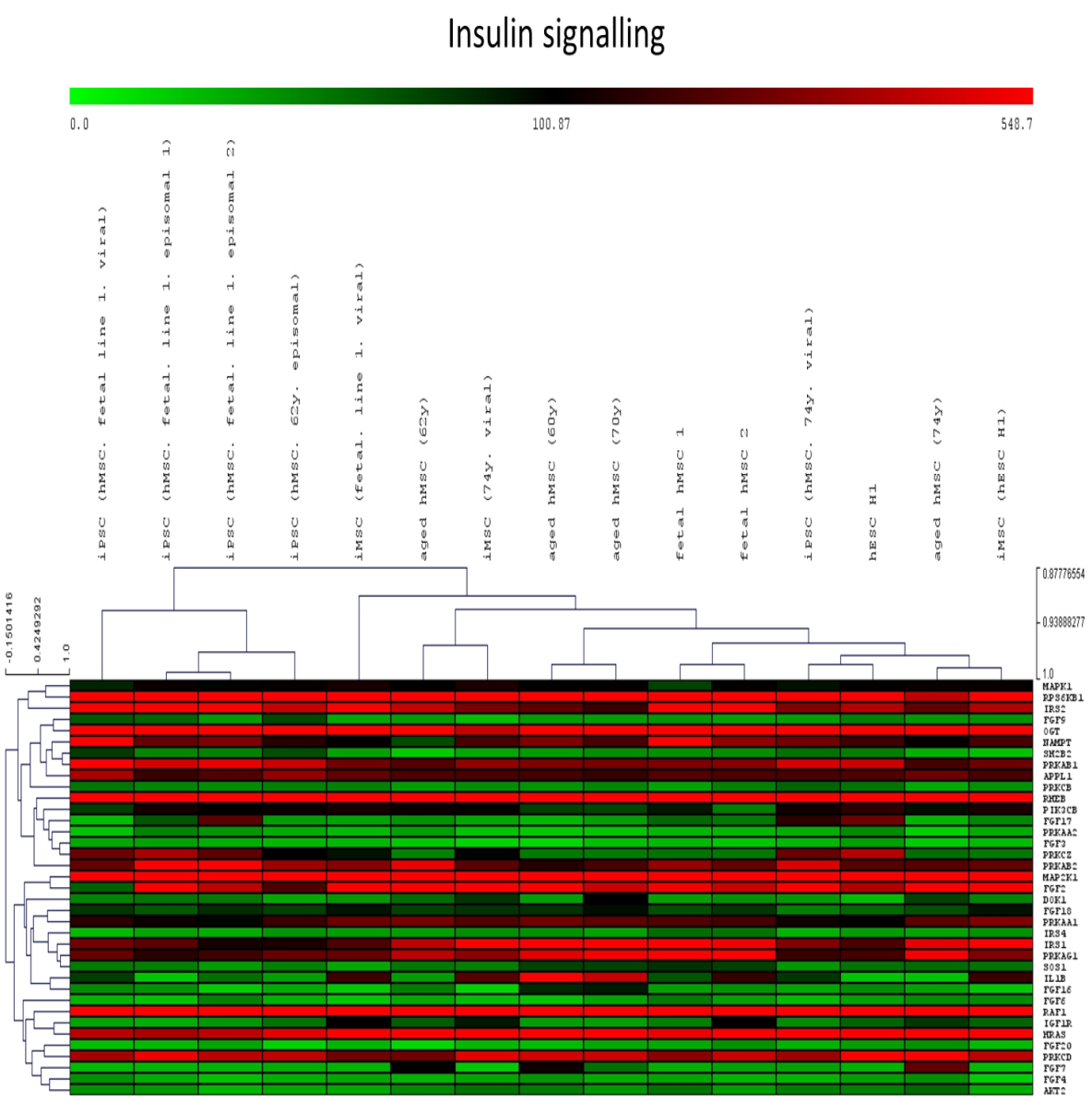

Figure 45 Effect of biological age of hMSCs on the gene expression related to insulin signalling in generated iMSCs compared hMSC-iPSCs and hMSCs.

Hierarchical clustering analysis showing similarities in gene expression related to insulin signalling comparing iMSCs of fetal and aged genetic background to hMSCs of different biological age, iPSCs and hESC H1. Heat map based on average signal detected using microarray-based gene expression profiling. Hierarchical clustering analysis based on Pearson correlation. Gene description Table 31.

In order to elucidate the potential residual gene expression patterns related to the metabolic instability theory of ageing (Brink et al. 2009) in iMSCs significantly up-and down-regulated genes of gene lists based on the GO-terms oxidative phosphorylation, TCA cycle, glycolysis, glutathione metabolism and insulin signalling that are differentially expressed in iMSC (merged samples of iMSC (fetal, line 1,

viral), iMSC (74y, viral) and iMSC (hESC H1)) against aged hMSCs (merged samples of aged hMSC (60y), aged hMSC (62y), aged hMSC (70y) and aged hMSC (74y)) were extracted from raw microarray data detected with an Illumina Bead Chip system. Through this analysis, genes related to glutathione metabolism were detected to be differentially expressed. More specifically, *GCLM* was down-regulated and *MGST2* was up-regulated. In addition, *PGAM1*, a gene involved in glycolysis was found to be down-regulated (Figure 46 A). Moreover, the expression of genes that are known to be regulated with age in human fibroblasts according to a recent study (Hashizume et al. 2015) was analysed in iMSCs compared to hMSCs of fetal and aged origin and corresponding iPSCs as well as hESC H1. Plotting of the genes revealed that higher expression levels of the gene *COX7A1* in aged hMSCs is down-regulated in the corresponding iPS cells and iMSCs. The genes *MRPL28*, *CAPRIN2*, *GCAT*, *EHHADH*, *ALDH5A1* and *SHMT2*, did not show ageing–related regulation or modulation upon pluripotency induction or redifferentiation. (Figure 46 B).

A

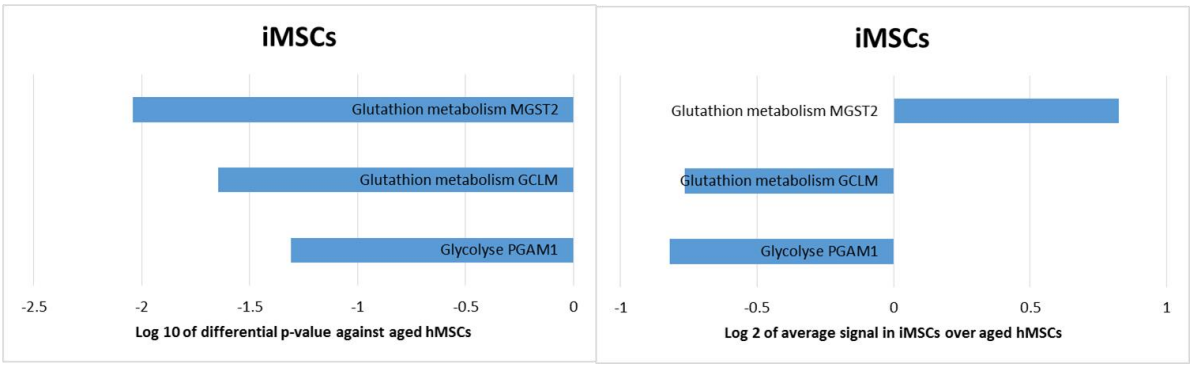

B

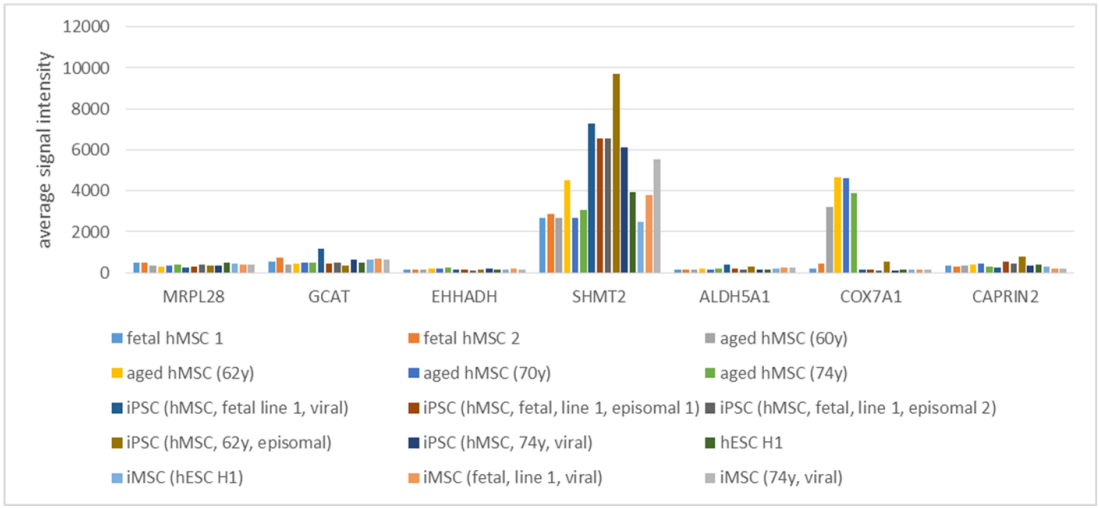

Figure 46 Expression patterns of genes with implications in the metabolic stability theory of ageing and known to be regulated with age in iMSCs.

(A) Genes of gene lists based on the GO-terms oxidative phosphorylation, TCA cycle, glycolysis, glutathione metabolism and insulin signalling that were differentially expressed in iMSC (merged samples of iMSC (fetal, line 1, viral), iMSC (74y, viral) and iMSC (hESC H1)) against aged hMSCs (merged samples of aged hMSC (60y), aged hMSC (62y), aged hMSC (70y) and aged hMSC (74y)). Left: log 10 of the differential p-values below 0.01 calculated by GenomeStudio of differentially expressed genes in iMSCs compared to aged hMSCs. Right: log 2 of the ratios of the average signals in iMSCs over aged hMSCs of the differentially expressed genes sorted according to the differential p-value. Gene expression was measured using an Illumina Bead Chip. (B) Hierarchical clustering analysis based on the Pearson correlation of the average signals of expression of genes described to be regulated with age in a recent study (Hashizume et al. 2015). Compared were iMSCs to hMSCs of fetal and aged origin, hMSC-iPSCs and hESC H1. Gene expression was measured using an Illumina Bead Chip.

4 Discussion

4.1 Characterisation of primary hMSCs and iPS-derived iMSCs

In the first step of this work, hMSCs derived from fetal and aged backgrounds were analysed towards fulfilment of the criteria for mesenchymal stem cells set by the International Society for Cellular Therapy (Dominici et al. 2006). Doing this, the fibroblast-like morphology and the expression of MSC surface markers CD90, CD73 and CD105 as well as the absence of hematopoietic markers could be confirmed by FACS and microarray proving the cell type identity of the hMSCs used in this study (Figure 4 A-C). However, the marker set of MSCs is still under debate (Lv et al. 2014). Moreover, the multipotency of hMSCs used in this study could be confirmed by the differentiation experiments and subsequent staining and quantification of marker gene expression and microarray based gene expression analysis (Figure 5 A-E). This is in line with the minimal criteria required for MSCs (Dominici et al. 2006). Yet, variation in trilineage differentiation between fetal and aged hMSCs might be due to an age-related shift from osteogenic to adipogenic potential described in a recent study (Kim et al. 2012).

In addition, iPSC (hMSC, fetal, line 1, viral), iPSC (hMSC, 74y, viral), iPSC (hMSC, fetal, line 1, episomal 1) and hESC H1 could successfully be differentiated into mesenchymal stem cell-like (iMSCs) using a previously described protocol (Yen Shun Chen et al. 2012). The generated showed MSC surface marker expression and trilineage differentiation (

Figure 34 A-C). These results are in line with the study applying the same protocol on fibroblast-derived iPS cells (Yen Shun Chen et al. 2012). Interestingly, osteogenic differentiation propensity seemed to be retained in iMSCs derived from hMSC-iPSCs compared to iMSC (hESC H1). Furthermore, adipocyte differentiation seemed to be less efficient or even impaired in comparison to the adipocyte differentiation of the parental hMSCs. Moreover, chondrocyte differentiation seemed to be impaired in iMSCs derived from fetal hMSC-iPSCs (

Figure 34 A). The possibility to derive mesenchymal stem cell-like cells from pluripotent cells was described in numerous studies (Barberi et al. 2005, Yen Shun Chen et al. 2012, Diederichs and Tuan 2014, Frobel et al. 2014, Hong et al. 2015, Ishiy et al. 2015, Kimbrel et al. 2014, Raynaud et al. 2013, Wang et al. 2014). One of these studies described variations in trilineage differentiation capacity of iMSCs, which is in line with our results (Diederichs and Tuan 2014). A further study described reduced adipogenesis but retention of osteogenic and adipogeneic differentiation potential in iMSCs (Kang et al. 2015), which is in line with the results of this study.

4.2 Negative effect of donor age on reprogramming efficiency

Reprogramming using retroviruses was more efficient than episomal plasmid-based reprogramming when pluripotency was induced in fetal hMSCs under normoxic conditions. Furthermore, hypoxic conditions enhanced the efficiency of viral and non-viral reprogramming efficiency in fetal hMSCs. Moreover, the combination of mTeSR 1 addition at day 14 and hypoxia enhanced the reprogramming efficiency of fetal hMSCs to 0.06% (Table 12). This is in line with a previously published report describing the same effect in fibroblasts (Yoshida et al. 2009). Interestingly, the reprogramming efficiency of aged hMSC (62y) was 0.04% and therefore as high as the reprogramming efficiency of fetal hMSCs reprogrammed using viruses and much higher than the reprogramming efficiency of aged hMSC (74y) with retroviruses and additional inhibitors (Table 12). A possible reason for this is that the addition of vitamin c might have had a much more positive effect on the reprogramming efficiency of aged hMSC (62y) than the inhibitor combination used to reprogram aged hMSC (74y). In conclusion, hMSC 1 could be reprogrammed more efficiently using viral reprogramming and episomal plasmid-based reprogramming than all aged hMSCs used in this study indicating a negative effect of donor age of hMSCs on the reprogramming efficiency. Moreover, this is the first study to describe the reprogramming of fetal hMSCs with viral and non-viral methods. However, there are numerous studies reporting the reprogramming of fetal stem cell types, such as amniotic fluid-derived stem cells (Moschidou et al. 2012, Wolfrum et al. 2010) showing effective reprogramming of fetal cells to iPSCs. Moreover, the reprogramming efficiency of retroviral reprogramming using *OCT4, SOX2, KLF4* and c-*MYC* was initially described to be 0.02% in fibroblasts (Takahashi et al. 2007). The reprogramming efficiency of fetal hMSCs was slightly higher under normoxic conditions with 0.03% (Table 12). One reason for this could be that fetal hMSCs are a younger cell type than the fibroblasts used in the study of Takahashi et al. (Takahashi et al. 2007). Furthermore, the reprogramming efficiency of hMSCs reprogrammed with *OCT4, SOX2, KLF4* and *c-MYC* as well as *SV40LT* and *hTERT* was described to be 0.003% (Park et al. 2008b). The reprogramming efficiency of fetal hMSCs was tenfold higher under normoxia and twentyfold higher under hypoxia with addition of mTeSR 1. Likewise, the reprogramming efficiency of aged hMSC (62y) was more than tenfold higher, whereas the reprogramming efficiency of hMSC aged (74y) was more than tenfold lower (Table 12). Furthermore, several studies have described successful reprogramming of bone marrow-derived hMSCs (Frobel et al. 2014, Ohnishi et al. 2012, Park et al. 2008a, Shao et al. 2013). One of these studies reported a reprogramming efficiency of 0.0002-0.0008% (Ohnishi et al. 2012). In addition, several studies in mice reported a lower reprogramming efficiency of biological older cells confirming the lower reprogramming efficiency of aged hMSCs compared to fetal hMSCs detected in this thesis project (Cheng et al. 2011, Kim et al. 2010, Li et al. 2009, Bo Wang et al. 2011).

4.3 Enhancement of reprogramming efficiency in hMSCs of fetal and aged background

Aged hMSCs could only be reprogrammed with retroviruses using inhibition of P53 as well as additional inhibition of MEK and TGF-β receptor inhibitor (Megges 2010) or addition of vitamin c. (Table 12; Figure 27 A). This is in line with reports describing the enhancing effects of these conditions in reprogramming (Gao et al. 2013, Kawamura et al. 2009, Lin et al. 2009). The treatment of aged hMSCs with small molecule inhibitors and with agents modulating ageing-related processes revealed that the most effective condition to enhance the reprogramming efficiency of aged hMSC (62y) was addition of vitamin c and mTeSR 1 from day 14 after nucleofection when the cells were reprogrammed using episomal plasmids. This is in line with the described effect of addition of mTeSR 1at day 14 during reprogramming in a recent study (Yu et al. 2011). Furthermore, the combination smM and vitamin c as well as the combination of P53 inhibition and smM yielded iPS colonies from aged hMSC (62y) (Figure 27 A). The combination smM was described to enhance episomal plasmid-based reprogramming (Yu et al. 2011). Interestingly, the same experimental conditions did not yield iPS colonies when aged hMSC (62y) were reprogrammed with retroviruses, which could be used to reprogram fetal hMSCs. In addition, viral reprogramming of fetal hMSCs was most efficient when conditioned medium or smM and mTeSR 1 were used during reprogramming. Furthermore, episomal plasmid-based reprogramming of fetal hMSCs was most efficient when only N2B27 medium was used without inhibitor in contrast to episomal plasmid-based reprogramming of aged hMSC (62y) (Figure 27 A-C). These results indicate that the used conditions might have had adverse effects on reprogramming of fetal hMSCs compared to aged hMSCs. An additional report described a reprogramming efficiency of 0.01% and the tenfold increase of it by using valproic acid, vitamin c and P53 inhibition in MSCs (Yulin et al. 2012). The same combination of additives resulted in a reprogramming efficiency of 0.02% in fetal hMSCs and no iPS cells in aged hMSCs in this study (Figure 27). As the results are form one reprogramming experiment per primary hMSC population more comparative reprogramming experiments need to be conducted to confirm these observations.

4.4 iPS characterisation

All hMSC iPS cell lines generated were confirmed to be pluripotent by embryoid body based undirected differentiation and immunofluorescence labelling of pluripotency markers as well as by the transcriptome-based test of pluripotency PluriTest (Müller et al. 2011) (Figure 15, Figure 16, Figure 17, Figure 20, Figure 21 and Figure 23 B). These results are in line with studies describing iPS generation by retroviral and episomal plasmid-based reprogramming (Takahashi et al. 2007, Yu et al. 2011, Yu et al. 2009). In addition, pluripotency of iPSC (hMSC, 74y, viral) was confirmed *in vivo* by a teratoma assay in NSG mice (Figure 23 A). However, the *in vivo* pluripotency confirmation of the remaining hMSC-iPSCs still remains to be determined. Yet, a comparison of the expression of

pluripotency-related genes of all hMSC-iPSCs to hESCs revealed, that iPSC (hMSC, fetal, line 1, viral) expressed lower levels of *NANOG* than all other iPSCs. However, *OCT4*, *SOX2*, *KLF4* and further marker genes were expressed. Likewise, iPSC (hMSC, 62y, episomal) expressed fewer pluripotency markers in a pattern similar to the expression in iPSC (hMSC, fetal, line 1, viral) (Figure 16 A). These results implicate that iPSC (hMSC, fetal, line 1, viral) and iPSC (hMSC, 62y, episomal) might be partially reprogrammed iPS cells (Buganim et al. 2012), which have to be cultured further to reach the fully reprogrammed state. However, the other hMSC-iPSC lines, which were not tested in a teratoma assay, are very likely fully reprogrammed, as their expression pattern of pluripotency-related genes was very similar to the pattern in hESCs (Figure 16 A). Further, confirmation of the expression of pluripotency marker genes for example via quantitative real-time PCR is necessary to confirm these results. In addition, the hMSC-iPSCs were confirmed to have originated from their parental cells by DNA fingerprinting (Figure 18 A-D) and hMSC-iPSCs derived by means of the episomal plasmid-based reprogramming method did not show plasmid-specific transgene expression, which makes it very likely that the episomal plasmids were diluted out and the iPS cell lines are transgene-free (Figure 19 A and B). Yet, for more robust confirmation of the absence of the episomal plasmids, further PCR-based tests using transgene-specific primers are necessary. A further possibility to confirm the absence of the episomal plasmids could be to use Southern Blotting to rule out integration of the episomal plasmids into the genomic DNA of the derived iPS cells. Moreover, the transcriptome analysis of hiPSCs, hESCs, fetal hMSCs and aged hMSCs revealed that all iPS cell lines were more similar to hESCs than to hMSC samples (Figure 24 A and B) which confirms the loss of hMSC properties and acquisition of transcriptional properties similar to pluripotent hESCs in the derived iPSCs. Interestingly, iPSC (hMSC, 74y, viral) were most similar to hESCs and iPSC (hMSC, fetal, line 1, viral) were the least similar sample compared to hESCs based on correlation of the transcriptomes. However, the iPS cell lines reprogrammed using episomal plasmids formed a similarity-based cluster revealing a potential common gene expression signature due to reprogramming technique. Interestingly, this was not the case for iPSCs derived by means of retroviruses (Figure 24 A and B). Yet, a clear age-related effect of the donor age on similarities of the transcriptomes of hMSC-derived iPSCs was not detectable with this method.

4.5 Age-related differences in pluripotency marker expression in hMSCs

Human first trimester bone marrow MSCs express the pluripotency markers OCT4, NANOG, REX-1, SSEA-3, SSEA-4, TRA-1-60, and TRA-1-81 (Guillot et al. 2007). Fetal hMSCs used in this study were found to express SSEA4, KLF4, c-MYC and with very faint immunofluorescence staining signals of OCT4 and SOX2. However, TRA1-60 and TRA-81 as well as NANOG were not present contradicting the study by Guillot et al. (Figure 9 A). In addition, high OCT4 expression in adult

hMSCs was described as marker for higher *in vitro* lifespan of these cells in a recent study, which is in line with the result of this thesis for fetal hMSCs (Piccinato et al. 2015). The differences in pluripotency marker expression between fetal and aged hMSCs (Figure 9 A, B and C) might have facilitated reprogramming of fetal hMSCs.

4.6 Ageing-related changes in cell cycle and implications for hMSC reprogramming

In addition, a FACS-based analysis of the cell cycle phases comparing fetal and aged hMSCs revealed that more cells were in the G2 phase of the cell cycle and less cells in the G1 and S phase in populations of aged hMSCs compared to fetal hMSCs (Figure 7 A). So far no study reported a higher number of cells in G2 in hMSC preparations from aged donors. Yet, a recent report described an induced cell cycle arrest in G2 in normal human keratinocytes from aged donors (Kim et al. 2015). It is likely that the higher number of aged hMSCs in the G2 phase of the cell cycle is induced by a higher frequency of DNA damage as the G2 checkpoint in the cell cycle is ensuring the proper segregation and stops the cell from entering into mitosis in case of DNA damage (Cuddihy and O'Connell 2003). Differences in proliferation between hMSCs of different age background were reported previously confirming the results (Beane et al. 2014). In addition, the higher proliferation rate of fetal hMSCs might have contributed to the different amounts of cells in the cell cycle phases, which was observed (Guillot et al. 2007). Moreover, the differences in the cell cycle phases and cell cycle-related genes (Figure 7 B) most likely have facilitated the reprogramming of fetal hMSCs as the cell cycle is modulated during pluripotency induction (Ghule et al. 2011).

4.7 Retention of hMSC-related gene expression patterns in hMSC-iPSCs and effect on differentiation propensity

In addition to ageing-related features, the results of this study support the notion that donor cell transcriptional memory in hMSC-iPSCs might be reflected in the differentiation propensity of hMSC-iPSCs. This was revealed by microarray-based gene expression analysis indicating the retention of genes involved in the skeletal system and implying a possible enhanced propensity of all hMSC-iPSCs to differentiate into osteoblasts. Indeed, iPSC (hMSC, 74y, viral) could be differentiated into osteoblasts more efficiently than hFF-derived iPSCs and genes associated with MSC-specific processes or tissues such as genes related to bone were up-regulated (Figure 33). So far, there are no studies supporting the context between MSC-specific donor cell memory in iPSCs derived from hMSCs from the bone marrow and the differentiation propensity of the respective iPSCs. However, there are reports claiming a variation of the donor cell memory depending on the clone or individual but not depending on the cell type of origin (Nasu et al. 2013, Shao et al. 2013) Yet, one study

described enhanced osteogenic potential of MSCs derived from iPSCs from MSCs of a dental source but not from bone marrow, which is in line with the results (Ishiy et al. 2015). Further, reports described that the iPSCs tend to differentiate more efficiently into the cell lineages of their somatic origin confirming our results (Kim et al. 2010, Kim et al. 2011, Ohi et al. 2011, Polo et al. 2010, Rizzi et al. 2012). However, a recent report described that the differentiation propensity of iPS cells is affected by the reprogramming factor selection (Buganim et al. 2014). Therefore, the enhanced osteogenic potential of hMSC-iPSCs might be due to the use of the combination of OCT4, SOX2, KLF4 and c-MYC as reprogramming factor combination.

4.8 Change of ageing-related features before and after iPS generation and redifferentiation to iMSCs in hMSCs of different age backgrounds

4.8.1 Genomic stability, DNA damage and DNA damage repair

The results of karyotyping analysis showed that fetal and most of the aged hMSCs were stable. Yet, aged hMSC (74y) showed karyotypic abnormalities (

Figure 6). As aged hMSC (74y) were derived from the oldest donor in this study, the aberrations might have been caused by telomere exhaustion due to high age in these cells. However, it has been reported that MSCs develop chromosomal aberrations in culture (Foudah et al. 2009). Furthermore, it has been shown that fibroblasts from older donors display higher chromosomal instability compared to young donors, confirming a likely effect of age on frequency of chromosomal aberrations seen in aged hMSCs (Kalfalah et al. 2015). Therefore, the higher reprogramming efficiency of fetal hMSCs could be due to higher genomic stability compared to aged hMSCs. However, iPSCs derived from aged hMSC (74y) had chromosomal instabilities (Figure 22) and could only be reprogrammed with P53 inhibition revealing that P53 might have hindered the reprogramming process (Megges 2010). The inhibiting role of P53 during reprogramming has been described previously confirming the enhancing role of P53 inhibition on reprogramming efficiency (Kawamura et al. 2009). Interestingly, the tetraploid karyotype might have been caused by P53 inhibition and not by age (Aylon and Oren 2011). In addition iPSC (hMSC, fetal, line 1, episomal 3) showed chromosomal aberrations however distinct from iPSC (hMSC, 74y, viral) (Figure 22). As the other iPS cell lines generated from fetal hMSC 1 had no karyotypical aberrations, the aberrant karyotype of iPSC (hMSC, fetal, line 1, episomal 3) might have been caused by *EBNA1* the open reading frame of which is on episomal plasmids and has been described to be involved in chromosomal instabilities in cancer (Kamranvar and Masucci 2011). Whether, iPSC (hMSC, fetal, line 1, viral) or iPSC (hMSC, 62y, episomal) carry karyotypical abnormalities was not analysed and therefore still remains to be determined. Interestingly, it is likely

that lower numbers of a DNA double-strand breaks are present in iPSC (hMSC, 74y, viral) compared to iPSCs derived from fetal hMSCs and from aged hMSC (62y) using episomal plasmids. In addition, aged hMSC (62y) showed phosphorylation of P53 implying the presence of a DNA damage response (Figure 28). These results imply a potentially higher likelihood that DNA lesions accumulate in episomal plasmid-derived iPSCs. Moreover, the expression patterns of genes involved in DNA damage repair were more similar between iMSCs irrespective of donor age or pluripotent cell line and fetal hMSCs than between iMSCs and aged hMSCs (Figure 39). This result indicates a change to a younger gene expression pattern of genes involved in the process of DNA damage repair during iMSC generation from aged hMSCs. Interestingly, this might be due to remodelling of the DNA damage repair pathways during pluripotency induction (Rocha et al. 2013). In addition, numerous studies reported the detection of genomic instabilities in iPS cells, which is in line with some of the results of this study (Ronen and Benvenisty 2012). Furthermore, the results indicate the need for thorough analysis of the genomic stability of iPS cells and iMSCs before application in therapy. Therefore, further experiments have to be conducted to analyse the impact of high age on the genomic stability of iPSCs. For example karyotyping of all iPS cell lines and iMSCs and a more detailed analysis of the DNA damage are necessary. Furthermore, array-based comparative genomic hybridisation (array CGH) or single nucleotide polymorphism arrays (SNP arrays) would help to get a more profound picture about of the age effect of hMSCs on genomic stability features of iPS cells and iMSCs derived from them.

4.8.2 Reactive oxygen species, oxidative DNA damage and oxidative stress response

A further hallmark of ageing are elevated levels of ROS and subsequent accumulation of oxidative DNA damage and oxidative stress in hMSCs of high age background (Stolzing et al. 2008). In line with that, elevated ROS levels were measured in hMSCs derived from 60 to 70-year-old donors compared to fetal hMSCs (Figure 8 A and B). In addition, functional annotation of differentially expressed genes revealed that genes involved in the response to oxidative stress are up-regulated in aged hMSCs (Table 10). Interestingly, elevated ROS levels were not only measured in MSCs of aged background but in MSCs of younger background after long-term cultivation (Geissler et al. 2012). The hMSCs in this study were not cultivated for a long term before the analysis was carried out making it more likely that the higher levels of ROS are an effect of high donor age. Whether the higher ROS levels detected in aged hMSCs correlate with high mitochondrial ROS remains to be determined. As the level of reactive oxygen species has implications in reprogramming of somatic cells to induced pluripotent stem cells (Hämäläinen et al. 2015, Prigione et al. 2010), the higher levels of intracellular ROS in aged hMSCs might have contributed to the age-related decline of reprogramming efficiency compared to fetal hMSCs (Table 12).

Moreover, immunofluorescence staining revealed that in both aged and fetal hMSCs the oxidative DNA damage was at similar levels on day six after transduction with the reprogramming factors (Figure 25 A). In addition, the level of oxidative DNA damage was lower in hMSCs at day 6 post-transduction compared to MSCs that were not transduced indicating early induction of oxidative damage-specific DNA repair pathways during cellular reprogramming (Figure 25 B). A recent report described that high glutathione peroxidase levels contribute to iPS-specific maintenance of genomic stability after pluripotency induction (Dannenmann et al. 2015). Therefore, the decrease in oxidative DNA damage after transduction could be due to induction of higher glutathione peroxidase levels. In contrast to that, oxidative DNA damage could be detected in iPSCs derived from hMSCs of fetal and aged background (Figure 28) and measurements of intracellular ROS levels revealed similar or higher ROS levels in iPSCs compared to hMSCs independent of age background (Figure 29 A). Furthermore, expression patterns of genes involved in the response to oxidative stress revealed similarity between fetal episomal iPSCs and between iPSCs derived from aged hMSCs making an effect of donor age on ROS levels and related gene expression less likely and a general modulation of ROS level upon reprogramming more likely (Figure 29 B). These results are in line with a recent report describing the modulation of ROS and related oxidative damage during reprogramming (Prigione et al. 2011b). In addition to that, the most effective condition in terms of enhancement of reprogramming efficiency in aged hMSCs was vitamin c in combination with culture in mTeSR 1 from day 14 post-nucleofection in episomal plasmid-based reprogramming of aged hMSC (62y) (Table 12). However, the same condition had not the same effect when fetal hMSCs were reprogrammed (Table 12) and for reprogramming of other primary hMSCs of aged background (data not shown). These results indicate that an oxidative stress-related roadblock was possibly inherent to aged hMSC (62y) rendering them more susceptible to reprogramming and enhancement of reprogramming through vitamin c compared to the other primary hMSCs. Yet, the results are from one reprogramming experiment and more research has to be conducted to confirm the significance of the effect of vitamin c in this context. Interestingly, the enhancing effect of vitamin c in reprogramming has been described underlining the result of this study (Tao Wang et al. 2011). Finally, iMSCs derived from aged hMSCs showed high similarity of expression patterns of genes involved in oxidative stress to their parental cells whereas iMSCs derived from fetal hMSCs and H1 were more similar to fetal hMSC 2 in this respect (Figure 41). This result indicates that the donor age of hMSCs might be reflected in iMSCs derived from them. Moreover, this result is contradicting studies describing the absence of age-related features in cells derived from iPSCs of aged origin using fibroblasts (Lapasset et al. 2011, Miller et al. 2013).

4.8.3 Effect of hMSC donor age on senescence and senescence-associated gene expression in iPSCs and iMSCs

Comparative staining of the senescence marker β-galactosidase in fetal hMSCs and aged hMSCs revealed an increase of the number of senescent cells in aged hMSCs compared to fetal hMSCs (Figure 7 D). Moreover, the expression patterns of genes involved in senescence differed in an age-dependent manner between aged hMSCs and fetal hMSCs (Figure 7 C). These results revealed higher numbers of senescent cells and differences in senescence-related gene expression in aged hMSCs compared to fetal hMSCs and hESCs. In addition, the more flat and senescent appearance of aged hMSCs compared to fetal hMSCs indicated a higher number of senescent cells in the population of aged hMSCs (Figure 4 A). This result is in line with a study describing senescence to be dependent on donor age in human hMSCs (Wagner et al. 2009). In addition, other studies in animal models reported an increased senescence in aged MSCs (Choudhery et al. 2012, Yu et al. 2011). One cause for the increased senescence in aged hMSCs in this thesis might be an increase of ROS levels (Jeong and Cho 2015). In addition, the differential regulation of senescence-associated genes in fetal and aged hMSCs compared to hESC H1 (Figure 7 C) might have contributed to the decline in reprogramming efficiency in aged hMSCs compared to fetal hMSCs as previous studies have shown that senescence and also higher donor age impairs cellular reprogramming (Banito et al. 2009, Trokovic et al. 2015). Yet, after pluripotency induction and redifferentiation to iMSCs, the expression patterns of genes involved in regulation of senescence were more similar between aged hMSCs and iMSCs of the same origin. Likewise, the expression patterns were more similar between fetal hMSCs and iMSCs derived from them and from hESC H1 (Figure 38 A). According to these results there seems to be a reflection of donor age in the transcriptional patterns of senesce-associated genes in iMSCs. In addition to that, expression patterns of senescence-associated genes were more similar between aged hMSCs and fetal iMSCs than between fetal hMSCs and aged iMSCs based on a further gene set involved in senescence (Figure 38 B), a result further indicating a senescence-related transcriptional signature rather to be present in iMSCs of aged background and therefore to reflect donor age. These results confirm recent studies describing the circumvention of senescence in aged somatic cells through reprogramming (Lapasset et al. 2011) and contradict studies describing lower senescence in cells derived from iPSCs of aged background (Frobel et al. 2014, Miller et al. 2013). However, further gene expression analysis revealed the rejuvenation of genes involved in negative regulation of cell proliferation (Table 16), which is in line with the above mentioned studies describing rejuvenation of iPS derived MSCs and other cell types (Frobel et al. 2014, Lapasset et al. 2011, Miller et al. 2013).

4.8.4 Ageing-related transcriptional changes before and after iPS generation and redifferentiation to iMSCs

The microarray based transcriptome analysis enabled the detection of the differences and similarities between the transcriptomes of fetal hMSCs, aged hMSCs and hESCs. The clustering dendrogram revealed a low similarity between hMSCs and hESCs as expected. In addition, the correlation of the transcriptomes of fetal hMSCs and hESCs was higher than the correlation between the transcriptomes of aged hMSCs and hESCs (Figure 10 A and B). This result might explain why fetal hMSCs could be reprogrammed to pluripotency with a higher efficiency than aged hMSCs in this study. Surprisingly, 847 genes were commonly differentially expressed in aged hMSC (62y) and aged hMSC (74y) compared to fetal hMSCs, which makes these two samples the least similar to fetal hMSC 1 (Figure 10 C). As these aged hMSC populations could be reprogrammed to iPSCs in contrast to the other aged hMSC samples, there might be a feature inherent to these two lines rendering them more susceptible to reprogramming although they are more distinct from fetal hMSC 1, which in turn showed high reprogramming efficiency. Furthermore, a process found to be down-regulated in aged hMSCs of this study was Notch signalling (Table 8). This confirms a previous study in mice showing reduced basal Notch signalling in hMSCs of aged mice (Mutyaba et al. 2014). In addition, Notch signalling has recently been described to be involved in the reprogramming process (Ichida et al. 2014). Therefore, altered Notch signalling in aged hMSCs might have contributed to lower reprogramming efficiency in aged hMSCs.

In addition, hierarchical clustering analysis of the transcriptomes did not reveal a clear age-related effect on the similarities of the transcriptomes of iPSCs with different age backgrounds (Figure 24 A and B). Moreover, the overlapping gene expression was significantly annotated to the gene ontology ageing in the cases of iPSC (hMSC, 62y, episomal) and iPSC (hMSC, 74y, viral) (Table 13). According to these results, an ageing-related gene expression signature is retained in hMSC-iPSCs. This adds further aspects to studies describing the rejuvenation of somatic cells of aged origin upon reprogramming (Lapasset et al. 2011, Prigione and Adjaye 2010) and shows that the retention of an age-related gene expression signature in iPSCs derived from aged hMSCs is something that needs to be considered when developing regenerative therapies with this technology.

Moreover, genes of the gene ontology term ageing were changed upon reprogramming in hMSCs of fetal and aged origin in a similar manner revealing no regulation of these genes according to donor age (Figure 32). This result is in line with recent studies on remodelling of ageing-related processes upon reprogramming (Lapasset et al. 2011, Prigione et al. 2010). The microarray-based gene expression analysis comparing differentially expressed genes between iPSCs and parental cells revealed more up than down-regulated genes upon reprogramming of hMSCs of both age backgrounds. In addition, the number of up or down-regulated genes was higher in the individual iPS cell lines revealing a high variance in the transcriptional processes taken place during reprogramming independent from donor

age (Figure 26). These results show that donor age might have an impact on reprogramming of hMSCs of aged background - an effect that has not been described so far. Comparative transcriptome analysis revealed a potentially age-dependent variation of the similarities between iMSCs and their parental cells (Figure 36 A and C). However, iMSCs had a transcriptome, which was more similar to hMSCs than to hESC H1 (Figure 36 A and B). Furthermore, the clustering dendrogram revealed a higher similarity between the transcriptomes of iMSC and hMSCs than iMSCs and iPSCs (Figure 36 A and D). This is in line with recent studies describing the derivation of mesenchymal stem cell-like cells from pluripotent cells (Frobel et al. 2014, Kimbrel et al. 2014, Wang et al. 2014). Interestingly, iMSCs shared more expressed genes with fetal hMSCs than with aged hMSCs (Figure 36 B). Yet, transcriptional differences related to ageing-associated processed could be detected between iMSCs of fetal and aged background (Table 15). However, more experiments need to be conducted to further confirm the effects of donor age on iMSC features.

4.8.5 Transcriptional changes related to the metabolic stability theory of ageing during reprogramming hMSCs and redifferentiation to iMSCs

The microarray-based gene expression analysis revealed the down-regulation of genes involved in the metabolic stability theory of ageing such as insulin response, insulin receptor signalling and glucose metabolism in aged hMSCs compared to fetal hMSCs (Table 10). These results are not in line with a recent study describing the up-regulation of insulin signalling in the tissue of aged mouse hearts. However, the same study described the down-regulation of oxidative phosphorylation in aged mice corroborating lower glycolysis seen in the results of this thesis (Brink et al. 2009). However, more detailed gene expression analysis revealed higher levels of two glycolysis-associated genes in fetal hMSCs compared to aged hMSC supporting age related down-regulation in hMSCs. These genes were *ALDOC* encoding an isoenzyme of fructose-1,6-(bis)phosphate aldolase and *PFKFB3* encoding the enzyme 6-phosphofructo-2-kinase/fructose-2,6-bisphosphatase 3 (Figure 11 B). Interestingly, a recent study found the up-regulation of the enzyme ALDOC in a canine model of ageing (Opii et al. 2008). Moreover, PFKFB3 is involved in the redox homeostasis in cancer (Seo and Lee 2014). In addition, genes involved in the response to insulin were down-regulated in aged hMSCs compared to fetal hMSCs (Table 10). This result is in line with the study of Brink et al. in which the regulated genes involved in insulin signalling were found to be down-regulated in the hearts of aged mice. However, none of the genes related to insulin signalling described in this study for aged hMSCs was found to be regulated by Brink et al. (Brink et al. 2009). Furthermore, genes involved in insulin signalling were found to be differentially expressed in hMSCs of elderly patients with osteoporosis, which is in line with the fining for hMSCs of aged background in this thesis (Zhou et al. 2015). Yet, the insulin

signalling-associated gene IRS2 was up-regulated in fetal hMSCs compared to aged hMSCs (Figure 11 B), which is not in line with the results of Brink et al. (Brink et al. 2009). Although there is no report on involvement of *IRS2* in ageing of hMSCs, enhanced INK4A/ARF locus expression could restore impaired IRS2 signalling in mice, which is not be in line with low IRS2 levels in aged hMSCs (Vinué et al. 2015). In contrast to that, GCLM was reported to be affected by age-related deregulation of circadian signalling during ageing in Drosophila and leads to temporal deregulation of the redox homeostasis (Klichko et al. 2015). Therefore, higher GCLM levels in aged hMSCs as detected in this study (Figure 11 B) could be responsible for higher ROS levels in aged hMSCs.

Yet, genes involved in the response to oxidative stress were significantly up-regulated in aged hMSCs as well as genes associated with glutathione metabolism, antioxidant activity and mitochondrion, however without significance (Table 10). These results are in line with Brink et al. who described up-regulation of glutathione metabolism-related genes in aged mice (Brink et al. 2009). Furthermore, several studies described the higher likelihood of MSC of aged background to show signs of oxidative stress and the involvement of decline in antioxidative capacity and mitochondrial metabolism in the ageing process in MSCs corroborating our results (Geissler et al. 2012, Shipounova et al. 2010).

Moreover, the gene *COX7A2*, encoding cytochrome c oxidase subunit VIIa polypeptide 2 (liver), was found to be up-regulated in aged hMSCs in this study and was annotated to the term mitochondrion (Table 10). The same gene was found by Brink et al. to be up-regulated in the heart of age mice (Brink et al. 2009). A further publication described the deregulation of *COX7A1*, encoding cytochrome c oxidase subunit VIIa polypeptide 1 (muscle), in aged human fibroblasts (Hashizume et al. 2015) - the expression of which was up-regulated in aged hMSCs compared to fetal hMSCs (Figure 11 A). Moreover, a recent publication based on a comparative meta-analysis of *in vivo* aged tissue shows the differential regulation of genes involved in oxidative phosphorylation in aged tissues underlining the possibility that the deregulation of the mitochondrial enzymes of the respiratory chain might be part of the ageing process in aged hMSCs in this study and possibly have interfered with pluripotency induction (Voutetakis et al. 2015).

Upon reprogramming, processes that were found to be changed in aged hMSCs compared to fetal hMSCs that are part of the metabolic stability theory of ageing were altered. Although functional annotation of overlapping gene expression between iPSCs and their parental fetal or aged hMSCs did not reveal that ageing associated metabolic processes are reflected in the iPSCs of different age backgrounds (Figure 31), the comparison between aged hMSCs and corresponding iPSCs elucidated a change in these processes upon reprogramming. Genes involved in glycolysis, oxidative phosphorylation, insulin signalling and glutathione peroxidase genes were down-regulated whereas genes associated to mitochondria were up-regulated in iPSCs derived from aged hMSCs compared to their parental cells (Table 14). This is in line with a recent study describing the down-regulation of genes involved in the response to oxidative stress and antioxidant enzymes as well as an up-regulation of mitochondrial biogenesis factors upon reprogramming of fibroblasts (Prigione et al. 2010).

However, the detected alteration of metabolic processes in iPSCs from aged hMSCs underpins a rejuvenated metabolic state as age-related up-regulation of glutathione metabolism and Insulin signalling described by Brink et al. (Brink et al. 2009) could not be detected in iPSCs from aged hMSCs compared to aged hMSCs (Table 14). Moreover, a recent study described the involvement of glycolysis in impairment of reprogramming in fibroblast further underlining the context between metabolic stability, pluripotency induction and age (Gupta et al. 2015).

Interestingly, the TCA cycle-associated gene *OGHDL* was expressed at much higher levels and significance in iPSCs from aged hMSCs than in aged hMSCs (Figure 30 B). As the TCA cycle was recently described to be involved in age-related changes of chromatin remodelling, the low expression of this gene in aged hMSCs might be a cause of age-specific regulations of TCA cycle and different chromatin dynamics (Salminen et al. 2014). As chromatin remodelling is taking place during cellular reprogramming (Apostolou and Hochedlinger 2013) the age-related decline in reprogramming efficiency in hMSCs might be eventually caused by the down-regulation of *OGHDL*. Moreover, *OGHDL* has been described as modifier of NF-κB function (Sen et al. 2012) and NF-κB was described to be involved in age-related interfere in reprogramming ageing (Soria-Valles et al. 2015) Therefore, low *OGHDL* levels in aged hMSCs might have interfered with NF-κB function and impaired reprogramming in aged hMSCs. In addition, microarray-based gene expression analysis revealed a lower expression of glycolysis-associated genes *GPDH* and *PFKP* as well as a lower expression of insulin signalling-related genes *PRKAG1*, *MAP2K1* and *IRS1* in iPSCs derived from aged hMSCs compared to their somatic origin (Figure 30 B). These results corroborate the down-regulation of insulin signalling and glycolysis upon reprogramming described in a recent study (Prigione et al. 2010). However, the down-regulation of glycolysis-associated genes is not in line with a study describing the enhancing effect of c-MYC on glycolytic capacity in iPSCs as c-MYC was used for reprogramming of aged hMSCs in this study (Folmes et al. 2013). Moreover, glutathione-associated genes *GGCT* and *CNDP2* were up-regulated whereas *GCLM* was down-regulated (Figure 30 B) indicating that glutathione metabolism is not entirely down-regulated in iPSCs derived from aged hMSCs compared to the parental cells. Interestingly, a recent study described the mediation of protection from oxidative DNA damage by *GPX2* in iPS cells (Dannenmann et al. 2015). Yet, the up-regulation of this gene through reprogramming could not be confirmed. In addition, the gene *COX7A1* that was up-regulated in aged hMSCs (Figure 11 A) and described to be deregulated in aged fibroblasts (Hashizume et al. 2015) was down-regulated upon reprogramming of aged hMSCs (Figure 30 A).

Moreover, upon redifferentiation of hMSC-iPSCs of different age backgrounds, processes metabolic stability were in part reverted to the level detected in the hMSCs before indicating a reflection of the donor age. Hierarchical clustering analysis showed that genes oxidative phosphorylation display an iPS-like pattern in fetal iMSCs whereas the pattern is close

aged hMSCs in H1 iMSCs and aged iMSCs (Figure 42). In addition, genes involved in glutathione metabolism showed hMSC-like patterns in H1 iMSCs and iPS-like patterns in hMSC-derived iMSCs (Figure 43). Yet, genes associated with glycolysis showed expression pattern similar to aged hMSCs in iMSCs derived from them whereas the expression patterns were iPS-like in H1 iMSCs and fetal iMSCs (Figure 44). However, Insulin signalling-related gene expression patterns were iPS-like in H1 derived iMSCs, similar to aged hMSC (62y) in iMSCs of aged background and more hMSC-like in fetal hMSC derived iMSCs (
Figure 45). Interestingly, the glutathione metabolism-associated gene *GCLM* encoding glutamate-cysteine ligase modifier subunit, was down-regulated compared to aged hMSCs in fetal hMSCs, aged iPSCs and iMSCs indicating the down-regulation of this gene upon reprogramming and the retention of the expression level upon redifferentiation of aged hMSCs (Figure 11 B; Figure 30 B; Figure 46 A) However, the glutathione metabolism-associated gene *MGST2* was up-regulated in iMSCs compared to aged hMSCs indicating a modulation of glutathione metabolism upon redifferentiation. These findings contradict in part the study of Brink et al. who described the down-regulation of genes involved in glutathione metabolism in aged mice (Brink et al. 2009). Furthermore, the glycolysis-associated gene *PGAM1* encoding phosphoglyceric acid mutase was down-regulated in iMSCs. Interestingly, Brink et al. have found that the TCA cycle is down-regulated in aged mice however glycolysis-associated genes were not deregulated in aged mouse tissues (Brink et al. 2009). In addition, a recent report described the down-regulation of genes involved in mitochondrial biogenesis upon differentiation of iPS cells which is not in line with the findings in this study as only one glycolysis-related genes was found to be down-regulated upon differentiation to iMSCs (Prigione and Adjaye 2010). This low number of differentially regulated genes in iMSCs compared to aged hMSCs indicates a rather aged-like phenotype of processes of the metabolic stability theory of ageing in iMSCs. Yet, further experiments have to be conducted to confirm a reflection of donor age in the expression of genes involved in metabolic stability-associated processes. If confirmed, these results would contradict recent studies describing a rejuvenated state of iMSCs and of cells derived from iPSCs (Frobel et al. 2014, Lapasset et al. 2011, Miller et al. 2013). However, the gene *COX7A1* was expressed at higher levels in aged hMSCs compared to fetal hMSCs but not in hMSC-iPSCs and iMSCs derived from aged hMSC (74y) (Figure 46 B). The up-regulation of *COX7A1* in ageing has been described (Hashizume et al. 2015), which would underline a rejuvenation by reprogramming and iMSC differentiation from aged hMSCs in this study. In contrast to that, the genes *MRPL28*, *CAPRIN2*, *GCAT*, *EHHADH*, *ALDH5A1* and *SHMT2*, which were described to be regulated with age in fibroblasts in the same publication, were not found to be regulated in this study.

4.8.6 Transcriptional changes related to cytoskeleton and niche interaction during reprogramming of hMSCs and redifferentiation to iMSCs

Mesenchymal stem cell ageing is associated with alterations in the interaction with their microenvironment (Reitinger et al. 2015). In this study the effect of donor age on expression of genes involves in cytoskeleton dynamics and niche interaction in hMSCs, hMSC-iPSCs and iMSCs of fetal and aged backgrounds could successfully be analysed utilizing microarray-based gene expression profiling. First, microarray data analysis revealed a down-regulation of genes involved in cytoskeleton organisation as well as an up-regulation of genes associated to the extracellular matrix (ECM), ECM interaction and to cell adhesion and migration in aged hMSCs (Table 9, Table 11). This result is in line with recent reports describing an impaired reaction of aged hMSCs to their environment, e.g. reaction to surface substrate stiffness and that genes involved in the interaction with extracellular matrix are up-regulated (Stolzing et al. 2011, Zhou et al. 2015). However, a further study described an age-related decline in the responsiveness to ECM in MSCs, which contradicts the finding of this thesis (Kasper et al. 2009). Moreover, an additional study described the up-regulation of genes associated with the regulation of ECM in human MSCs of elderly donors confirming the result of this work (Wagner et al. 2009). In contrast to that, the down-regulation of processes associated to the cytoskeleton in aged hMSCs compared to fetal hMSCs (Table 10) confirm studies describing age-related deregulation of the cytoskeleton in MSCs of the rat (Geissler et al. 2012, Kasper et al. 2009).
Interestingly, genes involved in actin cytoskeleton organisation and ECM were down-regulated upon reprogramming of aged hMSCs and genes involved in focal adhesion and ECM were down-regulated during reprogramming of fetal hMSCs (Table 14). These results indicate a possible reversion of the age-related transcriptional features involved in niche interaction and cytoskeleton during reprogramming. Interestingly, it has been described that changes in the regulation of extracellular matrix formulation modulates iPS generation (Li et al. 2014) indicating that the age-related features of ECM regulation in age hMSCs could have had an effect on the induction of pluripotency in these cells. Yet, genes associated to cell adhesion, and ECM interaction were down-regulated in iMSCs derived from aged hMSCs compared to iMSCs derived from fetal hMSCs (Table 15). Furthermore, the functional annotation of genes expressed in iPSCs and iMSCs but not in hMSCs revealed that processes related to cell adhesion are rejuvenated by reprogramming and that this is retained in iMSCs (Table 16). As genes involved in these processes were up-regulated in aged hMSCs compared to fetal hMSCs it is likely that reprogramming to iPSCs and subsequent redifferentiation reversed the niche interaction related gene expression patterns in aged hMSCs to a more fetal hMSC –like state. In addition, the up-regulation of ECM-associated genes has been described to be associated with ageing (Wagner et al. 2009). On the other hand, the down-regulation of genes involved in cellular adhesion were described to be associated with *in vitro* ageing of MSCs highlighting a rather aged-like

expression pattern of genes involved in these processes (Geissler et al. 2012). Likewise, genes involved in the regulation of the cytoskeleton were down-regulated in iMSCs of aged origin compared to iMSCs derived from fetal hMSCs (Table 15) indicating a retained age associated gene expression patterns of this category as the down-regulation of cytoskeleton dynamics were described for MSCs of aged background (Kasper et al. 2009). Although further experiments need to be conducted to confirm these results, they indicate reversion of ECM interaction in aged hMSCs by iMSC generation from them. However, adhesion- and cytoskeleton-associated processes are likely to be influenced by donor age in iMSCs.

4.9 General discussion

Human bone marrow derived mesenchymal stem cells are already widely tested in clinical trials for the use in future therapies (Mastri et al. 2014). However, their application potential is limited due to limited expansion possibilities and *in vitro* senescence, which increases with age (Baxter et al. 2004, Geissler et al. 2012, Stenderup et al. 2003). Furthermore, MSCs loose their differentiation potential in culture (Banfi et al. 2000, Bonab et al. 2006, Wagner et al. 2008), which leads to problems as high cell numbers are needed for cell therapy applications. Therefore, it is necessary to generate MSC cell populations for clinical applications, which are devoid of the limits associated with expansion and biological age and to circumvent senescence without using immortalisation that can lead to cancer cell-like features in hMSCs. The initial comparison of hMSCs of fetal and aged origin in this study revealed age-related decline in differentiation, proliferation, cell cycle regulation, elevated senescence and elevated ROS levels in aged hMSCs as well as differences in expression patterns of genes involved in metabolic processes and pathways regulating processes such as insulin signalling. Furthermore, age-related alterations in cytoskeleton dynamics and interaction with the extracellular matrix were detected. All of these features might have implications for reprogramming which are discussed above in detail.

A possible solution to the shortfalls of functional decline and senescence caused by biological or *in vitro* ageing of hMSCs is the differentiation of these cells from pluripotent stem cells such as human embryonic stem cells or induced pluripotent stem cells to generate mesenchymal stem cell-like cells (iMSCs) (Barberi et al. 2005, Yen Shun Chen et al. 2012, Diederichs and Tuan 2014, Frobel et al. 2014, Hong et al. 2015, Ishiy et al. 2015, Kimbrel et al. 2014, Raynaud et al. 2013, Wang et al. 2014).

Human embryonic stem cells have a very promising potential in regenerative medicine. However, ethical concerns and potential rejection of the hESC-derived cells in cell replacement therapy limit their application possibilities (Miyazaki et al. 2012). Induced pluripotent stem cells are very similar to human embryonic stem cells in terms of unlimited self-renewal and differentiation potential in all cell types of the three germ layers and represent an alternative to the use of hESCs. Moreover, the use of iPS cell derived cells in therapy allows a reduction of variance often seen in primary cells, which

commonly impairs the application potential of hMSCs (Takahashi et al. 2007). Reprogramming of hMSCs to iPSCs has been described by several studies (Frobel et al. 2014, Ohnishi et al. 2012, Park et al. 2008a, Shao et al. 2013). In this study iPS cells could be derived from hMSCs of fetal and aged origin. So far, no study described reprogramming of fetal femur-derived hMSCs. Moreover, features of generated iPSCs are most likely affected by high hMSCs donor age. Therefore, iPSCs derived from aged hMSCs have to be carefully evaluated before clinical application.

The generated hMSC-iPSCs were confirmed to be pluripotent by detection of marker expression as well as *in vitro*-, *in vivo*- and transcriptome-based pluripotency tests. The transcriptomes of the generated iPS cells were similar to the transcriptome of hESCs. Yet, two iPS cell lines were less similar to hESCs than all other iPS cell lines and expressed fewer pluripotency marker genes. Moreover, these iPS cell lines were confirmed to be pluripotent in *in vitro* and transcriptome-based tests. However, the reduced number of expressed pluripotency marker genes might indicate that these iPS cell lines were partially reprogrammed as described in a recent study in fibroblasts (Buganim et al. 2012). Therefore, further passaging of these iPS cell lines is necessary to induce the fully reprogrammed state in these iPS cell lines. Furthermore, karyotypical abnormalities were detected in iPS cell line derived from aged hMSC (74y). This result is in line with a study describing the detection of chromosomal aberrations in iPSCs derived from fibroblasts of an 84-year-old donor (Prigione et al. 2011a). Nevertheless, the iPS cell line derived from aged hMSC (74y) met all required characteristics of induced pluripotent stem cells and could successfully be re-differentiated into functional iMSCs. Therefore, it is important to develop strategies to ensure genomic stability in iPS cells derived from aged donors especially for applications of iMSCs in aged patients. Moreover, several studies reported the occurrence of genomic instabilities in iPSCs (Ronen and Benvenisty 2012). According to this, it is not clear whether the age of the hMSC donor is the only cause of the presence of chromosomal instabilities. Furthermore, karyotypical abnormalities depend upon the reprogramming methods. In a recent study the rate of karyotypical abnormalities in fibroblasts was described to be higher after retroviral reprogramming compared to episomal plasmid based reprogramming. However, among non-viral reprogramming methods episomal plasmid-based iPS cell generation showed higher occurrence of chromosomal instabilities than other methods such as mRNA-based reprogramming (Schlaeger et al. 2015).

Comparison of the transcriptomes of fetal and aged hMSCs confirmed the differential expression of genes involved in antioxidative processes, which is in line with the metabolic stability theory of ageing (Brink et al. 2009). However, other processes such as insulin signalling were regulated differently contradicting the metabolic stability theory of ageing (Brink et al. 2009). Upon reprogramming, expression patterns of genes involved in processes of the metabolic stability theory of ageing were changed in a way that is in line with a recent study characterising these changes in fibroblasts (Prigione et al. 2010). Yet, glutathione metabolism was not entirely down-regulated most probably

because it plays an important role in DNA damage protection in pluripotent cells (Dannenmann et al. 2015). However, after redifferentiation into iMSCs higher donor age seemed to be reflected in the expression patterns of genes involved in processes of metabolic stability theory of ageing. Interestingly, particular processes such as glutathione metabolism seemed to resemble a rejuvenated state.

Furthermore, comparative transcriptome analyses indicated that cytoskeleton related processes are down-regulated and processes involved in ECM interaction are up-regulated in aged hMSCs compared to fetal hMSCs. However, the ways in which these processes are involved in hMSC ageing are still debated (Kasper et al. 2009, Wagner et al. 2009). Furthermore, ECM-related gene expression changed upon reprogramming in fetal and aged hMSCs indicating that age-related differences in these processes in hMSCs might have an effect on the reprogramming process itself as described in a recent study (Li et al. 2014). Interestingly, processes involved in ECM interaction were up-regulated in iMSCs of aged background compared to iMSCs of a fetal background whereas they were down-regulated in aged hMSCs. Yet, the age-related down-regulation of cytoskeleton-associated processes was retained in iMSCs. Therefore, iMSC generation from aged hMSCs very likely represents a potential possibility to reverse age-related changes of ECM interaction but not cytoskeleton-related processes in aged hMSCs, which might potentially restore defective age-related niche interaction processes in aged hMSCs.

Furthermore, ROS levels were lower in fetal hMSCs compared to aged hMSCs and genes involved in response to oxidative stress were up-regulated in aged hMSCs compared to fetal hMSCs. Confirming this finding, higher ROS levels were described as hallmark of MSC ageing (Stolzing et al. 2008). In addition, oxidative DNA damage was lower at day six after viral transduction in both fetal and aged hMSCs, which could be due to early induction of processes involved in antioxidant production during reprogramming (Dannenmann et al. 2015). However, oxidative DNA damage could be detected in iPSCs derived from fetal and aged background and intracellular ROS levels were similar between iPSCs independent of donor age. Yet, genes involved in antioxidant processes were down-regulated in iPSCs however not in an age depended manner contradicting the study of Dannenmann et al. (Dannenmann et al. 2015). Moreover, elevated levels of ROS might have contributed to age-related decline of the reprogramming efficiency in hMSCs in this study as levels of ROS have implications in reprogramming (Hämäläinen et al. 2015, Prigione et al. 2010). Interestingly, vitamin c had the strongest enhancing effect on reprogramming efficiency of one primary population of the aged hMSCs analysed in the reprogramming experiments. Therefore, an oxidative stress-related roadblock in aged hMSCs is very likely. However, oxidative stress-related gene expression patterns seemed to be more similar to the parental hMSCs and therefore age-related in iMSCs. Yet, this is not in line with studies describing rejuvenation of iPS-derived cells and reversal of ageing features in mesenchymal stem cell-like cells from iPSCs (Frobel et al. 2014, Lapasset et al. 2011, Miller et al. 2013).

Moreover, higher numbers of senescent cells and age-related changes of senescence-associated gene expression are further aspects which very likely contributed to reduce preprograming efficiency in aged hMSCs as already described in several reports for fibroblasts (Banito et al. 2009, Li et al. 2009). Interestingly, senescence-related gene expression pattern were most probably age-dependent in iMSCs derived from aged hMSCs further contradicting publications describing reversal of ageing features in iPS-derived cells (Frobel et al. 2014, Lapasset et al. 2011, Miller et al. 2013). These results confirm that more research needs to be done involving more aged hMSC primary cell preparations and reprogramming as well as redifferentiation experiments in order get more detailed insights into senescence regulation in iMSCs before applying them in regenerative therapies.

A further aspect is that features of ageing are reversed upon reprogramming according to several studies (Koch et al. 2013, Lapasset et al. 2011, Marion et al. 2009, Prigione and Adjaye 2010, Prigione et al. 2011a, Suhr et al. 2009). This puts the ageing signature detected in this study into a different angle as detected age-related gene expression signatures in iPSCs might be distorted by introduced rejuvenation-like gene expression patterns. A more thorough analysis including more iPS cell lines and further aged hMSC samples is necessary to analyse this in more detail. On the other hand the reflected gene expression patterns in iPS cells can give valuable insights into the impairment of iPS cell application in an aged context and possible ways to rejuvenate primary hMSCs in order to be applied in a more efficient way in therapies of ageing-associated diseases.

Furthermore, the transcriptional comparison between hFF-derived iPSCs and hMSC-iPSCs revealed the up-regulation of MSC-specific genes such as genes involved in osteogenesis. Remarkably, hMSC-iPSCs differentiated into osteoblasts more efficiently than hFF-derived iPSCs most probably caused by the detected higher expression of bone-related genes. These results make the existence of an MSC-specific epigenetic memory as the basis of a functional memory of hMSC-iPSCs very likely as reported by others for other cell types (Kim et al. 2010, Kim et al. 2011, Ohi et al. 2011, Polo et al. 2010, Rizzi et al. 2012).

The iMSCs generated in this study displayed typical MSC surface marker combinations and were able to differentiate into osteoblasts, adipocytes and chondrocytes in line with the study and protocol that was used for iMSC generation (Yen Shun Chen et al. 2012). Although many publications reported the generation of iMSCs from iPSCs and also from hMSC-derived iPSCs (Barberi et al. 2005, Yen Shun Chen et al. 2012, Diederichs and Tuan 2014, Frobel et al. 2014, Hong et al. 2015, Ishiy et al. 2015, Kimbrel et al. 2014, Raynaud et al. 2013, Wang et al. 2014), there are no studies on transcriptional ageing features in iMSCs derived from iPSCs of different age backgrounds at this point.

The method to derive iMSCs used in this study (Yen Shun Chen et al. 2012), is one of several described protocols (Diederichs and Tuan 2014, Frobel et al. 2014, Hong et al. 2015, Ishiy et al. 2015, Kimbrel et al. 2014, Raynaud et al. 2013, Wang et al. 2014). Which protocol yields iMSCs closest to the somatic origin remains to be determined. One study compared several derivation methods yet

could not show which one is the most feasible to generate iMSCs closes to the somatic origin (Diederichs and Tuan 2014). However, several studies have reported the reversal of ageing-associated senescence through reprogramming and subsequent redifferentiation which could only partly be confirmed in this study (Frobel et al. 2014, Lapasset et al. 2011, Miller et al. 2013). A further result, supporting the notion that donor age is reflected in iMSCs is, that iMSCs from aged hMSCs showed a lower number of colony-forming unit fibroblastoid cells (CFU-f) than fetal hMSC derived iMSCs (Figure 35). This corroborates a study describing decreased numbers of CFU-f to correlate with donor age in hMSCs (Kuzmina et al. 2015). Likewise, others have reported the detection of age-related features of the donor cells in cells re-differentiated from iPSCs (Feng et al. 2010, Suhr et al. 2009).

The results of this study confirm the hypothesis that ageing-related features are retained in iPSCs however partly contradict studies, which reported a rejuvenation of cells derived from iPSCs. As the results are from one redifferentiation experiment they have to be confirmed with more iPS cell lines from further aged donors and redifferentiation experiments.

Ageing-related features such as DNA damage and processes involved in the metabolic stability theory of ageing as well as age-related alterations of processes associated with the niche interaction were most probably reversed into a rejuvenated state underlining how useful iPS technology is to tackle ageing-associated shortfalls of aged hMSCs. The presence of genomic instabilities, oxidative DNA damage and ageing-related transcriptional patterns in iPSCs give valuable insights into potential obstacles of applications of hMSC-iPSCs and iMSCs in the therapy of elderly patients.

Furthermore, aspects of donor age seemed to be reflected in iMSCs as differential expression patterns of genes involved in the metabolic stability theory of ageing, whereas senescence of primary hMSCs was circumvented indicating that further improvement is needed before iMSCs can be applied for cell therapy of age-related diseases and personalised cell replacement therapies in patients of high age.

5 Conclusion

Comparative reprogramming revealed a decline of reprogramming efficiency with age. However, fully reprogrammed iPS cells could be generated from aged and fetal hMSCs. Moreover, aged hMSCs could only be reprogrammed with additional vitamin c in combination with other inhibitors. Comparative analysis of ageing hallmarks and donor cell specific gene expression before and after pluripotency induction and redifferentiation into iMSCs revealed the following about their reflection in the generated cell-types:

- Transcriptional changes: Transcriptomes of fetal hMSCs were more similar to hESCs than the transcriptomes of aged hMSCs and hESCs. However, after pluripotency induction the transcriptome comparison indicated no age-related differences between iPS cells of different age background. Yet, there were indications that donor age negatively influenced the similarity of iMSCs to primary hMSCs.
- Expression of ageing-associated genes: The analysis of the overlapping gene expression between aged hMSCs and the corresponding iPS indicated the retention of genes with the gene ontology ageing as well as rentention of gene expression signatures related to MSC functions. Moreover, the gene expression pattern related to ageing was more similar between iMSCs of aged background and fetal hMSCs than between the same iMSCs and aged hMSCs.
- Somatic donor cell memory: Retained MSC-specific gene expression patterns had a positive effect on the differentiation propensity of hMSC-iPSCs towards osteoblasts, which is of interest for regenerative applications.
- Senescence: Age-related differences in senescence-associated gene expression patterns were likely maintained in iMSCs even after being changed in comparison to the parental primary hMSCs upon reprogramming to iPS cells.
- Genomic stability: Ageing in hMSCs seemed to be accompagnied by karyotypic abnormalities, which most probably was retained after reprogramming. On the other hand, DNA damage seemed to depend on reprogramming technique as DNA damage was present in episomal iPS from fetal hMSCs but not in iPS cells derived with retroviruses. Moreover, expression patterns of genes involved in DNA damage repair were more fetal-like in iMSCs of aged background.
- Metabolic stability: Age-related changes according to the metabolic stability theory of ageing were reflected in part in gene expression patterns most evidently in iMSCs. Anti-oxidative processes seemed to be changed in aged hMSCs. Upon reprogramming mitochondrial and glutathione metabolism were most likely changed irrespective of age. Moreover, insulin

signalling, oxidative phosphorylation and glycolysis seemed to reflect the age of the donor in iMSCs.

- Cytoskeleton, adhesion, ECM interaction: Cytoskeleton and adhesion-related processes were very likely regulated by age in hMSCs and seemed be changed upon reprogramming in the same manner irrespective of age. In iMSCs the results suggested a reintroduction of ageing-related changes of the cytoskeleton. However, ECM interaction and adhesion-related processes seemed not to reflect the donor age in iMSCs.
- Reactive oxygen species, oxidative stress: Age-related elevation of ROS levels in hMSCs was not present after pluripotency induction. However, oxidative DNA damage could be detected in iPS cells independent from donor age. Moreover, the response to oxidative stress most likely depended on age in hMSCs and iMSC and seemed to be down regulated in iPS cells independent from age.

Higher donor age led to less efficient pluripotency induction in hMSCs. In agreement with previous studies in fibroblasts, upon reprogramming of hMSCs age-related aspects such as senescence, impaired mitochondrial metabolism, defective DNA repair, elevated oxidative stress response, decline in anti-oxidative mechanisms and changes in adhesion and cytoskeleton properties were reverted to a different most likely more immature state. However, donor age and hMSC-specific functional properties were demonstrated to be reflected in iPS cells in this study. Upon iMSC differentiation, the results indicate that most ageing hallmarks found in aged hMSCs were reintroduced. However, DNA repair and glutathione metabolism resembled a more fetal-like state in iMSCs. Therefore, iPS generation from hMSCs of aged origin is a powerful tool to circumvent senescence of primary hMSCs and to enhance their differentiation potential. Yet, donor age has to be taken into account, as it seemed to be reflected in expression signatures of iPSCs from aged donors and in iMSCs derived from hMSCs of aged background. Hence, careful evaluation of the implications for the potential use of hMSCs-derived iPS cells and iMSCs in the context of high donor age is necessary. In particular, investigations that are more detailed and involve further aged hMSC samples will help to further elucidate the implications of ageing-related features present in autologous iPS cells and iMSCs and to optimise resulting potential shortfalls concerning regenerative efficiency. This will help to pave the way for applications of of these cells in regenerative cures for the use in age-related diseases and elderly patients.

6 References

Aasen, T., Raya, A., Barrero, M. J., Garreta, E., Consiglio, A., Gonzalez, F., Vassena, R., Bilić, J., Pekarik, V., Tiscornia, G., Edel, M., Boué, S. and Izpisúa Belmonte, J. C. (2008) Efficient and rapid generation of induced pluripotent stem cells from human keratinocytes. *Nature Biotechnology, 26*(11), pp. 1276-1284.

Alves, H., Mentink, A., Le, B., van Blitterswijk, C. A. and de Boer, J. (2013) Effect of antioxidant supplementation on the total yield, oxidative stress levels, and multipotency of bone marrow-derived human mesenchymal stromal cells. *Tissue Engineering. Part A, 19*(7-8), pp. 928-937.

Amit, M., Carpenter, M. K., Inokuma, M. S., Chiu, C. P., Harris, C. P., Waknitz, M. A., Itskovitz-Eldor, J. and Thomson, J. A. (2000) Clonally derived human embryonic stem cell lines maintain pluripotency and proliferative potential for prolonged periods of culture. *Developmental Biology, 227*(2), pp. 271-278.

Aoi, T., Yae, K., Nakagawa, M., Ichisaka, T., Okita, K., Takahashi, K., Chiba, T. and Yamanaka, S. (2008) Generation of pluripotent stem cells from adult mouse liver and stomach cells. *Science (New York, N.Y.), 321*(5889), pp. 699-702.

Apostolou, E. and Hochedlinger, K. (2013) Chromatin dynamics during cellular reprogramming. *Nature, 502*(7472), pp. 462-471.

Armstrong, L., Tilgner, K., Saretzki, G., Atkinson, S. P., Stojkovic, M., Moreno, R., Przyborski, S. and Lako, M. (2010) Human induced pluripotent stem cell lines show stress defense mechanisms and mitochondrial regulation similar to those of human embryonic stem cells. *Stem Cells (Dayton, Ohio), 28*(4), pp. 661-673.

Arpornmaeklong, P., Wang, Z., Pressler, M. J., Brown, S. E. and Krebsbach, P. H. (2010) Expansion and characterization of human embryonic stem cell-derived osteoblast-like cells. *Cellular Reprogramming, 12*(4), pp. 377-389.

Ashburner, M., Ball, C. A., Blake, J. A., Botstein, D., Butler, H., Cherry, J. M., Davis, A. P., Dolinski, K., Dwight, S. S., Eppig, J. T., Harris, M. A., Hill, D. P., Issel-Tarver, L., Kasarskis, A., Lewis, S., Matese, J. C., Richardson, J. E., Ringwald, M., Rubin, G. M. and Sherlock, G. (2000) Gene Ontology: tool for the unification of biology. *Nature Genetics, 25*(1), pp. 25-29.

Aubert, G. and Lansdorp, P. M. (2008) Telomeres and aging. *Physiological Reviews, 88*(2), pp. 557-579.

Avilion, A. A., Nicolis, S. K., Pevny, L. H., Perez, L., Vivian, N. and Lovell-Badge, R. (2003) Multipotent cell lineages in early mouse development depend on SOX2 function. *Genes & Development, 17*(1), pp. 126-140.

Aylon, Y. and Oren, M. (2011) p53: guardian of ploidy. *Molecular Oncology, 5*(4), pp. 315-323.

Babaie, Y., Herwig, R., Greber, B., Brink, T. C., Wruck, W., Groth, D., Lehrach, H., Burdon, T. and Adjaye, J. (2007) Analysis of Oct4-dependent transcriptional networks regulating self-renewal and pluripotency in human embryonic stem cells. *Stem Cells (Dayton, Ohio), 25*(2), pp. 500-510.

Baird, N. A., Douglas, P. M., Simic, M. S., Grant, A. R., Moresco, J. J., Wolff, S. C., Yates, J. R., Manning, G. and Dillin, A. (2014) HSF-1-mediated cytoskeletal integrity determines thermotolerance and life span. *Science (New York, N.Y.), 346*(6207), pp. 360-363.

Bajek, A., Czerwinski, M., Olkowska, J., Gurtowska, N., Kloskowski, T. and Drewa, T. (2012) Does aging of mesenchymal stem cells limit their potential application in clinical practice? *Aging Clinical and Experimental Research, 24*(5), pp. 404-411.

Baker, N., Boyette, L. B. and Tuan, R. S. (2015) Characterization of bone marrow-derived mesenchymal stem cells in aging. *Bone, 70*, pp. 37-47.

Ban, H., Nishishita, N., Fusaki, N., Tabata, T., Saeki, K., Shikamura, M., Takada, N., Inoue, M., Hasegawa, M., Kawamata, S. and Nishikawa, S.-I. (2011) Efficient generation of transgene-free human induced pluripotent stem cells (iPSCs) by temperature-sensitive Sendai virus vectors. *Proceedings of the National Academy of Sciences, 108*(34), pp. 14234-14239.

Banfi, A., Muraglia, A., Dozin, B., Mastrogiacomo, M., Cancedda, R. and Quarto, R. (2000) Proliferation kinetics and differentiation potential of ex vivo expanded human bone marrow stromal cells: Implications for their use in cell therapy. *Experimental Hematology, 28*(6), pp. 707-715.

Banito, A., Rashid, S. T., Acosta, J. C., Li, S., Pereira, C. F., Geti, I., Pinho, S., Silva, J. C., Azuara, V., Walsh, M., Vallier, L. and Gil, J. (2009) Senescence impairs successful reprogramming to pluripotent stem cells. *Genes & Development, 23*(18), pp. 2134-2139.

Bar-Nur, O., Russ, Holger A., Efrat, S. and Benvenisty, N. (2011) Epigenetic Memory and Preferential Lineage-Specific Differentiation in Induced Pluripotent Stem Cells Derived from Human Pancreatic Islet Beta Cells. *Cell Stem Cell, 9*(1), pp. 17-23.

Bara, J. J., Richards, R. G., Alini, M. and Stoddart, M. J. (2014) Concise Review: Bone Marrow-Derived Mesenchymal Stem Cells Change Phenotype Following In Vitro Culture: Implications for Basic Research and the Clinic. *STEM CELLS, 32*(7), pp. 1713-1723.

Barberi, T., Willis, L. M., Socci, N. D. and Studer, L. (2005) Derivation of Multipotent Mesenchymal Precursors from Human Embryonic Stem Cells. *PLoS Medicine, 2*(6).

Barbet, R., Peiffer, I., Hatzfeld, A., Charbord, P. and Hatzfeld, J. A. (2011) Comparison of Gene Expression in Human Embryonic Stem Cells, hESC-Derived Mesenchymal Stem Cells and Human Mesenchymal Stem Cells. *Stem Cells International, 2011*, pp. 368192.

Baxter, M. A., Wynn, R. F., Jowitt, S. N., Wraith, J. E., Fairbairn, L. J. and Bellantuono, I. (2004) Study of telomere length reveals rapid aging of human marrow stromal cells following in vitro expansion. *Stem Cells (Dayton, Ohio), 22*(5), pp. 675-682.

Beane, O. S., Fonseca, V. C., Cooper, L. L., Koren, G. and Darling, E. M. (2014) Impact of aging on the regenerative properties of bone marrow-, muscle-, and adipose-derived mesenchymal stem/stromal cells. *PloS One, 9*(12), pp. e115963.

Beauséjour, C. (2007) Bone marrow-derived cells: the influence of aging and cellular senescence. *Handbook of Experimental Pharmacology*, (180), pp. 67-88.

Bellin, M., Marchetto, M. C., Gage, F. H. and Mummery, C. L. (2012) Induced pluripotent stem cells: the new patient? *Nature Reviews. Molecular Cell Biology, 13*(11), pp. 713-726.

Ben-David, U., Mayshar, Y. and Benvenisty, N. (2011) Large-Scale Analysis Reveals Acquisition of Lineage-Specific Chromosomal Aberrations in Human Adult Stem Cells. *Cell Stem Cell, 9*(2), pp. 97-102.

Benjamini, Y. and Hochberg, Y. (1995) Controlling the False Discovery Rate: A Practical and Powerful Approach to Multiple Testing. *Journal of the Royal Statistical Society. Series B (Methodological), 57*(1), pp. 289-300.

Bernardo, M. E., Zaffaroni, N., Novara, F., Cometa, A. M., Avanzini, M. A., Moretta, A., Montagna, D., Maccario, R., Villa, R., Daidone, M. G., Zuffardi, O. and Locatelli, F. (2007) Human Bone Marrow–Derived Mesenchymal Stem Cells Do Not Undergo Transformation after Long-term In vitro Culture and Do Not Exhibit Telomere Maintenance Mechanisms. *Cancer Research, 67*(19), pp. 9142-9149.

Bilousova, G., Jun, D. H., King, K. B., De Langhe, S., Chick, W. S., Torchia, E. C., Chow, K. S., Klemm, D. J., Roop, D. R. and Majka, S. M. (2011) Osteoblasts derived from induced pluripotent stem cells form calcified structures in scaffolds both in vitro and in vivo. *Stem Cells (Dayton, Ohio), 29*(2), pp. 206-216.

Blasco, M. A. (2007) Telomere length, stem cells and aging. *Nature Chemical Biology, 3*(10), pp. 640-649.

Bodnar, A. G., Ouellette, M., Frolkis, M., Holt, S. E., Chiu, C. P., Morin, G. B., Harley, C. B., Shay, J. W., Lichtsteiner, S. and Wright, W. E. (1998) Extension of life-span by introduction of telomerase into normal human cells. *Science (New York, N.Y.), 279*(5349), pp. 349-352.

Bonab, M. M., Alimoghaddam, K., Talebian, F., Ghaffari, S. H., Ghavamzadeh, A. and Nikbin, B. (2006) Aging of mesenchymal stem cell in vitro. *BMC cell biology, 7*, pp. 14.

Bonnans, C., Chou, J. and Werb, Z. (2014) Remodelling the extracellular matrix in development and disease. *Nature Reviews. Molecular Cell Biology, 15*(12), pp. 786-801.

Bork, S., Pfister, S., Witt, H., Horn, P., Korn, B., Ho, A. D. and Wagner, W. (2010) DNA methylation pattern changes upon long-term culture and aging of human mesenchymal stromal cells. *Aging Cell, 9*(1), pp. 54-63.

Boulting, G. L., Kiskinis, E., Croft, G. F., Amoroso, M. W., Oakley, D. H., Wainger, B. J., Williams, D. J., Kahler, D. J., Yamaki, M., Davidow, L., Rodolfa, C. T., Dimos, J. T., Mikkilineni, S., MacDermott, A. B., Woolf, C. J., Henderson, C. E., Wichterle, H. and Eggan, K. (2011) A functionally characterized test set of human induced pluripotent stem cells. *Nature Biotechnology, 29*(3), pp. 279-286.

Boyd, N. L., Robbins, K. R., Dhara, S. K., West, F. D. and Stice, S. L. (2009) Human Embryonic Stem Cell–Derived Mesoderm-like Epithelium Transitions to Mesenchymal Progenitor Cells. *Tissue Engineering. Part A, 15*(8), pp. 1897-1907.

Boyer, L. A., Lee, T. I., Cole, M. F., Johnstone, S. E., Levine, S. S., Zucker, J. P., Guenther, M. G., Kumar, R. M., Murray, H. L., Jenner, R. G., Gifford, D. K., Melton, D. A., Jaenisch, R. and Young, R. A. (2005) Core transcriptional regulatory circuitry in human embryonic stem cells. *Cell, 122*(6), pp. 947-956.

Brink, T. C., Demetrius, L., Lehrach, H. and Adjaye, J. (2009) Age-related transcriptional changes in gene expression in different organs of mice support the metabolic stability theory of aging. *Biogerontology, 10*(5), pp. 549-564.

Buganim, Y., Faddah, D. A., Cheng, A. W., Itskovich, E., Markoulaki, S., Ganz, K., Klemm, S. L., van Oudenaarden, A. and Jaenisch, R. (2012) Single-cell expression analyses during cellular reprogramming reveal an early stochastic and a late hierarchic phase. *Cell, 150*(6), pp. 1209-1222.

Buganim, Y., Markoulaki, S., van Wietmarschen, N., Hoke, H., Wu, T., Ganz, K., Akhtar-Zaidi, B., He, Y., Abraham, B. J., Porubsky, D., Kulenkampff, E., Faddah, D. A., Shi, L., Gao, Q., Sarkar, S., Cohen, M., Goldmann, J., Nery, J. R., Schultz, M. D., Ecker, J. R., Xiao, A., Young, R. A., Lansdorp, P. M. and Jaenisch, R. (2014) The developmental potential of iPSCs is greatly influenced by reprogramming factor selection. *Cell Stem Cell, 15*(3), pp. 295-309.

Bustos, M. L., Huleihel, L., Kapetanaki, M. G., Lino-Cardenas, C. L., Mroz, L., Ellis, B. M., McVerry, B. J., Richards, T. J., Kaminski, N., Cerdenes, N., Mora, A. L. and Rojas, M. (2014) Aging Mesenchymal Stem Cells Fail to Protect Because of Impaired Migration and Antiinflammatory Response. *American Journal of Respiratory and Critical Care Medicine, 189*(7), pp. 787-798.

Calloni, R., Cordero, E. A. A., Henriques, J. A. P. and Bonatto, D. (2013) Reviewing and Updating the Major Molecular Markers for Stem Cells. *Stem Cells and Development, 22*(9), pp. 1455-1476.

Campagnoli, C., Roberts, I. A., Kumar, S., Bennett, P. R., Bellantuono, I. and Fisk, N. M. (2001) Identification of mesenchymal stem/progenitor cells in human first-trimester fetal blood, liver, and bone marrow. *Blood, 98*(8), pp. 2396-2402.

Campagnoli, C., Roberts, I. A. G., Kumar, S., Choolani, M., Bennett, P. R., Letsky, E. and Fisk, N. M. (2002) Expandability of haemopoietic progenitors in first trimester fetal and maternal blood: implications for non-invasive prenatal diagnosis. *Prenatal Diagnosis, 22*(6), pp. 463-469.

Campisi, J. (2011) Cellular senescence: putting the paradoxes in perspective. *Current Opinion in Genetics & Development, 21*(1), pp. 107-112.

Caplan, A. I. (1991) Mesenchymal stem cells. *Journal of Orthopaedic Research: Official Publication of the Orthopaedic Research Society, 9*(5), pp. 641-650.

Caplan, A. I. (2005) Review: mesenchymal stem cells: cell-based reconstructive therapy in orthopedics. *Tissue Engineering, 11*(7-8), pp. 1198-1211.

Caplan, A. I. (2009) Why are MSCs therapeutic? New data: new insight. *The Journal of Pathology, 217*(2), pp. 318-324.

Chambers, I., Colby, D., Robertson, M., Nichols, J., Lee, S., Tweedie, S. and Smith, A. (2003) Functional expression cloning of Nanog, a pluripotency sustaining factor in embryonic stem cells. *Cell, 113*(5), pp. 643-655.

Chan, Y. S., Yang, L. and Ng, H.-H. (2011) Transcriptional regulatory networks in embryonic stem cells. *Progress in Drug Research. Fortschritte Der Arzneimittelforschung. Progrès Des Recherches Pharmaceutiques, 67*, pp. 239-252.

Chen, G., Gulbranson, D. R., Hou, Z., Bolin, J. M., Ruotti, V., Probasco, M. D., Smuga-Otto, K., Howden, S. E., Diol, N. R., Propson, N. E., Wagner, R., Lee, G. O., Antosiewicz-Bourget, J., Teng, J. M. C. and Thomson, J. A. (2011) Chemically defined conditions for human iPSC derivation and culture. *Nature Methods, 8*(5), pp. 424-429.

Chen, J., Liu, H., Liu, J., Qi, J., Wei, B., Yang, J., Liang, H., Chen, Y., Chen, J., Wu, Y., Guo, L., Zhu, J., Zhao, X., Peng, T., Zhang, Y., Chen, S., Li, X., Li, D., Wang, T. and Pei, D. (2013) H3K9 methylation is a barrier during somatic cell reprogramming into iPSCs. *Nature Genetics, 45*(1), pp. 34-42.

Chen, T., Shen, L., Yu, J., Wan, H., Guo, A., Chen, J., Long, Y., Zhao, J. and Pei, G. (2011) Rapamycin and other longevity-promoting compounds enhance the generation of mouse induced pluripotent stem cells. *Aging Cell, 10*(5), pp. 908-911.

Chen, X., Yin, Z., Chen, J.-l., Shen, W.-l., Liu, H.-h., Tang, Q.-m., Fang, Z., Lu, L.-r., Ji, J. and Ouyang, H.-w. (2012) Force and scleraxis synergistically promote the commitment of human ES cells derived MSCs to tenocytes. *Scientific Reports, 2*, pp. 977.

Chen, Y. S., Pelekanos, R. A., Ellis, R. L., Horne, R., Wolvetang, E. J. and Fisk, N. M. (2012) Small molecule mesengenic induction of human induced pluripotent stem cells to generate mesenchymal stem/stromal cells. *Stem Cells Translational Medicine, 1*(2), pp. 83-95.

Cheng, Z., Ito, S., Nishio, N., Xiao, H., Zhang, R., Suzuki, H., Okawa, Y., Murohara, T. and Isobe, K.-I. (2011) Establishment of induced pluripotent stem cells from aged mice using bone marrow-derived myeloid cells. *Journal of Molecular Cell Biology, 3*(2), pp. 91-98.

Cheung, K. S. C., Sposito, N., Stumpf, P. S., Wilson, D. I., Sanchez-Elsner, T. and Oreffo, R. O. C. (2014) MicroRNA-146a Regulates Human Foetal Femur Derived Skeletal Stem Cell Differentiation by Down-Regulating SMAD2 and SMAD3. *PloS One, 9*(6).

Cho, Y. M., Kwon, S., Pak, Y. K., Seol, H. W., Choi, Y. M., Park, D. J., Park, K. S. and Lee, H. K. (2006) Dynamic changes in mitochondrial biogenesis and antioxidant enzymes during the spontaneous differentiation of human embryonic stem cells. *Biochemical and Biophysical Research Communications, 348*(4), pp. 1472-1478.

Choi, H. R., Cho, K. A., Kang, H. T., Lee, J. B., Kaeberlein, M., Suh, Y., Chung, I. K. and Park, S. C. (2011) Restoration of senescent human diploid fibroblasts by modulation of the extracellular matrix. *Aging Cell, 10*(1), pp. 148-157.

Chou, B.-K., Mali, P., Huang, X., Ye, Z., Dowey, S. N., Resar, L. M., Zou, C., Zhang, Y. A., Tong, J. and Cheng, L. (2011) Efficient human iPS cell derivation by a non-integrating plasmid from blood cells with unique epigenetic and gene expression signatures. *Cell Research, 21*(3), pp. 518-529.

Choudhery, M. S., Khan, M., Mahmood, R., Mehmood, A., Khan, S. N. and Riazuddin, S. (2012) Bone marrow derived mesenchymal stem cells from aged mice have reduced wound healing, angiogenesis, proliferation and anti-apoptosis capabilities. *Cell Biology International, 36*(8), pp. 747-753.

Collado, M., Blasco, M. A. and Serrano, M. (2007) Cellular senescence in cancer and aging. *Cell, 130*(2), pp. 223-233.

Collart-Dutilleul, P.-Y., Chaubron, F., De Vos, J. and Cuisinier, F. J. (2015) Allogenic banking of dental pulp stem cells for innovative therapeutics. *World Journal of Stem Cells, 7*(7), pp. 1010-1021.

Colony Forming Unit Assays for MSCs - Springer. in (2008) Prockop, D. J., Bunnell, B. A. and Phinney, D. G., (eds.): Humana Press.

Crisan, M., Chen, C.-W., Corselli, M., Andriolo, G., Lazzari, L. and Péault, B. (2009) Perivascular multipotent progenitor cells in human organs. *Annals of the New York Academy of Sciences, 1176*, pp. 118-123.

Cuddihy, A. R. and O'Connell, M. J. (2003) Cell-cycle responses to DNA damage in G2. *International Review of Cytology, 222*, pp. 99-140.

Curran, S. P. and Ruvkun, G. (2007) Lifespan regulation by evolutionarily conserved genes essential for viability. *PLoS genetics, 3*(4), pp. e56.

da Silva Meirelles, L., Chagastelles, P. C. and Nardi, N. B. (2006) Mesenchymal stem cells reside in virtually all post-natal organs and tissues. *Journal of Cell Science, 119*(Pt 11), pp. 2204-2213.

Daley, G. Q. (2014) Deriving blood stem cells from pluripotent stem cells for research and therapy. *Best Practice & Research Clinical Haematology, 27*(3–4), pp. 293-297.

Dannenmann, B., Lehle, S., Hildebrand, D. G., Kübler, A., Grondona, P., Schmid, V., Holzer, K., Fröschl, M., Essmann, F., Rothfuss, O. and Schulze-Osthoff, K. (2015) High glutathione and glutathione peroxidase-2 levels mediate cell-type-specific DNA damage protection in human induced pluripotent stem cells. *Stem Cell Reports, 4*(5), pp. 886-898.

Davidson, K. C., Adams, A. M., Goodson, J. M., McDonald, C. E., Potter, J. C., Berndt, J. D., Biechele, T. L., Taylor, R. J. and Moon, R. T. (2012) Wnt/β-catenin signaling promotes differentiation, not self-renewal, of human embryonic stem cells and is repressed by Oct4. *Proceedings of the National Academy of Sciences of the United States of America, 109*(12), pp. 4485-4490.

de Andrés, M. C., Kingham, E., Imagawa, K., Gonzalez, A., Roach, H. I., Wilson, D. I. and Oreffo, R. O. C. (2013) Epigenetic Regulation during Fetal Femur Development: DNA Methylation Matters. *PloS One, 8*(1).

de Magalhães, J. P. (2014) The scientific quest for lasting youth: prospects for curing aging. *Rejuvenation Research, 17*(5), pp. 458-467.

de Peppo, G. M., Svensson, S., Lennerås, M., Synnergren, J., Stenberg, J., Strehl, R., Hyllner, J., Thomsen, P. and Karlsson, C. (2010) Human embryonic mesodermal progenitors highly resemble human mesenchymal stem cells and display high potential for tissue engineering applications. *Tissue Engineering. Part A, 16*(7), pp. 2161-2182.

Demetrius, L. (2004) Caloric restriction, metabolic rate, and entropy. *The Journals of Gerontology. Series A, Biological Sciences and Medical Sciences, 59*(9), pp. B902-915.

Deyle, D. R., Khan, I. F., Ren, G., Wang, P.-R., Kho, J., Schwarze, U. and Russell, D. W. (2012) Normal collagen and bone production by gene-targeted human osteogenesis imperfecta iPSCs. *Molecular Therapy: The Journal of the American Society of Gene Therapy, 20*(1), pp. 204-213.

Diederichs, S. and Tuan, R. S. (2014) Functional comparison of human-induced pluripotent stem cell-derived mesenchymal cells and bone marrow-derived mesenchymal stromal cells from the same donor. *Stem Cells and Development, 23*(14), pp. 1594-1610.

Dimos, J. T., Rodolfa, K. T., Niakan, K. K., Weisenthal, L. M., Mitsumoto, H., Chung, W., Croft, G. F., Saphier, G., Leibel, R., Goland, R., Wichterle, H., Henderson, C. E. and Eggan, K. (2008)

Induced pluripotent stem cells generated from patients with ALS can be differentiated into motor neurons. *Science (New York, N.Y.), 321*(5893), pp. 1218-1221.

Dimri, G. P., Lee, X., Basile, G., Acosta, M., Scott, G., Roskelley, C., Medrano, E. E., Linskens, M., Rubelj, I. and Pereira-Smith, O. (1995) A biomarker that identifies senescent human cells in culture and in aging skin in vivo. *Proceedings of the National Academy of Sciences, 92*(20), pp. 9363-9367.

Dominici, M., Le Blanc, K., Mueller, I., Slaper-Cortenbach, I., Marini, F., Krause, D., Deans, R., Keating, A., Prockop, D. and Horwitz, E. (2006a) Minimal criteria for defining multipotent mesenchymal stromal cells. The International Society for Cellular Therapy position statement. *Cytotherapy, 8*(4), pp. 315-317.

Eghbali-Fatourechi, G. Z., Lamsam, J., Fraser, D., Nagel, D., Riggs, B. L. and Khosla, S. (2005) Circulating Osteoblast-Lineage Cells in Humans. *New England Journal of Medicine, 352*(19), pp. 1959-1966.

El-Serafi, A. T., Wilson, D. I., Roach, H. I. and Oreffo, R. O. (2011) Developmental plasticity of human foetal femur-derived cells in pellet culture: self assembly of an osteoid shell around a cartilaginous core. *European Cells & Materials, 21*, pp. 558-567.

Erices, A., Conget, P. and Minguell, J. J. (2000) Mesenchymal progenitor cells in human umbilical cord blood. *British Journal of Haematology, 109*(1), pp. 235-242.

Escacena, N., Quesada-Hernández, E., Capilla-Gonzalez, V., Soria, B. and Hmadcha, A. (2015) Bottlenecks in the Efficient Use of Advanced Therapy Medicinal Products Based on Mesenchymal Stromal Cells. *Stem Cells International, 2015*.

Esteban, M. A., Wang, T., Qin, B., Yang, J., Qin, D., Cai, J., Li, W., Weng, Z., Chen, J., Ni, S., Chen, K., Li, Y., Liu, X., Xu, J., Zhang, S., Li, F., He, W., Labuda, K., Song, Y., Peterbauer, A., Wolbank, S., Redl, H., Zhong, M., Cai, D., Zeng, L. and Pei, D. (2010) Vitamin C enhances the generation of mouse and human induced pluripotent stem cells. *Cell Stem Cell, 6*(1), pp. 71-79.

Estrada, J. C., Albo, C., Benguría, A., Dopazo, A., López-Romero, P., Carrera-Quintanar, L., Roche, E., Clemente, E. P., Enríquez, J. A., Bernad, A. and Samper, E. (2012) Culture of human mesenchymal stem cells at low oxygen tension improves growth and genetic stability by activating glycolysis. *Cell Death and Differentiation, 19*(5), pp. 743-755.

Evans, M. J. and Kaufman, M. H. (1981) Establishment in culture of pluripotential cells from mouse embryos. *Nature, 292*(5819), pp. 154-156.

Faggioli, F., Wang, T., Vijg, J. and Montagna, C. (2012) Chromosome-specific accumulation of aneuploidy in the aging mouse brain. *Human Molecular Genetics, 21*(24), pp. 5246-5253.

Fan, J., Robert, C., Jang, Y.-Y., Liu, H., Sharkis, S., Baylin, S. B. and Rassool, F. V. (2011) Human induced pluripotent cells resemble embryonic stem cells demonstrating enhanced levels of DNA repair and efficacy of nonhomologous end-joining. *Mutation Research, 713*(1-2), pp. 8-17.

Fan, M., Chen, W., Liu, W., Du, G.-Q., Jiang, S.-L., Tian, W.-C., Sun, L., Li, R.-K. and Tian, H. (2010) The Effect of Age on the Efficacy of Human Mesenchymal Stem Cell Transplantation after a Myocardial Infarction. *Rejuvenation Research, 13*(4), pp. 429-438.

Feng, Q., Lu, S.-J., Klimanskaya, I., Gomes, I., Kim, D., Chung, Y., Honig, G. R., Kim, K.-S. and Lanza, R. (2010) Hemangioblastic derivatives from human induced pluripotent stem cells exhibit limited expansion and early senescence. *Stem Cells (Dayton, Ohio), 28*(4), pp. 704-712.

Filareto, A., Parker, S., Darabi, R., Borges, L., Iacovino, M., Schaaf, T., Mayerhofer, T., Chamberlain, J. S., Ervasti, J. M., McIvor, R. S., Kyba, M. and Perlingeiro, R. C. R. (2013) An ex vivo gene therapy approach to treat muscular dystrophy using inducible pluripotent stem cells. *Nature Communications, 4*, pp. 1549.

Folmes, C. D. L., Martinez-Fernandez, A., Faustino, R. S., Yamada, S., Perez-Terzic, C., Nelson, T. J. and Terzic, A. (2013) Nuclear reprogramming with c-Myc potentiates glycolytic capacity of derived induced pluripotent stem cells. *Journal of Cardiovascular Translational Research, 6*(1), pp. 10-21.

Fontana, L., Partridge, L. and Longo, V. D. (2010) Extending healthy life span--from yeast to humans. *Science (New York, N.Y.), 328*(5976), pp. 321-326.

Forsberg, L. A., Rasi, C., Razzaghian, H. R., Pakalapati, G., Waite, L., Thilbeault, K. S., Ronowicz, A., Wineinger, N. E., Tiwari, H. K., Boomsma, D., Westerman, M. P., Harris, J. R., Lyle, R., Essand, M., Eriksson, F., Assimes, T. L., Iribarren, C., Strachan, E., O'Hanlon, T. P., Rider, L. G., Miller, F. W., Giedraitis, V., Lannfelt, L., Ingelsson, M., Piotrowski, A., Pedersen, N. L., Absher, D. and Dumanski, J. P. (2012) Age-related somatic structural changes in the nuclear genome of human blood cells. *American Journal of Human Genetics, 90*(2), pp. 217-228.

Foudah, D., Redaelli, S., Donzelli, E., Bentivegna, A., Miloso, M., Dalprà, L. and Tredici, G. (2009) Monitoring the genomic stability of in vitro cultured rat bone-marrow-derived mesenchymal stem cells. *Chromosome Research, 17*(8), pp. 1025-1039.

Frenette, P. S., Pinho, S., Lucas, D. and Scheiermann, C. (2013) Mesenchymal Stem Cell: Keystone of the Hematopoietic Stem Cell Niche and a Stepping-Stone for Regenerative Medicine. *Annual Review of Immunology, 31*(1), pp. 285-316.

Friedenstein, A. J., Deriglasova, U. F., Kulagina, N. N., Panasuk, A. F., Rudakowa, S. F., Luriá, E. A. and Ruadkow, I. A. (1974) Precursors for fibroblasts in different populations of hematopoietic cells as detected by the in vitro colony assay method. *Experimental Hematology, 2*(2), pp. 83-92.

Friedenstein, A. J., Petrakova, K. V., Kurolesova, A. I. and Frolova, G. P. (1968) Heterotopic of bone marrow. Analysis of precursor cells for osteogenic and hematopoietic tissues. *Transplantation, 6*(2), pp. 230-247.

Frobel, J., Hemeda, H., Lenz, M., Abagnale, G., Joussen, S., Denecke, B., Sarić, T., Zenke, M. and Wagner, W. (2014) Epigenetic rejuvenation of mesenchymal stromal cells derived from induced pluripotent stem cells. *Stem Cell Reports, 3*(3), pp. 414-422.

Fukuta, M., Nakai, Y., Kirino, K., Nakagawa, M., Sekiguchi, K., Nagata, S., Matsumoto, Y., Yamamoto, T., Umeda, K., Heike, T., Okumura, N., Koizumi, N., Sato, T., Nakahata, T., Saito, M., Otsuka, T., Kinoshita, S., Ueno, M., Ikeya, M. and Toguchida, J. (2014) Derivation of mesenchymal stromal cells from pluripotent stem cells through a neural crest lineage using small molecule compounds with defined media. *PloS One, 9*(12), pp. e112291.

Fusaki, N., Ban, H., Nishiyama, A., Saeki, K. and Hasegawa, M. (2009) Efficient induction of transgene-free human pluripotent stem cells using a vector based on Sendai virus, an RNA

virus that does not integrate into the host genome. *Proceedings of the Japan Academy, Series B, 85*(8), pp. 348-362.

Galende, E., Karakikes, I., Edelmann, L., Desnick, R. J., Kerenyi, T., Khoueiry, G., Lafferty, J., McGinn, J. T., Brodman, M., Fuster, V., Hajjar, R. J. and Polgar, K. (2010) Amniotic fluid cells are more efficiently reprogrammed to pluripotency than adult cells. *Cellular Reprogramming, 12*(2), pp. 117-125.

Galvin, K. E., Travis, E. D., Yee, D., Magnuson, T. and Vivian, J. L. (2010) Nodal Signaling Regulates the Bone Morphogenic Protein Pluripotency Pathway in Mouse Embryonic Stem Cells. *Journal of Biological Chemistry, 285*(26), pp. 19747-19756.

Gao, Y., Yang, L., Chen, L., Wang, X., Wu, H., Ai, Z., Du, J., Liu, Y., Shi, X., Wu, Y., Guo, Z. and Zhang, Y. (2013) Vitamin C facilitates pluripotent stem cell maintenance by promoting pluripotency gene transcription. *Biochimie, 95*(11), pp. 2107-2113.

Garinis, G. A., van der Horst, G. T. J., Vijg, J. and Hoeijmakers, J. H. J. (2008) DNA damage and ageing: new-age ideas for an age-old problem. *Nature Cell Biology, 10*(11), pp. 1241-1247.

Geissler, S., Textor, M., Kühnisch, J., Könnig, D., Klein, O., Ode, A., Pfitzner, T., Adjaye, J., Kasper, G. and Duda, G. N. (2012) Functional comparison of chronological and in vitro aging: differential role of the cytoskeleton and mitochondria in mesenchymal stromal cells. *PloS One, 7*(12), pp. e52700.

Geissler, S., Textor, M., Schmidt-Bleek, K., Klein, O., Thiele, M., Ellinghaus, A., Jacobi, D., Ode, A., Perka, C., Dienelt, A., Klose, J., Kasper, G., Duda, G. N. and Strube, P. (2013) In serum veritas-in serum sanitas? Cell non-autonomous aging compromises differentiation and survival of mesenchymal stromal cells via the oxidative stress pathway. *Cell Death & Disease, 4*, pp. e970.

Gharibi, B., Farzadi, S., Ghuman, M. and Hughes, F. J. (2014) Inhibition of Akt/mTOR attenuates age-related changes in mesenchymal stem cells. *Stem Cells (Dayton, Ohio), 32*(8), pp. 2256-2266.

Ghule, P. N., Medina, R., Lengner, C. J., Mandeville, M., Qiao, M., Dominski, Z., Lian, J. B., Stein, J. L., van Wijnen, A. J. and Stein, G. S. (2011) Reprogramming the pluripotent cell cycle: restoration of an abbreviated G1 phase in human induced pluripotent stem (iPS) cells. *Journal of Cellular Physiology, 226*(5), pp. 1149-1156.

Gładych, M., Andrzejewska, A., Oleksiewicz, U. and Estécio, M. R. H. (2015) Epigenetic mechanisms of induced pluripotency. *Contemporary Oncology (Poznań, Poland), 19*(1A), pp. A30-38.

Gokoh, M., Nishio, M., Nakamura, N., Matsuyama, S., Nakahara, M., Suzuki, S., Mitsumoto, M., Akutsu, H., Umezawa, A., Yasuda, K., Yuo, A. and Saeki, K. (2011) Early senescence is not an inevitable fate of human-induced pluripotent stem-derived cells. *Cellular Reprogramming, 13*(4), pp. 361-370.

Golpanian, S., El-Khorazaty, J., Mendizabal, A., DiFede, D. L., Suncion, V. Y., Karantalis, V., Fishman, J. E., Ghersin, E., Balkan, W. and Hare, J. M. (2015) Effect of aging on human mesenchymal stem cell therapy in ischemic cardiomyopathy patients. *Journal of the American College of Cardiology, 65*(2), pp. 125-132.

González, F., Georgieva, D., Vanoli, F., Shi, Z.-D., Stadtfeld, M., Ludwig, T., Jasin, M. and Huangfu, D. (2013) Homologous recombination DNA repair genes play a critical role in reprogramming to a pluripotent state. *Cell Reports, 3*(3), pp. 651-660.

González, M. A., Gonzalez-Rey, E., Rico, L., Büscher, D. and Delgado, M. (2009) Treatment of experimental arthritis by inducing immune tolerance with human adipose-derived mesenchymal stem cells. *Arthritis and Rheumatism, 60*(4), pp. 1006-1019.

Gore, A., Li, Z., Fung, H.-L., Young, J. E., Agarwal, S., Antosiewicz-Bourget, J., Canto, I., Giorgetti, A., Israel, M. A., Kiskinis, E., Lee, J.-H., Loh, Y.-H., Manos, P. D., Montserrat, N., Panopoulos, A. D., Ruiz, S., Wilbert, M. L., Yu, J., Kirkness, E. F., Izpisua Belmonte, J. C., Rossi, D. J., Thomson, J. A., Eggan, K., Daley, G. Q., Goldstein, L. S. B. and Zhang, K. (2011) Somatic coding mutations in human induced pluripotent stem cells. *Nature, 471*(7336), pp. 63-67.

Greber, B., Lehrach, H. and Adjaye, J. (2007) Fibroblast growth factor 2 modulates transforming growth factor beta signaling in mouse embryonic fibroblasts and human ESCs (hESCs) to support hESC self-renewal. *Stem Cells (Dayton, Ohio), 25*(2), pp. 455-464.

Green, D. R., Galluzzi, L. and Kroemer, G. (2011) Mitochondria and the autophagy-inflammation-cell death axis in organismal aging. *Science (New York, N.Y.), 333*(6046), pp. 1109-1112.

Gregg, S. Q., Gutiérrez, V., Robinson, A. R., Woodell, T., Nakao, A., Ross, M. A., Michalopoulos, G. K., Rigatti, L., Rothermel, C. E., Kamileri, I., Garinis, G. A., Stolz, D. B. and Niedernhofer, L. J. (2012) A mouse model of accelerated liver aging caused by a defect in DNA repair. *Hepatology (Baltimore, Md.), 55*(2), pp. 609-621.

Gronthos, S., Mankani, M., Brahim, J., Robey, P. G. and Shi, S. (2000) Postnatal human dental pulp stem cells (DPSCs) in vitro and in vivo. *Proceedings of the National Academy of Sciences of the United States of America, 97*(25), pp. 13625-13630.

Gruenloh, W., Kambal, A., Sondergaard, C., McGee, J., Nacey, C., Kalomoiris, S., Pepper, K., Olson, S., Fierro, F. and Nolta, J. A. (2011) Characterization and in vivo testing of mesenchymal stem cells derived from human embryonic stem cells. *Tissue Engineering. Part A, 17*(11-12), pp. 1517-1525.

Guillot, P. V., Gotherstrom, C., Chan, J., Kurata, H. and Fisk, N. M. (2007) Human first-trimester fetal MSC express pluripotency markers and grow faster and have longer telomeres than adult MSC. *Stem Cells (Dayton, Ohio), 25*(3), pp. 646-654.

Guillot, P. V., O'Donoghue, K., Kurata, H. and Fisk, N. M. (2006) Fetal stem cells: betwixt and between. *Seminars in Reproductive Medicine, 24*(5), pp. 340-347.

Gupta, M. K., Teo, A. K. K., Rao, T. N., Bhatt, S., Kleinridders, A., Shirakawa, J., Takatani, T., Hu, J., De Jesus, D. F., Windmueller, R., Wagers, A. J. and Kulkarni, R. N. (2015) Excessive Cellular Proliferation Negatively Impacts Reprogramming Efficiency of Human Fibroblasts. *Stem Cells Translational Medicine*.

Hacia, J. G., Lee, C. C. I., Jimenez, D. F., Karaman, M. W., Ho, V. V., Siegmund, K. D. and Tarantal, A. F. (2008) Age-related gene expression profiles of rhesus monkey bone marrow-derived mesenchymal stem cells. *Journal of Cellular Biochemistry, 103*(4), pp. 1198-1210.

Hajizadeh-Saffar, E., Tahamtani, Y., Aghdami, N., Azadmanesh, K., Habibi-Anbouhi, M., Heremans, Y., De Leu, N., Heimberg, H., Ravassard, P., Shokrgozar, M. A. and Baharvand, H. (2015)

Inducible VEGF expression by human embryonic stem cell-derived mesenchymal stromal cells reduces the minimal islet mass required to reverse diabetes. *Scientific Reports, 5*, pp. 9322.

Hämäläinen, R. H., Ahlqvist, K. J., Ellonen, P., Lepistö, M., Logan, A., Otonkoski, T., Murphy, M. P. and Suomalainen, A. (2015) mtDNA Mutagenesis Disrupts Pluripotent Stem Cell Function by Altering Redox Signaling. *Cell Reports, 11*(10), pp. 1614-1624.

Hanna, J., Saha, K., Pando, B., van Zon, J., Lengner, C. J., Creyghton, M. P., van Oudenaarden, A. and Jaenisch, R. (2009) Direct cell reprogramming is a stochastic process amenable to acceleration. *Nature, 462*(7273), pp. 595-601.

Hanna, J., Wernig, M., Markoulaki, S., Sun, C.-W., Meissner, A., Cassady, J. P., Beard, C., Brambrink, T., Wu, L.-C., Townes, T. M. and Jaenisch, R. (2007) Treatment of sickle cell anemia mouse model with iPS cells generated from autologous skin. *Science (New York, N.Y.), 318*(5858), pp. 1920-1923.

Hanna, J. H., Saha, K. and Jaenisch, R. (2010) Pluripotency and cellular reprogramming: facts, hypotheses, unresolved issues. *Cell, 143*(4), pp. 508-525.

Harman, D. (1965) THE FREE RADICAL THEORY OF AGING: EFFECT OF AGE ON SERUM COPPER LEVELS. *Journal of Gerontology, 20*, pp. 151-153.

Hart, A. H., Hartley, L., Ibrahim, M. and Robb, L. (2004) Identification, cloning and expression analysis of the pluripotency promoting Nanog genes in mouse and human. *Developmental Dynamics: An Official Publication of the American Association of Anatomists, 230*(1), pp. 187-198.

Hashizume, O., Ohnishi, S., Mito, T., Shimizu, A., Iashikawa, K., Nakada, K., Soda, M., Mano, H., Togayachi, S., Miyoshi, H., Okita, K. and Hayashi, J.-I. (2015) Epigenetic regulation of the nuclear-coded GCAT and SHMT2 genes confers human age-associated mitochondrial respiration defects. *Scientific Reports, 5*, pp. 10434.

Hay, D. C., Sutherland, L., Clark, J. and Burdon, T. (2004) Oct-4 knockdown induces similar patterns of endoderm and trophoblast differentiation markers in human and mouse embryonic stem cells. *Stem Cells (Dayton, Ohio), 22*(2), pp. 225-235.

Hayflick, L. and Moorhead, P. S. (1961) The serial cultivation of human diploid cell strains. *Experimental Cell Research, 25*, pp. 585-621.

Himeno, T., Kamiya, H., Naruse, K., Cheng, Z., Ito, S., Kondo, M., Okawa, T., Fujiya, A., Kato, J., Suzuki, H., Kito, T., Hamada, Y., Oiso, Y., Isobe, K. and Nakamura, J. (2013) Mesenchymal stem cell-like cells derived from mouse induced pluripotent stem cells ameliorate diabetic polyneuropathy in mice. *BioMed Research International, 2013*, pp. 259187.

Holzwarth, C., Vaegler, M., Gieseke, F., Pfister, S. M., Handgretinger, R., Kerst, G. and Müller, I. (2010) Low physiologic oxygen tensions reduce proliferation and differentiation of human multipotent mesenchymal stromal cells. *BMC cell biology, 11*, pp. 11.

Hong, H., Takahashi, K., Ichisaka, T., Aoi, T., Kanagawa, O., Nakagawa, M., Okita, K. and Yamanaka, S. (2009) Suppression of induced pluripotent stem cell generation by the p53-p21 pathway. *Nature, 460*(7259), pp. 1132-1135.

Hong, K.-S., Bae, D., Choi, Y., Kang, S.-W., Moon, S.-H., Lee, H. T. and Chung, H.-M. (2014) A Porous Membrane-Mediated Isolation of Mesenchymal Stem Cells from Human Embryonic Stem Cells. *Tissue Engineering Part C: Methods, 21*(3), pp. 322-329.

Hong, K.-S., Bae, D., Choi, Y., Kang, S.-W., Moon, S.-H., Lee, H. T. and Chung, H.-M. (2015) A porous membrane-mediated isolation of mesenchymal stem cells from human embryonic stem cells. *Tissue Engineering. Part C, Methods, 21*(3), pp. 322-329.

Horvath, S. (2013) DNA methylation age of human tissues and cell types. *Genome Biology, 14*(10), pp. R115.

Hossini, A. M., Megges, M., Prigione, A., Lichtner, B., Toliat, M. R., Wruck, W., Schröter, F., Nuernberg, P., Kroll, H., Makrantonaki, E., Zouboulis, C. C., Zoubouliss, C. C. and Adjaye, J. (2015) Induced pluripotent stem cell-derived neuronal cells from a sporadic Alzheimer's disease donor as a model for investigating AD-associated gene regulatory networks. *BMC genomics, 16*, pp. 84.

Hou, P., Li, Y., Zhang, X., Liu, C., Guan, J., Li, H., Zhao, T., Ye, J., Yang, W., Liu, K., Ge, J., Xu, J., Zhang, Q., Zhao, Y. and Deng, H. (2013) Pluripotent Stem Cells Induced from Mouse Somatic Cells by Small-Molecule Compounds. *Science, 341*(6146), pp. 651-654.

Hu, G.-W., Li, Q., Niu, X., Hu, B., Liu, J., Zhou, S.-M., Guo, S.-C., Lang, H.-L., Zhang, C.-Q., Wang, Y. and Deng, Z.-F. (2015) Exosomes secreted by human-induced pluripotent stem cell-derived mesenchymal stem cells attenuate limb ischemia by promoting angiogenesis in mice. *Stem Cell Research & Therapy, 6*(1), pp. 10.

Hu, J., Smith, L. A., Feng, K., Liu, X., Sun, H. and Ma, P. X. (2010) Response of human embryonic stem cell-derived mesenchymal stem cells to osteogenic factors and architectures of materials during in vitro osteogenesis. *Tissue Engineering. Part A, 16*(11), pp. 3507-3514.

Hu, K. and Slukvin, I. (2013) Generation of transgene-free iPSC lines from human normal and neoplastic blood cells using episomal vectors. *Methods in Molecular Biology (Clifton, N.J.), 997*, pp. 163-176.

Hu, K., Yu, J., Suknuntha, K., Tian, S., Montgomery, K., Choi, K.-D., Stewart, R., Thomson, J. A. and Slukvin, I. I. (2011) Efficient generation of transgene-free induced pluripotent stem cells from normal and neoplastic bone marrow and cord blood mononuclear cells. *Blood, 117*(14), pp. e109-e119.

Hu, X., Zhang, L., Mao, S.-Q., Li, Z., Chen, J., Zhang, R.-R., Wu, H.-P., Gao, J., Guo, F., Liu, W., Xu, G.-F., Dai, H.-Q., Shi, Yujiang G., Li, X., Hu, B., Tang, F., Pei, D. and Xu, G.-L. (2014) Tet and TDG Mediate DNA Demethylation Essential for Mesenchymal-to-Epithelial Transition in Somatic Cell Reprogramming. *Cell Stem Cell, 14*(4), pp. 512-522.

Huang, D. W., Sherman, B. T. and Lempicki, R. A. (2009) Systematic and integrative analysis of large gene lists using DAVID bioinformatics resources. *Nature Protocols, 4*(1), pp. 44-57.

Huangfu, D., Maehr, R., Guo, W., Eijkelenboom, A., Snitow, M., Chen, A. E. and Melton, D. A. (2008a) Induction of pluripotent stem cells by defined factors is greatly improved by small-molecule compounds. *Nature Biotechnology, 26*(7), pp. 795-797.

Huangfu, D., Osafune, K., Maehr, R., Guo, W., Eijkelenboom, A., Chen, S., Muhlestein, W. and Melton, D. A. (2008b) Induction of pluripotent stem cells from primary human fibroblasts with only Oct4 and Sox2. *Nature Biotechnology, 26*(11), pp. 1269-1275.

Hug, K. and Hermerén, G. (2011) Do we still need human embryonic stem cells for stem cell-based therapies? Epistemic and ethical aspects. *Stem Cell Reviews, 7*(4), pp. 761-774.

Hussein, S. M., Batada, N. N., Vuoristo, S., Ching, R. W., Autio, R., Närvä, E., Ng, S., Sourour, M., Hämäläinen, R., Olsson, C., Lundin, K., Mikkola, M., Trokovic, R., Peitz, M., Brüstle, O., Bazett-Jones, D. P., Alitalo, K., Lahesmaa, R., Nagy, A. and Otonkoski, T. (2011) Copy number variation and selection during reprogramming to pluripotency. *Nature, 471*(7336), pp. 58-62.

Hwang, N. S., Varghese, S., Lee, H. J., Zhang, Z., Ye, Z., Bae, J., Cheng, L. and Elisseeff, J. (2008) In vivo commitment and functional tissue regeneration using human embryonic stem cell-derived mesenchymal cells. *Proceedings of the National Academy of Sciences of the United States of America, 105*(52), pp. 20641-20646.

Hwang, N. S., Varghese, S., Zhang, Z. and Elisseeff, J. (2006) Chondrogenic differentiation of human embryonic stem cell-derived cells in arginine-glycine-aspartate-modified hydrogels. *Tissue Engineering, 12*(9), pp. 2695-2706.

Ichida, J. K., Tcw, J., T C W, J., Williams, L. A., Carter, A. C., Shi, Y., Moura, M. T., Ziller, M., Singh, S., Amabile, G., Bock, C., Umezawa, A., Rubin, L. L., Bradner, J. E., Akutsu, H., Meissner, A. and Eggan, K. (2014) Notch inhibition allows oncogene-independent generation of iPS cells. *Nature Chemical Biology, 10*(8), pp. 632-639.

Imaizumi, Y. and Okano, H. (2014) Modeling human neurological disorders with induced pluripotent stem cells. *Journal of Neurochemistry, 129*(3), pp. 388-399.

Ishiy, F. A. A., Fanganiello, R. D., Griesi-Oliveira, K., Suzuki, A. M., Kobayashi, G. S., Morales, A. G., Capelo, L. P. and Passos-Bueno, M. R. (2015) Improvement of In Vitro Osteogenic Potential through Differentiation of Induced Pluripotent Stem Cells from Human Exfoliated Dental Tissue towards Mesenchymal-Like Stem Cells. *Stem Cells International, 2015*, pp. 249098.

Ito, H. (2014) Clinical considerations of regenerative medicine in osteoporosis. *Current Osteoporosis Reports, 12*(2), pp. 230-234.

Jacob, K. D., Hooten, N. N., Trzeciak, A. R. and Evans, M. K. (2013) Markers of Oxidant Stress that are Clinically Relevant in Aging and Age-related Disease. *Mechanisms of ageing and development, 134*(0), pp. 139-157.

Jaenisch, R. and Young, R. (2008) Stem cells, the molecular circuitry of pluripotency and nuclear reprogramming. *Cell, 132*(4), pp. 567-582.

James, D., Levine, A. J., Besser, D. and Hemmati-Brivanlou, A. (2005) TGFbeta/activin/nodal signaling is necessary for the maintenance of pluripotency in human embryonic stem cells. *Development (Cambridge, England), 132*(6), pp. 1273-1282.

Jeck, W. R., Siebold, A. P. and Sharpless, N. E. (2012) Review: a meta-analysis of GWAS and age-associated diseases. *Aging Cell, 11*(5), pp. 727-731.

Jensen, J., Hyllner, J. and Björquist, P. (2009) Human embryonic stem cell technologies and drug discovery. *Journal of Cellular Physiology, 219*(3), pp. 513-519.

Jeong, S.-G. and Cho, G.-W. (2015) Endogenous ROS levels are increased in replicative senescence in human bone marrow mesenchymal stromal cells. *Biochemical and Biophysical Research Communications, 460*(4), pp. 971-976.

Jiang, J., Mohan, P. and Maxwell, C. A. (2013) The cytoskeletal protein RHAMM and ERK1/2 activity maintain the pluripotency of murine embryonic stem cells. *PloS One, 8*(9), pp. e73548.

Jin, G.-Z., Kim, T.-H., Kim, J.-H., Won, J.-E., Yoo, S.-Y., Choi, S.-J., Hyun, J. K. and Kim, H.-W. (2013) Bone tissue engineering of induced pluripotent stem cells cultured with macrochanneled polymer scaffold. *Journal of Biomedical Materials Research Part A, 101A*(5), pp. 1283-1291.

Judson, R. L., Babiarz, J. E., Venere, M. and Blelloch, R. (2009) Embryonic stem cell–specific microRNAs promote induced pluripotency. *Nature Biotechnology, 27*(5), pp. 459-461.

Jung, M., Peterson, H., Chavez, L., Kahlem, P., Lehrach, H., Vilo, J. and Adjaye, J. (2010) A data integration approach to mapping OCT4 gene regulatory networks operative in embryonic stem cells and embryonal carcinoma cells. *PloS One, 5*(5), pp. e10709.

Jurewicz, M., Yang, S., Augello, A., Godwin, J. G., Moore, R. F., Azzi, J., Fiorina, P., Atkinson, M., Sayegh, M. H. and Abdi, R. (2010) Congenic mesenchymal stem cell therapy reverses hyperglycemia in experimental type 1 diabetes. *Diabetes, 59*(12), pp. 3139-3147.

Kalfalah, F., Seggewiß, S., Walter, R., Tigges, J., Moreno-Villanueva, M., Bürkle, A., Ohse, S., Busch, H., Boerries, M., Hildebrandt, B., Royer-Pokora, B. and Boege, F. (2015) Structural chromosome abnormalities, increased DNA strand breaks and DNA strand break repair deficiency in dermal fibroblasts from old female human donors. *Aging, 7*(2), pp. 110-122.

Kamranvar, S. A. and Masucci, M. G. (2011) The Epstein-Barr virus nuclear antigen-1 promotes telomere dysfunction via induction of oxidative stress. *Leukemia, 25*(6), pp. 1017-1025.

Kanczler, J. M., Mirmalek-Sani, S.-H., Hanley, N. A., Ivanov, A. L., Barry, J. J. A., Upton, C., Shakesheff, K. M., Howdle, S. M., Antonov, E. N., Bagratashvili, V. N., Popov, V. K. and Oreffo, R. O. C. (2009) Biocompatibility and osteogenic potential of human fetal femur-derived cells on surface selective laser sintered scaffolds. *Acta Biomaterialia, 5*(6), pp. 2063-2071.

Kanehisa, M. and Goto, S. (2000) KEGG: kyoto encyclopedia of genes and genomes. *Nucleic Acids Research, 28*(1), pp. 27-30.

Kanehisa, M., Goto, S., Sato, Y., Kawashima, M., Furumichi, M. and Tanabe, M. (2014) Data, information, knowledge and principle: back to metabolism in KEGG. *Nucleic Acids Research, 42*(Database issue), pp. D199-205.

Kanfi, Y., Naiman, S., Amir, G., Peshti, V., Zinman, G., Nahum, L., Bar-Joseph, Z. and Cohen, H. Y. (2012) The sirtuin SIRT6 regulates lifespan in male mice. *Nature, 483*(7388), pp. 218-221.

Kang, K., Sun, L., Xiao, Y., Li, S.-H., Wu, J., Guo, J., Jiang, S.-L., Yang, L., Yau, T. M., Weisel, R. D., Radisic, M. and Li, R.-K. (2012) Aged Human Cells Rejuvenated by Cytokine Enhancement of Biomaterials for Surgical Ventricular Restoration. *Journal of the American College of Cardiology, 60*(21), pp. 2237-2249.

Kang, R., Zhou, Y., Tan, S., Zhou, G., Aagaard, L., Xie, L., Bünger, C., Bolund, L. and Luo, Y. (2015) Mesenchymal stem cells derived from human induced pluripotent stem cells retain adequate osteogenicity and chondrogenicity but less adipogenicity. *Stem Cell Research & Therapy, 6*(1), pp. 144.

Kapahi, P., Chen, D., Rogers, A. N., Katewa, S. D., Li, P. W.-L., Thomas, E. L. and Kockel, L. (2010) With TOR, less is more: a key role for the conserved nutrient-sensing TOR pathway in aging. *Cell Metabolism, 11*(6), pp. 453-465.

Kapahi, P. and Zid, B. (2004) TOR pathway: linking nutrient sensing to life span. *Science of aging knowledge environment: SAGE KE, 2004*(36), pp. PE34.

Karlsson, C., Emanuelsson, K., Wessberg, F., Kajic, K., Axell, M. Z., Eriksson, P. S., Lindahl, A., Hyllner, J. and Strehl, R. (2009) Human embryonic stem cell-derived mesenchymal progenitors—Potential in regenerative medicine. *Stem Cell Research, 3*(1), pp. 39-50.

Kasper, G., Mao, L., Geissler, S., Draycheva, A., Trippens, J., Kühnisch, J., Tschirschmann, M., Kaspar, K., Perka, C., Duda, G. N. and Klose, J. (2009) Insights into Mesenchymal Stem Cell Aging: Involvement of Antioxidant Defense and Actin Cytoskeleton. *STEM CELLS, 27*(6), pp. 1288-1297.

Katsara, O., Mahaira, L. G., Iliopoulou, E. G., Moustaki, A., Antsaklis, A., Loutradis, D., Stefanidis, K., Baxevanis, C. N., Papamichail, M. and Perez, S. A. (2011) Effects of donor age, gender, and in vitro cellular aging on the phenotypic, functional, and molecular characteristics of mouse bone marrow-derived mesenchymal stem cells. *Stem Cells and Development, 20*(9), pp. 1549-1561.

Kawamura, T., Suzuki, J., Wang, Y. V., Menendez, S., Morera, L. B., Raya, A., Wahl, G. M. and Belmonte, J. C. I. (2009) Linking the p53 tumour suppressor pathway to somatic cell reprogramming. *Nature, 460*(7259), pp. 1140-1144.

Kazak, L., Reyes, A. and Holt, I. J. (2012) Minimizing the damage: repair pathways keep mitochondrial DNA intact. *Nature Reviews. Molecular Cell Biology, 13*(10), pp. 659-671.

Kenyon, C. J. (2010) The genetics of ageing. *Nature, 464*(7288), pp. 504-512.

Khan, M., Mohsin, S., Khan, S. N. and Riazuddin, S. (2011) Repair of senescent myocardium by mesenchymal stem cells is dependent on the age of donor mice. *Journal of Cellular and Molecular Medicine, 15*(7), pp. 1515-1527.

Kida, Y. S., Kawamura, T., Wei, Z., Sogo, T., Jacinto, S., Shigeno, A., Kushige, H., Yoshihara, E., Liddle, C., Ecker, J. R., Yu, R. T., Atkins, A. R., Downes, M. and Evans, R. M. (2015) ERRs Mediate a Metabolic Switch Required for Somatic Cell Reprogramming to Pluripotency. *Cell Stem Cell, 16*(5), pp. 547-555.

Kim, D., Kim, C.-H., Moon, J.-I., Chung, Y.-G., Chang, M.-Y., Han, B.-S., Ko, S., Yang, E., Cha, K. Y., Lanza, R. and Kim, K.-S. (2009) Generation of Human Induced Pluripotent Stem Cells by Direct Delivery of Reprogramming Proteins. *Cell Stem Cell, 4*(6), pp. 472-476.

Kim, J. B., Sebastiano, V., Wu, G., Araúzo-Bravo, M. J., Sasse, P., Gentile, L., Ko, K., Ruau, D., Ehrich, M., van den Boom, D., Meyer, J., Hübner, K., Bernemann, C., Ortmeier, C., Zenke, M., Fleischmann, B. K., Zaehres, H. and Schöler, H. R. (2009) Oct4-Induced Pluripotency in Adult Neural Stem Cells. *Cell, 136*(3), pp. 411-419.

Kim, J. B., Zaehres, H., Wu, G., Gentile, L., Ko, K., Sebastiano, V., Araúzo-Bravo, M. J., Ruau, D., Han, D. W., Zenke, M. and Schöler, H. R. (2008) Pluripotent stem cells induced from adult neural stem cells by reprogramming with two factors. *Nature, 454*(7204), pp. 646-650.

Kim, K., Doi, A., Wen, B., Ng, K., Zhao, R., Cahan, P., Kim, J., Aryee, M. J., Ji, H., Ehrlich, L. I. R., Yabuuchi, A., Takeuchi, A., Cunniff, K. C., Hongguang, H., McKinney-Freeman, S., Naveiras, O., Yoon, T. J., Irizarry, R. A., Jung, N., Seita, J., Hanna, J., Murakami, P., Jaenisch, R., Weissleder, R., Orkin, S. H., Weissman, I. L., Feinberg, A. P. and Daley, G. Q. (2010) Epigenetic memory in induced pluripotent stem cells. *Nature, 467*(7313), pp. 285-290.

Kim, K., Zhao, R., Doi, A., Ng, K., Unternaehrer, J., Cahan, P., Hongguang, H., Loh, Y.-H., Aryee, M. J., Lensch, M. W., Li, H., Collins, J. J., Feinberg, A. P. and Daley, G. Q. (2011) Donor cell type can influence the epigenome and differentiation potential of human induced pluripotent stem cells. *Nature Biotechnology, 29*(12), pp. 1117-1119.

Kim, M., Kim, C., Choi, Y. S., Kim, M., Park, C. and Suh, Y. (2012) Age-related alterations in mesenchymal stem cells related to shift in differentiation from osteogenic to adipogenic potential: implication to age-associated bone diseases and defects. *Mechanisms of ageing and development, 133*(5), pp. 215-225.

Kim, R. H., Kang, M. K., Kim, T., Yang, P., Bae, S., Williams, D. W., Phung, S., Shin, K.-H., Hong, C. and Park, N.-H. (2015) Regulation of p53 during senescence in normal human keratinocytes. *Aging Cell*.

Kimbrel, E. A., Kouris, N. A., Yavanian, G. J., Chu, J., Qin, Y., Chan, A., Singh, R. P., McCurdy, D., Gordon, L., Levinson, R. D. and Lanza, R. (2014) Mesenchymal stem cell population derived from human pluripotent stem cells displays potent immunomodulatory and therapeutic properties. *Stem Cells and Development, 23*(14), pp. 1611-1624.

King, C. C. and Newton, A. C. (2004) The adaptor protein Grb14 regulates the localization of 3-phosphoinositide-dependent kinase-1. *The Journal of Biological Chemistry, 279*(36), pp. 37518-37527.

Kinoshita, T., Nagamatsu, G., Kosaka, T., Takubo, K., Hotta, A., Ellis, J. and Suda, T. (2011) Ataxia-telangiectasia mutated (ATM) deficiency decreases reprogramming efficiency and leads to genomic instability in iPS cells. *Biochemical and Biophysical Research Communications, 407*(2), pp. 321-326.

Klichko, V. I., Chow, E. S., Kotwica-Rolinska, J., Orr, W. C., Giebultowicz, J. M. and Radyuk, S. N. (2015) Aging alters circadian regulation of redox in Drosophila. *Frontiers in Genetics, 6*, pp. 83.

Koç, O. N., Gerson, S. L., Cooper, B. W., Dyhouse, S. M., Haynesworth, S. E., Caplan, A. I. and Lazarus, H. M. (2000) Rapid hematopoietic recovery after coinfusion of autologous-blood stem cells and culture-expanded marrow mesenchymal stem cells in advanced breast cancer patients receiving high-dose chemotherapy. *Journal of Clinical Oncology: Official Journal of the American Society of Clinical Oncology, 18*(2), pp. 307-316.

Koch, C. M., Reck, K., Shao, K., Lin, Q., Joussen, S., Ziegler, P., Walenda, G., Drescher, W., Opalka, B., May, T., Brümmendorf, T., Zenke, M., Saric, T. and Wagner, W. (2013) Pluripotent stem cells escape from senescence-associated DNA methylation changes. *Genome Research, 23*(2), pp. 248-259.

Koga, H., Shimaya, M., Muneta, T., Nimura, A., Morito, T., Hayashi, M., Suzuki, S., Ju, Y.-J., Mochizuki, T. and Sekiya, I. (2008) Local adherent technique for transplanting mesenchymal stem cells as a potential treatment of cartilage defect. *Arthritis Research & Therapy, 10*(4), pp. R84.

Komarov, P. G., Komarova, E. A., Kondratov, R. V., Christov-Tselkov, K., Coon, J. S., Chernov, M. V. and Gudkov, A. V. (1999) A chemical inhibitor of p53 that protects mice from the side effects of cancer therapy. *Science (New York, N.Y.), 285*(5434), pp. 1733-1737.

Kondoh, H., Lleonart, M. E., Nakashima, Y., Yokode, M., Tanaka, M., Bernard, D., Gil, J. and Beach, D. (2007) A high glycolytic flux supports the proliferative potential of murine embryonic stem cells. *Antioxidants & Redox Signaling, 9*(3), pp. 293-299.

Kopen, G. C., Prockop, D. J. and Phinney, D. G. (1999) Marrow stromal cells migrate throughout forebrain and cerebellum, and they differentiate into astrocytes after injection into neonatal mouse brains. *Proceedings of the National Academy of Sciences of the United States of America, 96*(19), pp. 10711-10716.

Kopher, R. A., Penchev, V. R., Islam, M. S., Hill, K. L., Khosla, S. and Kaufman, D. S. (2010) Human embryonic stem cell-derived CD34+ cells function as MSC progenitor cells. *Bone, 47*(4), pp. 718-728.

Koyama, N., Miura, M., Nakao, K., Kondo, E., Fujii, T., Taura, D., Kanamoto, N., Sone, M., Yasoda, A., Arai, H., Bessho, K. and Nakao, K. (2013) Human induced pluripotent stem cells differentiated into chondrogenic lineage via generation of mesenchymal progenitor cells. *Stem Cells and Development, 22*(1), pp. 102-113.

Kretlow, J. D., Jin, Y.-Q., Liu, W., Zhang, W. J., Hong, T.-H., Zhou, G., Baggett, L. S., Mikos, A. G. and Cao, Y. (2008) Donor age and cell passage affects differentiation potential of murine bone marrow-derived stem cells. *BMC cell biology, 9*, pp. 60.

Kuhn, K., Baker, S. C., Chudin, E., Lieu, M.-H., Oeser, S., Bennett, H., Rigault, P., Barker, D., McDaniel, T. K. and Chee, M. S. (2004) A novel, high-performance random array platform for quantitative gene expression profiling. *Genome Research, 14*(11), pp. 2347-2356.

Kuhn, L. T., Liu, Y., Boyd, N. L., Dennis, J. E., Jiang, X., Xin, X., Charles, L. F., Wang, L., Aguila, H. L., Rowe, D. W., Lichtler, A. C. and Goldberg, A. J. (2014) Developmental-like bone regeneration by human embryonic stem cell-derived mesenchymal cells. *Tissue Engineering. Part A, 20*(1-2), pp. 365-377.

Kuilman, T., Michaloglou, C., Mooi, W. J. and Peeper, D. S. (2010) The essence of senescence. *Genes & Development, 24*(22), pp. 2463-2479.

Kurtz, A. and Oh, S.-J. (2012) Age related changes of the extracellular matrix and stem cell maintenance. *Preventive Medicine, 54, Supplement*, pp. S50-S56.

Kuzmina, L. A., Petinati, N. A., Shipounova, I. N., Sats, N. V., Bigildeev, A. E., Zezina, E. A., Popova, M. D., Drize, N. J., Parovichnikova, E. N. and Savchenko, V. G. (2015) Analysis of multipotent mesenchymal stromal cells used for acute graft-versus-host disease prophylaxis. *European Journal of Haematology*.

Lamouille, S., Xu, J. and Derynck, R. (2014) Molecular mechanisms of epithelial–mesenchymal transition. *Nature Reviews Molecular Cell Biology, 15*(3), pp. 178-196.

Lapasset, L., Milhavet, O., Prieur, A., Besnard, E., Babled, A., Aït-Hamou, N., Leschik, J., Pellestor, F., Ramirez, J.-M., De Vos, J., Lehmann, S. and Lemaitre, J.-M. (2011) Rejuvenating senescent and centenarian human cells by reprogramming through the pluripotent state. *Genes & Development, 25*(21), pp. 2248-2253.

Laurent, L. C., Ulitsky, I., Slavin, I., Tran, H., Schork, A., Morey, R., Lynch, C., Harness, J. V., Lee, S., Barrero, M. J., Ku, S., Martynova, M., Semechkin, R., Galat, V., Gottesfeld, J., Izpisua Belmonte, J. C., Murry, C., Keirstead, H. S., Park, H.-S., Schmidt, U., Laslett, A. L., Muller, F.-J., Nievergelt, C. M., Shamir, R. and Loring, J. F. (2011) Dynamic changes in the copy number of pluripotency and cell proliferation genes in human ESCs and iPSCs during reprogramming and time in culture. *Cell Stem Cell, 8*(1), pp. 106-118.

Lee, E. J., Lee, H.-N., Kang, H.-J., Kim, K.-H., Hur, J., Cho, H.-J., Lee, J., Chung, H.-M., Cho, J., Cho, M.-Y., Oh, S.-K., Moon, S.-Y., Park, Y.-B. and Kim, H.-S. (2010) Novel embryoid body-based method to derive mesenchymal stem cells from human embryonic stem cells. *Tissue Engineering. Part A, 16*(2), pp. 705-715.

Lee, J., Sayed, N., Hunter, A., Au, Kin F., Wong, Wing H., Mocarski, Edward S., Pera, Renee R., Yakubov, E. and Cooke, John P. (2012) Activation of Innate Immunity Is Required for Efficient Nuclear Reprogramming. *Cell, 151*(3), pp. 547-558.

Lee, P., Martin, N. T., Nakamura, K., Azghadi, S., Amiri, M., Ben-David, U., Perlman, S., Gatti, R. A., Hu, H. and Lowry, W. E. (2013) SMRT compounds abrogate cellular phenotypes of ataxia telangiectasia in neural derivatives of patient-specific hiPSCs. *Nature Communications, 4*, pp. 1824.

Lee, R. H., Seo, M. J., Reger, R. L., Spees, J. L., Pulin, A. A., Olson, S. D. and Prockop, D. J. (2006) Multipotent stromal cells from human marrow home to and promote repair of pancreatic islets and renal glomeruli in diabetic NOD/scid mice. *Proceedings of the National Academy of Sciences of the United States of America, 103*(46), pp. 17438-17443.

Li, H., Collado, M., Villasante, A., Strati, K., Ortega, S., Cañamero, M., Blasco, M. A. and Serrano, M. (2009) The Ink4/Arf locus is a barrier for iPS cell reprogramming. *Nature, 460*(7259), pp. 1136-1139.

Li, T.-S. and Marbán, E. (2010) Physiological levels of reactive oxygen species are required to maintain genomic stability in stem cells. *Stem Cells (Dayton, Ohio), 28*(7), pp. 1178-1185.

Li, Y. and Geng, Y.-J. (2010) A potential role for insulin-like growth factor signaling in induction of pluripotent stem cell formation. *Growth hormone & IGF research: official journal of the Growth Hormone Research Society and the International IGF Research Society, 20*(6), pp. 391-398.

Li, Z., Dang, J., Chang, K.-Y. and Rana, T. M. (2014) MicroRNA-mediated regulation of extracellular matrix formation modulates somatic cell reprogramming. *RNA (New York, N.Y.), 20*(12), pp. 1900-1915.

Lian, Q., Lye, E., Suan Yeo, K., Khia Way Tan, E., Salto-Tellez, M., Liu, T. M., Palanisamy, N., El Oakley, R. M., Lee, E. H., Lim, B. and Lim, S.-K. (2007) Derivation of Clinically Compliant MSCs from CD105+, CD24− Differentiated Human ESCs. *STEM CELLS, 25*(2), pp. 425-436.

Lin, T., Ambasudhan, R., Yuan, X., Li, W., Hilcove, S., Abujarour, R., Lin, X., Hahm, H. S., Hao, E., Hayek, A. and Ding, S. (2009) A chemical platform for improved induction of human iPSCs. *Nature Methods, 6*(11), pp. 805-808.

Ling, L. S., Voskas, D. and Woodgett, J. R. (2013) Activation of PDK-1 maintains mouse embryonic stem cell self-renewal in a PKB-dependent manner. *Oncogene, 32*(47), pp. 5397-5408.

Liu, G.-H., Barkho, B. Z., Ruiz, S., Diep, D., Qu, J., Yang, S.-L., Panopoulos, A. D., Suzuki, K., Kurian, L., Walsh, C., Thompson, J., Boue, S., Fung, H. L., Sancho-Martinez, I., Zhang, K., Yates, J. and Izpisua Belmonte, J. C. (2011) Recapitulation of premature ageing with iPSCs from Hutchinson-Gilford progeria syndrome. *Nature, 472*(7342), pp. 221-225.

Liu, Y., Goldberg, A. J., Dennis, J. E., Gronowicz, G. A. and Kuhn, L. T. (2012) One-step derivation of mesenchymal stem cell (MSC)-like cells from human pluripotent stem cells on a fibrillar collagen coating. *PloS One, 7*(3), pp. e33225.

Liu, Y., Liu, N., Wu, D., Bi, Q. and Meng, S. (2015) The longevity of tor1Δ, sch9Δ, and ras2Δ mutants depends on actin dynamics in Saccharomyces cerevisiae. *Cell & Bioscience, 5*, pp. 18.

Liu, Y., Long, J. and Liu, J. (2014) Mitochondrial free radical theory of aging: Who moved my premise? *Geriatrics & Gerontology International, 14*(4), pp. 740-749.

Livak, K. J. and Schmittgen, T. D. (2001) Analysis of relative gene expression data using real-time quantitative PCR and the 2(-Delta Delta C(T)) Method. *Methods (San Diego, Calif.), 25*(4), pp. 402-408.

Loenarz, C. and Schofield, C. J. (2008) Expanding chemical biology of 2-oxoglutarate oxygenases. *Nature Chemical Biology, 4*(3), pp. 152-156.

López-Otín, C., Blasco, M. A., Partridge, L., Serrano, M. and Kroemer, G. (2013) The hallmarks of aging. *Cell, 153*(6), pp. 1194-1217.

Lord, C. J. and Ashworth, A. (2012) The DNA damage response and cancer therapy. *Nature, 481*(7381), pp. 287-294.

Luo, L., Kawakatsu, M., Guo, C.-W., Urata, Y., Huang, W.-J., Ali, H., Doi, H., Kitajima, Y., Tanaka, T., Goto, S., Ono, Y., Xin, H.-B., Hamano, K. and Li, T.-S. (2014) Effects of antioxidants on the quality and genomic stability of induced pluripotent stem cells. *Scientific Reports, 4*, pp. 3779.

Luo, M., Ling, T., Xie, W., Sun, H., Zhou, Y., Zhu, Q., Shen, M., Zong, L., Lyu, G., Zhao, Y., Ye, T., Gu, J., Tao, W., Lu, Z. and Grummt, I. (2013) NuRD Blocks Reprogramming of Mouse Somatic Cells into Pluripotent Stem Cells. *STEM CELLS, 31*(7), pp. 1278-1286.

Luzzani, C., Neiman, G., Garate, X., Questa, M., Solari, C., Fernandez Espinosa, D., García, M., Errecalde, A. L., Guberman, A., Scassa, M. E., Sevlever, G. E., Romorini, L. and Miriuka, S. G. (2015) A therapy-grade protocol for differentiation of pluripotent stem cells into mesenchymal stem cells using platelet lysate as supplement. *Stem Cell Research & Therapy, 6*, pp. 6.

Lv, F.-J., Tuan, R. S., Cheung, K. M. C. and Leung, V. Y. L. (2014) Concise Review: The Surface Markers and Identity of Human Mesenchymal Stem Cells. *STEM CELLS, 32*(6), pp. 1408-1419.

Madeira, A., da Silva, C. L., dos Santos, F., Camafeita, E., Cabral, J. M. S. and Sá-Correia, I. (2012) Human mesenchymal stem cell expression program upon extended ex-vivo cultivation, as revealed by 2-DE-based quantitative proteomics. *PloS One, 7*(8), pp. e43523.

Mah, N., Wang, Y., Liao, M.-C., Prigione, A., Jozefczuk, J., Lichtner, B., Wolfrum, K., Haltmeier, M., Flöttmann, M., Schaefer, M., Hahn, A., Mrowka, R., Klipp, E., Andrade-Navarro, M. A. and Adjaye, J. (2011) Molecular insights into reprogramming-initiation events mediated by the OSKM gene regulatory network. *PloS One, 6*(8), pp. e24351.

Mahmood, A., Harkness, L., Schrøder, H. D., Abdallah, B. M. and Kassem, M. (2010) Enhanced differentiation of human embryonic stem cells to mesenchymal progenitors by inhibition of TGF-beta/activin/nodal signaling using SB-431542. *Journal of Bone and Mineral Research: The Official Journal of the American Society for Bone and Mineral Research, 25*(6), pp. 1216-1233.

Mahmoudi, S. and Brunet, A. (2012) Aging and reprogramming: a two-way street. *Current Opinion in Cell Biology, 24*(6), pp. 744-756.

Mali, P., Chou, B.-K., Yen, J., Ye, Z., Zou, J., Dowey, S., Brodsky, R. A., Ohm, J. E., Yu, W., Baylin, S. B., Yusa, K., Bradley, A., Meyers, D. J., Mukherjee, C., Cole, P. A. and Cheng, L. (2010) Butyrate Greatly Enhances Derivation of Human Induced Pluripotent Stem Cells by Promoting Epigenetic Remodeling and the Expression of Pluripotency-Associated Genes. *STEM CELLS, 28*(4), pp. 713-720.

Marión, R. M., Strati, K., Li, H., Murga, M., Blanco, R., Ortega, S., Fernandez-Capetillo, O., Serrano, M. and Blasco, M. A. (2009) A p53-mediated DNA damage response limits reprogramming to ensure iPS cell genomic integrity. *Nature, 460*(7259), pp. 1149-1153.

Marion, R. M., Strati, K., Li, H., Tejera, A., Schoeftner, S., Ortega, S., Serrano, M. and Blasco, M. A. (2009) Telomeres acquire embryonic stem cell characteristics in induced pluripotent stem cells. *Cell Stem Cell, 4*(2), pp. 141-154.

Mason, C. and Dunnill, P. (2008) A brief definition of regenerative medicine. *Regenerative Medicine, 3*(1), pp. 1-5.

Mastri, M., Lin, H. and Lee, T. (2014) Enhancing the efficacy of mesenchymal stem cell therapy. *World Journal of Stem Cells, 6*(2), pp. 82-93.

Masuda, S., Miyagawa, S., Fukushima, S., Sougawa, N., Okimoto, K., Tada, C., Saito, A. and Sawa, Y. (2015) Eliminating residual iPS cells for safety in clinical application. *Protein & Cell, 6*(7), pp. 469-471.

Matin, M. M., Walsh, J. R., Gokhale, P. J., Draper, J. S., Bahrami, A. R., Morton, I., Moore, H. D. and Andrews, P. W. (2004) Specific knockdown of Oct4 and beta2-microglobulin expression by RNA interference in human embryonic stem cells and embryonic carcinoma cells. *Stem Cells (Dayton, Ohio), 22*(5), pp. 659-668.

Maynard, S., Swistowska, A. M., Lee, J. W., Liu, Y., Liu, S.-T., Da Cruz, A. B., Rao, M., de Souza-Pinto, N. C., Zeng, X. and Bohr, V. A. (2008) Human embryonic stem cells have enhanced repair of multiple forms of DNA damage. *Stem Cells (Dayton, Ohio), 26*(9), pp. 2266-2274.

Mayshar, Y., Ben-David, U., Lavon, N., Biancotti, J.-C., Yakir, B., Clark, A. T., Plath, K., Lowry, W. E. and Benvenisty, N. (2010) Identification and classification of chromosomal aberrations in human induced pluripotent stem cells. *Cell Stem Cell, 7*(4), pp. 521-531.

Medvedev, S. P., Grigor'eva, E. V., Shevchenko, A. I., Malakhova, A. A., Dementyeva, E. V., Shilov, A. A., Pokushalov, E. A., Zaidman, A. M., Aleksandrova, M. A., Plotnikov, E. Y., Sukhikh, G. T. and Zakian, S. M. (2010) Human Induced Pluripotent Stem Cells Derived from Fetal Neural Stem Cells Successfully Undergo Directed Differentiation into Cartilage. *Stem Cells and Development, 20*(6), pp. 1099-1112.

Megges, M., Geissler, S., Duda, G. N. and Adjaye, J. (2015) Generation of an iPS cell line from bone marrow derived mesenchymal stromal cells from an elderly patient. *Stem Cell Research, 15*(3), pp. 565-568.

Megges, M. M. (2010) *Cellular reprogramming of human mesenchymal stem cells derived from young and old individuals using viral and non-viral approaches*. Unpublished Master Thesis, Beuth Hochschule für Technik Berlin, Berlin.

Miller, J. and Studer, L. (2014) Aging in iPS cells. *Aging, 6*(4), pp. 246-247.

Miller, J. D., Ganat, Y. M., Kishinevsky, S., Bowman, R. L., Liu, B., Tu, E. Y., Mandal, P. K., Vera, E., Shim, J.-w., Kriks, S., Taldone, T., Fusaki, N., Tomishima, M. J., Krainc, D., Milner, T. A., Rossi, D. J. and Studer, L. (2013) Human iPSC-based modeling of late-onset disease via progerin-induced aging. *Cell Stem Cell, 13*(6), pp. 691-705.

Mirmalek-Sani, S.-H., Stokes, P. J., Tare, R. S., Ralph, E. J., Inglis, S., Hanley, N. A., Houghton, F. D. and Oreffo, R. O. C. (2009) Derivation of a novel undifferentiated human foetal phenotype in serum-free cultures with BMP-2. *Journal of Cellular and Molecular Medicine, 13*(9b), pp. 3541-3555.

Mirmalek-Sani, S.-H., Tare, R. S., Morgan, S. M., Roach, H. I., Wilson, D. I., Hanley, N. A. and Oreffo, R. O. C. (2006) Characterization and Multipotentiality of Human Fetal Femur–Derived Cells: Implications for Skeletal Tissue Regeneration. *STEM CELLS, 24*(4), pp. 1042-1053.

Miyazaki, S., Yamamoto, H., Miyoshi, N., Takahashi, H., Suzuki, Y., Haraguchi, N., Ishii, H., Doki, Y. and Mori, M. (2012) Emerging Methods for Preparing iPS Cells. *Japanese Journal of Clinical Oncology, 42*(9), pp. 773-779.

Moiseeva, O., Bourdeau, V., Roux, A., Deschênes-Simard, X. and Ferbeyre, G. (2009) Mitochondrial dysfunction contributes to oncogene-induced senescence. *Molecular and Cellular Biology, 29*(16), pp. 4495-4507.

Molina-Estevez, F. J., Lozano, M. L., Navarro, S., Torres, Y., Grabundzija, I., Ivics, Z., Samper, E., Bueren, J. A. and Guenechea, G. (2013) Brief report: impaired cell reprogramming in nonhomologous end joining deficient cells. *Stem Cells (Dayton, Ohio), 31*(8), pp. 1726-1730.

Moretti, A., Bellin, M., Welling, A., Jung, C. B., Lam, J. T., Bott-Flügel, L., Dorn, T., Goedel, A., Höhnke, C., Hofmann, F., Seyfarth, M., Sinnecker, D., Schömig, A. and Laugwitz, K.-L. (2010) Patient-specific induced pluripotent stem-cell models for long-QT syndrome. *The New England Journal of Medicine, 363*(15), pp. 1397-1409.

Morgan, J. T., Raghunathan, V. K., Chang, Y.-R., Murphy, C. J. and Russell, P. (2015) The intrinsic stiffness of human trabecular meshwork cells increases with senescence. *Oncotarget, 6*(17), pp. 15362-15374.

Moschidou, D., Mukherjee, S., Blundell, M. P., Drews, K., Jones, G. N., Abdulrazzak, H., Nowakowska, B., Phoolchund, A., Lay, K., Ramasamy, T. S., Cananzi, M., Nettersheim, D., Sullivan, M., Frost, J., Moore, G., Vermeesch, J. R., Fisk, N. M., Thrasher, A. J., Atala, A., Adjaye, J., Schorle, H., De Coppi, P. and Guillot, P. V. (2012) Valproic acid confers functional pluripotency to human amniotic fluid stem cells in a transgene-free approach. *Molecular Therapy: The Journal of the American Society of Gene Therapy, 20*(10), pp. 1953-1967.

Moskalev, A. A., Shaposhnikov, M. V., Plyusnina, E. N., Zhavoronkov, A., Budovsky, A., Yanai, H. and Fraifeld, V. E. (2013) The role of DNA damage and repair in aging through the prism of Koch-like criteria. *Ageing Research Reviews, 12*(2), pp. 661-684.

Mostoslavsky, R., Chua, K. F., Lombard, D. B., Pang, W. W., Fischer, M. R., Gellon, L., Liu, P., Mostoslavsky, G., Franco, S., Murphy, M. M., Mills, K. D., Patel, P., Hsu, J. T., Hong, A. L., Ford, E., Cheng, H.-L., Kennedy, C., Nunez, N., Bronson, R., Frendewey, D., Auerbach, W., Valenzuela, D., Karow, M., Hottiger, M. O., Hursting, S., Barrett, J. C., Guarente, L., Mulligan, R., Demple, B., Yancopoulos, G. D. and Alt, F. W. (2006) Genomic instability and aging-like phenotype in the absence of mammalian SIRT6. *Cell, 124*(2), pp. 315-329.

Müller, F.-J., Schuldt, B. M., Williams, R., Mason, D., Altun, G., Papapetrou, E. P., Danner, S., Goldmann, J. E., Herbst, A., Schmidt, N. O., Aldenhoff, J. B., Laurent, L. C. and Loring, J. F. (2011) A bioinformatic assay for pluripotency in human cells. *Nature Methods, 8*(4), pp. 315-317.

Murakami, S. (2006) Stress resistance in long-lived mouse models. *Experimental Gerontology, 41*(10), pp. 1014-1019.

Mutyaba, P. L., Belkin, N. S., Lopas, L., Gray, C. F., Dopkin, D., Hankenson, K. D. and Ahn, J. (2014) Notch signaling in mesenchymal stem cells harvested from geriatric mice. *Journal of Orthopaedic Trauma, 28 Suppl 1*, pp. S20-23.

Nasu, A., Ikeya, M., Yamamoto, T., Watanabe, A., Jin, Y., Matsumoto, Y., Hayakawa, K., Amano, N., Sato, S., Osafune, K., Aoyama, T., Nakamura, T., Kato, T. and Toguchida, J. (2013) Genetically Matched Human iPS Cells Reveal that Propensity for Cartilage and Bone Differentiation Differs with Clones, not Cell Type of Origin. *PloS One, 8*(1).

Nayler, S., Gatei, M., Kozlov, S., Gatti, R., Mar, J. C., Wells, C. A., Lavin, M. and Wolvetang, E. (2012) Induced pluripotent stem cells from ataxia-telangiectasia recapitulate the cellular phenotype. *Stem Cells Translational Medicine, 1*(7), pp. 523-535.

Nejadnik, H., Diecke, S., Lenkov, O. D., Chapelin, F., Donig, J., Tong, X., Derugin, N., Chan, R. C. F., Gaur, A., Yang, F., Wu, J. C. and Daldrup-Link, H. E. (2015) Improved approach for chondrogenic differentiation of human induced pluripotent stem cells. *Stem Cell Reviews, 11*(2), pp. 242-253.

Ng, C. P., Sharif, A. R. M., Heath, D. E., Chow, J. W., Zhang, C. B. Y., Chan-Park, M. B., Hammond, P. T., Chan, J. K. Y. and Griffith, L. G. (2014) Enhanced ex vivo expansion of adult mesenchymal stem cells by fetal mesenchymal stem cell ECM. *Biomaterials, 35*(13), pp. 4046-4057.

Nichols, J., Zevnik, B., Anastassiadis, K., Niwa, H., Klewe-Nebenius, D., Chambers, I., Schöler, H. and Smith, A. (1998) Formation of pluripotent stem cells in the mammalian embryo depends on the POU transcription factor Oct4. *Cell, 95*(3), pp. 379-391.

Nori, S., Okada, Y., Yasuda, A., Tsuji, O., Takahashi, Y., Kobayashi, Y., Fujiyoshi, K., Koike, M., Uchiyama, Y., Ikeda, E., Toyama, Y., Yamanaka, S., Nakamura, M. and Okano, H. (2011) Grafted human-induced pluripotent stem-cell-derived neurospheres promote motor functional recovery after spinal cord injury in mice. *Proceedings of the National Academy of Sciences of the United States of America, 108*(40), pp. 16825-16830.

Ohi, Y., Qin, H., Hong, C., Blouin, L., Polo, J. M., Guo, T., Qi, Z., Downey, S. L., Manos, P. D., Rossi, D. J., Yu, J., Hebrok, M., Hochedlinger, K., Costello, J. F., Song, J. S. and Ramalho-Santos, M. (2011) Incomplete DNA methylation underlies a transcriptional memory of somatic cells in human iPS cells. *Nature Cell Biology, 13*(5), pp. 541-549.

Ohmine, S., Squillace, K. A., Hartjes, K. A., Deeds, M. C., Armstrong, A. S., Thatava, T., Sakuma, T., Terzic, A., Kudva, Y. and Ikeda, Y. (2012) Reprogrammed keratinocytes from elderly type 2 diabetes patients suppress senescence genes to acquire induced pluripotency. *Aging, 4*(1), pp. 60-73.

Ohnishi, H., Oda, Y., Aoki, T., Tadokoro, M., Katsube, Y., Ohgushi, H., Hattori, K. and Yuba, S. (2012) A comparative study of induced pluripotent stem cells generated from frozen, stocked bone marrow- and adipose tissue-derived mesenchymal stem cells. *Journal of Tissue Engineering and Regenerative Medicine, 6*(4), pp. 261-271.

Oki, K., Tatarishvili, J., Wood, J., Koch, P., Wattananit, S., Mine, Y., Monni, E., Tornero, D., Ahlenius, H., Ladewig, J., Brüstle, O., Lindvall, O. and Kokaia, Z. (2012) Human-Induced Pluripotent Stem Cells form Functional Neurons and Improve Recovery After Grafting in Stroke-Damaged Brain. *STEM CELLS, 30*(6), pp. 1120-1133.

Okita, K., Ichisaka, T. and Yamanaka, S. (2007) Generation of germline-competent induced pluripotent stem cells. *Nature, 448*(7151), pp. 313-317.

Okita, K., Matsumura, Y., Sato, Y., Okada, A., Morizane, A., Okamoto, S., Hong, H., Nakagawa, M., Tanabe, K., Tezuka, K.-i., Shibata, T., Kunisada, T., Takahashi, M., Takahashi, J., Saji, H. and Yamanaka, S. (2011) A more efficient method to generate integration-free human iPS cells. *Nature Methods, 8*(5), pp. 409-412.

Okita, K., Nakagawa, M., Hyenjong, H., Ichisaka, T. and Yamanaka, S. (2008) Generation of Mouse Induced Pluripotent Stem Cells Without Viral Vectors. *Science, 322*(5903), pp. 949-953.

Olivier, E. N., Rybicki, A. C. and Bouhassira, E. E. (2006) Differentiation of human embryonic stem cells into bipotent mesenchymal stem cells. *Stem Cells (Dayton, Ohio), 24*(8), pp. 1914-1922.

Onder, T. T., Kara, N., Cherry, A., Sinha, A. U., Zhu, N., Bernt, K. M., Cahan, P., Marcarci, B. O., Unternaehrer, J., Gupta, P. B., Lander, E. S., Armstrong, S. A. and Daley, G. Q. (2012) Chromatin-modifying enzymes as modulators of reprogramming. *Nature, 483*(7391), pp. 598-602.

Ono, M., Hamada, Y., Horiuchi, Y., Matsuo-Takasaki, M., Imoto, Y., Satomi, K., Arinami, T., Hasegawa, M., Fujioka, T., Nakamura, Y. and Noguchi, E. (2012) Generation of Induced Pluripotent Stem Cells from Human Nasal Epithelial Cells Using a Sendai Virus Vector. *PloS One, 7*(8), pp. e42855.

Opii, W. O., Joshi, G., Head, E., Milgram, N. W., Muggenburg, B. A., Klein, J. B., Pierce, W. M., Cotman, C. W. and Butterfield, D. A. (2008) Proteomic identification of brain proteins in the canine model of human aging following a long-term treatment with antioxidants and a

program of behavioral enrichment: relevance to Alzheimer's disease. *Neurobiology of Aging, 29*(1), pp. 51-70.

Pan, L., Chen, S., Weng, C., Call, G., Zhu, D., Tang, H., Zhang, N. and Xie, T. (2007) Stem cell aging is controlled both intrinsically and extrinsically in the Drosophila ovary. *Cell Stem Cell, 1*(4), pp. 458-469.

Park, I.-H., Arora, N., Huo, H., Maherali, N., Ahfeldt, T., Shimamura, A., Lensch, M. W., Cowan, C., Hochedlinger, K. and Daley, G. Q. (2008a) Disease-specific induced pluripotent stem cells. *Cell, 134*(5), pp. 877-886.

Park, I.-H., Zhao, R., West, J. A., Yabuuchi, A., Huo, H., Ince, T. A., Lerou, P. H., Lensch, M. W. and Daley, G. Q. (2008b) Reprogramming of human somatic cells to pluripotency with defined factors. *Nature, 451*(7175), pp. 141-146.

Passos, J. F., Saretzki, G., Ahmed, S., Nelson, G., Richter, T., Peters, H., Wappler, I., Birket, M. J., Harold, G., Schaeuble, K., Birch-Machin, M. A., Kirkwood, T. B. L. and von Zglinicki, T. (2007) Mitochondrial dysfunction accounts for the stochastic heterogeneity in telomere-dependent senescence. *PLoS biology, 5*(5), pp. e110.

Piccinato, C. A., Sertie, A. L., Torres, N., Ferretti, M. and Antonioli, E. (2015) High OCT4 and Low p16(INK4A) Expressions Determine In Vitro Lifespan of Mesenchymal Stem Cells. *Stem Cells International, 2015*, pp. 369828.

Pilch, D. R., Sedelnikova, O. A., Redon, C., Celeste, A., Nussenzweig, A. and Bonner, W. M. (2003) Characteristics of gamma-H2AX foci at DNA double-strand breaks sites. *Biochemistry and Cell Biology = Biochimie Et Biologie Cellulaire, 81*(3), pp. 123-129.

Pittenger, M. F., Mackay, A. M., Beck, S. C., Jaiswal, R. K., Douglas, R., Mosca, J. D., Moorman, M. A., Simonetti, D. W., Craig, S. and Marshak, D. R. (1999) Multilineage potential of adult human mesenchymal stem cells. *Science (New York, N.Y.), 284*(5411), pp. 143-147.

Polentes, J., Jendelova, P., Cailleret, M., Braun, H., Romanyuk, N., Tropel, P., Brenot, M., Itier, V., Seminatore, C., Baldauf, K., Turnovcova, K., Jirak, D., Teletin, M., Côme, J., Tournois, J., Reymann, K., Sykova, E., Viville, S. and Onteniente, B. (2012) Human induced pluripotent stem cells improve stroke outcome and reduce secondary degeneration in the recipient brain. *Cell Transplantation, 21*(12), pp. 2587-2602.

Polo, J. M., Anderssen, E., Walsh, R. M., Schwarz, B. A., Nefzger, C. M., Lim, S. M., Borkent, M., Apostolou, E., Alaei, S., Cloutier, J., Bar-Nur, O., Cheloufi, S., Stadtfeld, M., Figueroa, M. E., Robinton, D., Natesan, S., Melnick, A., Zhu, J., Ramaswamy, S. and Hochedlinger, K. (2012) A molecular roadmap of reprogramming somatic cells into iPS cells. *Cell, 151*(7), pp. 1617-1632.

Polo, J. M., Liu, S., Figueroa, M. E., Kulalert, W., Eminli, S., Tan, K. Y., Apostolou, E., Stadtfeld, M., Li, Y., Shioda, T., Natesan, S., Wagers, A. J., Melnick, A., Evans, T. and Hochedlinger, K. (2010) Cell type of origin influences the molecular and functional properties of mouse induced pluripotent stem cells. *Nature Biotechnology, 28*(8), pp. 848-855.

Poyton, R. O., Ball, K. A. and Castello, P. R. (2009) Mitochondrial generation of free radicals and hypoxic signaling. *Trends in endocrinology and metabolism: TEM, 20*(7), pp. 332-340.

Prigione, A. and Adjaye, J. (2010) Modulation of mitochondrial biogenesis and bioenergetic metabolism upon in vitro and in vivo differentiation of human ES and iPS cells. *The International Journal of Developmental Biology, 54*(11-12), pp. 1729-1741.

Prigione, A., Fauler, B., Lurz, R., Lehrach, H. and Adjaye, J. (2010) The Senescence-Related Mitochondrial/Oxidative Stress Pathway is Repressed in Human Induced Pluripotent Stem Cells. *STEM CELLS, 28*(4), pp. 721-733.

Prigione, A., Hossini, A. M., Lichtner, B., Serin, A., Fauler, B., Megges, M., Lurz, R., Lehrach, H., Makrantonaki, E., Zouboulis, C. C. and Adjaye, J. (2011a) Mitochondrial-associated cell death mechanisms are reset to an embryonic-like state in aged donor-derived iPS cells harboring chromosomal aberrations. *PloS One, 6*(11), pp. e27352.

Prigione, A., Lichtner, B., Kuhl, H., Struys, E. A., Wamelink, M., Lehrach, H., Ralser, M., Timmermann, B. and Adjaye, J. (2011b) Human induced pluripotent stem cells harbor homoplasmic and heteroplasmic mitochondrial DNA mutations while maintaining human embryonic stem cell-like metabolic reprogramming. *Stem Cells (Dayton, Ohio), 29*(9), pp. 1338-1348.

Rakovic, A., Seibler, P. and Klein, C. (2015) iPS models of Parkin and PINK1. *Biochemical Society Transactions, 43*(2), pp. 302-307.

Rando, T. A. (2006) Stem cells, ageing and the quest for immortality. *Nature, 441*(7097), pp. 1080-1086.

Rando, T. A. and Wyss-Coray, T. (2014) Stem cells as vehicles for youthful regeneration of aged tissues. *The Journals of Gerontology. Series A, Biological Sciences and Medical Sciences, 69 Suppl 1*, pp. S39-42.

Raynaud, C. M., Halabi, N., Elliott, D. A., Pasquier, J., Elefanty, A. G., Stanley, E. G. and Rafii, A. (2013) Human embryonic stem cell derived mesenchymal progenitors express cardiac markers but do not form contractile cardiomyocytes. *PloS One, 8*(1), pp. e54524.

Reinisalo, M., Kårlund, A., Koskela, A., Kaarniranta, K. and Karjalainen, R. O. (2015) Polyphenol Stilbenes: Molecular Mechanisms of Defence against Oxidative Stress and Aging-Related Diseases. *Oxidative Medicine and Cellular Longevity, 2015*, pp. 340520.

Reitinger, S., Schimke, M., Klepsch, S., de Sneeuw, S., Yani, S. L., Gaßner, R., Ertl, P. and Lepperdinger, G. (2015) Systemic impact molds mesenchymal stromal/stem cell aging. *Transfusion and Apheresis Science, 52*(3), pp. 285-289.

Reuter, S., Gupta, S. C., Chaturvedi, M. M. and Aggarwal, B. B. (2010) Oxidative stress, inflammation, and cancer: how are they linked? *Free Radical Biology & Medicine, 49*(11), pp. 1603-1616.

Rizzi, R., Di Pasquale, E., Portararo, P., Papait, R., Cattaneo, P., Latronico, M. V. G., Altomare, C., Sala, L., Zaza, A., Hirsch, E., Naldini, L., Condorelli, G. and Bearzi, C. (2012) Post-natal cardiomyocytes can generate iPS cells with an enhanced capacity toward cardiomyogenic re-differentation. *Cell Death and Differentiation, 19*(7), pp. 1162-1174.

Rocha, C. R. R., Lerner, L. K., Okamoto, O. K., Marchetto, M. C. and Menck, C. F. M. (2013) The role of DNA repair in the pluripotency and differentiation of human stem cells. *Mutation Research, 752*(1), pp. 25-35.

Rogakou, E. P., Pilch, D. R., Orr, A. H., Ivanova, V. S. and Bonner, W. M. (1998) DNA double-stranded breaks induce histone H2AX phosphorylation on serine 139. *The Journal of Biological Chemistry, 273*(10), pp. 5858-5868.

Rohani, L., Johnson, A. A., Arnold, A. and Stolzing, A. (2014) The aging signature: a hallmark of induced pluripotent stem cells? *Aging Cell, 13*(1), pp. 2-7.

Ronen, D. and Benvenisty, N. (2012) Genomic stability in reprogramming. *Current Opinion in Genetics & Development, 22*(5), pp. 444-449.

Røsland, G. V., Svendsen, A., Torsvik, A., Sobala, E., McCormack, E., Immervoll, H., Mysliwietz, J., Tonn, J.-C., Goldbrunner, R., Lønning, P. E., Bjerkvig, R. and Schichor, C. (2009) Long-term Cultures of Bone Marrow–Derived Human Mesenchymal Stem Cells Frequently Undergo Spontaneous Malignant Transformation. *Cancer Research, 69*(13), pp. 5331-5339.

Saeed, A. I., Bhagabati, N. K., Braisted, J. C., Liang, W., Sharov, V., Howe, E. A., Li, J., Thiagarajan, M., White, J. A. and Quackenbush, J. (2006) TM4 microarray software suite. *Methods in Enzymology, 411*, pp. 134-193.

Saeed, A. I., Sharov, V., White, J., Li, J., Liang, W., Bhagabati, N., Braisted, J., Klapa, M., Currier, T., Thiagarajan, M., Sturn, A., Snuffin, M., Rezantsev, A., Popov, D., Ryltsov, A., Kostukovich, E., Borisovsky, I., Liu, Z., Vinsavich, A., Trush, V. and Quackenbush, J. (2003) TM4: a free, open-source system for microarray data management and analysis. *BioTechniques, 34*(2), pp. 374-378.

Sakurai, K., Talukdar, I., Patil, Veena S., Dang, J., Li, Z., Chang, K.-Y., Lu, C.-C., Delorme-Walker, V., DerMardirossian, C., Anderson, K., Hanein, D., Yang, C.-S., Wu, D., Liu, Y. and Rana, Tariq M. (2014) Kinome-wide Functional Analysis Highlights the Role of Cytoskeletal Remodeling in Somatic Cell Reprogramming. *Cell Stem Cell, 14*(4), pp. 523-534.

Salminen, A., Kaarniranta, K., Hiltunen, M. and Kauppinen, A. (2014) Krebs cycle dysfunction shapes epigenetic landscape of chromatin: novel insights into mitochondrial regulation of aging process. *Cellular Signalling, 26*(7), pp. 1598-1603.

Saretzki, G., Walter, T., Atkinson, S., Passos, J. F., Bareth, B., Keith, W. N., Stewart, R., Hoare, S., Stojkovic, M., Armstrong, L., von Zglinicki, T. and Lako, M. (2008) Downregulation of Multiple Stress Defense Mechanisms During Differentiation of Human Embryonic Stem Cells. *STEM CELLS, 26*(2), pp. 455-464.

Sato, N., Meijer, L., Skaltsounis, L., Greengard, P. and Brivanlou, A. H. (2004) Maintenance of pluripotency in human and mouse embryonic stem cells through activation of Wnt signaling by a pharmacological GSK-3-specific inhibitor. *Nature Medicine, 10*(1), pp. 55-63.

Schlaeger, T. M., Daheron, L., Brickler, T. R., Entwisle, S., Chan, K., Cianci, A., DeVine, A., Ettenger, A., Fitzgerald, K., Godfrey, M., Gupta, D., McPherson, J., Malwadkar, P., Gupta, M., Bell, B., Doi, A., Jung, N., Li, X., Lynes, M. S., Brookes, E., Cherry, A. B. C., Demirbas, D., Tsankov, A. M., Zon, L. I., Rubin, L. L., Feinberg, A. P., Meissner, A., Cowan, C. A. and Daley, G. Q. (2015) A comparison of non-integrating reprogramming methods. *Nature Biotechnology, 33*(1), pp. 58-63.

Sen, T., Sen, N., Noordhuis, M. G., Ravi, R., Wu, T. C., Ha, P. K., Sidransky, D. and Hoque, M. O. (2012) OGDHL is a modifier of AKT-dependent signaling and NF-κB function. *PloS One, 7*(11), pp. e48770.

Seo, M. and Lee, Y.-H. (2014) PFKFB3 regulates oxidative stress homeostasis via its S-glutathionylation in cancer. *Journal of Molecular Biology, 426*(4), pp. 830-842.

Sethe, S., Scutt, A. and Stolzing, A. (2006) Aging of mesenchymal stem cells. *Ageing Research Reviews, 5*(1), pp. 91-116.

Shamji, A. F., Kuruvilla, F. G. and Schreiber, S. L. (2000) Partitioning the transcriptional program induced by rapamycin among the effectors of the Tor proteins. *Current biology: CB, 10*(24), pp. 1574-1581.

Shao, K., Koch, C., Gupta, M. K., Lin, Q., Lenz, M., Laufs, S., Denecke, B., Schmidt, M., Linke, M., Hennies, H. C., Hescheler, J., Zenke, M., Zechner, U., Šarić, T. and Wagner, W. (2013) Induced pluripotent mesenchymal stromal cell clones retain donor-derived differences in DNA methylation profiles. *Molecular Therapy: The Journal of the American Society of Gene Therapy, 21*(1), pp. 240-250.

Shaw, A. C., Panda, A., Joshi, S. R., Qian, F., Allore, H. G. and Montgomery, R. R. (2011) Dysregulation of human Toll-like receptor function in aging. *Ageing Research Reviews, 10*(3), pp. 346-353.

Shipounova, I. N., Svinareva, D. A., Petrova, T. V., Lyamzaev, K. G., Chernyak, B. V., Drize, N. I. and Skulachev, V. P. (2010) Reactive oxygen species produced in mitochondria are involved in age-dependent changes of hematopoietic and mesenchymal progenitor cells in mice. A study with the novel mitochondria-targeted antioxidant SkQ1. *Mechanisms of ageing and development, 131*(6), pp. 415-421.

Siegel, G., Kluba, T., Hermanutz-Klein, U., Bieback, K., Northoff, H. and Schäfer, R. (2013) Phenotype, donor age and gender affect function of human bone marrow-derived mesenchymal stromal cells. *BMC medicine, 11*, pp. 146.

Singh, R., Shen, W., Kuai, D., Martin, J. M., Guo, X., Smith, M. A., Perez, E. T., Phillips, M. J., Simonett, J. M., Wallace, K. A., Verhoeven, A. D., Capowski, E. E., Zhang, X., Yin, Y., Halbach, P. J., Fishman, G. A., Wright, L. S., Pattnaik, B. R. and Gamm, D. M. (2013) iPS cell modeling of Best disease: insights into the pathophysiology of an inherited macular degeneration. *Human Molecular Genetics, 22*(3), pp. 593-607.

Sivakumar, R., Koga, H., Selvendiran, K., Maeyama, M., Ueno, T. and Sata, M. (2009) Autocrine loop for IGF-I receptor signaling in SLUG-mediated epithelial-mesenchymal transition. *International Journal of Oncology, 34*(2), pp. 329-338.

Smith, Z. D., Nachman, I., Regev, A. and Meissner, A. (2010) Dynamic single-cell imaging of direct reprogramming reveals an early specifying event. *Nature Biotechnology, 28*(5), pp. 521-526.

Somers, A., Jean, J.-C., Sommer, C. A., Omari, A., Ford, C. C., Mills, J. A., Ying, L., Sommer, A. G., Jean, J. M., Smith, B. W., Lafyatis, R., Demierre, M.-F., Weiss, D. J., French, D. L., Gadue, P., Murphy, G. J., Mostoslavsky, G. and Kotton, D. N. (2010) Generation of transgene-free lung disease-specific human induced pluripotent stem cells using a single excisable lentiviral stem cell cassette. *Stem Cells (Dayton, Ohio), 28*(10), pp. 1728-1740.

Soria-Valles, C., Osorio, F. G., Gutiérrez-Fernández, A., De Los Angeles, A., Bueno, C., Menéndez, P., Martín-Subero, J. I., Daley, G. Q., Freije, J. M. P. and López-Otín, C. (2015) NF-κB activation impairs somatic cell reprogramming in ageing. *Nature Cell Biology, 17*(8), pp. 1004-1013.

Soyombo, A. A., Wu, Y., Kolski, L., Rios, J. J., Rakheja, D., Chen, A., Kehler, J., Hampel, H., Coughran, A. and Ross, T. S. (2013) Analysis of induced pluripotent stem cells from a BRCA1 mutant family. *Stem Cell Reports, 1*(4), pp. 336-349.

Srikanth, P. and Young-Pearse, T. L. (2014) Stem cells on the brain: modeling neurodevelopmental and neurodegenerative diseases using human induced pluripotent stem cells. *Journal of Neurogenetics, 28*(1-2), pp. 5-29.

Stadtfeld, M., Apostolou, E., Ferrari, F., Choi, J., Walsh, R. M., Chen, T., Ooi, S. S. K., Kim, S. Y., Bestor, T. H., Shioda, T., Park, P. J. and Hochedlinger, K. (2012) Ascorbic acid prevents loss of Dlk1-Dio3 imprinting and facilitates generation of all-iPS cell mice from terminally differentiated B cells. *Nature Genetics, 44*(7), pp. 831-831.

Stadtfeld, M., Maherali, N., Breault, D. T. and Hochedlinger, K. (2008) Defining Molecular Cornerstones during Fibroblast to iPS Cell Reprogramming in Mouse. *Cell Stem Cell, 2*(3), pp. 230-240.

Stenderup, K., Justesen, J., Clausen, C. and Kassem, M. (2003) Aging is associated with decreased maximal life span and accelerated senescence of bone marrow stromal cells. *Bone, 33*(6), pp. 919-926.

Stolzing, A., Colley, H. and Scutt, A. (2011) Effect of age and diabetes on the response of mesenchymal progenitor cells to fibrin matrices. *International Journal of Biomaterials, 2011*, pp. 378034.

Stolzing, A., Jones, E., McGonagle, D. and Scutt, A. (2008) Age-related changes in human bone marrow-derived mesenchymal stem cells: Consequences for cell therapies. *Mechanisms of ageing and development, 129*(3), pp. 163-173.

Stolzing, A. and Scutt, A. (2006) Age-related impairment of mesenchymal progenitor cell function. *Aging Cell, 5*(3), pp. 213-224.

Studer, L., Vera, E. and Cornacchia, D. (2015) Programming and Reprogramming Cellular Age in the Era of Induced Pluripotency. *Cell Stem Cell, 16*(6), pp. 591-600.

Suh, Y., Atzmon, G., Cho, M.-O., Hwang, D., Liu, B., Leahy, D. J., Barzilai, N. and Cohen, P. (2008) Functionally significant insulin-like growth factor I receptor mutations in centenarians. *Proceedings of the National Academy of Sciences of the United States of America, 105*(9), pp. 3438-3442.

Suhr, S. T., Chang, E. A., Rodriguez, R. M., Wang, K., Ross, P. J., Beyhan, Z., Murthy, S. and Cibelli, J. B. (2009) Telomere dynamics in human cells reprogrammed to pluripotency. *PloS One, 4*(12), pp. e8124.

Suhr, S. T., Chang, E. A., Tjong, J., Alcasid, N., Perkins, G. A., Goissis, M. D., Ellisman, M. H., Perez, G. I. and Cibelli, J. B. (2010) Mitochondrial rejuvenation after induced pluripotency. *PloS One, 5*(11), pp. e14095.

Sun, Y., Li, W., Lu, Z., Chen, R., Ling, J., Ran, Q., Jilka, R. L. and Chen, X.-D. (2011) Rescuing replication and osteogenesis of aged mesenchymal stem cells by exposure to a young extracellular matrix. *The FASEB Journal, 25*(5), pp. 1474-1485.

Suzuki, E., Fujita, D., Takahashi, M., Oba, S. and Nishimatsu, H. (2015) Adipose tissue-derived stem cells as a therapeutic tool for cardiovascular disease. *World Journal of Cardiology, 7*(8), pp. 454-465.

Suzuki, H., Shibata, R., Kito, T., Ishii, M., Li, P., Yoshikai, T., Nishio, N., Ito, S., Numaguchi, Y., Yamashita, J. K., Murohara, T. and Isobe, K. (2010) Therapeutic angiogenesis by transplantation of induced pluripotent stem cell-derived Flk-1 positive cells. *BMC cell biology, 11*(1), pp. 72.

Takahashi, K., Tanabe, K., Ohnuki, M., Narita, M., Ichisaka, T., Tomoda, K. and Yamanaka, S. (2007) Induction of Pluripotent Stem Cells from Adult Human Fibroblasts by Defined Factors. *Cell, 131*(5), pp. 861-872.

Takahashi, K. and Yamanaka, S. (2006) Induction of Pluripotent Stem Cells from Mouse Embryonic and Adult Fibroblast Cultures by Defined Factors. *Cell, 126*(4), pp. 663-676.

Takenaka, C., Nishishita, N., Takada, N., Jakt, L. M. and Kawamata, S. (2010) Effective generation of iPS cells from CD34+ cord blood cells by inhibition of p53. *Experimental Hematology, 38*(2), pp. 154-162.

Takeuchi, M., Takeuchi, K., Ozawa, Y., Kohara, A. and Mizusawa, H. (2009) Aneuploidy in immortalized human mesenchymal stem cells with non-random loss of chromosome 13 in culture. *In Vitro Cellular and Developmental Biology - Animal, 45*(5-6), pp. 290-299.

Thomas, S. M., Kagan, C., Pavlovic, B. J., Burnett, J., Patterson, K., Pritchard, J. K. and Gilad, Y. (2015) Reprogramming LCLs to iPSCs Results in Recovery of Donor-Specific Gene Expression Signature. *PLoS genetics, 11*(5), pp. e1005216.

Thomson, J. A., Itskovitz-Eldor, J., Shapiro, S. S., Waknitz, M. A., Swiergiel, J. J., Marshall, V. S. and Jones, J. M. (1998) Embryonic Stem Cell Lines Derived from Human Blastocysts. *Science, 282*(5391), pp. 1145-1147.

Tilgner, K., Neganova, I., Moreno-Gimeno, I., Al-Aama, J. Y., Burks, D., Yung, S., Singhapol, C., Saretzki, G., Evans, J., Gorbunova, V., Gennery, A., Przyborski, S., Stojkovic, M., Armstrong, L., Jeggo, P. and Lako, M. (2013) A human iPSC model of Ligase IV deficiency reveals an important role for NHEJ-mediated-DSB repair in the survival and genomic stability of induced pluripotent stem cells and emerging haematopoietic progenitors. *Cell Death and Differentiation, 20*(8), pp. 1089-1100.

Trivedi, P. and Hematti, P. (2007) Simultaneous generation of CD34+ primitive hematopoietic cells and CD73+ mesenchymal stem cells from human embryonic stem cells cocultured with murine OP9 stromal cells. *Experimental Hematology, 35*(1), pp. 146-154.

Trivedi, P. and Hematti, P. (2008) Derivation and immunological characterization of mesenchymal stromal cells from human embryonic stem cells. *Experimental Hematology, 36*(3), pp. 350-359.

Trokovic, R., Weltner, J., Noisa, P., Raivio, T. and Otonkoski, T. (2015) Combined negative effect of donor age and time in culture on the reprogramming efficiency into induced pluripotent stem cells. *Stem Cell Research, 15*(1), pp. 254-262.

Tsai, C.-C., Chen, Y.-J., Yew, T.-L., Chen, L.-L., Wang, J.-Y., Chiu, C.-H. and Hung, S.-C. (2011) Hypoxia inhibits senescence and maintains mesenchymal stem cell properties through down-regulation of E2A-p21 by HIF-TWIST. *Blood, 117*(2), pp. 459-469.

Uccelli, A., Moretta, L. and Pistoia, V. (2008) Mesenchymal stem cells in health and disease. *Nature Reviews Immunology, 8*(9), pp. 726-736.

Utikal, J., Polo, J. M., Stadtfeld, M., Maherali, N., Kulalert, W., Walsh, R. M., Khalil, A., Rheinwald, J. G. and Hochedlinger, K. (2009) Immortalization eliminates a roadblock during cellular reprogramming into iPS cells. *Nature, 460*(7259), pp. 1145-1148.

Valavanidis, A., Vlachogianni, T. and Fiotakis, C. (2009) 8-hydroxy-2' -deoxyguanosine (8-OHdG): A critical biomarker of oxidative stress and carcinogenesis. *Journal of Environmental Science and Health. Part C, Environmental Carcinogenesis & Ecotoxicology Reviews, 27*(2), pp. 120-139.

Vallier, L., Alexander, M. and Pedersen, R. A. (2005) Activin/Nodal and FGF pathways cooperate to maintain pluripotency of human embryonic stem cells. *Journal of Cell Science, 118*(Pt 19), pp. 4495-4509.

Vallier, L., Mendjan, S., Brown, S., Chng, Z., Teo, A., Smithers, L. E., Trotter, M. W. B., Cho, C. H. H., Martinez, A., Rugg-Gunn, P., Brons, G. and Pedersen, R. A. (2009) Activin/Nodal signalling maintains pluripotency by controlling Nanog expression. *Development (Cambridge, England), 136*(8), pp. 1339-1349.

Vangsness, C. T., Sternberg, H. and Harris, L. (2015) Umbilical Cord Tissue Offers the Greatest Number of Harvestable Mesenchymal Stem Cells for Research and Clinical Application: A Literature Review of Different Harvest Sites. *Arthroscopy: The Journal of Arthroscopic & Related Surgery: Official Publication of the Arthroscopy Association of North America and the International Arthroscopy Association, 31*(9), pp. 1836-1843.

Villa-Diaz, L. G., Brown, S. E., Liu, Y., Ross, A. M., Lahann, J., Parent, J. M. and Krebsbach, P. H. (2012) Derivation of mesenchymal stem cells from human induced pluripotent stem cells cultured on synthetic substrates. *Stem Cells (Dayton, Ohio), 30*(6), pp. 1174-1181.

Vinué, Á., Andrés-Blasco, I., Herrero-Cervera, A., Piqueras, L., Andrés, V., Burks, D. J., Sanz, M. J. and González-Navarro, H. (2015) Ink4/Arf locus restores glucose tolerance and insulin sensitivity by reducing hepatic steatosis and inflammation in mice with impaired IRS2-dependent signalling. *Biochimica Et Biophysica Acta, 1852*(9), pp. 1729-1742.

Vitale, G., Brugts, M. P., Ogliari, G., Castaldi, D., Fatti, L. M., Varewijck, A. J., Lamberts, S. W., Monti, D., Bucci, L., Cevenini, E., Cavagnini, F., Franceschi, C., Hofland, L. J., Mari, D. and Janssen, J. (2012) Low circulating IGF-I bioactivity is associated with human longevity: findings in centenarians' offspring. *Aging, 4*(9), pp. 580-589.

Voutetakis, K., Chatziioannou, A., Gonos, E. S. and Trougakos, I. P. (2015) Comparative Meta-Analysis of Transcriptomics Data during Cellular Senescence and In Vivo Tissue Ageing. *Oxidative Medicine and Cellular Longevity, 2015*, pp. 732914.

Wagner, W., Bork, S., Horn, P., Krunic, D., Walenda, T., Diehlmann, A., Benes, V., Blake, J., Huber, F.-X., Eckstein, V., Boukamp, P. and Ho, A. D. (2009) Aging and replicative senescence have related effects on human stem and progenitor cells. *PloS One, 4*(6), pp. e5846.

Wagner, W., Bork, S., Lepperdinger, G., Joussen, S., Ma, N., Strunk, D. and Koch, C. (2010) How to track cellular aging of mesenchymal stromal cells? *Aging, 2*(4), pp. 224-230.

Wagner, W., Horn, P., Castoldi, M., Diehlmann, A., Bork, S., Saffrich, R., Benes, V., Blake, J., Pfister, S., Eckstein, V. and Ho, A. D. (2008) Replicative senescence of mesenchymal stem cells: a continuous and organized process. *PloS One, 3*(5), pp. e2213.

Wang, B., Miyagoe-Suzuki, Y., Yada, E., Ito, N., Nishiyama, T., Nakamura, M., Ono, Y., Motohashi, N., Segawa, M., Masuda, S. and Takeda, S. i. (2011) Reprogramming efficiency and quality of induced Pluripotent Stem Cells (iPSCs) generated from muscle-derived fibroblasts of mdx mice at different ages. *PLoS currents, 3*, pp. RRN1274.

Wang, C., Jurk, D., Maddick, M., Nelson, G., Martin-Ruiz, C. and von Zglinicki, T. (2009) DNA damage response and cellular senescence in tissues of aging mice. *Aging Cell, 8*(3), pp. 311-323.

Wang, T., Chen, K., Zeng, X., Yang, J., Wu, Y., Shi, X., Qin, B., Zeng, L., Esteban, M. A., Pan, G. and Pei, D. (2011) The histone demethylases Jhdm1a/1b enhance somatic cell reprogramming in a vitamin-C-dependent manner. *Cell Stem Cell, 9*(6), pp. 575-587.

Wang, X., Kimbrel, E. A., Ijichi, K., Paul, D., Lazorchak, A. S., Chu, J., Kouris, N. A., Yavanian, G. J., Lu, S.-J., Pachter, J. S., Crocker, S. J., Lanza, R. and Xu, R.-H. (2014) Human ESC-derived MSCs outperform bone marrow MSCs in the treatment of an EAE model of multiple sclerosis. *Stem Cell Reports, 3*(1), pp. 115-130.

Wang, Y. and Adjaye, J. (2011) A cyclic AMP analog, 8-Br-cAMP, enhances the induction of pluripotency in human fibroblast cells. *Stem Cell Reviews, 7*(2), pp. 331-341.

Warren, L., Manos, P. D., Ahfeldt, T., Loh, Y.-H., Li, H., Lau, F., Ebina, W., Mandal, P. K., Smith, Z. D., Meissner, A., Daley, G. Q., Brack, A. S., Collins, J. J., Cowan, C., Schlaeger, T. M. and Rossi, D. J. (2010) Highly Efficient Reprogramming to Pluripotency and Directed Differentiation of Human Cells with Synthetic Modified mRNA. *Cell Stem Cell, 7*(5), pp. 618-630.

Watanabe, A., Yamada, Y. and Yamanaka, S. (2013) Epigenetic regulation in pluripotent stem cells: a key to breaking the epigenetic barrier. *Philosophical Transactions of the Royal Society of London. Series B, Biological Sciences, 368*(1609), pp. 20120292.

Watanabe, K., Ueno, M., Kamiya, D., Nishiyama, A., Matsumura, M., Wataya, T., Takahashi, J. B., Nishikawa, S., Nishikawa, S.-i., Muguruma, K. and Sasai, Y. (2007) A ROCK inhibitor permits survival of dissociated human embryonic stem cells. *Nature Biotechnology, 25*(6), pp. 681-686.

Wei, X., Yang, X., Han, Z.-p., Qu, F.-f., Shao, L. and Shi, Y.-f. (2013) Mesenchymal stem cells: a new trend for cell therapy. *Acta Pharmacologica Sinica, 34*(6), pp. 747-754.

Wen, Y., Wani, P., Zhou, L., Baer, T., Phadnis, S. M., Reijo Pera, R. A. and Chen, B. (2013) Reprogramming of fibroblasts from older women with pelvic floor disorders alters cellular behavior associated with donor age. *Stem Cells Translational Medicine, 2*(2), pp. 118-128.

West, A. P., Brodsky, I. E., Rahner, C., Woo, D. K., Erdjument-Bromage, H., Tempst, P., Walsh, M. C., Choi, Y., Shadel, G. S. and Ghosh, S. (2011) TLR signaling augments macrophage bactericidal activity through mitochondrial ROS. *Nature, 472*(7344), pp. 476-480.

Wolfrum, K., Wang, Y., Prigione, A., Sperling, K., Lehrach, H. and Adjaye, J. (2010) The LARGE principle of cellular reprogramming: lost, acquired and retained gene expression in foreskin and amniotic fluid-derived human iPS cells. *PloS One, 5*(10), pp. e13703.

Wolfson, M., Budovsky, A., Tacutu, R. and Fraifeld, V. (2009) The signaling hubs at the crossroad of longevity and age-related disease networks. *The International Journal of Biochemistry & Cell Biology, 41*(3), pp. 516-520.

Xu, R.-H., Peck, R. M., Li, D. S., Feng, X., Ludwig, T. and Thomson, J. A. (2005) Basic FGF and suppression of BMP signaling sustain undifferentiated proliferation of human ES cells. *Nature Methods, 2*(3), pp. 185-190.

Yagi, T., Ito, D., Okada, Y., Akamatsu, W., Nihei, Y., Yoshizaki, T., Yamanaka, S., Okano, H. and Suzuki, N. (2011) Modeling familial Alzheimer's disease with induced pluripotent stem cells. *Human Molecular Genetics, 20*(23), pp. 4530-4539.

Yagi, T., Kosakai, A., Ito, D., Okada, Y., Akamatsu, W., Nihei, Y., Nabetani, A., Ishikawa, F., Arai, Y., Hirose, N., Okano, H. and Suzuki, N. (2012) Establishment of induced pluripotent stem cells from centenarians for neurodegenerative disease research. *PloS One, 7*(7), pp. e41572.

Yang, H., Aprecio, R. M., Zhou, X., Wang, Q., Zhang, W., Ding, Y. and Li, Y. (2014) Therapeutic effect of TSG-6 engineered iPSC-derived MSCs on experimental periodontitis in rats: a pilot study. *PloS One, 9*(6), pp. e100285.

Yao, J., Jiang, S.-L., Liu, W., Liu, C., Chen, W., Sun, L., Liu, K.-Y., Jia, Z.-B., Li, R.-K. and Tian, H. (2012) Tissue inhibitor of matrix metalloproteinase-3 or vascular endothelial growth factor transfection of aged human mesenchymal stem cells enhances cell therapy after myocardial infarction. *Rejuvenation Research, 15*(5), pp. 495-506.

Yoshida, Y., Takahashi, K., Okita, K., Ichisaka, T. and Yamanaka, S. (2009) Hypoxia enhances the generation of induced pluripotent stem cells. *Cell Stem Cell, 5*(3), pp. 237-241.

Yu, J., Chau, K. F., Vodyanik, M. A., Jiang, J. and Jiang, Y. (2011) Efficient feeder-free episomal reprogramming with small molecules. *PloS One, 6*(3), pp. e17557.

Yu, J., Hu, K., Smuga-Otto, K., Tian, S., Stewart, R., Slukvin, I. I. and Thomson, J. A. (2009) Human induced pluripotent stem cells free of vector and transgene sequences. *Science (New York, N.Y.), 324*(5928), pp. 797-801.

Yu, J., Vodyanik, M. A., Smuga-Otto, K., Antosiewicz-Bourget, J., Frane, J. L., Tian, S., Nie, J., Jonsdottir, G. A., Ruotti, V., Stewart, R., Slukvin, I. I. and Thomson, J. A. (2007) Induced Pluripotent Stem Cell Lines Derived from Human Somatic Cells. *Science, 318*(5858), pp. 1917-1920.

Yu, J. M., Wu, X., Gimble, J. M., Guan, X., Freitas, M. A. and Bunnell, B. A. (2011) Age-related changes in mesenchymal stem cells derived from rhesus macaque bone marrow. *Aging Cell, 10*(1), pp. 66-79.

Yulin, X., Lizhen, L., Lifei, Z., Shan, F., Ru, L., Kaimin, H. and Huang, H. (2012) Efficient generation of induced pluripotent stem cells from human bone marrow mesenchymal stem cells. *Folia Biologica, 58*(6), pp. 221-230.

Zappia, E., Casazza, S., Pedemonte, E., Benvenuto, F., Bonanni, I., Gerdoni, E., Giunti, D., Ceravolo, A., Cazzanti, F., Frassoni, F., Mancardi, G. and Uccelli, A. (2005) Mesenchymal stem cells ameliorate experimental autoimmune encephalomyelitis inducing T-cell anergy. *Blood, 106*(5), pp. 1755-1761.

Zhang, C. and Cuervo, A. M. (2008) Restoration of chaperone-mediated autophagy in aging liver improves cellular maintenance and hepatic function. *Nature Medicine, 14*(9), pp. 959-965.

Zhang, D., Yan, B., Yu, S., Zhang, C., Wang, B., Wang, Y., Wang, J., Yuan, Z., Zhang, L. and Pan, J. (2015) Coenzyme Q10 inhibits the aging of mesenchymal stem cells induced by D-galactose through Akt/mTOR signaling. *Oxidative Medicine and Cellular Longevity, 2015*, pp. 867293.

Zhang, H., Fazel, S., Tian, H., Mickle, D. A. G., Weisel, R. D., Fujii, T. and Li, R.-K. (2005) Increasing donor age adversely impacts beneficial effects of bone marrow but not smooth muscle myocardial cell therapy. *American Journal of Physiology - Heart and Circulatory Physiology, 289*(5), pp. H2089-H2096.

Zhang, J., Guan, J., Niu, X., Hu, G., Guo, S., Li, Q., Xie, Z., Zhang, C. and Wang, Y. (2015) Exosomes released from human induced pluripotent stem cells-derived MSCs facilitate cutaneous wound healing by promoting collagen synthesis and angiogenesis. *Journal of Translational Medicine, 13*, pp. 49.

Zhang, J., Li, Y., Chen, J., Cui, Y., Lu, M., Elias, S. B., Mitchell, J. B., Hammill, L., Vanguri, P. and Chopp, M. (2005) Human bone marrow stromal cell treatment improves neurological functional recovery in EAE mice. *Experimental Neurology, 195*(1), pp. 16-26.

Zhang, J., Lian, Q., Zhu, G., Zhou, F., Sui, L., Tan, C., Mutalif, R. A., Navasankari, R., Zhang, Y., Tse, H.-F., Stewart, C. L. and Colman, A. (2011) A human iPSC model of Hutchinson Gilford Progeria reveals vascular smooth muscle and mesenchymal stem cell defects. *Cell Stem Cell, 8*(1), pp. 31-45.

Zhang, J., Nuebel, E., Daley, G. Q., Koehler, C. M. and Teitell, M. A. (2012) Metabolic regulation in pluripotent stem cells during reprogramming and self-renewal. *Cell Stem Cell, 11*(5), pp. 589-595.

Zhang, S., Jiang, Y. Z., Zhang, W., Chen, L., Tong, T., Liu, W., Mu, Q., Liu, H., Ji, J., Ouyang, H. W. and Zou, X. (2013) Neonatal desensitization supports long-term survival and functional integration of human embryonic stem cell-derived mesenchymal stem cells in rat joint cartilage without immunosuppression. *Stem Cells and Development, 22*(1), pp. 90-101.

Zhang, W., Li, J., Suzuki, K., Qu, J., Wang, P., Zhou, J., Liu, X., Ren, R., Xu, X., Ocampo, A., Yuan, T., Yang, J., Li, Y., Shi, L., Guan, D., Pan, H., Duan, S., Ding, Z., Li, M., Yi, F., Bai, R., Wang, Y., Chen, C., Yang, F., Li, X., Wang, Z., Aizawa, E., Goebl, A., Soligalla, R. D., Reddy, P., Esteban, C. R., Tang, F., Liu, G.-H. and Belmonte, J. C. I. (2015) Aging stem cells. A Werner syndrome stem cell model unveils heterochromatin alterations as a driver of human aging. *Science (New York, N.Y.), 348*(6239), pp. 1160-1163.

Zhang, Z.-X., Guan, L.-X., Zhang, K., Wang, S., Cao, P.-C., Wang, Y.-H., Wang, Z. and Dai, L.-J. (2007) Cytogenetic analysis of human bone marrow-derived mesenchymal stem cells passaged in vitro. *Cell Biology International, 31*(6), pp. 645-648.

Zhao, R. and Daley, G. Q. (2008) From fibroblasts to iPS cells: induced pluripotency by defined factors. *Journal of Cellular Biochemistry, 105*(4), pp. 949-955.

Zhao, Y., Yin, X., Qin, H., Zhu, F., Liu, H., Yang, W., Zhang, Q., Xiang, C., Hou, P., Song, Z., Liu, Y., Yong, J., Zhang, P., Cai, J., Liu, M., Li, H., Li, Y., Qu, X., Cui, K., Zhang, W., Xiang, T., Wu, Y., Zhao, Y., Liu, C., Yu, C., Yuan, K., Lou, J., Ding, M. and Deng, H. (2008) Two supporting factors greatly improve the efficiency of human iPSC generation. *Cell Stem Cell, 3*(5), pp. 475-479.

Zhou, S., Greenberger, J. S., Epperly, M. W., Goff, J. P., Adler, C., Leboff, M. S. and Glowacki, J. (2008a) Age-related intrinsic changes in human bone-marrow-derived mesenchymal stem cells and their differentiation to osteoblasts. *Aging Cell, 7*(3), pp. 335-343.

Zhou, Z., Gao, M., Liu, Q. and Tao, M. D. J. (2015) Comprehensive transcriptome analysis of mesenchymal stem cells in elderly patients with osteoporosis. *Aging Clinical and Experimental Research*.

Zhu, S., Li, W., Zhou, H., Wei, W., Ambasudhan, R., Lin, T., Kim, J., Zhang, K. and Ding, S. (2010) Reprogramming of human primary somatic cells by OCT4 and chemical compounds. *Cell Stem Cell, 7*(6), pp. 651-655.

Zuk, P. A., Zhu, M., Mizuno, H., Huang, J., Futrell, J. W., Katz, A. J., Benhaim, P., Lorenz, H. P. and Hedrick, M. H. (2001) Multilineage cells from human adipose tissue: implications for cell-based therapies. *Tissue Engineering, 7*(2), pp. 211-228.

7 Appendix

7.1 Supplementary Material and Methods

7.1.1 Cell culture

7.1.1.1 MEF maintenance medium

Media components used to make 500ml of medium:
445ml of DMEM, high Glucose, (Life Technologies)
50ml of FBS (10%, Biochrom AG)
5ml of Penicillin-Streptomycin (1/100, Life Technologies)
All components were mixed and filtered with a 500ml Vacuum Filter/Storage Bottle System, 0.22µm pore diameter, 19.6cm² Membrane (Corning, 430756)

7.1.1.2 hMSC maintenance medium

Components for 500ml:
440ml MEM α, nucleosides, GlutaMAX™ (Life technologies)
50ml of FBS (10%, Biochrom AG)
5ml of Penicillin-Streptomycin (1:100, Life Technologies)
5ml Non-Essential Amino Acids (1:100, Life Technologies)
All components were mixed and filtered with a 500ml Vacuum Filter/Storage Bottle System, 0.22µm pore diameter, 19.6cm² Membrane (Corning, 430756)

7.1.1.3 Pluripotent stem cell maintenance medium (unconditioned medium)

Components for 500ml:
400ml of Knockout ™ DMEM (Life Technologies)
100ml of Knockout ™ Serum Replacement (20%, Life Technologies)
5ml of 200mM L-glutamine (1/100, Life Technologies)
5ml of Penicillin-Streptomycin (1/100, Life Technologies)
5ml of Non-Essential Amino Acids (1/100, Life Technologies)
All components were mixed and filtered with a 500ml Vacuum Filter/Storage Bottle System, 0.22µm pore diameter, 19.6cm² Membrane (Corning, 430756)

Media additions after filtering:
-35µl of 1.4 M β-mercaptoethanol (Sigma-Aldrich)
-respective volume of 8µg/ml FGF2 stock solution when the medium is used to a final concentration of 4ng/ml FGF2

7.1.1.4 N2B27 medium (defined medium)

Components for 500ml:
470ml of DMEM/F12 (Life Technologies)
5ml of N2 Supplement (100 x , Life Technologies)
10ml of B27 Supplement minus Vitamin A (50x, Life Technologies)
3.4ml of BSA (Bovine Albumin FractionV, 7.5%, Life Technologies)
5ml of 200mM L-glutamine (1/100, Life Technologies)
5ml of Penicillin-Streptomycin (1/100, Life Technologies)
5ml of Non-Essential Amino Acids (1/100, Life Technologies)
All components were mixed and filtered with a 500ml Vacuum Filter/Storage Bottle System, 0.22µm pore diameter, 19.6cm² Membrane (Corning, 430756)

Media additions after filtering:
-35µl of 1.4 M β-mercaptoethanol (Sigma-Aldrich)
-respective volume of 8µg/ml FGF2 stock solution when the medium is used to a final concentration of 4ng/ml FGF2

Mercaptoethanol solution for unconditioned medium

14.3M β-mercaptoethanol (Sigma-Aldrich) was diluted 1:10 in PBS, filtered and stored at −20°C in 40µl aliquots. Aliquots were thawed and used immediately.

8 µg/ml FGF2 stock solution

50µg recombinant human basic fibroblast growth factor (FGF2, Peprotech,100-18B) were reconstituted in 5ml of PBS with 0.2% BSA (Bovine Serum Albumin, Fraction V, 99% purity, Sigma-Aldrich, A9418). The BSA solution was filtered with a 22µm pore size syringe filter (Corning,431225) before the solution was aliquotted and stored at -20°C.

7.1.2 Polymerase chain reaction

7.1.2.1 10 x-B1 buffer

500mM Tris-Cl pH 8.8

200mM (NH4)2SO4

15mM MgCl2

0.1% Tween 20

7.1.2.2 6 x loading buffer

0.2% Bromophenol Blue

60% Glycerol

60mM EDTA

7.1.2.3 20 x SB buffer for electrophoresis

8g	NaOH
45g	Boric Acid

ad 1l with $_{dd}$H2O, adjust pH to 8.0

7.1.2.4 5 x TBE Buffer

10g	Boric acid
30.25g	Tris base
1.86g	EDTA

ad 1l with $_{dd}$H2O, adjust pH to 8.6.

7.1.3 Amplification of plasmid DNA

7.1.3.1 LB medium

10g	NaCl
10g	Peptone (Roth)
5g	Yeast Extract (Sigma-Aldrich)

in 1l $_{dd}H_2O$

7.1.4 Characterisation of hMSCs and iMSCs

7.1.4.1 2% Alizarin Red S staining solution

2g Alizarin Red S

100ml distilled water

The solution was mixed well and the pH was adjusted to 4.2 using 10% ammonium hydroxide.

7.1.4.2 Oil Red O staining

0.5% Oil Red O solution:

0.5g Oil Red O (Sigma-Aldrich)

100ml 2-Propanol (Merck)

The solution has to be freshly prepared before use. Furthermore, it has to be heated for several minutes at 95ºC and filtered with filter paper (Schleicher & Schüll).

Oil Red O solution for immediate application

6 parts of 0.5% Oil Red O in 2-Propanol

4 parts of distilled water

The solution was mixed and filtered using filter paper (Schleicher & Schüll)

7.1.5 iPS generation using retroviruses

7.1.5.1 HEK293T medium

For 500ml medium:

445ml Iscove's Modified Dulbecco's Medium (IMDM) (Life Technologies)

50ml of FBS (10%, BIOCHROM)

5ml of Penicillin-Streptomycin (1/100, Life Technologies)

5ml of 200mM L-glutamine (1/100, Life Technologies)

All components were mixed and filtered with a 500ml Vacuum Filter/Storage Bottle System, 0.22µm pore diameter, 19.6cm² Membrane (Corning, 430756)

7.1.5.2 2 x HBS solution

281mM NaCl

100mM HEPES

1.5mM Na2HPO4

pH 7.12

filtered with 0.22µM pore size filter

7.1.6 Episomal plasmid-based reprogramming

7.1.6.1 Vector maps

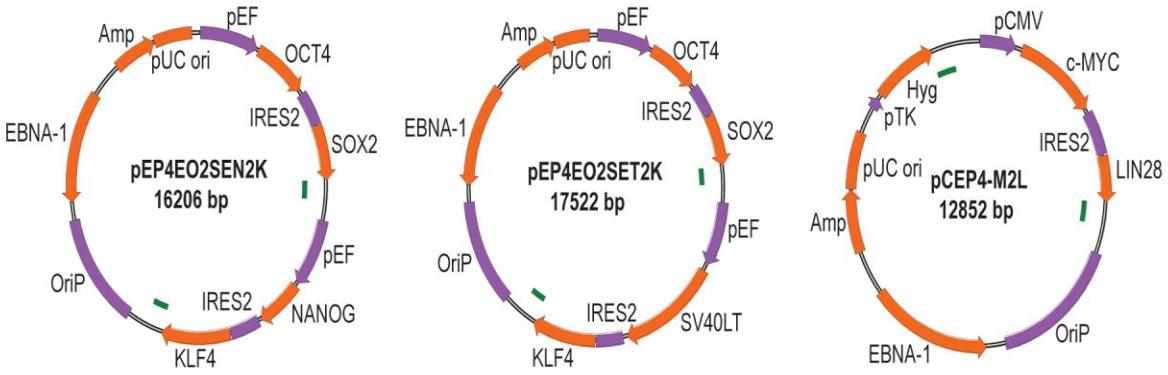

Figure 47 Vector maps of the episomal plasmids used as combination for non-viral reprogramming of hMSCs.

Picture taken from Yu et al. (Yu et al. 2011) pCMV: the cytomegalovirus immediate-early promoter; IRES2: internal ribosome entry site 2, pEF: the eukaryotic elongation 1α promoter.

7.2 Gene sets used for hierarchical clustering analysis

Table 17 Genes related to bone cell differentiation used for hMSC characterisation.

Name	Description
ACVR1	Homo sapiens activin A receptor, type I (ACVR1)
AMELX	Homo sapiens amelogenin (amelogenesis imperfecta 1, X-linked) (AMELX), transcript variant 1
BGLAP	Homo sapiens bone gamma-carboxyglutamate (gla) protein (osteocalcin) (BGLAP)
BMP6	Homo sapiens bone morphogenetic protein 6 (BMP6)
CHRD	Homo sapiens chordin (CHRD)
CITED1	Homo sapiens Cbp/p300-interacting transactivator, with Glu/Asp-rich carboxy-terminal domain, 1 (CITED1)
CREB3L1	Homo sapiens cAMP responsive element binding protein 3-like 1 (CREB3L1)
CYR61	Homo sapiens cysteine-rich, angiogenic inducer, 61 (CYR61)
DDX21	Homo sapiens DEAD (Asp-Glu-Ala-Asp) box polypeptide 21 (DDX21)
DLX5	Homo sapiens distal-less homeobox 5 (DLX5)
DNAJC13	Homo sapiens DnaJ (Hsp40) homolog, subfamily C, member 13 (DNAJC13)
GDF10	Homo sapiens growth differentiation factor 10 (GDF10)
HEMGN	Homo sapiens hemogen (HEMGN), transcript variant 1
HSPE1	Homo sapiens heat shock 10kDa protein 1 (chaperonin 10) (HSPE1)
LIMD1	Homo sapiens LIM domains containing 1 (LIMD1)
LRRC17	Homo sapiens leucine rich repeat containing 17 (LRRC17), transcript variant 2
MRC2	Homo sapiens mannose receptor, C type 2 (MRC2)
MSX2	Homo sapiens msh homeobox 2 (MSX2)
MYBBP1A	Homo sapiens MYB binding protein (P160) 1a (MYBBP1A)
MYOC	Homo sapiens myocilin, trabecular meshwork inducible glucocorticoid response (MYOC)
NBR1	Homo sapiens neighbor of BRCA1 gene 1 (NBR1), transcript variant 2
NELL1	Homo sapiens NEL-like 1 (chicken) (NELL1)
NF1	Homo sapiens neurofibromin 1 (NF1), transcript variant 1
NPNT	Homo sapiens nephronectin (NPNT)
OSTN	Homo sapiens osteocrin (OSTN)
RRAS2	Homo sapiens related RAS viral (r-ras) oncogene homolog 2 (RRAS2)
RRBP1	Homo sapiens ribosome binding protein 1 homolog 180kDa (dog) (RRBP1), transcript variant 1
SMOC1	Homo sapiens SPARC related modular calcium binding 1 (SMOC1), transcript variant 1
SNAI1	Homo sapiens snail homolog 1 (Drosophila) (SNAI1)
SNAI2	Homo sapiens snail homolog 2 (Drosophila) (SNAI2)
SOX8	Homo sapiens SRY (sex determining region Y)-box 8 (SOX8)
SP7	Homo sapiens Sp7 transcription factor (SP7)
SYNCRIP	Homo sapiens synaptotagmin binding, cytoplasmic RNA interacting protein (SYNCRIP)
TWIST1	Homo sapiens twist homolog 1 (Drosophila) (TWIST1)
TWIST2	twist family bHLH transcription factor 2
UCMA	Homo sapiens upper zone of growth plate and cartilage matrix associated (UCMA)

Table 18 Genes annotated to the GO-term cell cycle regulation used to characterise primary hMSCs.

Name	Description
BAP1	Homo sapiens BRCA1 associated protein-1 (ubiquitin carboxy-terminal hydrolase) (BAP1)
BEX2	Homo sapiens brain expressed X-linked 2 (BEX2)
BOP1	Homo sapiens block of proliferation 1 (BOP1)
CABLES1	Homo sapiens Cdk5 and Abl enzyme substrate 1 (CABLES1), transcript variant 1
CABLES2	Homo sapiens Cdk5 and Abl enzyme substrate 2 (CABLES2)
CCNB1	Homo sapiens cyclin B1 (CCNB1)
CCNB2	Homo sapiens cyclin B2 (CCNB2)
CCNDBP1	Homo sapiens cyclin D-type binding-protein 1 (CCNDBP1), transcript variant 2
CCNE1	Homo sapiens cyclin E1 (CCNE1), transcript variant 1
CCNE2	Homo sapiens cyclin E2 (CCNE2), transcript variant 2
CCNF	Homo sapiens cyclin F (CCNF)
CCNG1	Homo sapiens cyclin G1 (CCNG1), transcript variant 2
CCNG2	Homo sapiens cyclin G2 (CCNG2)
CCNI	Homo sapiens cyclin I (CCNI)
CDC25A	Homo sapiens cell division cycle 25 homolog A (S. pombe) (CDC25A), transcript variant 1
CDK3	Homo sapiens cyclin-dependent kinase 3 (CDK3)
CDKL1	Homo sapiens cyclin-dependent kinase-like 1 (CDC2-related kinase) (CDKL1)
CDKL4	Homo sapiens cyclin-dependent kinase-like 4 (CDKL4)
CENPF	Homo sapiens centromere protein F, 350/400ka (mitosin) (CENPF)
DOT1L	Homo sapiens DOT1-like, histone H3 methyltransferase (S. cerevisiae) (DOT1L)
E2F5	Homo sapiens E2F transcription factor 5, p130-binding (E2F5), transcript variant 1
EP300	Homo sapiens E1A binding protein p300 (EP300)
ESX1	Homo sapiens ESX homeobox 1 (ESX1)
FIGNL1	Homo sapiens fidgetin-like 1 (FIGNL1), transcript variant 1
FOXM1	Homo sapiens forkhead box M1 (FOXM1), transcript variant 2
GADD45A	Homo sapiens growth arrest and DNA-damage-inducible, alpha (GADD45A)
GADD45B	Homo sapiens growth arrest and DNA-damage-inducible, beta (GADD45B)
GADD45G	Homo sapiens growth arrest and DNA-damage-inducible, gamma (GADD45G)
GAS2L1	Homo sapiens growth arrest-specific 2 like 1 (GAS2L1), transcript variant 1
GNB2L1	Homo sapiens guanine nucleotide binding protein (G protein), beta polypeptide 2-like 1 (GNB2L1)
GRK5	Homo sapiens G protein-coupled receptor kinase 5 (GRK5)
INHA	Homo sapiens inhibin, alpha (INHA)
JUND	Homo sapiens jun D proto-oncogene (JUND)
LIN37	Homo sapiens lin-37 homolog (C. elegans) (LIN37)
LIN52	Homo sapiens lin-52 homolog (C. elegans) (LIN52)
LIN54	Homo sapiens lin-54 homolog (C. elegans) (LIN54)
LIN9	Homo sapiens lin-9 homolog (C. elegans) (LIN9)
MADD	Homo sapiens MAP-kinase activating death domain (MADD), transcript variant 5
NANOS3	Homo sapiens nitric oxide synthase 3 (endothelial cell) (NOS3)
OVOL2	Homo sapiens ovo-like 2 (Drosophila) (OVOL2)
PES1	Homo sapiens pescadillo homolog 1, containing BRCT domain (zebrafish) (PES1)
PHACTR4	Homo sapiens phosphatase and actin regulator 4 (PHACTR4), transcript variant 2
PLCB1	Homo sapiens phospholipase C, beta 1 (phosphoinositide-specific) (PLCB1), transcript variant 1
PLK1	Homo sapiens polo-like kinase 1 (Drosophila) (PLK1)
PRR11	Homo sapiens proline rich 11 (PRR11)
PTPRC	Homo sapiens protein tyrosine phosphatase, receptor type, C (PTPRC), transcript variant 2
RBBP4	Homo sapiens retinoblastoma binding protein 4 (RBBP4)
RBL1	Homo sapiens retinoblastoma-like 1 (p107) (RBL1), transcript variant 1
RBL2	Homo sapiens retinoblastoma-like 2 (p130) (RBL2)
SIRT2	Homo sapiens sirtuin (silent mating type information regulation 2 homolog) 2 (S. cerevisiae) (SIRT2), transcript variant 1
SON	Homo sapiens SON DNA binding protein (SON), transcript variant f
SPIN2A	Homo sapiens spindlin family, member 2A (SPIN2A)
SPIN2B	Homo sapiens spindlin family, member 2B (SPIN2B), transcript variant 2
TARDBP	Homo sapiens TAR DNA binding protein (TARDBP)
TRIM36	Homo sapiens tripartite motif-containing 36 (TRIM36), transcript variant 2
TRNP1	Homo sapiens TMF1-regulated nuclear protein 1 (TRNP1)
UHRF2	Homo sapiens ubiquitin-like with PHD and ring finger domains 2 (UHRF2)
WEE1	Homo sapiens WEE1 homolog (S. pombe) (WEE1)
YY1AP1	Homo sapiens YY1 associated protein 1 (YY1AP1), transcript variant 2
ZNF703	PREDICTED: Homo sapiens zinc finger protein 703 (ZNF703)

Table 19 Genes annotated to senescence used to charactersise primary hMSCs and iMSCs.

Name	Description
ABL1	Homo sapiens c-abl oncogene 1, receptor tyrosine kinase (ABL1), transcript variant b
AKT1	Homo sapiens v-akt murine thymoma viral oncogene homolog 1 (AKT1), transcript variant 3
ALDH1A3	Homo sapiens aldehyde dehydrogenase 1 family, member A3 (ALDH1A3)
ATM	Homo sapiens ataxia telangiectasia mutated (ATM), transcript variant 1
BMI1	Homo sapiens BMI1 polycomb ring finger oncogene (BMI1)
CALR	Homo sapiens calreticulin (CALR)
CCNA2	Homo sapiens cyclin A2 (CCNA2)
CCNB1	Homo sapiens cyclin B1 (CCNB1)
CCND1	Homo sapiens cyclin D1 (CCND1)
CCNE1	Homo sapiens cyclin E1 (CCNE1), transcript variant 1
CD44	Homo sapiens CD44 molecule (Indian blood group) (CD44), transcript variant 5
CDC25C	Homo sapiens cell division cycle 25 homolog C (S. pombe) (CDC25C), transcript variant 1
CDK2	Homo sapiens cyclin-dependent kinase 2 (CDK2), transcript variant 1
CDK4	Homo sapiens cyclin-dependent kinase 4 (CDK4)
CDK6	Homo sapiens cyclin-dependent kinase 6 (CDK6)
CDKN1A	Homo sapiens cyclin-dependent kinase inhibitor 1A (p21, Cip1) (CDKN1A), transcript variant 1
CDKN1B	Homo sapiens cyclin-dependent kinase inhibitor 1B (p27, Kip1) (CDKN1B)
CDKN1C	Homo sapiens cyclin-dependent kinase inhibitor 1C (p57, Kip2) (CDKN1C)
CDKN2A	Homo sapiens cyclin-dependent kinase inhibitor 2A (melanoma, p16, inhibits CDK4) (CDKN2A), transcript variant 4
CDKN2B	Homo sapiens cyclin-dependent kinase inhibitor 2B (p15, inhibits CDK4) (CDKN2B), transcript variant 2
CDKN2C	Homo sapiens cyclin-dependent kinase inhibitor 2C (p18, inhibits CDK4) (CDKN2C), transcript variant 1
CDKN2D	Homo sapiens cyclin-dependent kinase inhibitor 2D (p19, inhibits CDK4) (CDKN2D), transcript variant 2
CHEK1	Homo sapiens CHK1 checkpoint homolog (S. pombe) (CHEK1)
CHEK2	Homo sapiens CHK2 checkpoint homolog (S. pombe) (CHEK2), transcript variant 1
CITED2	Homo sapiens Cbp/p300-interacting transactivator, with Glu/Asp-rich carboxy-terminal domain, 2 (CITED2), transcript variant 1
COL1A1	Homo sapiens collagen, type I, alpha 1 (COL1A1)
COL3A1	Homo sapiens collagen, type III, alpha 1 (COL3A1)
CREG1	Homo sapiens cellular repressor of E1A-stimulated genes 1 (CREG1)
E2F1	Homo sapiens E2F transcription factor 1 (E2F1)
E2F3	Homo sapiens E2F transcription factor 3 (E2F3)
EGR1	Homo sapiens early growth response 1 (EGR1)
ETS1	Homo sapiens v-ets erythroblastosis virus E26 oncogene homolog 1 (avian) (ETS1)
ETS2	Homo sapiens v-ets erythroblastosis virus E26 oncogene homolog 2 (avian) (ETS2)
FN1	Homo sapiens fibronectin 1 (FN1), transcript variant 6
GADD45A	Homo sapiens growth arrest and DNA-damage-inducible, alpha (GADD45A)
GLB1	Homo sapiens galactosidase, beta 1 (GLB1), transcript variant 179423
GSK3B	Homo sapiens glycogen synthase kinase 3 beta (GSK3B)
HRAS	Homo sapiens v-Ha-ras Harvey rat sarcoma viral oncogene homolog (HRAS), transcript variant 1
ID1	Homo sapiens inhibitor of DNA binding 1, dominant negative helix-loop-helix protein (ID1), transcript variant 2
IFNG	Homo sapiens interferon, gamma (IFNG)
IGF1	Homo sapiens insulin-like growth factor 1 (somatomedin C) (IGF1)
IGF1R	Homo sapiens insulin-like growth factor 1 receptor (IGF1R)
IGFBP3	Homo sapiens insulin-like growth factor binding protein 3 (IGFBP3), transcript variant 2
IGFBP5	Homo sapiens insulin-like growth factor binding protein 5 (IGFBP5)
IGFBP7	Homo sapiens insulin-like growth factor binding protein 7 (IGFBP7)
ING1	Homo sapiens inhibitor of growth family, member 1 (ING1), transcript variant 1
IRF3	Homo sapiens interferon regulatory factor 3 (IRF3)
IRF5	Homo sapiens interferon regulatory factor 5 (IRF5), transcript variant 1
IRF7	Homo sapiens interferon regulatory factor 7 (IRF7), transcript variant b
MAP2K1	Homo sapiens mitogen-activated protein kinase kinase 1 (MAP2K1)
MAP2K3	Homo sapiens mitogen-activated protein kinase kinase 3 (MAP2K3), transcript variant A
MAP2K6	Homo sapiens mitogen-activated protein kinase kinase 6 (MAP2K6)
MAPK14	Homo sapiens mitogen-activated protein kinase 14 (MAPK14), transcript variant 3
MDM2	Homo sapiens Mdm2 p53 binding protein homolog (mouse) (MDM2), transcript variant MDM2
MORC3	Homo sapiens MORC family CW-type zinc finger 3 (MORC3)
MYC	Homo sapiens v-myc myelocytomatosis viral oncogene homolog (avian) (MYC)
NBN	Homo sapiens nibrin (NBN), transcript variant 2
NFKB1	Homo sapiens nuclear factor of kappa light polypeptide gene enhancer in B-cells 1 (NFKB1)
NOX4	Homo sapiens NADPH oxidase 4 (NOX4)
PCNA	Homo sapiens proliferating cell nuclear antigen (PCNA), transcript variant 2
PIK3CA	Homo sapiens phosphoinositide-3-kinase, catalytic, alpha polypeptide (PIK3CA)
PLAU	Homo sapiens plasminogen activator, urokinase (PLAU)
PRKCD	Homo sapiens protein kinase C, delta (PRKCD), transcript variant 1
PTEN	Homo sapiens phosphatase and tensin homolog (PTEN)
RB1	Homo sapiens retinoblastoma 1 (RB1)
RBL1	Homo sapiens retinoblastoma-like 1 (p107) (RBL1), transcript variant 1
RBL2	Homo sapiens retinoblastoma-like 2 (p130) (RBL2)
SERPINB2	Homo sapiens serpin peptidase inhibitor, clade B (ovalbumin), member 2 (SERPINB2)
SERPINE1	Homo sapiens serpin peptidase inhibitor, clade E (nexin, plasminogen activator inhibitor type 1), member 1 (SERPINE1)
SIRT1	Homo sapiens sirtuin (silent mating type information regulation 2 homolog) 1 (S. cerevisiae) (SIRT1)
SOD1	Homo sapiens superoxide dismutase 1, soluble (SOD1)
SOD2	Homo sapiens superoxide dismutase 2, mitochondrial (SOD2), nuclear gene encoding mitochondrial protein, transcript variant 3
SPARC	Homo sapiens secreted protein, acidic, cysteine-rich (osteonectin) (SPARC)
TBX2	Homo sapiens T-box 2 (TBX2)
TBX3	Homo sapiens T-box 3 (TBX3), transcript variant 1
TERF2	Homo sapiens telomeric repeat binding factor 2 (TERF2)
TERT	Homo sapiens telomerase reverse transcriptase (TERT), transcript variant 1
TGFB1	Homo sapiens transforming growth factor, beta 1 (TGFB1)
TGFB1I1	Homo sapiens transforming growth factor beta 1 induced transcript 1 (TGFB1I1), transcript variant 2
THBS1	Homo sapiens thrombospondin 1 (THBS1)
TP53	Homo sapiens tumor protein p53 (TP53)
TP53BP1	Homo sapiens tumor protein p53 binding protein 1 (TP53BP1)
TWIST1	Homo sapiens twist homolog 1 (Drosophila) (TWIST1)
VIM	Homo sapiens vimentin (VIM)

Table 20 Genes annotated to response to oxidative stress used to characterise primary hMSCs, iPSCs and iMSCs.

Name	Description
ANGPTL7	Homo sapiens angiopoietin-like 7 (ANGPTL7)
DUOX1	Homo sapiens dual oxidase 1 (DUOX1), transcript variant 1
DUOX2	Homo sapiens dual oxidase 2 (DUOX2)
DUSP1	Homo sapiens dual specificity phosphatase 1 (DUSP1)
GPX1	Homo sapiens glutathione peroxidase 1 (GPX1), transcript variant 2
GPX2	Homo sapiens glutathione peroxidase 2 (gastrointestinal) (GPX2)
GPX3	Homo sapiens glutathione peroxidase 3 (plasma) (GPX3)
GPX4	Homo sapiens glutathione peroxidase 4 (phospholipid hydroperoxidase) (GPX4), transcript variant 2
GPX6	Homo sapiens glutathione peroxidase 6 (olfactory) (GPX6)
HMOX2	Homo sapiens heme oxygenase (decycling) 2 (HMOX2)
HNF1A	Homo sapiens transcription factor 1, hepatic; LF-B1, hepatic nuclear factor (HNF1), albumin proximal factor (TCF1)
KRT1	Homo sapiens keratin 1 (KRT1)
LIAS	Homo sapiens lipoic acid synthetase (LIAS), nuclear gene encoding mitochondrial protein, transcript variant 2
LPO	Homo sapiens lactoperoxidase (LPO)
LRRK2	Homo sapiens leucine-rich repeat kinase 2 (LRRK2)
MPO	Homo sapiens myeloperoxidase (MPO), nuclear gene encoding mitochondrial protein
MSRA	Homo sapiens methionine sulfoxide reductase A (MSRA)
MSRB2	Homo sapiens methionine sulfoxide reductase B2 (MSRB2)
MSRB3	Homo sapiens methionine sulfoxide reductase B3 (MSRB3), transcript variant 1
OXR1	Homo sapiens oxidation resistance 1 (OXR1)
OXSR1	Homo sapiens oxidative-stress responsive 1 (OXSR1)
PARK7	Homo sapiens Parkinson disease (autosomal recessive, early onset) 7 (PARK7)
PDLIM1	Homo sapiens PDZ and LIM domain 1 (PDLIM1)
PTGS1	Homo sapiens prostaglandin-endoperoxide synthase 1 (prostaglandin G/H synthase and cyclooxygenase) (PTGS1), transcript variant 2
PXDNL	Homo sapiens peroxidasin homolog (Drosophila)-like (PXDNL)
RCAN1	Homo sapiens regulator of calcineurin 1 (RCAN1), transcript variant 2
RGS14	Homo sapiens regulator of G-protein signaling 14 (RGS14)
SCARA3	Homo sapiens scavenger receptor class A, member 3 (SCARA3), transcript variant 2
SELK	Homo sapiens selenoprotein K (SELK)
SEPP1	Homo sapiens selenoprotein P, plasma, 1 (SEPP1), transcript variant 1
SRXN1	Homo sapiens sulfiredoxin 1 homolog (S. cerevisiae) (SRXN1)
STK25	Homo sapiens serine/threonine kinase 25 (STE20 homolog, yeast) (STK25)
TPO	Homo sapiens thyroid peroxidase (TPO), transcript variant 2
TRPM2	Homo sapiens transient receptor potential cation channel, subfamily M, member 2 (TRPM2), transcript variant S
VNN1	Homo sapiens vanin 1 (VNN1)

Table 21 Genes annotated to pluripotency used to charactersise primary hMSCs and iPSCs.

Name	Description
ALPL	Homo sapiens alkaline phosphatase, liver/bone/kidney (ALPL), transcript variant 1
CD9	Homo sapiens CD9 molecule (CD9)
CER1	Homo sapiens cerberus 1, cysteine knot superfamily, homolog (Xenopus laevis) (CER1)
DNMT3B	Homo sapiens DNA (cytosine-5-)-methyltransferase 3 beta (DNMT3B), transcript variant 1
DPPA4	Homo sapiens developmental pluripotency associated 4 (DPPA4)
ESRRB	Homo sapiens estrogen-related receptor beta (ESRRB)
FGF4	Homo sapiens fibroblast growth factor 4 (heparin secretory transforming protein 1, Kaposi sarcoma oncogene) (FGF4)
FOXD3	Homo sapiens forkhead box D3 (FOXD3)
GABRB3	Homo sapiens gamma-aminobutyric acid (GABA) A receptor, beta 3 (GABRB3), transcript variant 1
GAL	Homo sapiens galanin prepropeptide (GAL)
GDF3	Homo sapiens growth differentiation factor 3 (GDF3)
GRB7	Homo sapiens growth factor receptor-bound protein 7 (GRB7), transcript variant 1
IFITM1	Homo sapiens interferon induced transmembrane protein 1 (9-27) (IFITM1)
KLF4	Homo sapiens Kruppel-like factor 4 (gut) (KLF4)
LEFTY1	Homo sapiens left-right determination factor 1 (LEFTY1)
LEFTY2	Homo sapiens left-right determination factor 2 (LEFTY2)
LIN28	Homo sapiens lin-28 homolog (C. elegans) (LIN28)
MYC	Homo sapiens v-myc myelocytomatosis viral oncogene homolog (avian) (MYC)
MYCN	Homo sapiens v-myc myelocytomatosis viral related oncogene, neuroblastoma derived (avian) (MYCN)
NANOG	Homo sapiens Nanog homeobox (NANOG)
NODAL	Homo sapiens nodal homolog (mouse) (NODAL)
NR5A2	Homo sapiens nuclear receptor subfamily 5, group A, member 2 (NR5A2), transcript variant 2
PODXL	Homo sapiens podocalyxin-like (PODXL), transcript variant 1
POU5F1	Homo sapiens POU class 5 homeobox 1 (POU5F1), transcript variant 1
SOX2	Homo sapiens SRY (sex determining region Y)-box 2 (SOX2)
TDGF1	Homo sapiens teratocarcinoma-derived growth factor 1 (TDGF1)
TERT	Homo sapiens telomerase reverse transcriptase (TERT), transcript variant 1
UTF1	Homo sapiens undifferentiated embryonic cell transcription factor 1 (UTF1)
ZFP42	Homo sapiens zinc finger protein 42 homolog (mouse) (ZFP42)

Table 22 Genes annotated to ageing used to characterise iPSCs and iMSCs.

Name	Description
APOD	Homo sapiens apolipoprotein D (APOD)
ATM	Homo sapiens ataxia telangiectasia mutated (ATM), transcript variant 1
C2orf40	Homo sapiens chromosome 2 open reading frame 40 (C2orf40)
CASP7	Homo sapiens caspase 7, apoptosis-related cysteine peptidase (CASP7), transcript variant gamma
CIITA	Homo sapiens class II, major histocompatibility complex, transactivator (CIITA)
CISD2	Homo sapiens CDGSH iron sulfur domain 2 (CISD2)
CITED2	Homo sapiens Cbp/p300-interacting transactivator, with Glu/Asp-rich carboxy-terminal domain, 2 (CITED2), transcript variant 1
ENG	Homo sapiens endoglin (Osler-Rendu-Weber syndrome 1) (ENG)
FADS1	Homo sapiens fatty acid desaturase 1 (FADS1)
HELT	Homo sapiens HES/HEY-like transcription factor (HELT)
ID2	Homo sapiens inhibitor of DNA binding 2, dominant negative helix-loop-helix protein (ID2)
IDE	Homo sapiens insulin-degrading enzyme (IDE)
ING2	Homo sapiens inhibitor of growth family, member 2 (ING2)
KRT16	Homo sapiens keratin 16 (focal non-epidermolytic palmoplantar keratoderma) (KRT16)
KRT25	Homo sapiens keratin 25 (KRT25)
KRT33B	Homo sapiens keratin 33B (KRT33B)
KRT83	Homo sapiens keratin 83 (KRT83)
KRTAP4-3	keratin associated protein 4-3
KRTAP4-5	Homo sapiens keratin associated protein 4-5 (KRTAP4-5)
KRTAP4-7	Homo sapiens keratin associated protein 4-7 (KRTAP4-7)
KRTAP4-8	keratin associated protein 4-8
LOXL2	Homo sapiens lysyl oxidase-like 2 (LOXL2)
LRRK2	Homo sapiens leucine-rich repeat kinase 2 (LRRK2)
MAGEA2	Homo sapiens melanoma antigen family A, 2 (MAGEA2), transcript variant 3
MARCH5	Homo sapiens membrane-associated ring finger (C3HC4) 5 (MARCH5)
MIF	Homo sapiens macrophage migration inhibitory factor (glycosylation-inhibiting factor) (MIF)
MORC3	Homo sapiens MORC family CW-type zinc finger 3 (MORC3)
NEK4	Homo sapiens NIMA (never in mitosis gene a)-related kinase 4 (NEK4)
NOX4	Homo sapiens NADPH oxidase 4 (NOX4)
NPM1	Homo sapiens nucleophosmin (nucleolar phosphoprotein B23, numatrin) (NPM1), transcript variant 2
NUAK1	Homo sapiens NUAK family, SNF1-like kinase, 1 (NUAK1)
OPA1	Homo sapiens optic atrophy 1 (autosomal dominant) (OPA1), nuclear gene encoding mitochondrial protein, transcript variant 1
PDCD4	Homo sapiens programmed cell death 4 (neoplastic transformation inhibitor) (PDCD4), transcript variant 2
PLA2R1	Homo sapiens phospholipase A2 receptor 1, 180kDa (PLA2R1), transcript variant 2
PNPT1	Homo sapiens polyribonucleotide nucleotidyltransferase 1 (PNPT1)
ROMO1	Homo sapiens chromosome 20 open reading frame 52 (C20orf52)
RSL1D1	Homo sapiens ribosomal L1 domain containing 1 (RSL1D1)
SOD2	Homo sapiens superoxide dismutase 2, mitochondrial (SOD2), nuclear gene encoding mitochondrial protein, transcript variant 3
SPEF2	Homo sapiens sperm flagellar 2 (SPEF2), transcript variant 2
TBX2	Homo sapiens T-box 2 (TBX2)
TBX3	Homo sapiens T-box 3 (TBX3), transcript variant 1
TSPO	Homo sapiens translocator protein (18kDa) (TSPO), transcript variant PBR
TWIST1	Homo sapiens twist homolog 1 (Drosophila) (TWIST1)
VASH1	Homo sapiens vasohibin 1 (VASH1)
ZKSCAN3	Homo sapiens zinc finger with KRAB and SCAN domains 3 (ZKSCAN3)
ZNF277	Homo sapiens zinc finger protein 277 (ZNF277)

Table 23 Gene of the UNIGENE annotation bone normal 3d differentially expressed between hMSC-derived and hFF-derived iPSCs.

Name	Descripton
ABCE1	Homo sapiens ATP-binding cassette, sub-family E (OABP), member 1 (ABCE1), transcript variant 2
AES	Homo sapiens amino-terminal enhancer of split (AES), transcript variant 2
ARPC4	Homo sapiens actin related protein 2/3 complex, subunit 4, 20kDa (ARPC4), transcript variant 2
ATP6V0C	PREDICTED: Homo sapiens ATPase, H+ transporting, lysosomal 16kDa, V0 subunit c (ATP6V0C)
BCAT1	Homo sapiens branched chain aminotransferase 1, cytosolic (BCAT1)
BCLAF1	Homo sapiens BCL2-associated transcription factor 1 (BCLAF1), transcript variant 1
C5ORF51	Homo sapiens chromosome 5 open reading frame 51 (C5orf51)
C7ORF28B	Homo sapiens chromosome 7 open reading frame 28B (C7orf28B)
CAV1	Homo sapiens caveolin 1, caveolae protein, 22kDa (CAV1)
CBFB	Homo sapiens core-binding factor, beta subunit (CBFB), transcript variant 2
CBX1	Homo sapiens chromobox homolog 1 (HP1 beta homolog Drosophila) (CBX1)
CCT6A	Homo sapiens chaperonin containing TCP1, subunit 6A (zeta 1) (CCT6A), transcript variant 1
CEP55	Homo sapiens centrosomal protein 55kDa (CEP55)
COL11A1	Homo sapiens collagen, type XI, alpha 1 (COL11A1), transcript variant A
COL12A1	Homo sapiens collagen, type XII, alpha 1 (COL12A1), transcript variant short
COL5A2	Homo sapiens collagen, type V, alpha 2 (COL5A2)
COL6A1	Homo sapiens collagen, type VI, alpha 1 (COL6A1)
COL6A2	Homo sapiens collagen, type VI, alpha 2 (COL6A2), transcript variant 2C2
COL9A2	Homo sapiens collagen, type IX, alpha 2 (COL9A2)
CPA4	Homo sapiens carboxypeptidase A4 (CPA4)
CYTH3	Homo sapiens cytohesin 3 (CYTH3)
DDX55	Homo sapiens DEAD (Asp-Glu-Ala-Asp) box polypeptide 55 (DDX55)
DIAPH1	Homo sapiens diaphanous homolog 1 (Drosophila) (DIAPH1)
DLGAP5	Homo sapiens discs, large (Drosophila) homolog-associated protein 5 (DLGAP5)
DLX1	Homo sapiens distal-less homeobox 1 (DLX1), transcript variant 1
EFR3A	Homo sapiens EFR3 homolog A (S. cerevisiae) (EFR3A)
EIF5A	Homo sapiens eukaryotic translation initiation factor 5A (EIF5A)
EPHX1	Homo sapiens epoxide hydrolase 1, microsomal (xenobiotic) (EPHX1)
EPM2AIP1	Homo sapiens EPM2A (laforin) interacting protein 1 (EPM2AIP1)
EXTL2	Homo sapiens exostoses (multiple)-like 2 (EXTL2), transcript variant 1
FAM129B	Homo sapiens family with sequence similarity 129, member B (FAM129B), transcript variant 2
FOXD1	Homo sapiens forkhead box D1 (FOXD1)
FOXO4	Homo sapiens forkhead box O4 (FOXO4)
GGCT	Homo sapiens gamma-glutamyl cyclotransferase (GGCT)
GLIPR1	Homo sapiens GLI pathogenesis-related 1 (GLIPR1)
GPR176	Homo sapiens G protein-coupled receptor 176 (GPR176)
GSTT1	Homo sapiens glutathione S-transferase theta 1 (GSTT1)
H2AFX	Homo sapiens H2A histone family, member X (H2AFX)
INO80E	Homo sapiens INO80 complex subunit E (INO80E)
IPO8	Homo sapiens importin 8 (IPO8)
ITGA11	Homo sapiens integrin, alpha 11 (ITGA11)
ITGAV	Homo sapiens integrin, alpha V (vitronectin receptor, alpha polypeptide, antigen CD51) (ITGAV)
ITGB1BP1	Homo sapiens integrin beta 1 binding protein 1 (ITGB1BP1), transcript variant 2
JAK1	Homo sapiens Janus kinase 1 (JAK1)
LDOC1	Homo sapiens leucine zipper, down-regulated in cancer 1 (LDOC1)
LEFTY2	Homo sapiens left-right determination factor 2 (LEFTY2)
MKI67IP	Homo sapiens MKI67 (FHA domain) interacting nucleolar phosphoprotein (MKI67IP)
MYL9	Homo sapiens myosin, light chain 9, regulatory (MYL9), transcript variant 1
NFIX	Homo sapiens nuclear factor I/X (CCAAT-binding transcription factor) (NFIX)
NLN	Homo sapiens neurolysin (metallopeptidase M3 family) (NLN)
NQO2	Homo sapiens NAD(P)H dehydrogenase, quinone 2 (NQO2)
NRP1	Homo sapiens neuropilin 1 (NRP1), transcript variant 1
PA2G4	Homo sapiens proliferation-associated 2G4, 38kDa (PA2G4)
PARL	Homo sapiens presenilin associated, rhomboid-like (PARL), nuclear gene encoding mitochondrial protein, transcript variant 1
PDSS1	Homo sapiens prenyl (decaprenyl) diphosphate synthase, subunit 1 (PDSS1)
PNN	Homo sapiens pinin, desmosome associated protein (PNN)
PODXL	Homo sapiens podocalyxin-like (PODXL), transcript variant 1
PPAT	Homo sapiens phosphoribosyl pyrophosphate amidotransferase (PPAT)
PRPF3	Homo sapiens PRP3 pre-mRNA processing factor 3 homolog (S. cerevisiae) (PRPF3)
PRRX1	Homo sapiens paired related homeobox 1 (PRRX1), transcript variant pmx-1a
PRSS23	Homo sapiens protease, serine, 23 (PRSS23)
RCAN1	Homo sapiens regulator of calcineurin 1 (RCAN1), transcript variant 2
RPA1	Homo sapiens replication protein A1, 70kDa (RPA1)
SET	Homo sapiens SET translocation (myeloid leukemia-associated) (SET)
SHISA2	Homo sapiens shisa homolog 2 (Xenopus laevis) (SHISA2)
SLC25A46	Homo sapiens solute carrier family 25, member 46 (SLC25A46)
SMO	Homo sapiens smoothened homolog (Drosophila) (SMO)
SPATS2L	Homo sapiens spermatogenesis associated, serine-rich 2-like (SPATS2L), transcript variant 2
SPP1	Homo sapiens secreted phosphoprotein 1 (SPP1), transcript variant 2
ST3GAL5	Homo sapiens ST3 beta-galactoside alpha-2,3-sialyltransferase 5 (ST3GAL5), transcript variant 2
SYDE1	Homo sapiens synapse defective 1, Rho GTPase, homolog 1 (C. elegans) (SYDE1)
TCERG1	Homo sapiens transcription elongation regulator 1 (TCERG1), transcript variant 1
TERF1	Homo sapiens telomeric repeat binding factor (NIMA-interacting) 1 (TERF1), transcript variant 1
TGFB1I1	Homo sapiens transforming growth factor beta 1 induced transcript 1 (TGFB1I1), transcript variant 2
TGFBR2	Homo sapiens transforming growth factor, beta receptor II (70/80kDa) (TGFBR2), transcript variant 1
THBS2	Homo sapiens thrombospondin 2 (THBS2)
TM2D2	Homo sapiens TM2 domain containing 2 (TM2D2), transcript variant 1
TMED2	Homo sapiens transmembrane emp24 domain trafficking protein 2 (TMED2)
TMEM48	Homo sapiens transmembrane protein 48 (TMEM48)
TMPO	Homo sapiens thymopoietin (TMPO), transcript variant 1
TRMT5	Homo sapiens TRM5 tRNA methyltransferase 5 homolog (S. cerevisiae) (TRMT5)
USMG5	Homo sapiens up-regulated during skeletal muscle growth 5 homolog (mouse) (USMG5)
VAMP2	Homo sapiens vesicle-associated membrane protein 2 (synaptobrevin 2) (VAMP2)
VIM	Homo sapiens vimentin (VIM)
XRCC5	Homo sapiens X-ray repair complementing defective repair in Chinese hamster cells 5 (double-strand-break rejoining; Ku autoantigen, 80kDa) (XRCC5)
ZNF195	Homo sapiens zinc finger protein 195 (ZNF195)
ZNF271	Homo sapiens zinc finger protein 271 (ZNF271)
ZNF286A	Homo sapiens zinc finger protein 286A (ZNF286A)
ZNF33B	Homo sapiens zinc finger protein 33B (ZNF33B)

Table 24 MSC-specific marker genes and other MSC-associated genes expressed in iMSCs.

MSC-specific markers	
Name	Description
ALCAM	Homo sapiens activated leukocyte cell adhesion molecule (ALCAM)
ANPEP	Homo sapiens alanyl (membrane) aminopeptidase (aminopeptidase N, aminopeptidase M, microsomal aminopeptidase, CD13, p150) (ANPEP)
BMP2	Homo sapiens bone morphogenetic protein 2 (BMP2)
CASP3	Homo sapiens caspase 3, apoptosis-related cysteine peptidase (CASP3), transcript variant beta
CD44	Homo sapiens CD44 molecule (Indian blood group) (CD44), transcript variant 5
ENG (CD105)	Homo sapiens endoglin (Osler-Rendu-Weber syndrome 1) (ENG)
ERBB2 (HER2)	Homo sapiens v-erb-b2 erythroblastic leukemia viral oncogene homolog 2, neuro/glioblastoma derived oncogene homolog (avian) (ERBB2), transcript variant 1
FUT4	Homo sapiens fucosyltransferase 4 (alpha (1,3) fucosyltransferase, myeloid-specific) (FUT4)
ITGAV	Homo sapiens integrin, alpha V (vitronectin receptor, alpha polypeptide, antigen CD51) (ITGAV)
NT5E (CD73)	Homo sapiens 5'-nucleotidase, ecto (CD73) (NT5E)
PDGFRB	Homo sapiens platelet-derived growth factor receptor, beta polypeptide (PDGFRB)
THY1 (CD90)	Homo sapiens Thy-1 cell surface antigen (THY1)
VCAM1	Homo sapiens vascular cell adhesion molecule 1 (VCAM1), transcript variant 1
Other genes associated with MSCs	
Name	Description
ANXA5	Homo sapiens annexin A5 (ANXA5)
COL1A1	Homo sapiens collagen, type I, alpha 1 (COL1A1)
CTNNB1	Homo sapiens catenin (cadherin-associated protein), beta 1, 88kDa (CTNNB1), transcript variant 2
IL10	Homo sapiens interleukin 10 (IL10)
IL6	Homo sapiens interleukin 6 (interferon, beta 2) (IL6)
ITGB1	Homo sapiens integrin, beta 1 (fibronectin receptor, beta polypeptide, antigen CD29 includes MDF2, MSK12) (ITGB1), transcript variant 1A
KITLG	Homo sapiens KIT ligand (KITLG), transcript variant b
MIF	Homo sapiens macrophage migration inhibitory factor (glycosylation-inhibiting factor) (MIF)
MMP2	Homo sapiens matrix metallopeptidase 2 (gelatinase A, 72kDa gelatinase, 72kDa type IV collagenase) (MMP2)
NES	Homo sapiens nestin (NES)
NUDT6	Homo sapiens nudix (nucleoside diphosphate linked moiety X)-type motif 6 (NUDT6), transcript variant 1
PIGS	Homo sapiens phosphatidylinositol glycan anchor biosynthesis, class S (PIGS)
SerpinE1	Homo sapiens serpin peptidase inhibitor, clade E (nexin, plasminogen activator inhibitor type 1), member 1 (SERPINE1)
TGFB3	Homo sapiens transforming growth factor, beta 3 (TGFB3)
VEGFA	Homo sapiens vascular endothelial growth factor A (VEGFA), transcript variant 2

Table 25 Genes related to MSC-differentiation expressed in iMSCs.

Osteogenesis	
Name	Descripton
HDAC1	Homo sapiens histone deacetylase 1 (HDAC1)
PTK2	Homo sapiens PTK2 protein tyrosine kinase 2 (PTK2), transcript variant 1
RUNX2	Homo sapiens runt-related transcription factor 2 (RUNX2), transcript variant 1
SMURF1	Homo sapiens SMAD specific E3 ubiquitin protein ligase 1 (SMURF1), transcript variant 2
Adipogenesis	
Name	Descripton
PPARG	Homo sapiens peroxisome proliferator-activated receptor gamma (PPARG), transcript variant 2
RHOA	Homo sapiens ras homolog gene family, member A (RHOA)
RUNX2	Homo sapiens runt-related transcription factor 2 (RUNX2), transcript variant 1
Chondrogenesis	
Name	Descripton
BMP4	Homo sapiens bone morphogenetic protein 4 (BMP4), transcript variant 1
HAT1	Homo sapiens histone acetyltransferase 1 (HAT1), transcript variant 1
KAT2B	K(lysine) acetyltransferase 2B
SOX9	Homo sapiens SRY (sex determining region Y)-box 9 (campomelic dysplasia, autosomal sex-reversal) (SOX9)
TGFB1	Homo sapiens transforming growth factor, beta 1 (TGFB1)
Myogenesis	
Name	Descripton
ACTA2	Homo sapiens actin, alpha 2, smooth muscle, aorta (ACTA2)
JAG1	Homo sapiens jagged 1 (Alagille syndrome) (JAG1)
NOTCH1	Homo sapiens Notch homolog 1, translocation-associated (Drosophila) (NOTCH1)
Tenogenesis	
Name	Descripton
GDF15 (PLAB)	Homo sapiens growth differentiation factor 15 (GDF15)

Table 26 Genes annotated to regulation of senescence used to characterise iMSCs.

Name	Descripton
ABL1	Homo sapiens c-abl oncogene 1, receptor tyrosine kinase (ABL1), transcript variant b
ARNTL	Homo sapiens aryl hydrocarbon receptor nuclear translocator-like (ARNTL), transcript variant 2
BCL2L12	Homo sapiens BCL2-like 12 (proline rich) (BCL2L12), transcript variant 3
BCL6	Homo sapiens B-cell CLL/lymphoma 6 (zinc finger protein 51) (BCL6), transcript variant 1
BMPR1A	Homo sapiens bone morphogenetic protein receptor, type IA (BMPR1A)
CDK6	Homo sapiens cyclin-dependent kinase 6 (CDK6)
CDKN2A	Homo sapiens cyclin-dependent kinase inhibitor 2A (melanoma, p16, inhibits CDK4) (CDKN2A), transcript variant 4
HMGA1	Homo sapiens high mobility group AT-hook 1 (HMGA1), transcript variant 6
HMGA2	Homo sapiens high mobility group AT-hook 2 (HMGA2), transcript variant 2
ING2	Homo sapiens inhibitor of growth family, member 2 (ING2)
NEK4	Homo sapiens NIMA (never in mitosis gene a)-related kinase 4 (NEK4)
NEK6	Homo sapiens NIMA (never in mitosis gene a)-related kinase 6 (NEK6)
NUAK1	Homo sapiens NUAK family, SNF1-like kinase, 1 (NUAK1)
PNPT1	Homo sapiens polyribonucleotide nucleotidyltransferase 1 (PNPT1)
RSL1D1	Homo sapiens ribosomal L1 domain containing 1 (RSL1D1)
SIRT1	Homo sapiens sirtuin (silent mating type information regulation 2 homolog) 1 (S. cerevisiae) (SIRT1)
TERF2	Homo sapiens telomeric repeat binding factor 2 (TERF2)
TERT	Homo sapiens telomerase reverse transcriptase (TERT), transcript variant 1
TP63	Homo sapiens tumor protein p63
TWIST1	Homo sapiens twist homolog 1 (Drosophila) (TWIST1)
VASH1	Homo sapiens vasohibin 1 (VASH1)
ZKSCAN3	Homo sapiens zinc finger with KRAB and SCAN domains 3 (ZKSCAN3)
ZNF277	Homo sapiens zinc finger protein 277 (ZNF277)

Table 27 Genes annotated to regulation of DNA damage repair used to characterise iMSCs.

Name	Descripton
APEX1	Homo sapiens APEX nuclease (multifunctional DNA repair enzyme) 1 (APEX1), transcript variant 3
APEX2	Homo sapiens APEX nuclease (apurinic/apyrimidinic endonuclease) 2 (APEX2), nuclear gene encoding mitochondrial protein
ATXN3	Homo sapiens ataxin 3 (ATXN3), transcript variant 2
BRCA1	Homo sapiens breast cancer 1, early onset (BRCA1), transcript variant BRCA1-delta14-17
BRCA2	Homo sapiens breast cancer 2, early onset (BRCA2)
BRIP1	Homo sapiens BRCA1 interacting protein C-terminal helicase 1 (BRIP1)
CCNH	Homo sapiens cyclin H (CCNH)
CCNO	Homo sapiens cyclin O (CCNO)
CDK7	Homo sapiens cyclin-dependent kinase 7 (MO15 homolog, Xenopus laevis, cdk-activating kinase) (CDK7)
DDB1	Homo sapiens damage-specific DNA binding protein 1, 127kDa (DDB1)
DDB2	Homo sapiens damage-specific DNA binding protein 2, 48kDa (DDB2)
DMC1	Homo sapiens DMC1 dosage suppressor of mck1 homolog, meiosis-specific homologous recombination (yeast) (DMC1)
ERCC1	Homo sapiens excision repair cross-complementing rodent repair deficiency, complementation group 1 (includes overlapping antisense sequence) (ERCC1), transcript variant 2
ERCC2	Homo sapiens excision repair cross-complementing rodent repair deficiency, complementation group 2 (xeroderma pigmentosum D) (ERCC2)
ERCC3	Homo sapiens excision repair cross-complementing rodent repair deficiency, complementation group 3 (xeroderma pigmentosum group B complementing) (ERCC3)
ERCC4	Homo sapiens excision repair cross-complementing rodent repair deficiency, complementation group 4 (ERCC4)
ERCC5	Homo sapiens excision repair cross-complementing rodent repair deficiency, complementation group 5 (ERCC5)
ERCC6	Homo sapiens excision repair cross-complementing rodent repair deficiency, complementation group 6 (ERCC6)
ERCC8	Homo sapiens excision repair cross-complementing rodent repair deficiency, complementation group 8 (ERCC8), transcript variant 2
FEN1	Homo sapiens flap structure-specific endonuclease 1 (FEN1)
LIG1	Homo sapiens ligase I, DNA, ATP-dependent (LIG1)
LIG3	Homo sapiens ligase III, DNA, ATP-dependent (LIG3), nuclear gene encoding mitochondrial protein, transcript variant alpha
LIG4	Homo sapiens ligase IV, DNA, ATP-dependent (LIG4), transcript variant 1
MLH1	Homo sapiens mutL homolog 1, colon cancer, nonpolyposis type 2 (E. coli) (MLH1)
MLH3	Homo sapiens mutL homolog 3 (E. coli) (MLH3), transcript variant 1
MMS19	Homo sapiens MMS19-like (MET18 homolog, S. cerevisiae) (MMS19L)
MPG	Homo sapiens N-methylpurine-DNA glycosylase (MPG), transcript variant 1
MRE11A	Homo sapiens MRE11 meiotic recombination 11 homolog A (S. cerevisiae) (MRE11A), transcript variant 1
MSH2	Homo sapiens mutS homolog 2, colon cancer, nonpolyposis type 1 (E. coli) (MSH2)
MSH3	Homo sapiens mutS homolog 3 (E. coli) (MSH3)
MSH4	Homo sapiens mutS homolog 4 (E. coli) (MSH4)
MSH5	Homo sapiens mutS homolog 5 (E. coli) (MSH5), transcript variant 3
MSH6	Homo sapiens mutS homolog 6 (E. coli) (MSH6)
MUTYH	Homo sapiens mutY homolog (E. coli) (MUTYH), transcript variant gamma2
NEIL1	Homo sapiens nei endonuclease VIII-like 1 (E. coli) (NEIL1)
NEIL2	Homo sapiens nei like 2 (E. coli) (NEIL2)
NEIL3	Homo sapiens nei endonuclease VIII-like 3 (E. coli) (NEIL3)
NTHL1	Homo sapiens nth endonuclease III-like 1 (E. coli) (NTHL1)
OGG1	Homo sapiens 8-oxoguanine DNA glycosylase (OGG1), nuclear gene encoding mitochondrial protein, transcript variant 2a
PARP1	Homo sapiens poly (ADP-ribose) polymerase family, member 1 (PARP1)
PARP2	Homo sapiens poly (ADP-ribose) polymerase 2 (PARP2), transcript variant 2
PARP3	Homo sapiens poly (ADP-ribose) polymerase family, member 3 (PARP3), transcript variant 2
PMS1	Homo sapiens PMS1 postmeiotic segregation increased 1 (S. cerevisiae) (PMS1)
PMS2	Homo sapiens PMS2 postmeiotic segregation increased 2 (S. cerevisiae) (PMS2), transcript variant 1
PNKP	Homo sapiens polynucleotide kinase 3'-phosphatase (PNKP)
POLB	Homo sapiens polymerase (DNA directed), beta (POLB)
POLD3	Homo sapiens polymerase (DNA-directed), delta 3, accessory subunit (POLD3)
POLL	Homo sapiens polymerase (DNA directed), lambda (POLL)
PRKDC	Homo sapiens protein kinase, DNA-activated, catalytic polypeptide (PRKDC), transcript variant 2
RAD21	Homo sapiens RAD21 homolog (S. pombe) (RAD21)
RAD23A	Homo sapiens RAD23 homolog A (S. cerevisiae) (RAD23A)
RAD23B	Homo sapiens RAD23 homolog B (S. cerevisiae) (RAD23B)
RAD50	Homo sapiens RAD50 homolog (S. cerevisiae) (RAD50), transcript variant 2
RAD51	Homo sapiens RAD51 homolog (RecA homolog, E. coli) (S. cerevisiae) (RAD51), transcript variant 1
RAD51B	Homo sapiens RAD51-like 1 (S. cerevisiae) (RAD51L1), transcript variant 2
RAD51C	Homo sapiens RAD51 homolog C (S. cerevisiae) (RAD51C), transcript variant 1
RAD51D	Homo sapiens RAD51-like 3 (S. cerevisiae) (RAD51L3), transcript variant 1
RAD52	Homo sapiens RAD52 homolog (S. cerevisiae) (RAD52)
RAD54L	Homo sapiens RAD54-like (S. cerevisiae) (RAD54L)
RPA1	Homo sapiens replication protein A1, 70kDa (RPA1)
RPA3	Homo sapiens replication protein A3, 14kDa (RPA3)
SLK	Homo sapiens STE20-like kinase (yeast) (SLK)
SMUG1	Homo sapiens single-strand-selective monofunctional uracil-DNA glycosylase 1 (SMUG1)
TDG	thymine DNA glycosylase
TREX1	Homo sapiens three prime repair exonuclease 1 (TREX1), transcript variant 1
UNG	Homo sapiens uracil-DNA glycosylase (UNG), nuclear gene encoding mitochondrial protein, transcript variant 1
XAB2	Homo sapiens XPA binding protein 2 (XAB2)
XPA	Homo sapiens xeroderma pigmentosum, complementation group A (XPA)
XPC	Homo sapiens xeroderma pigmentosum, complementation group C (XPC)
XRCC1	Homo sapiens X-ray repair complementing defective repair in Chinese hamster cells 1 (XRCC1)
XRCC2	Homo sapiens X-ray repair complementing defective repair in Chinese hamster cells 2 (XRCC2)
XRCC3	Homo sapiens X-ray repair complementing defective repair in Chinese hamster cells 3 (XRCC3), transcript variant 3
XRCC4	Homo sapiens X-ray repair complementing defective repair in Chinese hamster cells 4 (XRCC4), transcript variant 2
XRCC5	Homo sapiens X-ray repair complementing defective repair in Chinese hamster cells 5 (double-strand-break rejoining; Ku autoantigen, 80kDa) (XRCC5)
XRCC6	Homo sapiens X-ray repair complementing defective repair in Chinese hamster cells 6 (XRCC6)

Table 28 Genes annotated to regulation of oxidative phosphorylation used to characterise iMSCs.

Name	Descripton
ATP5C1	Homo sapiens ATP synthase, H+ transporting, mitochondrial F1 complex, gamma polypeptide 1 (ATP5C1), nuclear gene encoding mitochondrial protein, transcript variant 2
ATP5D	Homo sapiens ATP synthase, H+ transporting, mitochondrial F1 complex, delta subunit (ATP5D), nuclear gene encoding mitochondrial protein, transcript variant 1
COQ7	Homo sapiens coenzyme Q7 homolog, ubiquinone (yeast) (COQ7)
COX10	Homo sapiens COX10 homolog, cytochrome c oxidase assembly protein, heme A: farnesyltransferase (yeast) (COX10), nuclear gene encoding mitochondrial protein
COX15	Homo sapiens COX15 homolog, cytochrome c oxidase assembly protein (yeast) (COX15), nuclear gene encoding mitochondrial protein, transcript variant 1
COX4I1	Homo sapiens cytochrome c oxidase subunit IV isoform 1 (COX4I1)
COX5A	Homo sapiens cytochrome c oxidase subunit Va (COX5A), nuclear gene encoding mitochondrial protein
CYCS	Homo sapiens cytochrome c, somatic (CYCS), nuclear gene encoding mitochondrial protein
KCTD14	Homo sapiens potassium channel tetramerisation domain containing 14 (KCTD14)
LRRK2	Homo sapiens leucine-rich repeat kinase 2 (LRRK2)
MT-CO2	mitochondrially encoded cytochrome c oxidase II
MT-CYB	mitochondrially encoded cytochrome b
MT-ND1	mitochondrially encoded NADH dehydrogenase 1
MT-ND2	mitochondrially encoded NADH dehydrogenase 2
MT-ND3	mitochondrially encoded NADH dehydrogenase 3
MT-ND4	mitochondrially encoded NADH dehydrogenase 4
MT-ND4L	mitochondrially encoded NADH 4L dehydrogenase
MT-ND5	mitochondrially encoded NADH dehydrogenase 5
NDUFA1	Homo sapiens NADH dehydrogenase (ubiquinone) 1 alpha subcomplex, 1, 7.5kDa (NDUFA1), nuclear gene encoding mitochondrial protein
NDUFA10	Homo sapiens NADH dehydrogenase (ubiquinone) 1 alpha subcomplex, 10, 42kDa (NDUFA10), nuclear gene encoding mitochondrial protein
NDUFA2	NADH dehydrogenase (ubiquinone) 1 alpha subcomplex, 2
NDUFA3	Homo sapiens NADH dehydrogenase (ubiquinone) 1 alpha subcomplex, 3, 9kDa (NDUFA3)
NDUFA4	Homo sapiens NADH dehydrogenase (ubiquinone) 1 alpha subcomplex, 4, 9kDa (NDUFA4), nuclear gene encoding mitochondrial protein
NDUFA5	Homo sapiens NADH dehydrogenase (ubiquinone) 1 alpha subcomplex, 5, 13kDa (NDUFA5), nuclear gene encoding mitochondrial protein
NDUFA6	NADH dehydrogenase (ubiquinone) 1 alpha subcomplex, 6
NDUFA7	Homo sapiens NADH dehydrogenase (ubiquinone) 1 alpha subcomplex, 7, 14.5kDa (NDUFA7)
NDUFA8	Homo sapiens NADH dehydrogenase (ubiquinone) 1 alpha subcomplex, 8, 19kDa (NDUFA8), nuclear gene encoding mitochondrial protein
NDUFA9	Homo sapiens NADH dehydrogenase (ubiquinone) 1 alpha subcomplex, 9, 39kDa (NDUFA9)
NDUFAB1	Homo sapiens NADH dehydrogenase (ubiquinone) 1, alpha/beta subcomplex, 1, 8kDa (NDUFAB1)
NDUFB1	Homo sapiens NADH dehydrogenase (ubiquinone) 1 beta subcomplex, 1, 7kDa (NDUFB1)
NDUFB10	Homo sapiens NADH dehydrogenase (ubiquinone) 1 beta subcomplex, 10, 22kDa (NDUFB10)
NDUFB2	Homo sapiens NADH dehydrogenase (ubiquinone) 1 beta subcomplex, 2, 8kDa (NDUFB2), nuclear gene encoding mitochondrial protein
NDUFB3	Homo sapiens NADH dehydrogenase (ubiquinone) 1 beta subcomplex, 3, 12kDa (NDUFB3)
NDUFB4	Homo sapiens NADH dehydrogenase (ubiquinone) 1 beta subcomplex, 4, 15kDa (NDUFB4), nuclear gene encoding mitochondrial protein
NDUFB5	Homo sapiens NADH dehydrogenase (ubiquinone) 1 beta subcomplex, 5, 16kDa (NDUFB5), nuclear gene encoding mitochondrial protein
NDUFB6	Homo sapiens NADH dehydrogenase (ubiquinone) 1 beta subcomplex, 6, 17kDa (NDUFB6), nuclear gene encoding mitochondrial protein, transcript variant 1
NDUFB7	Homo sapiens NADH dehydrogenase (ubiquinone) 1 beta subcomplex, 7, 18kDa (NDUFB7), nuclear gene encoding mitochondrial protein
NDUFB8	Homo sapiens NADH dehydrogenase (ubiquinone) 1 beta subcomplex, 8, 19kDa (NDUFB8)
NDUFB9	NADH dehydrogenase (ubiquinone) 1 beta subcomplex, 9
NDUFC1	Homo sapiens NADH dehydrogenase (ubiquinone) 1, subcomplex unknown, 1, 6kDa (NDUFC1)
NDUFC2	Homo sapiens NADH dehydrogenase (ubiquinone) 1, subcomplex unknown, 2, 14.5kDa (NDUFC2)
NDUFC2-KCT	NDUFC2-KCTD14 readthrough
NDUFS1	Homo sapiens NADH dehydrogenase (ubiquinone) Fe-S protein 1, 75kDa (NADH-coenzyme Q reductase) (NDUFS1), nuclear gene encoding mitochondrial protein
NDUFS2	Homo sapiens NADH dehydrogenase (ubiquinone) Fe-S protein 2, 49kDa (NADH-coenzyme Q reductase) (NDUFS2)
NDUFS3	Homo sapiens NADH dehydrogenase (ubiquinone) Fe-S protein 3, 30kDa (NADH-coenzyme Q reductase) (NDUFS3)
NDUFS4	Homo sapiens NADH dehydrogenase (ubiquinone) Fe-S protein 4, 18kDa (NADH-coenzyme Q reductase) (NDUFS4)
NDUFS5	Homo sapiens NADH dehydrogenase (ubiquinone) Fe-S protein 5, 15kDa (NADH-coenzyme Q reductase) (NDUFS5)
NDUFS6	Homo sapiens NADH dehydrogenase (ubiquinone) Fe-S protein 6, 13kDa (NADH-coenzyme Q reductase) (NDUFS6)
NDUFS7	Homo sapiens NADH dehydrogenase (ubiquinone) Fe-S protein 7, 20kDa (NADH-coenzyme Q reductase) (NDUFS7)
NDUFS8	Homo sapiens NADH dehydrogenase (ubiquinone) Fe-S protein 8, 23kDa (NADH-coenzyme Q reductase) (NDUFS8)
NDUFV1	Homo sapiens NADH dehydrogenase (ubiquinone) flavoprotein 1, 51kDa (NDUFV1)
NDUFV2	Homo sapiens NADH dehydrogenase (ubiquinone) flavoprotein 2, 24kDa (NDUFV2)
NDUFV3	Homo sapiens NADH dehydrogenase (ubiquinone) flavoprotein 3, 10kDa (NDUFV3), nuclear gene encoding mitochondrial protein, transcript variant 2
SDHC	Homo sapiens succinate dehydrogenase complex, subunit C, integral membrane protein, 15kDa (SDHC), nuclear gene encoding mitochondrial protein, transcript variant 4
TAZ	Homo sapiens tafazzin (cardiomyopathy, dilated 3A (X-linked); endocardial fibroelastosis 2; Barth syndrome) (TAZ), transcript variant 2
UQCC2	ubiquinol-cytochrome c reductase complex assembly factor 2
UQCR10	ubiquinol-cytochrome c reductase, complex III subunit X
UQCRB	Homo sapiens ubiquinol-cytochrome c reductase binding protein (UQCRB)
UQCRC1	Homo sapiens ubiquinol-cytochrome c reductase core protein I (UQCRC1)
UQCRC2	Homo sapiens ubiquinol-cytochrome c reductase core protein II (UQCRC2)
UQCRH	Homo sapiens ubiquinol-cytochrome c reductase hinge protein (UQCRH)
UQCRHL	ubiquinol-cytochrome c reductase hinge protein like

Table 29 Genes annotated to glutathione metabolism used to characterise iMSCs.

Name	Descripton
CNDP2	Homo sapiens CNDP dipeptidase 2 (metallopeptidase M20 family) (CNDP2)
GCLC	Homo sapiens glutamate-cysteine ligase, catalytic subunit (GCLC)
GCLM	Homo sapiens glutamate-cysteine ligase, modifier subunit (GCLM)
GGCT	Homo sapiens gamma-glutamyl cyclotransferase (GGCT)
GGT1	Homo sapiens gamma-glutamyltransferase 1 (GGT1), transcript variant 1
GGT2	gamma-glutamyltransferase 2
GSS	Homo sapiens glutathione synthetase (GSS)
HAGH	Homo sapiens hydroxyacylglutathione hydrolase (HAGH), nuclear gene encoding mitochondrial protein, transcript variant 1
HAGHL	Homo sapiens hydroxyacylglutathione hydrolase-like (HAGHL), transcript variant 2
MGST2	Homo sapiens microsomal glutathione S-transferase 2 (MGST2)
OPLAH	Homo sapiens 5-oxoprolinase (ATP-hydrolysing) (OPLAH)

Table 30 Genes annotated to regulation of glycolysis used to characterise iMSCs.

Name	Descripton
ALDOA	Homo sapiens aldolase A, fructose-bisphosphate (ALDOA), transcript variant 2
ALDOB	Homo sapiens aldolase B, fructose-bisphosphate (ALDOB)
ALDOC	Homo sapiens aldolase C, fructose-bisphosphate (ALDOC)
ENO1	Homo sapiens enolase 1, (alpha) (ENO1)
ENO2	Homo sapiens enolase 2 (gamma, neuronal) (ENO2)
ENO3	Homo sapiens enolase 3 (beta, muscle) (ENO3), transcript variant 1
GAPDH	Homo sapiens glyceraldehyde-3-phosphate dehydrogenase (GAPDH)
GAPDHS	Homo sapiens glyceraldehyde-3-phosphate dehydrogenase, spermatogenic (GAPDHS)
GCK	Homo sapiens glucokinase (hexokinase 4) (GCK), transcript variant 3
GPI	Homo sapiens glucose phosphate isomerase (GPI)
HK1	Homo sapiens hexokinase 1 (HK1), nuclear gene encoding mitochondrial protein, transcript variant 5
HK2	Homo sapiens hexokinase 2 (HK2)
HK3	Homo sapiens hexokinase 3 (white cell) (HK3), nuclear gene encoding mitochondrial protein
PFKFB1	Homo sapiens 6-phosphofructo-2-kinase/fructose-2,6-biphosphatase 1 (PFKFB1)
PFKFB2	Homo sapiens 6-phosphofructo-2-kinase/fructose-2,6-biphosphatase 2 (PFKFB2), transcript variant 1
PFKFB3	Homo sapiens 6-phosphofructo-2-kinase/fructose-2,6-biphosphatase 3 (PFKFB3)
PFKFB4	Homo sapiens 6-phosphofructo-2-kinase/fructose-2,6-biphosphatase 4 (PFKFB4)
PFKL	Homo sapiens phosphofructokinase, liver (PFKL), transcript variant 2
PFKM	Homo sapiens phosphofructokinase, muscle (PFKM)
PFKP	Homo sapiens phosphofructokinase, platelet (PFKP)
PGAM1	Homo sapiens phosphoglycerate mutase 1 (brain) (PGAM1)
PGAM2	Homo sapiens phosphoglycerate mutase 2 (muscle) (PGAM2)
PGK1	Homo sapiens phosphoglycerate kinase 1 (PGK1)
PKLR	Homo sapiens pyruvate kinase, liver and RBC (PKLR), nuclear gene encoding mitochondrial protein, transcript variant 2
PPP2R5D	Homo sapiens protein phosphatase 2, regulatory subunit B', delta isoform (PPP2R5D), transcript variant 2
TPI1	Homo sapiens triosephosphate isomerase 1 (TPI1)

Table 31 Genes annotated to insulin-signalling used to characterise iMSCs.

Name	Descripton
AKT2	Homo sapiens v-akt murine thymoma viral oncogene homolog 2 (AKT2)
APPL1	Homo sapiens adaptor protein, phosphotyrosine interaction, PH domain and leucine zipper containing 1 (APPL1)
DOK1	Homo sapiens docking protein 1, 62kDa (downstream of tyrosine kinase 1) (DOK1)
FGF16	Homo sapiens fibroblast growth factor 16 (FGF16)
FGF17	Homo sapiens fibroblast growth factor 17 (FGF17)
FGF18	Homo sapiens fibroblast growth factor 18 (FGF18)
FGF2	Homo sapiens fibroblast growth factor 2 (basic) (FGF2)
FGF20	Homo sapiens fibroblast growth factor 20 (FGF20)
FGF3	Homo sapiens fibroblast growth factor 3 (murine mammary tumor virus integration site (v-int-2) oncogene homolog) (FGF3)
FGF4	Homo sapiens fibroblast growth factor 4 (heparin secretory transforming protein 1, Kaposi sarcoma oncogene) (FGF4)
FGF6	Homo sapiens fibroblast growth factor 6 (FGF6)
FGF7	Homo sapiens fibroblast growth factor 7 (keratinocyte growth factor) (FGF7)
FGF9	Homo sapiens fibroblast growth factor 9 (glia-activating factor) (FGF9)
HRAS	Homo sapiens v-Ha-ras Harvey rat sarcoma viral oncogene homolog (HRAS), transcript variant 1
IGF1R	Homo sapiens insulin-like growth factor 1 receptor (IGF1R)
IL1B	Homo sapiens interleukin 1, beta (IL1B)
IRS1	Homo sapiens insulin receptor substrate 1 (IRS1)
IRS2	Homo sapiens insulin receptor substrate 2 (IRS2)
IRS4	Homo sapiens insulin receptor substrate 4 (IRS4)
MAP2K1	Homo sapiens mitogen-activated protein kinase kinase 1 (MAP2K1)
MAPK1	Homo sapiens mitogen-activated protein kinase 1 (MAPK1), transcript variant 2
MTOR	mechanistic target of rapamycin (serine/threonine kinase)
NAMPT	Homo sapiens nicotinamide phosphoribosyltransferase (NAMPT)
OGT	Homo sapiens O-linked N-acetylglucosamine (GlcNAc) transferase (UDP-N-acetylglucosamine:polypeptide-N-acetylglucosaminyl transferase) (OGT), transcript variant 1
PIK3CB	Homo sapiens phosphoinositide-3-kinase, catalytic, beta polypeptide (PIK3CB)
PRKAA1	Homo sapiens protein kinase, AMP-activated, alpha 1 catalytic subunit (PRKAA1), transcript variant 2
PRKAA2	Homo sapiens protein kinase, AMP-activated, alpha 2 catalytic subunit (PRKAA2)
PRKAB1	Homo sapiens protein kinase, AMP-activated, beta 1 non-catalytic subunit (PRKAB1)
PRKAB2	Homo sapiens protein kinase, AMP-activated, beta 2 non-catalytic subunit (PRKAB2)
PRKAG1	Homo sapiens protein kinase, AMP-activated, gamma 1 non-catalytic subunit (PRKAG1), transcript variant 2
PRKCB	protein kinase C, beta
PRKCD	Homo sapiens protein kinase C, delta (PRKCD), transcript variant 1
PRKCZ	Homo sapiens protein kinase C, zeta (PRKCZ), transcript variant 1
RAF1	Homo sapiens v-raf-1 murine leukemia viral oncogene homolog 1 (RAF1)
RHEB	Homo sapiens Ras homolog enriched in brain (RHEB)
RPS6KB1	Homo sapiens ribosomal protein S6 kinase, 70kDa, polypeptide 1 (RPS6KB1)
SH2B2	Homo sapiens SH2B adaptor protein 2 (SH2B2)
SOS1	Homo sapiens son of sevenless homolog 1 (Drosophila) (SOS1)

Publications

- Luther, J., Driessler, F., Megges, M., Hess, A., Herbort, B., Mandic, V., Zaiss, M.M., Reichardt, A., Zech, C., Tuckermann, J.P., Calkhoven, C.F., Wagner, E.F., Schett, G., David, J.-P., 2011. Elevated Fra-1 expression causes severe lipodystrophy. J. Cell. Sci. 124, 1465–1476. doi:10.1242/jcs.079855
- Prigione, A., Hossini, A.M., Lichtner, B., Serin, A., Fauler, B., Megges, M., Lurz, R., Lehrach, H., Makrantonaki, E., Zouboulis, C.C., Adjaye, J., 2011. Mitochondrial-associated cell death mechanisms are reset to an embryonic-like state in aged donor-derived iPS cells harboring chromosomal aberrations. PLoS ONE 6, e27352. doi:10.1371/journal.pone.0027352
- Al-Nbaheen, M., Vishnubalaji, R., Ali, D., Bouslimi, A., Al-Jassir, F., Megges, M., Prigione, A., Adjaye, J., Kassem, M., Aldahmash, A., 2013. Human stromal (mesenchymal) stem cells from bone marrow, adipose tissue and skin exhibit differences in molecular phenotype and differentiation potential. Stem Cell Rev 9, 32–43. doi:10.1007/s12015-012-9365-8
- Méniel, V., Megges, M., Young, M.A., Cole, A., Sansom, O.J., Clarke, A.R., 2015. Apc and p53 interaction in DNA damage and genomic instability in hepatocytes. Oncogene 34, 4118–4129. doi:10.1038/onc.2014.342
- Hossini, A.M., Megges, M., Prigione, A., Lichtner, B., Toliat, M.R., Wruck, W., Schröter, F., Nuernberg, P., Kroll, H., Makrantonaki, E., Zouboulis, C.C., Zoubouliss, C.C., Adjaye, J., 2015. Induced pluripotent stem cell-derived neuronal cells from a sporadic Alzheimer's disease donor as a model for investigating AD-associated gene regulatory networks. BMC Genomics 16, 84. doi:10.1186/s12864-015-1262-5 (equal first author)
- Megges, M., Geissler, S., Duda, G.N., Adjaye, J., 2015. Generation of an iPS cell line from bone marrow-derived mesenchymal stromal cells from an elderly patient. Stem Cell Research 15, 565–568. doi:10.1016/j.scr.2015.10.003
- Megges, M., Geissler, S., Wruck W., Textor M., Duda, G.N., Adjaye, J., Bone marrow MSC-derived iPS cells retain a transcriptional memory and differentiation capacity specific to the parental cell-type. Manuscript in preparation
- Megges, M., Spitzhorn L., Ncube A., Wruck W., Oreffo R., Adjaye, J., Mesenchymal stem cells derived from iPS cells from aged individuals acquire fetal characteristics. Manuscript in preparation

Selbstständigkeitserklärung

Hiermit bestätige ich, dass ich diese Promotionsschrift selbstständig verfasst habe. Ich habe keine anderen Quellen und Hilfsmittels außer den von mir angegebenen verwendet. Darüber hinaus habe ich bisher keine Promotion an der Freien Universität Berlin oder einer anderen Universität absolviert oder eine Doktorarbeit eingereicht.

Matthias Mark Megges Berlin, 30.10.2015

Parts of this work are published in:

Megges M, Geissler S, Duda GN, Adjaye J. Generation of an iPS cell line from bone marrow derived mesenchymal stromal cells from an elderly patient. Stem Cell Res. 2015;15(3):565-8.

http://dx.doi.org/10.1016/j.scr.2015.10.003

Megges M, Oreffo ROC, Adjaye J. Episomal plasmid-based generation of induced pluripotent stem cells from fetal femur-derived human mesenchymal stromal cells. Stem Cell Res. 2016;16(1):128-32.

http://dx.doi.org/10.1016/j.scr.2015.12.013